Defining the functions of Wnt/β-catenin signalling in muscle stem cells

by

Shuang Cui

Thesis
Submitted to Flinders University
for the degree of

Doctor of Philosophy

College of Medicine and Public Health

May 2019

TABLE OF CONTENTS

LIST OF FIGURES

LIST OF TABLES

SUMMARY

Canonical Wnt signalling regulates muscle stem cell/myoblast differentiation, but there have been conflicting reports about the requirement for β-catenin in adult regenerative myogenesis. Wnt is also known to be a key player in fibrosis in many tissues. That Wnt may be a double edged sword in muscle repair, promoting myogenesis but also contributing to pathogenic fibrosis, suggests a pressing need to better understand the molecular processes of Wnt signalling in these contexts.

To better understand the role of β-catenin in myogenesis we used CRISPR to generate β-catenin null primary adult mouse myoblasts *in vitro*. β-catenin null myoblasts showed greatly impaired spontaneous and Wnt3a-induced differentiation. RNA-seq analysis showed a strong delay in activation of the global myogenic differentiation program after Wnt treatment, thus confirming the requirement for β-catenin in myogenesis. β-catenin interacts with TCF/LEF factors but also with the muscle regulatory factor MyoD, and it was unclear which regulatory complex may be involved in myogenesis. Using ChIP-seq analysis, we showed that Wnt induced activating histone modifications at genomic regions that contain MyoD (E-box) binding elements, but not TCF/LEF elements. We also found that Wnt increased binding of MyoD to E-box elements in wild-type myoblasts but not β-catenin null cells. Among the gene targets that were found to be controlled by MyoD and β-catenin is the membrane fusion protein Myomaker, which we propose as a novel effector of Wnt signalling in myoblasts. To explicitly test whether TCF/LEF is required for myogenic differentiation, we used a variant of β-catenin that cannot interact with TCF/LEF in rescue studies in β-catenin null myoblasts. The mutant β-catenin variant rescued the differentiation capacity of null myoblasts as effectively as wild-type β-catenin. Together these data indicate that Wnt promotes adult

myogenesis in a β-catenin-dependent and likely MyoD-dependent, but TCF/LEF-independent, manner.

β-catenin-TCF/LEF-CBP complexes are known to be involved in fibrosis in many contexts. Because we found no requirement for β-catenin-TCF/LEF complexes in myogenesis, we postulated that inhibition of this complex would not impair myogenesis, but might reduce fibrosis mediated by muscle fibroblasts/FAPs. In support of this, preliminary evidence suggests that a small molecule inhibitor of β-catenin-TCF/LEF-CBP complexes inhibits activation of fibroblasts *in vitro* and *in vivo* without inhibiting myogenic differentiation. In contrast, similar chemical inhibitor studies suggest that β-catenin-MRFs/MEFs-p300 complexes may be required for myogenic differentiation.

Wnt/β-catenin signalling was shown to inhibit Pax7 expression at the protein level in myoblasts. Wnt also induced expression of the myogenic miRNAs miR-133b and miR-206 in a β-catenin-dependent manner. miR-206 was previously reported to post-transcriptionally repress Pax7; our studies showed that miR-133b is likely to be a more potent inhibitor of Pax7 and confirmed that β-catenin is absolutely required to relieve Pax7-mediated inhibition of differentiation.

Overall, the findings reported in this thesis prompt the following conclusions about the role of Wnt/β-catenin signalling in myogenesis: 1. β-catenin regulates muscle stem cell differentiation by inducing miRNA-mediated Pax7 degradation to relieve Pax7's inhibitory effect on differentiation; 2. β-catenin works in concert with MyoD and p300 to positively regulate the differentiation-associated transcriptional network comprised of transcription factors, miRNAs, and mechanochemical effectors such as cytoskeletal remodelling and membrane fusion proteins. Moreover, given that the pro-differentiation and pro-fibrotic programs driven by Wnt/β-catenin are likely

mediated by different coactivators, these might be functionally separated as part of a therapeutic strategy for muscle fibrosis associated with muscle degenerative diseases such as DMD.

DECLARATION

I certify that this thesis:

1. does not incorporate without acknowledgement any material previously submitted for a degree or diploma in any university; and

2. to the best of my knowledge and belief, does not contain any material previously published or written by another person except where due reference is made in the text.

Shuang Cui

July 2018

ACKNOWLEDGEMENTS

First and foremost, I would like to express my gratitude to my supervisor Dr. Robyn Meech for her excellent guidance and mentorship throughout my Ph.D training. She is professional, knowledgeable and more importantly, she is so kind, patient and incredibly supportive of her students. Under her supervision, I have gained tremendous skills, both in research and in life. I am grateful to work with her in the past years. I am also grateful to my co-supervisor Professor Ross McKinnon for his help during my Ph.D candidature.

Thanks to all the staff and students in Department of Clinical Pharmacology, particularly in our lab-Professor Peter Mackenzie, Dr. Dong Gui Hu, Dr. Lu Lu, Alex Haines, Siti Mubarokah, Dr. Julie-Ann Hulin, Dhilushi Wijayakumara, and many others.

Thanks to Flinders University and China Scholarship Council for providing me financial support.

Finally, I would like to thank my family: my parents, my parent's in-law for giving me love, encouragement and financial support during these years. Thanks to my husband Dr. Liang Li, for his love and tremendous support in my everyday life. I also appreciate the coming of my little baby who is now swimming in my tummy and bringing me a lot of happiness.

PUBLICATIONS

- ***Cui, S.***, Li, L., Yu, R.T., Downes, M., Evans, R.M., Hulin, J.A., Makarenkova, H.P., and Meech, R. (2019). beta-Catenin is essential for differentiation of primary myoblasts via cooperation with MyoD and alpha-catenin. Development *146*.
- ***Cui, S.***, Li, L., Mubarokah, S.N., and Meech, R. (2019). Wnt/beta-catenin signaling induces the myomiRs miR-133b and miR-206 to suppress Pax7 and induce the myogenic differentiation program. J Cell Biochem. Epub ahead of print.
- Hulin, J.A., Nguyen, T.D., ***Cui, S***., Makarenkova, H. and Meech, R. (2016) Barx2 and Pax7 regulate Axin2 expression in myoblasts by interaction with β-catenin and chromatin remodelling. Stem Cells. 34(8):2169-82.

CONFERENCE PRESENTATIONS

- Oral presentation- ***Cui, S***., Makarenkova, H., Downes M., Yu R. and Meech, R. 'Wnt regulated muscle stem cell differentiation requires β-catenin', Combio annual meeting, Adelaide, Australia, Oct, 2017.
- Poster presentation- ***Cui, S***., Makarenkova, H., Downes M., Yu R. and Meech, R. 'Wnt regulates muscle stem cell differentiation require β-catenin', International Society for Stem Cell Research (ISSCR) annual meeting, Boston, USA, June, 2017.
- Oral presentation- ***Cui, S***., Downes M., Yu R. and Meech, R. 'Wnt regulated muscle stem cell differentiation requires β-catenin', Australian Society for Stem Cell Research (ASSCR) annual meeting, Sydney, Australia, May, 2017.

- Poster presentation- ***Cui, S***., Downes M., Yu R. and Meech, R.'Wnt regulates muscle stem cell differentiation require β-catenin', Australian Society for Stem Cell Research (ASSCR) annual meeting, Perth, Australia, December, 2016.
- Poster presentation- ***Cui, S***. and Meech, R. 'Wnt regulates primary myoblast differentiation through miRNA mediated Pax7 degradation', Australia and New Zealand Society for Cell and Developmental Biology (ANZSCDB) meeting, Adelaide, Australia, November, 2016.
- Oral presentation- ***Cui, S***. and Meech, R. 'Wnt regulates primary myoblast differentiation through miRNA mediated Pax7 degradation', AMSR National Scientific conference, Adelaide, Australia, June, 2016.
- Poster presentation- ***Cui, S***. and Meech, R. 'Wnt regulates primary myoblast differentiation through miRNA mediated Pax7 degradation', Gage Conference, Canberra, Australia, April, 2016.

AWARDS

Flinders University Research Student Travel Grant to attend and present at the ISSCR annual meeting, Boston 2017.

ASSCR Student Travel Grant to attend and present at the ASSCR annual meeting, Sydney 2017.

ASSCR Student Travel Grant to attend and present at the ASSCR annual meeting, Perth 2016.

ABBREVIATIONS

APC	adenomatous polyposis coli
ARM	armadillo
AT	acetyltransferase
ATCC	American Type Culture Collection
bFGF	basic fibroblast growth factor
bHLH	basic helix-loop-helix
BMP	bone morphogenetic protein
bp	base pair
BSA	bovine serum albumin
Cas9	CRISPR-associated protein 9
CBP	CREB binding protein
cDNA	complementary DNA
ChIP	chromatin immunoprecipitation
ChIP-seq	chromatin immunoprecipitation sequencing
CK	casein kinase
CREB	cAMP response element-binding protein
CRISPR	clustered regularly interspaced short palindromic repeats
CRISPRi	CRISPR interference
crRNA	CRISPR RNA
CTX	cardiotoxin
DAPI	4’, 6-diamidino-2-phenylindole
DMD	Duchenne muscular dystrophy
DMEM	Dulbecco’s modified Eagle’s medium
DMSO	dimethyl sulfoxide
DNA	deoxyribonucleic acid
Dvl	Dishevelled

E. coli	*Escherichia coli*
EDTA	ethylenediaminetetraacetic acid
FACS	fluorescence-activated cell sorting
FBS	foetal bovine serum
Fzd	Frizzled
GFP	green fluorescent protein
Gro	Groucho
GSK	glycogen synthase kinase
HAT	histone acetyltransferase
HDAC	histone deacetylase
kb	kilobase
KO	knockout
LB	Luria broth
LEF	lymphocyte enhancer factor
LRP	low density lipoprotein receptor-related protein
MADS	MCM1, agamous, deficiens, serum response factor
MEF	myocyte enhancer factor
miRNA	microRNA
MQ	Milli-Q
MRF	myogenic regulatory factor
mRNA	messenger RNA
MyHC	myosin heavy chain
NC	negative control
PAGE	polyacrylamide gel electrophoresis
PAM	protospacer adjacent motif
PBS	phosphate buffered saline
PCR	polymerase chain reaction
PEG	Polyethylglycol

Pen-strep	penicillin streptomycin
PIC	proteinase inhibitor cocktail
PLB	passive lysis buffer
PNK	proteinase K
RIPA	radioimmunoprecipitation assay
RNA	ribonucleic acid
RT-PCR	reverse-transcription PCR
SB	sodium borate
SDM	site-directed mutagenesis
SDS	sodium dodecyl sulphate
SEM	standard error of the mean
SF	serum free
sgRNA	single guide RNA
Shh	sonic hedgehog
TA	tibialis anterior
TAE	tris-acetate EDTA
TBE	tris-borate EDTA
TBS	tris-buffered saline
TBST	tris-buffered saline-Tween-20
TCF	T-cell factor
TE	tris-EDTA
TGF-β	transforming growth factor beta
TLE	transducin-like enhancer of split
TMX	tamoxifen
tracrRNA	trans-activating CRISPR RNA
Tris	tris[hydroxymethyl]aminomethane
UTR	untranslated region
WT	wild-type

CHAPTER 1: Literature Review

1.1 Muscle stem cell differentiation and muscle regeneration

1.1.1 Skeletal muscle and its function

Skeletal muscle is one of the three types of muscle tissue, which accounts for approximately 40% of adult human body mass and comprises 50-75% of all body proteins. Attached to the skeleton by strong tendons or directly connected to the bone, skeletal muscle is under voluntary control and is capable of contracting, which is vital for producing movement, maintaining posture, stabilising joints and generating heat. Moreover, skeletal muscle is a reservoir of amino acids and glycogen for supporting other tissues; these can be released from muscle contributing to maintaining blood glucose levels during starvation.

Skeletal muscle is composed of various integrated tissue units including myofibres, blood vessels, nerve fibres and associated connective tissue. A myofibre is a multinucleated muscle cell that forms by the fusion of myoblasts during embryonic and foetal development (Mintz and Baker, 1967). Connective tissue comprises three layers which compartmentalise the myofibres (Figure 1.1).

The outside layer of connective tissue surrounding the muscle is known as the epimysium. The epimysium maintains the integrity of skeletal muscle structure and separates skeletal muscle from other tissue to allow it to move independently.

Fibres within muscles are organised into individual bundles called fascicles, and surrounded by the middle layer of connective tissue referred to as the perimysium. The perimysium separates fascicles and allows the fascicles to be independently innervated by specific nerves.

Within a fascicle, individual muscle fibre is surrounded by a thin connective tissue layer composed of collagen and reticular fibres named the endomysium. The endomysium supplies the muscle fibre with extracellular fluid as well as nutrients

acquired via blood. Each muscle fibre has a cell membrane called a sarcolemma; the cytoplasm within it is named a sarcoplasm, and the functional unit of skeletal muscle is referred to as a sarcomere. The sarcomere is mainly composed of contractile myofilaments, cytoskeletal proteins, and other supportive or regulatory proteins, and it also stores calcium ions. The two most abundant myofilaments are actin (thin filament) and myosin (thick filament), which comprise almost 70-80% of total protein in the sarcomere. Muscle contraction is achieved when the myosin head binds to actin filaments; then myosin works as a motor to drive filament sliding repetitively. Moreover, the molecular events during muscle contraction are initiated by the release of calcium which is stored in the sarcoplasm.

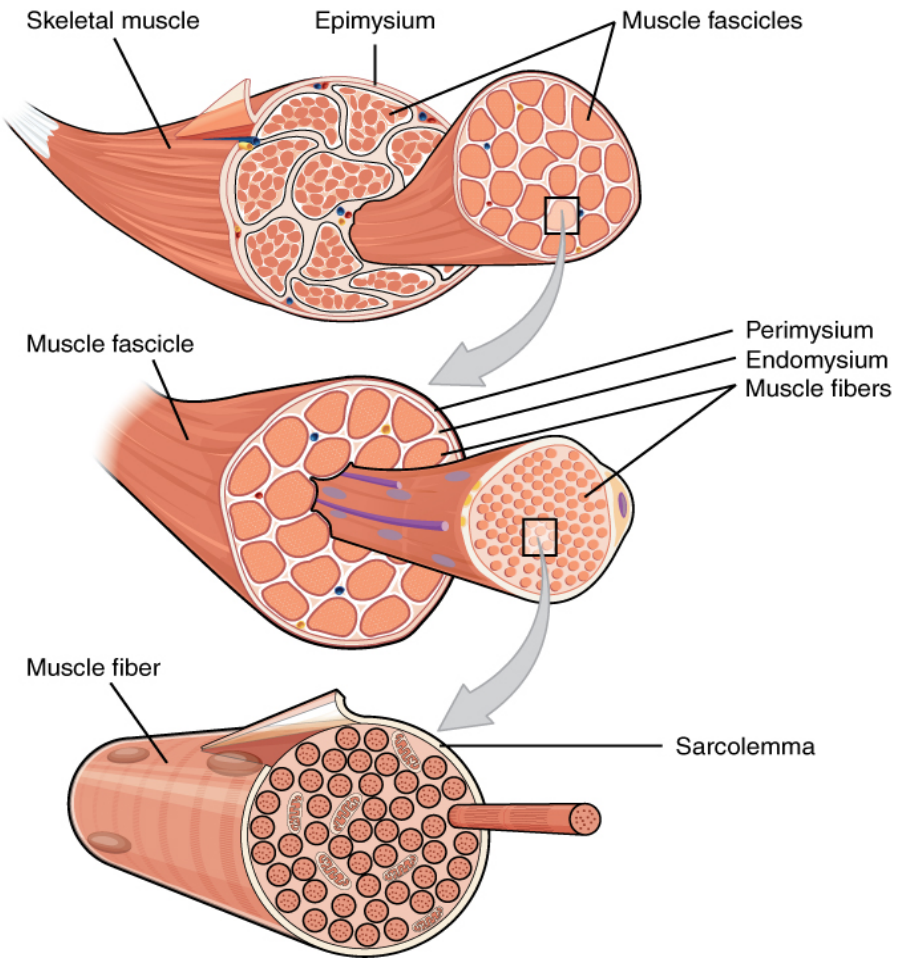

Figure 1.1: Structure of skeletal muscle

Skeletal muscle is mainly composed of fascicles and connective tissue with three layers: epimysium, perimysium and endomysium. Within a fascicle are bundles of individual

muscle fibres each surrounded by a sarcolemma. Figure obtained from http://oerpub.github.io/epubjs-demo-book/content/m46476.xhtml.

1.1.2 Satellite cells and their function

Skeletal muscles are capable of robust regeneration, with the full re-establishment of muscle function occurring within three weeks after severe injury (Rosenblatt, 1992). The efficient regeneration is also supported by the evidence that the function of muscle is restored even when the muscle was removed, minced and replaced in the muscle bed in a rat model (Studitsky, 1965). Moreover, the regeneration of muscle showed consistency after repeated injury in rodents (Luz et al., 2002).

During muscle regeneration, myoblasts fuse together or fuse with damaged myofibres to re-establish the functional unit of muscle. The cells which account for muscle generation postnatally in skeletal muscle are called adult muscle stem cells, also termed satellite cells.

Discovered half a century ago (Mauro, 1961), satellite cells are small, mononuclear and adjacent to the multinucleated myofibres (Enesco and Puddy, 1964; Mauro, 1961; Moss and Leblond, 1971). They were originally observed to be positioned between the sarcolemma and basement membrane of muscle fibres (Muir et al., 1965) (Figure 1.2), and this unique location is now defined as their niche. Later on, [^{3}H] thymidine labelling and tracing experiments suggested that satellite cells are quiescent in adult muscle but can quickly enter the cell cycle, undergo mitosis, and contribute to myofibre nuclei following muscle injury (Snow, 1977). More evidence came from single myofibre culture experiments, which demonstrated that satellite cells give rise to proliferating myoblasts that differentiate into myotubes during regeneration (Bischoff, 1975; Konigsberg et al., 1975). In addition to giving rise to differentiation-competent myoblasts, satellite cells are capable of self-renewing to

maintain their population and thus maintain long-term regenerative capacity (Collins et al., 2005). Satellite cells are usually considered to be monopotent stem cells that follow only the myogenic fate *in vivo*, although they may be manipulated into acquiring different mesenchymal fates *in vitro*.

There is evidence that the regenerative capability of satellite cells is limited and may be exceeded in disease states. For example the pool of satellite cells may be exhausted due to repeated cycles of activation and hence replicative senescence due to telomere shortening in the context of muscular dystrophy (Sacco et al., 2010). Other studies have posited that changes in satellite cell function, rather than abundance, are primarily involved in muscular dystrophy (Chang et al., 2016). Furthermore, the number of satellite cells and their functionality both decline with age, probably due to the change in systemic and local environmental, as well as intrinsic factors (Beccafico et al., 2011; Carlson and Conboy, 2007; Renault et al., 2002).

Satellite cells are identified by the expression of the paired box transcription factor Pax7 (Seale et al., 2000), , the receptor for hepatocyte growth factor (HGF) called c-met (Cornelison and Wold, 1997), and the myogenic factor 5 (Myf5) (Beauchamp et al., 2000; Cornelison and Wold, 1997).

Developmentally, satellite cells are mainly derived from the central region of the dermomyotome of the somite, which was demonstrated by lineage-tracing experiments using GFP electroporation into somites or quail-chick cell grafting experiments (Gros et al., 2005; Schienda et al., 2006). Previously satellite cells were thought to be homogeneous muscle progenitors. However, recent findings suggested that satellite cells are heterogeneous in terms of gene expression profile, myogenic differentiation potential, stemness and fate determination (Collins et al., 2005; Kuang

et al., 2007; Ono et al., 2010).

The turnover of myonuclei in adult mammalian skeletal muscle is infrequent (Schmalbruch and Lewis, 2000). Minor injury caused by wear and tear can be repaired efficiently, but severe damage due to major injury, or genetic disorders or other pathological conditions resulting in fibre instability/rupture, is associated with a series of events collectively referred to as muscle regeneration. These events include myofibre necrosis, inflammation, satellite cell activation, derived myoblast proliferation, and differentiation into functional myofibres. Satellite cells play a crucial role during muscle regeneration (Murphy et al., 2011; Sambasivan et al., 2011), which is supported by the evidence that deletion of Pax7-positive cells (satellite cells) in adult mice completely abolishes muscle regeneration (Lepper et al., 2011; Sambasivan et al., 2011).

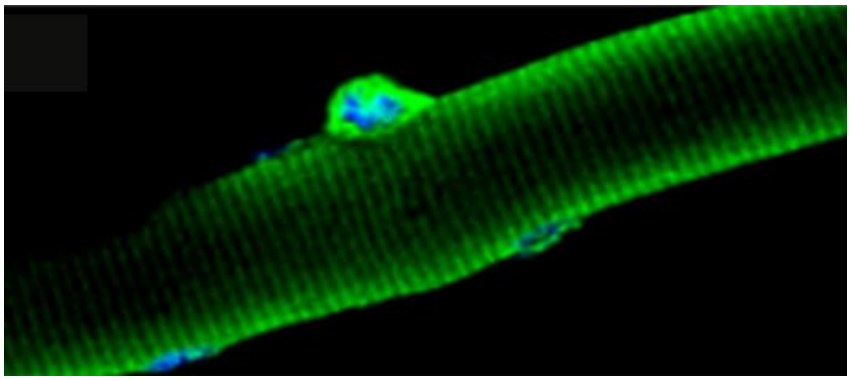

Figure 1.1: Fluorescence microscopic image of mitotic satellite cells
Satellite cells are labelled by a yellow fluorescent protein and DNA is stained in blue. Figure obtained from (Bentzinger et al., 2010).

1.1.3 Myogenesis

The process of generating muscle, both embryonically and during post-natal life, is called myogenesis, and can be divided into distinct phases as described here.

Embryonic myogenesis is governed by the interplay of extrinsic signals, and intrinsic

regulatory factors. Mesoderm-derived primitive myogenic cells, expressing Pax3 and Pax7, are regulated by surrounding signalling cues, such as sonic hedgehog (Shh), bone morphogenetic proteins (BMPs) and wingless-type MMTV integration site (Wnt) family of proteins (Sambasivan and Tajbakhsh, 2007). Furthermore, myogenic progression is modulated by Pax3/Pax7 and myogenic regulatory factors (MRFs) that will be discussed in detail in section 1.1.5 (Rudnicki et al., 2008a). Most skeletal muscle such as trunk and limb muscles arise from the dorsal part of the somite (Christ and Ordahl, 1995) termed the dermomyotome. Myogenic precursor cells migrate from the central region of the dermomyotome toward the myotome and extensively proliferate and differentiate, thereby contributing to the growth of myotome and the development of embryonic and fetal truck muscles (Kassar-Duchossoy et al., 2005; Relaix et al., 2005).

During the perinatal period, juvenile satellite cells proliferate broadly and quickly in their niche. After the period of postnatal muscle growth is complete, the remaining satellite cells reside in myofibre-associated niches and cease to proliferate or differentiate.

In adult, skeletal myogenesis (i.e. for muscle regeneration) relies on the activity of satellite cells. Adult satellite cells are quiescent until injury or degeneration of muscle fibres, whereupon satellite cells can undergo symmetric divisions and asymmetric divisions. Symmetric division is for the expansion of satellite cell pool and asymmetric division is for the concomittant generation of myogenic progenitors and self-renewal. Symmetric division is activated by the planar cell polarity (PCP) pathway, which promotes the equal distribution of polarity effectors such as Vangl2 in the daughter cells (Le Grand et al., 2009). Asymmetric division involves the different distribution of cell fate determinants in the daughter cells, such as Pax7 and

MRFs (Figure 1.3). It is important that, symmetric and asymmetric divisions in satellite cells be appropriately balanced duirng myogenesis; imbalance of these divisions may lead to impaired muscle regeneration, and/or be involved in pathological muscle conditions.

As a canonical marker of satellite cells, Pax7 promotes satellite cell proliferation and myogenic commitment, but represses genes that induce terminal myogenic differentiation (Soleimani et al., 2012). The levels of four different MRFs are upregulated during myogenic progression. The MRFs include MyoD, myogenic factor 5 (Myf5), myogenic factor 6 (Myf6; previously called MRF4), and myogenin (Yablonka-Reuveni and Rivera, 1994; Zammit et al., 2002). Once committed to the myogenic lineage, Pax7 is downregulated while the level of MyoD is maintained to activate the transcription of myogenic genes and upregulate myogenin, which is followed by the fusion of differentiated myoblasts for repair. However, a small subset of myoblasts maintain Pax7 but downregulate MyoD, and eventually exit from the cell cycle, and return to quiescence to maintain the satellite cell reservoir for future rounds of injury and repair (Day et al., 2007; Nagata et al., 2006; Olguin and Olwin, 2004).

The extrinsic signalling cues regulating adult myogenesis will be discussed later in section 1.2. Next, I will focus on the role of the critical intrinsic transcriptional factors Pax7 and MRFs.

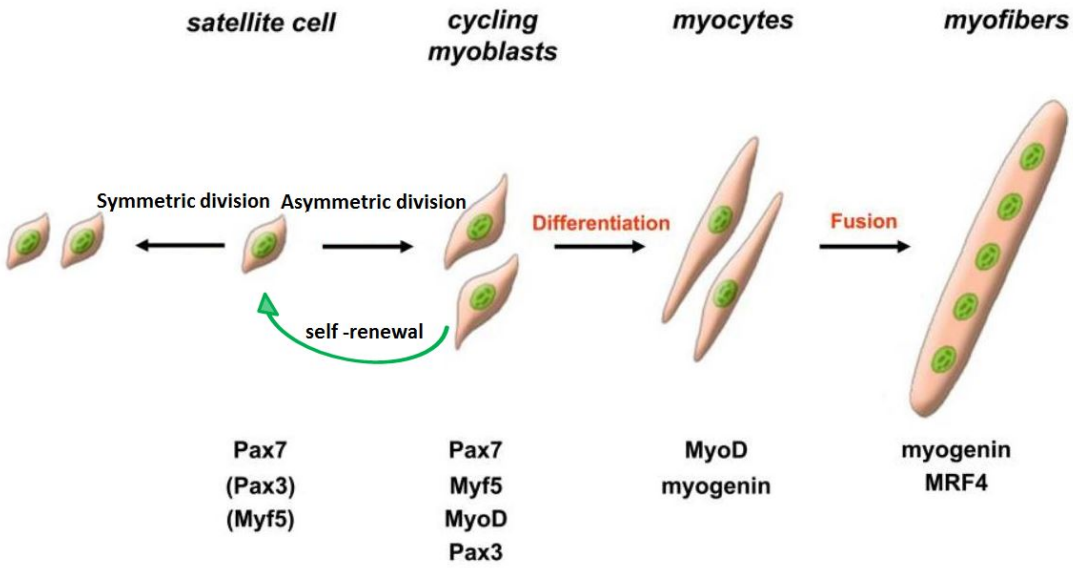

Figure 1.2: Schematic of adult myogenesis

Pax7 (or Pax3)-expressing quiescent adult satellite cells become activated upon injury or other stimuli and start to co-express Myf5, and MyoD. These cells can undergo symmetric divisions to expand satellite cell pool and asymmetric divisions to produce myogenic progenitors and also self-renewal. After asymmetric divisions, the majority of daughter cells down-regulate Pax7 to enter the proliferative phase of myogenic lineage progression; myogenin and other myogenic genes are subsequently upregulated as cells progress towards terminal differentiation. The minority of satellite cells downregulate MyoD, exit the cell cycle and return to quiescence to replenish the satellite cell reservoir. Figure modified from (Le Grand and Rudnicki, 2007).

1.1.4 Pax7

Pax7 and Pax3 belong to the paired-homeobox transcription factor family; they bind to the same DNA motifs (Soleimani et al., 2012) and lie genetically upstream of MRFs (Buckingham and Relaix, 2007).

Pax7 and Pax3 have some overlapping functions but are generally not redundant in terms of myogenic fate specification and myogenic progression. During development of the early embryo, Pax7 and Pax3 are co-expressed in the dermomyotome (DM) in cells that give rise to primitive muscle progenitors that also express MRFs (Kassar-Duchossoy et al., 2005). However, at later stages of development, Pax3 is

downregulated whereas the level of Pax7 is maintained. In adult muscle, Pax3 is expressed at low levels, other than in satellite cells within a restricted subset of muscles (e.g. diaphragm), where it is expressed at a similar level to Pax7 (Kassar-Duchossoy et al., 2005). Pax3 cannot compensate for the loss of Pax7 in the satellite cells in adult animals (Kuang et al., 2006).

As mentioned above, Pax7 is uniformly expressed in quiescent and activated satellite cells, and is rapidly downregulated during differentiation of committed myoblasts (Olguin and Olwin, 2004; Zammit et al., 2004). In *ex vivo* culture of myoblasts, a subpopulation of cells maintain the expression of Pax7 while downregulating the level of MyoD; these cells remain undifferentiated and resemble quiescent satellite cells. Mesenchymal cells can be induced to enter the myogenic lineage by ectopic expression of MyoD; however co-expression of Pax7 in these cells represses this myogenic conversion via inhibiting MyoD activity (Olguin and Olwin, 2004). These studies showed that Pax7 repressed myogenesis through altering stability of MyoD protein, rather than acting transcriptionally. Myogenin, which is activated by MyoD, regulates Pax7 activity by influencing Pax7 levels (Olguin et al., 2007). These studies demonstrate that reciprocal inhibitions exist between Pax7 and MRFs. During muscle regeneration, activated satellite cells possessing higher levels of Pax7 are less prone to commitment, which further supports the idea that a primary role of Pax7 is to prevent inappropriate myogenic differentiation (Rocheteau et al., 2012).

Mutation of Pax7 in mice and *in vitro* knockdown experiments both showed the importance of Pax7 in satellite cell survival, and proliferation of committed myoblasts (Kawabe et al., 2012; Kuang et al., 2006; McKinnell et al., 2008; Oustanina et al., 2004; Seale et al., 2000). Specifically, satellite cells in postnatal mice with germline deletion of Pax7 (Pax7-/-) mice failed to proliferate and

exhibited precocious differentiation, which led to loss of the myogenic lineage and reduction of muscle size, and the null mice died within three weeks of birth (Kuang et al., 2006; Oustanina et al., 2004; Seale et al., 2000). Knockdown of Pax7 using siRNA in cultured myoblasts or satellite cells led to cell cycle arrest and dysregulation of Myf5 (Kawabe et al., 2012; McKinnell et al., 2008).

Further insight into Pax7 function comes from a ChIP-seq study performed using epitope tagged-Pax7 expressed in cultured myoblasts. The study identified multiple DNA motifs which may be bound by Pax7; these motifs were involved in the activation of genes associated with myogenic specification, myoblast proliferation and inhibition of differentiation (Soleimani et al., 2012).

Overall, these data suggest that Pax7 plays a critical role in the regulation of satellite cell survival, proliferation and myogenic capability.

While the requirement of Pax7 for postnatal muscle growth is well defined, whether Pax7 is essential in adult life has been somewhat more controversial. A study by Lepper *et al.* (Lepper et al., 2009) suggested that Pax7 was entirely dispensable for adult myogenesis. In the study they showed that, in mice with a conditional tamoxifen-inducible Pax7 null allele, deletion of Pax7 specifically in satellite cells of adult mice, did not lead to any deficit in muscle regeneration efficiency or satellite cell function after muscle damage. In contrast, two subsequent studies by Gunther *et al.* (Günther et al., 2013) and von Maltzahn *et al.* (von Maltzahn et al., 2013) concluded that Pax7 was indispensable for adult satellite cell function and muscle regeneration.

Intriguingly, the genotype of the conditional tamoxifen-inducible Pax7 null mice used in the later studies was exactly the same as that generated by Lepper *et al.*, but

the regimen employed to induce deletion of Pax7 was different (Table 1.1). In the study by Lepper et al, tamoxifen (TMX) was injected to induce deletion of Pax7 only prior the injury, and there was no administration post-injury (Lepper et al., 2009). The strategies used by Gunther *et al.* and von Maltzahn *et al.* had a more extended regimen of TMX treatment before and after injury and during repair. With this extended TMX induction regimen, they showed the regenerative capacity and the function of satellite cells were severely compromised after Pax7 was deleted. The muscle tissue was gradually lost, but necrotic fibres and fibrotic tissue were massively increased. Furthermore, loss of Pax7 in the satellite cells reduced their proliferative capability due to precocious differentiation.

Table 1.1: Strategies used to inactivate Pax7 in different studies

STUDY	STRATEGY
Lepper *et al.* (2009)	Tamoxifen was administered and repeated five times consecutively before the injection of cardiotoxin (CTX); no additional injection during muscle repair.
Gunther *et al.* (2013)	TMX was administered before and sustained during muscle regeneration.
von Maltzahn *et al.* (2013)	Tamoxifen was injected four times and maintained with a tamoxifen diet throughout the whole experiment.

The limitations of Cre lox technology, and specifically the TMX-dependent CreER(T2) recombinase used throughout these experiments, may account for these distinct results. The successful recombination of genes relies on the activity, of the CreER(T2) fusion protein, which is induced by TMX with a half-life of about one

week. Hence, the continued administration of TMX during repair should sustain CreER activity and minimize the number of cells that may escape recombination. In contrast, when TMX is only administered before injury as in the Lepper *et al.* study; 'recombination-escaper' cells are proposed to exist. These cells function as normal satellite cells, and may be selectively expanded to meet the demands for repair, hence hiding the deficiency of the correctly recombined Pax7 null cells.

The turnover period of the target protein is another concern in studies such as these. If the chase period (after TMX-induced recombination) is shorter than the protein turnover time, then the residual level of functional protein would be underestimated. Moreover, TMX-treated $Pax7^{CRE/loxP\text{-}Le}$ mice have been shown to express a truncated mRNA from the recombined Pax7 allele at a high level, and this variant Pax7 mRNA may be translated into a protein that potentially has residual activity. These various observations may explain why later studies that used longer TMX treatment and chase times than Lepper *et al* observed significantly impaired muscle repair. Overall, the consensus in the muscle biology research field is now that Pax7 is essential for the regulation of satellite cells during adult muscle regeneration, and this is consistent with its roles in developmental myogenesis (Lepper et al., 2009; Oustanina et al., 2004; Relaix et al., 2006).

One important area of Pax7 biology that has not yet been discussed here is the post-transcriptional regulation of Pax7 by microRNAs. A number of miRNAs appear to target the Pax7 3'UTR, including two miRNAs defined as myomiRs because they were previously shown to be expressed exclusively in muscle and to have important roles in myogenesis. This thesis examined the roles of miRNAs in Wnt/β-catenin-mediated regulation of Pax7, and these studies are presented in Chapter 4. The prior literature on the regulation of Pax7 by myomiRs and other miRNAs is reviewed in

the introduction of Chapter 4.

1.1.5 MRFs

Specification of the skeletal myogenic lineage and the process of muscle differentiation is controlled by MRFs. Exclusively expressed in skeletal muscle, MRFs comprise four transcription factors Myf5, MyoD, myogenin and MRF4 (also known as Myf6) as previously defined in section 1.1.3.

All of the MRFs belong to the family of bHLH transcriptional factors, which contains two categories: class I and class II. Class I are ubiquitously expressed E-proteins and class II are tissue-specific expressed proteins that include the muscle expressed MRFs and the neurally-expressed bHLH factors (such as NeuroD). bHLH transcription factors contain an α-helical basic domain which guides the binding of bHLH factors to the consensus sequence CANNTG (E-box) and a HLH domain which allows Class II bHLH factors to homodimerise or to heterodimerise with the ubiquitous E proteins (Massari and Murre, 2000). MRFs normally dimerise with E-proteins. The preferred DNA binding motif for MyoD is CAGCTG/CAGGTG. The specific E-box sequence recognized and the dimers formed by the bHLH factors determine the various functions of different bHLH factors during development (Fairman et al., 1993).

MyoD was the first MRF identified, and was discovered by the screening of a cDNA library. The ability of MyoD to convert non-muscle lineage cells into muscle cells is striking (Davis et al., 1987). Later on, myogenin was identified as the second MRF, which induced myoblasts to become differentiated into myofibres (Wright et al., 1989). The Myf5 and MRF4 genes were identified later based in part on homology to MyoD (Braun et al., 1989; Rhodes and Konieczny, 1989).

Myf5 is induced during asymmetric satellite cell division, and the induction requires

Pax7 to trigger the recruitment of a histone methyltransferase complex to the Myf5 locus; this subsequently modifies the chromatin to stimulate the transcription of Myf5 (McKinnell et al., 2008). Translation of Myf5 is subject to regulation by miRNA-31, which is important for the increase in its protein level during activation of quiescent satellite cells (Crist et al., 2012).

MyoD is regulated by homeobox factors Six1 and Six4 during embryonic myogenesis, and is also activated by coordinated FoxO3 and Pax3/Pax7 in myoblasts (Grifone et al., 2005; Hu et al., 2008). After MyoD is induced, histone acetylation occurs at the *Myogenin* gene promoter, and chromatin remodelling factors Swi/Snf and RNA polymerase II (Pol II) are recruited to activate myogenin expression (Ivana et al., 2005). Meanwhile, Myf5 is repressed, and coincidently myoblasts exit the cell cycle and become committed to differentiation (Conerly et al., 2016; Liu et al., 2012). Activated MyoD and myogenin induce MRF4 and other myogenic genes to drive formation of fused myofibres. When the myofibre is mature, MyoD and myogenin are downregulated, whereas MRF4 is maintained at a high level (Hinterberger et al., 1991).

Genetic deletion of the MRFs in mice has been studied extensively to identify their function in myogenesis and the relationships between each family member. Mice lacking MyoD were viable and fertile with normal skeletal muscle, and Myf5 mRNA was elevated postnatally (Rudnicki et al., 1992). Inactivation of Myf5 led to abnormal rib development so that the mice died perinatally; however, no apparent skeletal muscle abnormalities were found, and MyoD was normally expressed and activated at the correct time (Braun et al., 1994; Braun et al., 1992). These results indicated that MyoD and Myf5 have partial functional redundancy. However, either MyoD or Myf5 is required for myogenesis, as there was no skeletal muscle formed

when both of them were inactivated. The myogenic program in the double mutant mice was profoundly affected, and the mice were immobile and died perinatally (Rudnicki et al., 1993).

Homozygous mutations in *Myog* were lethal perinatally due to a major deficit in skeletal muscle (Hasty et al., 1993; Nabeshima et al., 1993). Although myoblasts were present in the normal number, skeletal muscle was not functional owing to reduced fibre density and decreased muscle mass. MyoD was normally expressed, but myosin heavy chain and actin expression were lacking. These results indicated that myogenin is not required for myogenic lineage specification but is essential for later myogenic differentiation.

The phenotypes of *Mrf4* deleted mice were variable regarding severity of the muscle phenotype (Braun and Arnold, 1995; Patapoutian et al., 1995; Zhang et al., 1995). One of the *Mrf4* null mouse strains had a phenotype similar to the *Myf5* knockout, and the Myf5 mRNA level correlated with the phenotype of MRF4 mutation. Due to the adjacent location of *MRF4* and *Myf5* genes on the same chromosome, it was hypothesised that the phenotype in these *Mrf4* deleted mutated mice might be caused by the cis effects of *Mrf4* on the *Myf5* locus. Interestingly, when the *Mrf4* gene is normally expressed in *Myf5*:*Myod* double mutant mice, skeletal muscle is formed (Kassar-Duchossoy et al., 2004). This study suggests that *Mrf4* could also act upstream of *Myod* to determine myogenic identity apart from promoting differentiation.

These studies collectively suggest that the different MRFs have distinct roles in myogenesis overall, but also have particular functions that overlap to some degree.

1.1.6 MEFs

Myocyte enhancer factor 2 (MEF2) is another critical myogenic transcriptional

factor, and it is named based on its role in regulating/enhancing myogenic differentiation (Gossett et al., 1989). Unlike the myogenic bHLH factors, MEF2 is expressed not only in skeletal muscle but also in cardiac tissue, smooth muscle, lymphocytes, neurons and in bone of vertebrates; moreover homologues are expressed similarly in Drosophila.

MEF2 belongs to the family of MADS (MCM1, agamous, deficiens, serum response factor) box transcription factors, with four isoforms (MEF2A, B, C, D) found in vertebrates (Breitbart et al., 1993; McDermott et al., 1993; Yu et al., 1992). All MEF2 proteins contain three functional domains: MADS domain at the N-terminus for DNA binding, a central domain, and a transactivation domain at C-terminus (Potthoff and Olson, 2007). The MADS domain is highly conserved, while the transactivation domain is divergent. MEF2 binds to A-T rich DNA sequences in the control regions of specific targets, acting combinatorially with other transcriptional factors to regulate their target genes (Gossett et al., 1989).

Drosophila that have a mutation in *Mef2* still form myoblasts, but these myoblasts cannot undergo myogenic differentiation, which indicates that MEF2 is required for myogenesis in this system (Bour et al., 1995; Lilly et al., 1995). Loss of *Mef2c* in mice leads to embryonic lethality due to failure of heart development (Lin et al., 1997); deletions of *Mef2a* and *Mef2d* have little effect on skeletal muscle (Potthoff et al., 2007). MEF2 genes have some functional redundancy and recent work shows that combined deletion of *Mef2a*, *2c*, and *2d*, but not individual deletions, prevents differentiation of mouse satellite cells (Liu et al., 2014).

MEF2 does not exert myogenic function alone; it needs to collaborate with MRFs (i.e. via combinatorial binding to targets) to activate myogenic differentiation-associated genes. In addition, MEF2 and MRFs regulate each other's expression. For

example, during vertebrate skeletal muscle differentiation, MEF2 activity can be induced by bHLH factors, such as myogenin; activated MEF2 binds to a MEF2 site in the promoter of *myog*, thus forming a positive feedback loop to amplify the expression of myogenin (Edmondson et al., 1992; Molkentin and Olson, 1996). Hence, bHLH transcription factors and MEF2 form a regulatory network and cooperate to promote myogenic progression.

MEF2C was also shown to negatively regulate its own expression via activating the histone deacetylase HDAC9 (Haberland et al., 2007). Many other factors are reported to also influence MEF2C activity, such as phosphatases, acetylases, deacetylases and calcium (via a calcium-sensitive co-repressor) (Du et al., 2008; Grégoire et al., 2006; Grégoire et al., 2007; Han et al., 1997; Kato et al., 2000; Wu et al., 2000).

1.2 Wnt signalling in myogenesis

Wnt signalling is a conserved and ancient pathway that is involved in essentially every aspect of embryonic development and in adult tissue homeostasis (Logan and Nusse, 2004). Mutations in the components of Wnt signalling are frequently associated with birth defects, reflecting their important roles in cellular processes required for developmental morphogenesis including cell proliferation, differentiation, migration and adhesion. Dysregulation of Wnt pathways is also associated with cancer, for example in the majority of colorectal cancers, β-catenin is accumulated due to mutation of Wnt pathway genes adenomatosis polyposis coli (APC) or Axin (Bienz and Clevers, 2000). Moreover, Wnt is increasingly linked to degenerative diseases (Moon et al., 2002; Peifer and Polakis, 2000). These observations suggest that Wnt pathways control similar fundamental cell behaviors in adult tissues as they do during development (Clevers, 2006).

The name Wnt derives from the fusion of the gene names *wingless* (*Drosophlia*) and *int-1* (vertebrate). The *Wnt* genes encode a family of secreted glycoproteins that contain 19 members in mammals. All Wnts contain a signal sequence, conserved highly charged amino acids, and multiple glycosylation sites. Although Wnts have similar sequences, their functions are distinct, this is in part because the proteins are subject to different modifications, thereby altering their ability to interact with different receptors and activate diverse signalling pathways (Kühl et al., 2000; Nusse et al., 2008).

Wnt signalling can be divided into two categories according to whether β-catenin is the main transcriptional effector of the signal: β-catenin dependent canonical Wnt signalling, and β-catenin independent non-canonical Wnt signalling. Canonical Wnts (those that signal via the canonical β-catenin pathway) include Wnt1, Wnt2, Wnt2b, Wnt3, Wnt3a, Wnt7b, Wnt8, Wnt8b and Wnt10a whereas non-canonical Wnts include Wnt5a, Wnt5b, Wnt6, Wnt11 and others. This project is focused on canonical Wnt signalling; hence although some non-canonical Wnts also have important roles in muscle, their mechanisms of action will not be discussed here.

1.2.1 Mechanisms of Canonical Wnt signalling

Canonical Wnt signalling is relatively well studied and thought to be controlled mainly by the regulation of β-catenin stability. This pathway is described below. When the Wnt protein ligand is absent, canonical Wnt signalling is off, as cytoplasmic β-catenin is degraded by the destruction complex (Figure 1.4, left). The destruction complex is composed of the scaffold protein Axin, glycogen synthase kinase 3 (GSK3), tumour suppressor adenomatosis polyposis coli (APC), casein kinase 1α (CK1α) and protein phosphatase 2A (PP2A) (Gordon and Nusse, 2006; He et al., 2004). β-catenin is phosphorylated by CK1α and GSK3, and subsequently

recognised by a subunit of the E3 ubiquitin ligase beta-transducin repeats-containing protein (β-TrCP), which leads to its ubiquitin-dependent degradation in the proteasome (He et al., 2004). The continuous destruction of cytoplasmic β-catenin prevents its accumulation in the nucleus where Wnt-responsive genes are silenced by the combination of T-cell factor/lymphoid enhancer factor (TCF/LEF) and Groucho/transducin-like Enhancer of split (Gro/TLE) family repressor proteins.

Binding of canonical Wnt ligands (e.g.Wnt3a and Wnt1) to the receptor complex on the membrane activates the signalling pathway (Figure 1.4, right). The receptor complex includes the seven-transmembrane protein Frizzled (Fzd) and its partner, low-density lipoprotein receptor-related protein 5 and 6 (LRP5/6). Once the Wnt ligand binds to its receptor, CK1α and GSK3 phosphorylate LRP receptors, which lead to the recruitment of scaffolding protein Dishevelled (Dvl) to the membrane. Dvl is further activated after polymerisation (Metcalfe et al., 2010), and subsequently Axin is recruited to the Fzd/LRP receptors, and the destruction complex is inactivated. Consequently, β-catenin is stabilised, accumulates in the cytoplasm and then translocates into the nucleus where it binds to TCF/LEF factors, thereby displacing the Gro/TLE repressors (Daniels and Weis, 2005b) and recruiting coactivators to initiate the transcription of target genes (Hecht et al., 2000b; Takemaru and Moon, 2000a). Several co-activators interact with β-catenin and may promote different transcriptional programs. To date the coactivators that might be specifically involved in myogenesis have not been well defined. This thesis includes studies of coactivators that may mediate myogenesis and other functions of Wnt/ β-catenin signalling (such as fibrosis as discussed in section 1.2.5). These studies are presented in Chapter 5 and the prior literature on coactivators that are involved in β-catenin activity are reviewed in the introduction to Chapter 5.

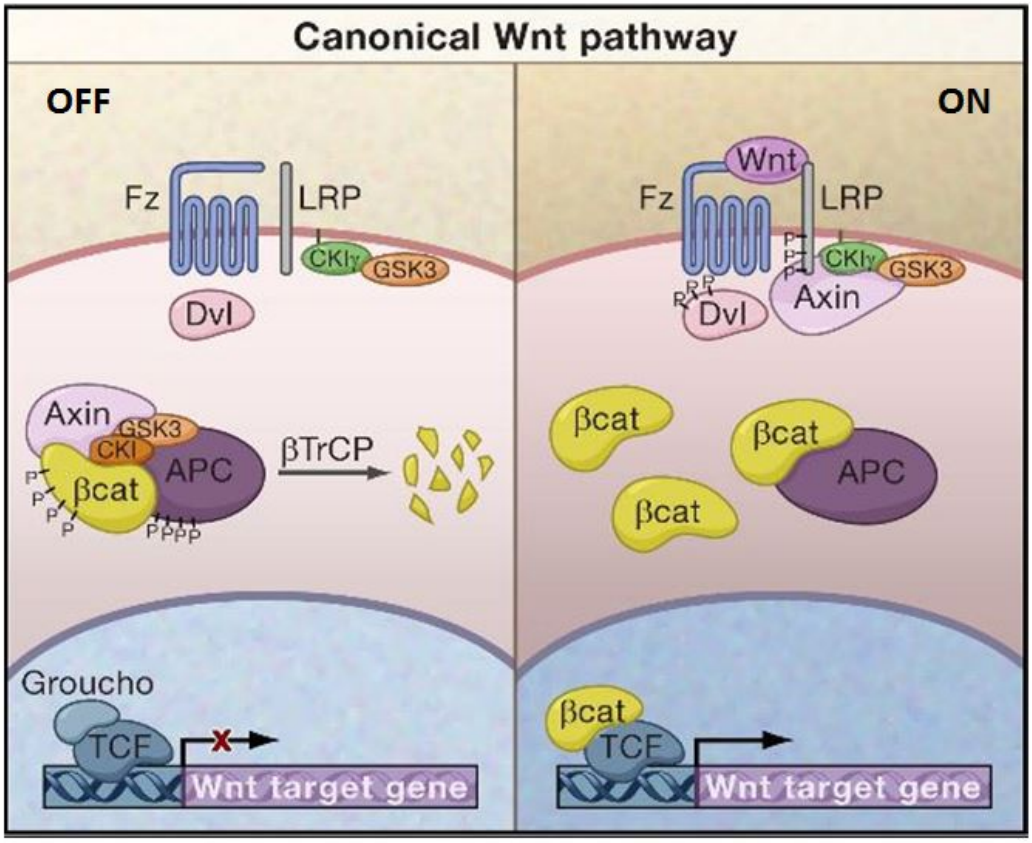

Figure 1.3: Canonical Wnt signalling pathway

In the classic Wnt signalling pathway, the status is off unless Wnt ligand binds to its receptors Fzd and LRP5/6. Upon binding of Wnt ligand, the LRP receptors are phosphorylated by CK1α and GSK3 and then Dvl is recruited and activated. Next, Axin is recruited to the receptor, and the destruction complex is disabled. Consequently, β-catenin is stabilised and able to accumulate in the cytoplasm. β-catenin translocates into the nucleus and binds to TCF/LEF factors, displacing Gro/TLE repressors and recruiting coactivators, thereby activating the target gene. Figure obtained from (Clevers, 2006).

1.2.2 Wnt signalling during muscle development

During embryonic development, Wnt signalling is essential for muscle formation (Cossu and Borello, 1999). In the early embryo, Wnts are expressed from the neural tube and help maintain Pax3 and Pax7 expression in premyogenic cells in the somites. Wnt signals also induce expression of Myf5 and MyoD in somites and in the dermomyotome. Blocking Wnt signals with a soluble antagonist reduces muscle formation suggesting that it plays a key role in myogenic lineage specification

(Borello et al., 1999). Although Wnts are critical in embryonic myogenesis, because the focus of this study is adult myogenesis, the roles of Wnts and other developmental signals in embryogenesis will not be further expanded on here but are reviewed in (von Maltzahn et al., 2012).

1.2.3 Wnt signalling in the adult satellite cell niche

In their niche, satellite cells directly interact with the myofibre and basal lamina. Other cell types close to the niche also contribute to the regulation of satellite cells via paracrine signalling, and these cells include endothelial cells (Christov et al., 2007), fibro/adipogenic progenitors (Joe et al., 2010) and anti-inflammatory macrophages, which emerge during muscle repair (Arnold et al., 2007). Extracellular signalling cues are secreted by the above cell types for the regulation of satellite cell fate and control of myogenesis. The secretion of extracellular signalling molecules is triggered by the niche due to environmental factor changes. Among these multiple signalling cues, Wnt signalling plays a crucial role in the regulation of myogenic cells.

During adult myogenesis, myogenic cell differentiation and satellite cell self-renewal are precisely regulated and balanced to ensure the replenishment of the satellite cell pool and maintain their capability for repair. Wnt signalling is essential for this fine tuned regulation during muscle regeneration; in general, non-canonical Wnt modulates muscle stem cell self-renewal and muscle growth, while canonical Wnt signalling appears to regulate adult myogenic differentiation as discussed in more detail below.

Non-canonical Wnt7a has been implicated in the regulation of satellite cell proliferation post muscle injury (Le Grand et al., 2009). During regeneration, Wnt7a binds to the Fzd7 receptor, and induces satellite cell division symmetrically via

planar cell polarity (PCP) pathway. Wnt7a overexpression in the skeletal muscle significantly increased the number of satellite cells and improved muscle repair (Le Grand et al., 2009).

Several studies have suggested that various canonical Wnts and the central effector β-catenin are important for adult myogenesis. Following acute injury, β-catenin was highly induced in satellite cells in the regenerating tibialis anterior (TA) muscle, which indicated that satellite cells respond to canonical Wnt signalling during muscle repair (Polesskaya et al., 2003). A study in cell culture (using the C2 immortal myoblast line and primary human myoblasts) showed that canonical Wnt1 cooperated with insulin to induce MyoD and myogenin, and also increased the size and fusion of myotubes during the late stage of differentiation (Rochat et al., 2004). *In vivo*, the application of Wnt3a at an early stage of muscle regeneration led to the premature differentiation of myogenic progenitors, which further proved the strong stimulatory effect of canonical Wnt signalling on myogenic differentiation (von Maltzahn et al., 2012). Similarly, canonical Wnt agonist R-spondin, which increases the strength of Wnt signalling by increasing surface levels of the LRP6 coreceptor, has been reported to promote skeletal myogenesis (Han et al., 2011). Conversely, injection of the Wnt inhibitor sFRP3 during muscle during repair led to the reduction in number and a decrease in size of newly formed myotubes (Brack et al., 2008a).

Importantly, ectopic application of Wnt ligands/agonists *in vivo* not only induces precocious differentiation of myogenic cells, but also results in depletion of the satellite cell/myoblast reservoir and is hence deleterious to overall regeneration efficiency. In normal regeneration, canonical Wnt signalling is carefully balanced with Notch signalling, which promotes muscle stem cell self-renewal and the proliferative expansion phase of the myogenic progression (Brack et al., 2008a). The

suppression of proliferation and onset of differentiation is due to a temporal switch from Notch to Wnt signalling via the regulation of common mediator GSK3β. Inhibition of Wnt repressor GSK3β with LiCl, which leads to β-catenin accumulation, was shown to be sufficient to stimulate myogenic differentiation (van der Velden et al., 2006). Altogether, these studies demonstrate that canonical Wnt signalling is important for the control of adult myogenesis, but that its activity must be tightly controlled for optimal regeneration efficiency.

1.2.4 β-catenin may have multiple functions in muscle stem cells

As the key mediator of canonical Wnt signalling, β-catenin exerts multiple functions at different subcellular locations. At the plasma membrane junctions, β-catenin stabilises cadherins through the interaction with α-catenin, which dynamically interacts with actin cytoskeleton; in the cytoplasm, the level of β-catenin is regulated by the destruction complex; in the nucleus, β-catenin interacts with multiple coactivators and regulates target gene transcription.

β-catenin is evolutionary conserved and belongs to the family of the armadillo (ARM) repeat proteins, with the prototypical armadillo protein being identifed in *Drosphila*. Encoded by *CTNNB1*, the human β-catenin protein has 781 amino acid residues and contains three domains: the N-terminal domain, the armadillo repeats and the C-terminal domain (Xu and Kimelman, 2007). The N-terminal domain is mainly responsible for the binding of β-TrCP, which leads to its ubiquitin-dependent degradation; the curved ARM provides binding sites for various ligands; the C-terminal domain is for transactivation when DNA is recruited. The ARM domain is the core component, is well conserved and comprises 12 armadillo repeats with 42 amino acids in each. The 12 repeats form a positively charged groove that can bind to more than 20 different partners. Interestingly, these binding partners often share

overlapping binding sites within the scaffold, which indicates they cannot bind to β-catenin at the same time. The terminal domains are less conserved than the ARM domain, but they are involved in the mediation of protein interactions as well. Many of the proteins which interact with β-catenin are also involved in the regulation of cell adhesion and Wnt signalling.

1.2.4.1 Function of β-catenin as an adhesion molecule

β-catenin mediates cell adhesion through the coordination of cadherin. Cadherins are single transmembrane proteins that are composed of an extracellular domain and a cytoplasmic domain (Gumbiner, 2000). The extracellular domain is rod-like and comprises five repeats that are bound by Ca^{2+} ions. The cytoplasmic tail binds with β-catenin and forms the homophilic cadherin-catenin complex. There are multiple cadherins expressed in different cell types. During myogenesis, N-cadherin is expressed. β-catenin interacts with the distal region of the cytoplasmic domain while a different catenin family protein p120 catenin (also known as delta catenin) binds to the region close to the membrane (Niessen and Gumbiner, 1998; Reynolds et al., 1994). Another catenin family protein called α-catenin dynamically shuttles between β-catenin and the actin cytoskeleton. α-catenin binds to the cadherin-β-catenin complex in the monomeric state, whereas it binds to the actin cytoskeleton in the dimeric state for the regulation of actin assembly (Drees et al., 2005). These complexes all mediate coordination of membrane adhesion with cytoskeletal remodelling events and are likely, although not proven, to be important for the processes of myogenic differentiation including migration, adhesion and cell fusion.

1.2.4.2 Controversial roles of β-catenin in Wnt-regulated muscle stem cell differentiation

Canonical Wnt signalling is considered to be important in the regulation of adult myogenesis. However, the underlying mechanisms by which Wnts modulate the

behaviour of adult satellite cells/myoblasts remain unclear. In particular, a variety of *in vitro* studies have concluded different functions for β-catenin. Moreover there have been recent conflicting reports regarding the requirement for β-catenin in satellite cells *in vivo*.

Researchers have used various different strategies to block β-catenin signalling in muscle stem cells *in vitro*; these inhibition studies resulted in distinct outcomes. Otto *et al*. (Otto et al., 2008) showed that the proliferation of activated satellite cells on the myofibre significantly decreased after treatment with epigallocatechin-3-gallate (EGCG), which leads to the breakdown of β-catenin. Similar to this, Tanaka *et al*. (Tanaka et al., 2011) reported that the proliferation of C2C12 myoblasts was suppressed by KH535, a β-catenin/TCF complex inhibitor. These studies suggested a role for β-catenin in myoblast proliferation. In contrast, Kim *et al*. (Kim et al., 2008b) found that the myotube formation of C2C12 cells was inhibited by shRNA targeting β-catenin, which indicated that the differentiation, rather than the proliferation, of myoblasts is suppressed by β-catenin inhibition. Similarly, a study by Brack *et al*. (Brack et al., 2008a) showed reduced myofibre differentiation when the Wnt attenuator sFRP3 was added to committed myogenic cells in culture. However, another study by Gavard *et al*. (Gavard et al., 2004) showed that β-catenin siRNA led to the increase in myogenin expression in primary myoblasts, which suggested that β-catenin supression increases myogenic differentiation. Thus the role of β-catenin in satellite cells/myoblasts *in vitro* is still not entirely resolved.

Most surprisingly, an *in vivo* study by Murphy *et al*. (Murphy et al., 2014a) suggested that β-catenin is not required cell autonomously for muscle regeneration. Using a conditional β-catenin null mouse model in which β-catenin was deleted using a satellite cell specific (Pax7 locus-driven) TAM-inducible Cre-ERT2 allele,

they found that absence of β-catenin did not affect the proliferation or the differentiation of satellite cells after injury in adult mice. As described further in Chapter 3, this finding is now also controversial, because a subsequent study using similar methodologies did not reproduce the key findings of Murphy *et al.*, and instead found that loss of β-catenin impaired regeneration (Rudolf et al., 2016b).

Overall, it is likely that β-catenin plays dual roles in muscle stem cells, in cell adhesion/cytoskeletal remodelling and in transcriptional signalling. However, whether any of these functions are actually required for satellite cells/myoblasts to undertake muscle regeneration in response to Wnt signals remains somewhat controversial.

1.2.5 Wnt and fibrosis

In addition to the important role of canonical Wnt signalling in myogenesis by modulating the functions of satellite cells and myoblasts, Wnt signalling can also affect other processes in muscle; an important one of which is fibrosis.

Wnt signalling has been reported to be elevated in aged muscle and in patients with myopathies such as Duchenne muscular dystrophy (DMD) (Brack et al., 2007; Liu et al., 2016). Aging is associated with increased fibrotic tissue and impaired muscle regenerative potential, while muscular dystrophies are often accompanied by progressive fibrosis and muscle loss. Excessive Wnt, both systemic and locally produced, is proposed to be one of the factors that may drive fibrotic processes in muscle.

In adult mice, overexpression of Wnt3a by electroporation of CMV-Wnt3a in the tibialis anterior (TA) muscle led to the increase of abnormal matrix deposition, which is one principal characteristic of fibrosis (Le Grand et al., 2009).

Canonical Wnt is reported to be essential for fibroblast activation and necessary for the transforming growth factor beta (TGF-β) signalling-mediated fibrosis (Akhmetshina et al., 2012). TGF-β activates canonical Wnt by the inhibition of the expression of Wnt repressor DKK1 in a p38-dependent manner. Activated Wnt3a decreased fibroblast proliferation, but promoted cell migration and myofibroblast formation and differentiation (Carthy et al., 2011). These effects are explained in part by the enhanced canonical Wnt signalling upregulating TGF-β signalling via SMAD2 phosphorylation (Carthy et al., 2011). Altogether, canonical Wnt and TGF-β signalling markedly contribute to the pathogenesis of fibrotic disease as they enhance each other and amplify the effects through positive circuitries. The precise role of β-catenin in fibrosis is not well defined and in particular the transcriptional complexes that may mediate fibroblast activation, including coactivators involved, is a topic that is addressed further in Chapter 5.

Apart from fibroblast activation, canonical Wnt signalling has been reported induce a myogenic to fibrogenic lineage conversion, In particular, one study showed that Wnt3a protein application resulted in myogenic progenitors being converted to the fibrogenic lineage *in vitro* (Brack et al., 2007). In addition, they found that Wnt3a injection in young mice one day post-muscle injury led to an increase in connective tissue deposition and reduction of regenerative capacity *in vivo* (Brack et al., 2007). Conversely, administration of Wnt antagonist Dickkopf-1 (DKK1) in skeletal muscle reduced fibrosis in aged mice and also in *mdx* mice (Brack et al., 2007; Trensz et al., 2010). However, in these studies, it remains unclear the extent to which the *in vivo* effects of Wnt agonism and antagonism on fibrosis were due to the conversion of myoblasts to fibroblasts, versus the activation of fibroblasts already resident in the muscle.

1.3 CRISPR

1.3.1 Principle of CRISPR technology

CRISPR/Cas9 is a relatively new genome editing technology that has triggered a revolution in laboratories, and its use is rapidly expanding in the fields of biomedical research and therapeutic application. Compared to previous genome editing tools, such as site-directed zinc-finger nucleases (ZFNs) and transcription activator-like effector nucleases (TALENs), CRISPR is much more powerful as it is more efficient and easier to use in a wide array of cell types and organisms. CRISPR has already been widely applied in genome editing to create gene knockout models, imaging and synthetic biology.

CRISPR/Cas9 technology originates from the type II CRISPR-Cas (clustered regularly interspaced short palindromic repeats) adaptive bacterial defense system and utilises short RNAs to guide the endonuclease Cas9 precisely to defined target DNA locations within complex genomes.

The single guide RNA (sgRNA) is the fusion of CRISPR RNA (crRNA) and a trans-activating crRNA (tracrRNA). sgRNA pairs with the target DNA sequence via the 5' region, with the existence of a protospacer adjacent motif (PAM) close to the target loci (Figure 1.5). The 3' part of the sgRNA enables Cas9 (CRISPR-associated protein 9) nuclease to bind to the target DNA sites and cleave it, hence double strand breaks are generated and DNA is subsequently repaired by non-homologous end joining (NHEJ), or replaced by homology-directed repair (HDR) if an appropriate template is available. This leads to deletion, insertion, substitution or replacement at the target DNA site of interest.

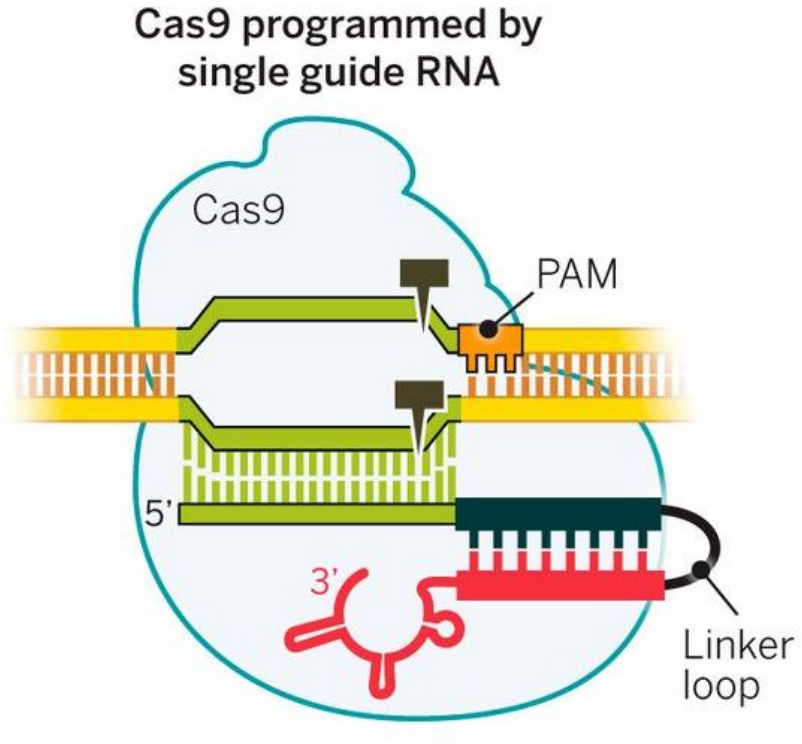

Figure 1.4: Structure of the CRISPR-Cas9 complex

The CRISPR/Cas9 complex is composed of Cas9 protein with guide RNA. The 5' part of the guide RNA is a short sequence of approximately 20 nt, which pairs with the target DNA loci at the presence of the adjacent PAM sequence; the 3' part of the guide RNA binds to the Cas9 protein and produces a double-strand DNA break at the recognised site. Figure obtained from (Doudna and Charpentier, 2014).

1.3.2 Development and application of CRISPR

In 1987, the CRISPR sequence was first described in *E.coli* as short direct repeats separated by short sequences (Ishino et al., 1987). In 2000, CRISPR sequences were found in diverse bacteria and archaea (Mojica et al., 2000). Subsequently, CRISPR sequences were predicted to be involved in DNA damage repair or gene regulation (Guy et al., 2004). This was followed by the presumption that CRISPR-Cas was an adaptive immune system in bacteria, as the repeat sequences were identified as being derived from virus and plasmid (Pourcel et al., 2005). Infection experiments proved this idea and identified the functions of Cas9 domains, tracrRNA and crRNA (CRISPR, 2011; Gasiunas et al., 2012). In 2013, Cong *et al*. (Cong et al., 2013)

developed and utilised the type II CRISPR/Cas9 system for precise genome editing in mammalian cells. In 2014, the crystal structure of Cas9 nuclease was resolved (Nishimasu et al., 2014).

Since 2013, the number of papers about CRISPR modifications, optimisations and applications has exploded. To date, over 4,000 articles and reviews about CRISPR have been published.

More recently, the CRISPR/Cas9 system has been modified for use for gene regulation in mammalian cells in two variants called CRISPR interference and activation (CRISPRi/a). In this system, the catalytic domain of Cas9 is deactivated, leading to the formation of dCas9, which does not cut DNA but can be used to alter transcription at the targeted site (Qi et al., 2013). After fusing with VP64 or KRAB, dCas9 is able to efficiently activate or inhibit the target transcription in eukaryotes (Gilbert et al., 2013). Owing to the specific recognition by dCas9-guide RNA, the off-target activity of CRISPRi/a is very low.

The CRISPR/dCas9 system was further modified for the multicolour labelling of chromosome loci to achieve 4D imaging in living cells (Ma et al., 2015). Cas9 variants from three bacteria were used; they were catalytically inactivated, fused with green, red or blue fluorescent proteins and guided by different sgRNAs to three loci. This CRISPR multicolour labelling technique allows for the imaging of different genomic loci in live cells simultaneously.

The technology of CRISPR/Cas9 is continuously being optimised to improve the specificity and reduce the off-target effects, such as through the use of newer endonucleases such as Cpf1 and Cas9-nickase (Ran et al., 2013; Zetsche et al., 2015).

CRISPR/Cas9 has been used in numerous basic research studies and also for translational applications. For example, CRISPR/Cas9 has been applied to anti-PD-1 therapy in cancer. PD-1 is an immune-suppressor protein that is expressed of the surface of tumour cells and prevents their recognition by the immune system; reducing the PD-1 level by CRISPR/Cas9 appears to activate T cells to target cancer cells (Rupp et al., 2017; Su et al., 2017). This CRISPR/Cas9 suppression approach has entered phase I clinical trials.

Gene correction by CRISPR/Cas9 has also been explored for treating disease due to genetic defects. In muscle, CRISPR/Cas9 has been combined with adeno-associated viral (AAV) delivery to treat muscular dystrophy in a in a mouse model of Duchenne muscular dystrophy (DMD) (Bengtsson et al., 2017). DMD is caused by the mutation of the *dystrophin* gene, which encodes a structural protein in myofibers. A muscle-restricted specific Cas9 cassette was designed and delivered by AAV vector in muscle; consequently the mutated *dystrophin* gene was corrected, the dystrophin protein was successfully expressed, and muscle function was improved. Whether such gene therapy applications will have clinical utility remains to be known. In the studies described in this thesis, CRISPR is used experimentally as a means to create a cell autonomous null β-catenin model in primary myoblasts as is described further in the Aims section below.

1.4 Aims

The overarching goal of this project is to understand how Wnt signalling controls the behaviour of myoblasts; in particular, how Wnt effects are mediated at a molecular and cellular level by β-catenin and other effectors. The detailed specific aims of the project and their rationale are as described below:

Aim 1: To create β-catenin null adult primary myoblasts *in vitro* using CRISPR and

to use these null myoblasts to define the requirement for β-catenin in adult myoblast differentiation *in vitro.* These studies allow us to assess the cell autonomous function of β-catenin using a method that is not subject to the limitations/confounds of homologous recombination *in vivo*.

Aim 2: To define the mechanism of action of β-catenin in myoblast differentiation *in vitro,* using transcriptomic and epigenomic tools including RNA-seq profiling, histone ChIP-seq profiling and MyoD ChIP-seq profiling. Together these methods allow us to identify the transcriptional program induced by Wnt/β-catenin signalling and identify the DNA motifs associated with this gene activation, as well as to explore the relationship between β-catenin and MyoD in gene regulation.

Aim 3: To generate mutant forms of β-catenin that cannot interact with various partners such as TCF/LEF proteins in the nucleus, or alpha-catenin at membrane junctions, and to introduce these mutant proteins into β-catenin null myoblasts. This allows us to assess the relative roles of β-catenin/TCF transcriptional complexes, and of β-catenin-alpha-catenin membrane complexes in myogenesis.

Aim 4: To explore the role of Wnt-regulated miRNAs including the myomiRs miRNA-206 and miRNA-133b in Pax7 regulation downstream of Wnt/β-catenin signalling. This allows us to, for the first time, identify a direct pathway from Wnt to the post-transcriptional downregulation of Pax7, which is required for myogenesis.

Aim 5: To define the mechanisms by which Wnt/β-catenin signalling promotes fibrosis, and in particular to determine whether different β-catenin-coactivator complexes are involved in the activation of pro-myogenic versus pro-fibrotic gene expression programs. This study explores the possibility that the pro-fibrotic effects of Wnt/β-catenin can be selectively pharmacologically inhibited *in vivo* without

disrupting myogenesis.

Aims 1-3 are completed in Chapter 3, Aim 4 is completed in Chapter 4, and Aim 5 is completed in Chapter 5.

CHAPTER 2: Materials and Methods

2.1 Materials

2.1.1 Mice

The Wnt-reporter TOP-EGFP mice were obtained from the RIKEN BioResource Center (RBRC02229) and were genotyped for the presence of GFP. All mice were housed in the Animal Facility in the School of Medicine, Flinders University, and all maintenance and breeding of mice was performed by trained technical staff within the facility.

2.1.2 Mammalian cell lines and bacterial strains

Primary myoblasts were isolated from TA muscle of TP1-Venus mice from the RIKEN BioResource Centre (strain RBRC02229). HEK293T cells and C3H 10T1/2 (Clone 8) cells were obtained from the American Type Culture Collection (ATCC, Manassas, VA, USA). The DH5α *Escherichia coli (E. coli)* strain was originally purchased from the ATCC.

2.1.3 Vectors

Vectors used in this study are listed in Table 2.1.

Table 2.1: Vectors used in this thesis

Name	Source	Usage
LentiCRISPR V2	Addgene	Lentivector backbone
pCMV-dvrp8.2	Addgene	2nd generation lentiviral packaging plasmid
pRSV-Rev	Addgene	3rd generation lentiviral packaging plasmid
pMD2.G (VSV-G)	Addgene	VSV-G envelope expressing plasmid
pMSCV	Addgene	Retroviral vector backbone
pGL3-basic	Promega	Luciferase assay
pGL3-promoter	Promega	Luciferase assay
pRL-Null	Promega	Luciferase assay
pMM043-GFP	Assoc. Prof. Michael Michael (Flinders University, South Australia)	Transfection

pcDNA3.0	Addgene	Transfection

2.1.4 Buffers

The following buffer formulae were used throughout this project.

Coomassie Blue Stain: 10% (v/v) acetic acid; 0.006% (w/v) Coomassie Blue dye in MQ H_2O.

ChIP buffers:

Lysis buffer 1: 1 % Nonidet P40; 15 mM Tris pH 8.0; 0.5 mM EGTA; 15 mM NaCl; 60 mM KCl; 300 mM Sucrose; 0.5 mM B-mercatoptoethanol.

Lysis buffer 2: 1 % SDS; 10 mM EDTA; 50 mM Tris pH 8.0.

Dilution buffer: 0.01% SDS; 1% Triton X-100; 1.2 mM EDTA; 16.7 mM Tris pH 8.0; 150 mM NaCl.

High Salt Wash Buffer: 0.1% SDS; 1% Triton X-100; 1 mM EDTA; 20 mM TrisCl pH 8.0; 500 mM NaCl.

LiCl Buffer: 1% NP-40; 1% deoxycholic acid sodium salt; 1 mM EDTA; 10 mM Tris pH 8.0; 250 mM LiCl.

TE Buffer: 1 mM EDTA; 10 mM Tris pH 8.0.

Elution Buffer: 20 mM Tris pH 8.0; 5 mM EDTA; 50 mM NaCl; 1% SDS.

6 × DNA loading dye: 0.25% (w/v) bromophenol blue; 0.25% (w/v) xylene cyanol FF; 30% (v/v) glycerol.

GTS running buffer: 25 mM Tris; 192 mM glycine; 0.1% SDS.

Isopropanol Fixing Solution: 10% (v/v) acetic acid; 25% (v/v) isopropanol in MQ H_2O.

LB medium: 10 g of tryptone; 5 g of yeast extract; 10 g of NaCl in 1 L deionised water, pH 7.0, autoclaved.

1 × Phosphate buffered saline (PBS): 137 mM NaCl; 2.7 mM KCl; 10 mM Na_2HPO_4; 2 mM KH_2PO_4, pH 7.4.

RIPA buffer: 50 mM Tris; 150 mM NaCl; 0.1% SDS; 0.5% sodium deoxycholate; 1% NP-40.

1 × SDS-PAGE running buffer: 25 mM Tris pH 8.3; 192 mM glycine; 0.1% SDS.

1 × SDS-PAGE transfer buffer: 25 mM Tris pH 8.3; 192 mM glycine; 20% methanol

4 × SDS protein loading dye: 40% glycerol; 240 mM Tris/HCl pH 6.8; 8% SDS; 0.04% bromophenol blue; 5% beta-mercaptoethanol (added fresh).

1 × Sodium borate (SB) buffer: 0.8 g of NaOH; 2.35 g of boric acid in 1 L deionized water.

Staining buffer: PBS containing 1% BSA and 0.01% sodium azide.

1 × TBE: 89 mM Tris; 89 mM boric acid; 2 mM EDTA; pH 8.3.

Transfer buffer: 25 mM Tris; 190 mM glycine; 20% methanol.

1 × Tris-acetate EDTA (TAE) electrophoresis buffer: 40 mM Tris pH 8; 20 mM acetic acid; 1 mM EDTA.

0.5 × Tris-borate EDTA (TBE) electrophoresis buffer: 40 mM Tris pH 8.3; 45 mM boric acid; 1 mM EDTA.

Tris-buffered saline (TBS): 50 mM Tris pH 7.4; 150 mM NaCl.

2.1.5 Reagents

Reagents used in this thesis are listed in Table 2.2. All chemicals used were of analytical grade.

Table 2.2: Reagents used in this thesis

Reagent	Supplier
Bacterial Culture	
Agar	Amresco, Solon, OH, USA
Ampicillin	Aspen Pharmacare, KwaZulu-Natal, South Africa
Kanamycin	Sigma, St Louis, MO, USA
Luria Broth (LB) EZMix	Amresco
Buffer Chemicals	
Acetic acid	Ajax Finechem, Seven Hills, NSW, Australia
Bovine serum albumin (BSA) solution (100 mg/ml)	New England Biolabs (NEB), Beverley, MA, USA
$CaCl_2$.2H2O	Ajax Finechem
Dimethyl sulfoxide (DMSO)	Merck, Darmstadt, Germany
DMSO for molecular biology	Sigma-Aldrich, Castle Hill, NSW Australia
Ethylenediaminetetra-acetic acid, di-sodium salt (EDTA)	Biochemicals, Gymea, NSW, Australia
Glycerol	Amresco
Glycine	Amresco
HCl	VWR International, Radnor, PA, USA
Isopropanol	Chem-Supply, Gillman, SA, Australia
KCl	Amresco
KH_2PO_4	Amresco
LiCl	Sigma
Methanol	RCI Labscan, Bangkok, Thailand

$MgCl_2.6H_2O$	Amresco
Na_2HPO_4	Ajax Finechem
NaCl	Biochemicals
Nonidet P-40	Fluka Analytical (Honeywell), Morris Plains, NJ, USA
Polyethylglycol (PEG)	Sigma
Proteinase K	NEB
Sodium dodecyl sulphate (SDS)	A.G. Scientific, San Diego, CA, USA
Sucrose	Sigma
Tris[hydroxymethyl]aminomethane (Tris)	Astral Scientific, Gymea, NSW, Australia
Chromatin Immunoprecipitation (ChIP)	
ChIP grade Protein G magnetic beads	Cell Signaling Technology, Danvers, MA, USA
EGTA	Sigma
Formaldehyde	Sigma
DNA Detection, Purification and Modification	
100 bp DNA ladder	NEB
1 Kb DNA ladder	NEB
30% Acrylamide/Bis solution 19:1	Bio-Rad, Hercules, CA, USA
Agarose	Biochemicals
Ethidium bromide	Amresco
GelRed	Biotium Inc., Hayward, CA, USA
Lambda DNA-HindIII Digest	NEB
QIAGEN Plasmid Midiprep kit	Qiagen, Clifton Hill, VIC, Australia
QIAprep Spin Miniprep kit	Qiagen
QIAquick Gel Extraction kit	Qiagen
QIAquick PCR Purification kit	Qiagen
Quick Ligation kit	NEB
Restriction enzymes	NEB

Immunostaining and Cell Labelling	
Bovine serum albumin (BSA)	Sigma
Triton X-100	Sigma
Vybrant Dil cell-labelling solution	Invitrogen (Life Technologies), Carlsbad, CA, USA
Inhibitors of β-catenin Coactivators	
ICG-001	ApexBio, Houston, TX, USA (A8217)
IQ-1	ApexBio (B7700)
Mammalian Tissue Culture	
Dulbecco's modified Eagle's medium (DMEM)	Invitrogen (Life Technologies)
Foetal calf serum	Bovogen, Keilor East, VIC, Australia
Ham's F-10 Nutrient Mix	Thermo Scientific, Scoresby, VIC, Australia
MEM non-essential amino acids	Invitrogen (Life Technologies)
Murine FGF-basic	Peprotech, Rocky Hill, NJ, USA
Penicillin Streptomycin (Pen Strep)	Life Technologies
Puromycin	Astral Scientific
Tissue culture flasks and plates	Nunc, Roskilde, Denmark
Trypan blue	Sigma Chemical Co, St Louis, MO, USA
Trypsin-EDTA	Invitrogen (Life Technologies)
Polymerase Chain Reaction (PCR)	
Deoxynucleotide-triphosphate mix (dNTP)	NEB
GoTaq qPCR master mix	Promega, Madison, WI, USA
Oligonucleotides	Geneworks, Thebarton, SA, Australia or Integrated DNA Technologies, Coralville, IA, USA
Phire HotStart DNA Polymerase	Thermo Scientific
Phusion High-Fidelity DNA Polymerase	Thermo Scientific
RNA Purification and cDNA Synthesis	
Amplification grade DNaseI	Life Technologies
Chloroform	VWR

NxGen M-MuLV Reverse Transcriptase	Lucigen, Middleton, WI, USA
NxGen RNase Inhibitor	Lucigen
TRIzol	Life Technologies
Transfection and Reporter Gene Assays	
Dual-Luciferase Reporter Assay System	Promega
Lipofectamine® 2000	Invitrogen (Life Technologies)
Lipofectamine® LTX with Plus™ Reagent	Invitrogen (Life Technologies)
Western Blot	
30% Acrylamide/Bis solution (29:1)	BioRad
Ammonium persulphate (APS)	Amresco
BioRad Protein Assay Reagent	BioRad
Complete Proteinase Inhibitor tablets	Roche Diagnostics, Mannheim, Germany
Coomassie G-250	Sigma
N,N,N',N'-Tetramethyl-1-,2-diaminomethane (Temed)	Sigma Chemical Co
Protein Standard I	Bruker Daltonics, Billerica, MA, USA
Skim milk powder	Fonterra Brands, NZ
SuperSignal West Pico chemiluminescent (ECL) HRP substrate	Thermo Scientific
Trans-blot nitrocellulose membrane	BioRad
Tween-20	Biochemicals
Primary Myoblast Isolation	
Basic fibroblast growth factor (murine)	Cell Signaling Technology
Collagen	Gibco (Life Technologies), Waltham, MA, USA
Collagenase	Gibco (Life Technologies)
Dispase	Gibco (Life Technologies)
Primary Antibodies	
CD34 PE rat-anti-mouse	BD Pharmingen, Franklin Lakes, NJ, USA (551387)
CD45 APC rat-anti-mouse	BD Pharmingen (559864)

DAPI (4’,6-diamidino-2-phenylindole)	Sigma
Gapdh	Sigma (G9545)
Histone H3K acetylation	Millipore, Burlington, MA, USA (06-599)
Histone H3K4 tri-methylation	Millipore (07-473)
Histone H3K27 tri-methylation	Millipore (07-449)
MyHC (MF20)	DSHB, Iowa City, IA, USA
MyoD	Santa Cruz Biotechnology, Santa Cruz, CA, USA (M-318)
Myog (F5D)	DSHB
Normal rabbit IgG	Cell Signaling Technology (2779S)
Pax7	Santa Cruz (sc-7748)
ScaI FITC rat-anti-mouse	BD Pharmingen (557405)
β-actin	Invitrogen (Life Technologies)
β-catenin	Santa Cruz (sc-7199)
β-catenin	Cell Signaling Technology (9562L)
Secondary Antibodies	
Anti-goat HRP	Sigma (A5420)
Anti-mouse HRP	Abcam, Cambridge, UK (6820)
Anti-rabbit HRP	Jackson ImmunoResearch, West Grove, PA, USA
Donkey-anti-goat Alexa 546	Jackson ImmunoResearch (7191)
Donkey-anti-mouse Cy3	Jackson ImmunoResearch (715-165-150)
Donkey-anti-mouse Cy5	Jackson ImmunoResearch (26558)
DyLight 488 Horse-anti-mouse	Vector Laboratories, Burlingame, CA, USA (DI-2488)
DyLight 594 Goat-anti-rabbit	Vector Laboratories (DI-1594)
IRDye® 680LT Donkey anti-Mouse IgG (H + L)	LI-COR, Lincoln, NE, USA (P/N 925-68022)
IRDye® 800CW Donkey anti-Rabbit IgG (H + L)	LI-COR (P/N 925-32213)

2.1.6 Primers

All primers were purchased desalt purified and listed in the 5' to 3' direction.

Primers used in this thesis are listed below in Table 2.3 to Table 2.8.

Table 2.3: CRISPR primers

β-catenin Exon5 CRISPR F:	CACCGCATCTGAGGGGAGCGCATGA
β-catenin Exon5 CRISPR R:	AAACTCATGCGCTCCCCTCAGATG
β-catenin exon5 CRISPR screening F:	AGGTGGTAGTTAATAAAGCTGCTG
β-catenin exon5 CRISPR screening R:	CAGCAAGCCCTCGCGGTGG

Table 2.4: Site-Directed Mutagenesis primers

β-catenin K312E SDM F:	GAGAGCGACCTCATCATTCTGGCCAGTGG
β-catenin K312E SDM R:	ATGAGGTCGCTCTCTTGATTGCCATAAGC
β-catenin K435E SDM F:	CAAAAACGACATGATGGTGTGCCAAGTGG
β-catenin K435E SDM R:	CATCATGTCGTTTTTGTAATTATTGCAAGTGAGG
β-catenin T120V122 SDM F:	CATCCCGCTAATGCCCAGCGCTTGGCTGAACC
β-catenin T120V122 SDM R:	GCGCTGGGCATTAGCGGGATGAGCAGCGTCAAAC
Pax7 miR-133b SDM F:	CGCTTGTCAAGATCATAATGATCTGCCCG
Pax7 miR-133b SDM R:	TATGATCTTGACAAGCGTTGGAATGTTGCTC

Table 2.5: Mmu-miRNA mimics and inhibitors

Mmu-miR-206 mimics:	UGGAAUGUAAGGAAGUGUGUGG
	ACACACUUCCUUACAUUCCAUU
Mmu-miR-133b mimics:	UUUGGUCCCCUUCAACCAGCUA
	GCUGGUUGAAGGGGACCAAAUU
Mmu-miR-206 inhibitors:	CCACACACUUCCUUACAUUCCA
Mmu-miR-133b inhibitors:	UAGCUGGUUGAAGGGGACCAAA

Table 2.6: qPCR primers

pri-miR1-2 F:	GCTAATCTCCGCACTGGATC
pri-miR1-2 R:	TGGAAGTCATCCTCCTGGAAAG
pri-miR133a-1 F:	GAACAGCAGTGTAGGACATATGC
pri-miR133a-1 R:	CCATGTGTAATCAATGCATAGCTAC
pri-miR133b F:	CTTTCAAGCTCTGTGAGAGGTTAG
pri-miR133b R:	CTTCCTTCTTGGGAACATAAGGC
pri-miR206 F:	CTGCCTGTTAGGCCAAGATGG
pri-miR206 R:	CTGAGAGTAGATGTGAAGGATGTTGG
RPS26 F:	AGGTGCAGAAGGCTGAGG
RPS26 R:	GGTTCTCCCGAGTGATGAAG
Axin2 F:	GAGAGTGAGCGGCAGAGC
Axin2 R:	CGGCTGACTCGTTCTCCT
MyoD F:	CCGCCTGAGCAAAGTGAATG
MyoD R:	GCGGTCCAGGTGCGTAGAA
Myogenin F:	CCTTGCTCAGCTCCCTCA
Myogenin R:	TGGGAGTTGCATTCACTGG
Fst F:	AAGCATTCTGGATCTTGCAACT
Fst R:	GATAGGAAAGCTGTAGTCCTGGTC
Mef2c F:	GGTGCTGACGGGAACAAC
Mef2c R:	CAGTTTTCAATGCTTTTGTTGG
Pax7 F:	ACCACTTGGCTACAGTGTGGA
Pax7 R:	AGTAGGCTTGTCCCGTTTCC
Col1a1 F:	CTGCTGGTGAGAGAGGTGAAC
Col1a1 R:	ACCAAGGTCTCCAGGAACAC
Col1a2 F:	CTGGTGCACAGGGTGTGA
Col1a2 R:	CTCCTGCTTGACCTGGAGTT
Ctgf F:	TGACCTGGAGGAAAACATTAAGA
Ctgf R:	AGCCCTGTATGTCTTCACACTG

Table 2.7: ChIP-PCR primers

rDNA1 F:	GCGGCCTGCGCCGCGCGTGG
rDNA1 R:	CCCGCGATTTCGCCAGCCGT
Axin2 T3 F:	TACCTCCCTTCCAGGACC
Axin2 T3 R:	CCTCCGGGCGCTTCCAAC
Myogenin promoter F:	GAATCACATGTAATCCACTGGA
Myogenin promoter R:	ACGCCAACTGCTGGGTGCCA
Fst promoter F:	AGAAGACAGTTGTTTGGGTGC
Fst promoter R:	GCGGCGGCGAGGTCACC
Tmem8c promoter F:	AGCAGCCCTGACCGCAG
Tmem8c promoter R:	AGAATATATTAGAGGCAAGTGCATAC

Table 2.8: Mature miRNA qPCR primers

mmu-miR-1 F:	CGCAGTGGAATGTAAAGAAGTAT
mmu-miR-1 R:	GCAGGTCCAGTTTTTTTTTTTTTTATAC
mmu-miR-133a F:	CAGTTTGGTCCCCTTCAACC

mmu-miR-133a R:	CAGGTCCAGTTTTTTTTTTTTTTA
mmu-miR-133b F:	CAGTTTGGTCCCCTTCAACC
mmu-miR-133b R:	CAGGTCCAGTTTTTTTTTTTTTTC
Universal:	CAGGTCCAGTTTTTTTTTTTTTT
SnoRNA234 F:	CAGCTTTTGGAACTGAATCTAAGTGAT
SnoRNA234 R:	GTCCAGTTTTTTTTTTTTTTTCTCAGTGG
mmu-miR-let-7b F:	TGAGGTAGTAGGTTGTGTGG
mmu-miR-let-7b R:	CAGGTCCAGTTTTTTTTTTTTTTTAAC
mmu-miR-495 F:	GCAGAAACAAACATGGTGCACTT
mmu-miR-495 R:	CAGGTCCAGTTTTTTTTTTTTTTTTTAAG
mmu-miR-1192 F:	GCAGAAACAAACAAACAGACC
mmu-miR-1192 R:	CAGGTCCAGTTTTTTTTTTTTTTTAATT
mmu-miR 23a/b-3p F:	GCAGATCACATTGCCAGGGA
mmu-miR 23b-3p R:	CAGGTCCAGTTTTTTTTTTTTTTTGGTA
mmu-miR 23a-3p R:	CAGGTCCAGTTTTTTTTTTTTTTTGGAA
mmu-miR-431 F:	GCAGTGTCTTGCAGGCCGTCA
mmu-miR-431 R:	CAGGTCCAGTTTTTTTTTTTTTTTTGC
mmu-miR-183 F:	GCAGTATGGCACTGGTAGAATTC
mmu-miR-183 R:	CAGGTCCAGTTTTTTTTTTTTTTTTAGT
mmu-miR-22-3p F:	GCAGAAGCTGCCAGTTGAAGAAC
mmu-miR-22-3p R:	CAGGTCCAGTTTTTTTTTTTTTTTTACA
mmu-miR-335-5p F:	GCAGTCAAGAGCAATAACGAAAAAT
mmu-miR-335-5p R:	CAGGTCCAGTTTTTTTTTTTTTTTTAC
mmu-miR-150-5p F:	GCAGTCTCCCAACCCTTGTACC
mmu-miR-150-5p R:	CAGGTCCAGTTTTTTTTTTTTTTTTCAC
mmu-miR-410 F:	GCAGAATATAACACAGATGGCC
mmu-miR-410 R:	CAGGTCCAGTTTTTTTTTTTTTTTTACA
mmu-miR-16 F:	GCAGTAGCAGCACGTAAATATTG
mmu-miR-16 R:	CAGGTCCAGTTTTTTTTTTTTTTTTCGC
mmu-miR-15a F:	GCAGTAGCAGCACATAATGGTTT
mmu-miR-15a R:	CAGGTCCAGTTTTTTTTTTTTTTTTCAC
mmu-miR-143 F:	GCAGTGAGATGAAGCACTGTAG
mmu-miR-143 R:	CAGGTCCAGTTTTTTTTTTTTTTTTGAG

2.2 Methods

2.2.1 Preparation of plasmid DNA

Routine preparation of plasmid DNA was performed using the QIAprep Spin Plasmid Miniprep Kit (Qiagen), according to the manufacturer's instructions. DNA was eluted using 40 µl H_2O and stored at $-20^{\circ}C$.

2.2.2 Large-scale plasmid purification

When larger amounts of plasmid DNA were required, the QIAGEN Plasmid Midi

Kit was used, according to the manufacturer's instructions. Plasmid DNA was eluted with 400 µl TE buffer and stored at −20°C.

2.2.3 Cell genomic DNA isolation

Cells were harvested by trypsinisation, and the pellet collected by centrifugation at 5,000 × g for 5 minutes. Media was removed, and cell pellet was resuspended in 300 µl TNES buffer with 17 µl PNK. This digestion was incubated at 55°C for 1 hour. Eighty four microlitres of 6M NaCl was added and the tube was shaken vigorously by hand for 15 seconds. Samples were centrifuged at 13,000 × g for 5 minutes to precipitate protein and other debris. The supernatant was removed and transferred to fresh tubes, and genomic DNA was precipitated by addition of 300 µl cold 95% ethanol. DNA was spun down at 13,000 × g for 10 minutes. The supernatant was removed, and the pellet was washed with 70% ethanol and spun again for 10 minutes, then left to air dry for 20-30 minutes. The DNA pellet was resuspended in 40 µl EB buffer.

2.2.4 Analysis of DNA size, purity and concentration

DNA samples were assessed for size, purity and concentration using agarose gel electrophoresis. Agarose was mixed with 1 × TAE or 1 × TBE, and melted in a microwave oven and cast into mini gels ranging from 1% – 2.5% agarose. Before loading into the wells, DNA samples were mixed with 6 × DNA loading dye in 1 × TAE or 1 × TBE buffer. Gels were visualised using a UV transilluminator coupled to a CCD camera (ChemiDoc, BioRad). Comparison of DNA bands with DNA molecular markers (New England Biolabs) allowed estimation of DNA size and concentration. Accurate measurement of DNA concentration was performed using a NanoDrop 2000 spectrophotometer (Thermo Scientific).

2.2.5 Restriction enzyme digestion

Restriction digests of DNA were performed using restriction enzymes from New England Biolabs according to the manufacturer's instructions. Reaction volumes ranged from 5–50 µl, while reaction times ranged from 1 hour to overnight as specified by the manufacturer.

2.2.6 Gel extraction of DNA fragments

Digested DNA fragments or plasmids required for cloning were run on a large-well agarose gel at 90 V. The gel was then immersed in GelRed DNA stain (Biotium) for 20 minutes, and DNA bands were visualised using a Safe Imager bright light transilluminator (Invitrogen). Bands were excised from gels using a clean scalpel blade, and DNA was purified using the QIAquick Gel Extraction Kit according to the manufacturer's instructions, with a 30 µl elution volume. One microlitre of the gel extraction was checked for purity and concentration on an agarose gel or using the NanoDrop spectrophotometer.

2.2.7 Dephosphorylation of plasmids with Antarctic Phosphatase

Linearised vectors with compatible ends were treated with Antarctic Phosphatase (New England Biolabs), which catalyses the removal of 5' phosphate groups from DNA, thereby preventing self-religation. Treatment with Antarctic Phosphatase thus reduces the background number of colonies on transformation plates resulting from religated, singly-cut vector without the desired insert. Five units of Antarctic Phosphatase were added to restriction digests in 1 × Antarctic Phosphatase buffer (New England Biolabs), and reactions were incubated for 15 minutes at 37°C and then heat inactivated at 65°C for 5 minutes.

2.2.8 Ligating DNA fragments into plasmid vectors

Ligations were performed in 10 µl reaction volumes, containing 0.5–2 units of T4 DNA ligase, 1 × ligase buffer (New England Biolabs) and an approximate 3:1 molar

ratio of insert to vector DNA, with the amount of vector DNA in the range of 10–100 ng. A control reaction containing vector but lacking insert DNA was prepared identically to determine the number of background colonies resulting from the vector DNA alone. Following incubation for 1 hour at room temperature, 5 µl of the ligation reaction was transformed into competent cells.

2.2.9 Site-directed mutagenesis

PCR reactions for site-directed mutagenesis were set up as 50 µl reactions containing the following: 0.5 µl of Phusion High-Fidelity DNA Polymerase, 10 µl of 5 × Phusion HF buffer, 1 µl of 10 mM dNTP, 1.25 µl of 100 ng/µl forward primer, 1.25 µl of 100 ng/µl reverse primer, and 50 ng of the plasmid. The PCR cycling parameters are displayed in Table 2.9.

Table 2.9: Site-directed mutagenesis PCR cycling parameters

Stage	Temperature (°C)	Time (minutes)	Number of cycles
Initial denaturation	98	1	1
Denaturation	98	0.5	18
Annealing	55	1	
Extension	72	2.5	

Three hundred units of DpnI (New England Biolabs) were added into 20 µl of the PCR reaction to digest the methylated, non-mutated DNA template. Five microlitres of the digested products were used for transformation.

2.2.10 Transformation

Competent *E. coli* cells were thawed on ice (approximately 20-30 minutes). DNA (usually 100 pg to 100 ng) was mixed into 20-50 µl of competent cells in a microcentrifuge tube. The competent cell/DNA mixture was incubated on ice for 20-

30 minutes, and then heat shocked for 45 seconds at 42°C. The tube was chilled again on ice for 2 minutes. LB or SOC media (500-900 µl, without antibiotics) was added and cultured in a 37°C shaking incubator for 45 minutes. Either an aliquot, or the entire transformation mixture was plated onto a 10 cm LB agar plate containing the appropriate antibiotic (Ampicillin at a concentration of 100 µg/ml, or Kanamycin at a concentration at 25 µg/ml). Plates were incubated at 37°C overnight.

2.2.11 Generation of high competency *E. Coli* DH5α cells

High competency cells were needed for transformation with lentivector. The method to generate competent *E. coli* cells is based on the original Inoue method (Inoue et al., 1990). Transformation buffer containing 10 mM of PIPES (1,4-Piperazinediethanesulfonic acid), 15 mM of $CaCl_2.2H_2O$, 250 mM of KCl and 55 mM of $MnCl_2$ at pH 6.7-6.8, was filtered (0.22 µm) and kept at 4°C. DH5α cells were incubated in SOC medium on a shaker (150-250 rpm) at 18°C until they reached a culture density of between 0.4-0.6 O.D. (600 nm) and then centrifuged at 3,000 × g and chilled on ice. Cells were then washed with 1/3 volume of ice-cold transformation buffer and chilled on ice for 10 minutes before further centrifugation. Cells were re-suspended with 1/12.5 volume of ice-cold transformation buffer with 7% glycerol. Cells were dispensed into 100 µl aliquots, frozen with dry ice and stored at -80°C.

2.2.12 RNA extraction

2.2.12.1 Extraction of RNA from monolayer cells

To extract total RNA, cells were washed in 1 × PBS and harvested in 1 ml TRIzol per 10-25cm^2 of surface area, as per the manufacturer's protocol. Briefly, the TRIzol (containing lysed cells) was transferred to 1.5 ml microcentrifuge tubes, and 200 µl of chloroform per 1 ml of TRIzol was added to each sample and mixed vigorously. Tubes were centrifuged at 12,000 × g, 4°C for 15 minutes and the aqueous (top)

layer containing the RNA was removed to a fresh tube. RNA was precipitated by the addition of 500 µl isopropanol per 1 ml TRIzol initially used, then incubated at room temperature for 10 minutes and centrifuged again at 12,000 × g, 4°C for 10 minutes. A final 75% ethanol wash of the RNA pellet was done with 1 ml ethanol per 1 ml TRIzol and centrifuged under the same conditions as previously described. The RNA pellet was air-dried, resuspended in 20-30 µl RNase-free H_2O and heated to 65°C for 10 minutes to resuspend.

2.2.12.2 Extraction of RNA from primary tissue

Harvested murine tissue was stored in RNALater (Invitrogen). RNA from tissue was extracted using the same TRIzol method and protocol as described above. However, tissue samples were first sliced into small pieces using a razor blade and then homogenised in a microcentrifuge tube in a small amount of TRIzol (100-200 µl) using a UV-sterilised hand micro-pestle. Generally a final volume of 1 ml TRIzol was sufficient for most tissue samples. The remainder of the protocol was performed as previously described. All RNA samples were stored at -20°C until required.

2.2.13 Quality check of RNA

Following extraction, RNA concentration was determined using a NanoDrop 2000 UV-Vis spectrophotometer (Thermo Scientific). The concentration of the RNA was determined at 260 nm while the ratios of absorbance at 260 nm: 280 nm of 2.0 were considered pure. In addition to checking by spectrophotometry, the quality of the extracted RNA (2 µg) was also checked using gel electrophoresis to detect the 18s and 28s ribosomal RNA.

2.2.14 cDNA synthesis

Two micrograms of total RNA extracted by TRIzol was treated with one unit amplification grade DNase I in 20 mM Tris-HCl (pH 8.4), 2 mM $MgCl_2$ and 50 mM

KCl for 15 minutes at room temperature. EDTA was added to 2.5 mM, and the sample was incubated at 65°C for 10 minutes to inactivate the DNase I. cDNA was generated from DNase-treated RNA in a random hexamer-primed M-MuLV reverse transcriptase reaction using the Lucigen NxGen M-MulV Reverse Transcriptase. One microgram (8 µl) of RNA was added to a 20 µl reaction initially containing 1 µl 10 mM dNTPs, 1 µl 53 ng/µl random hexamers (NEB) and 6 µl water. Following a 5 minute incubation at 65°C and 2 minutes cooling on ice, the reaction was brought up to a total of 20 µl by the addition of 2 µl 10 × M-MulV Reverse Transcriptase buffer, 1 µl RNase inhibitor (Lucigen) and 1 µl Reverse Transcriptase (Lucigen). RNA was reverse transcribed at 42°C for 1 hour and the reaction stopped by heating to 90°C for 10 minutes. Before use in PCR, the cDNA was diluted 1:5 in sterile RNase-free water.

2.2.15 Quantitative real-time PCR

To quantify levels of mRNA transcripts present in extracted RNA samples, real-time PCR was used. The general set-up used for all reactions was: 16 µl reactions containing 2 × GoTaq qPCR Master Mix, 0.5 µM each primer and template cDNA equivalent to 20-40 ng input RNA. The general PCR cycling conditions used for quantitative analysis were: an activation period of 15 minutes at 95°C; 40 cycles of 95°C for 15 seconds, specific annealing temperature (60-62°C) for 15 seconds, and 72°C for 20 seconds; and a ramped melt analysis between 55 and 95°C with 4 second, 1°C steps. Data were acquired during the 72°C extension phase of each cycle.

Quantitative poly-A tailed RTPCR to measure mature miRNA levels was performed as below: RNA was poly-A tailed using poly (A) polymerase (NEB) and reverse-transcribed using a poly-T adaptor. The reverse primer for each miRNA contains the

poly-T sequence and 3-5 nucleotides of target-specific sequence at the 3’ end of the miRNA. The forward primer contains 16-18 nt of target-specific sequence at the 5’ end of the miRNA.

2.2.16 Preparation of lysates

Cultured mammalian cells from which protein was to be extracted were washed by PBS and scraped off the base of the well in 50-200 µl RIPA buffer with the volume dependent on cell number. To further promote cell lysis, lysates were incubated at 4°C for 10 minutes. Cellular debris was removed via centrifugation at 8,000 × g for 10 minutes at 4°C, and protein lysates were stored at -20°C.

2.2.17 Protein concentration determination

The concentration of total protein in RIPA lysates was determined using Bio-Rad Protein Assay reagent (Bio-Rad, NSW, Australia) as per the manufacturer’s instructions. Using a 96-well plate, 2 µl RIPA lysate was added to 100 µl 1 × Protein Assay reagent and the absorbance measured at 595 nm in a plate reader (DTX 880 Multimode Detector; Beckman Coulter). Protein concentration was calculated against the 595 nm absorbances of a BSA standard curve of known concentrations (0, 0.1, 0.2, 0.4, 0.6 and 1 µg/ml).

2.2.18 SDS-PAGE and Western blotting

Protein samples (30 µg) were loaded onto 7.5% polyacrylamide gels (Invitrogen, Carlsbad, CA, USA) after boiling in 4 × SDS sample buffer containing 10% β-mercaptoethanol for 5 minutes at 95°C. Electrophoresis was performed between 100-120 V using GTS running buffer, followed by transfer to a 0.2 µm PVDF membrane (GE Healthcare) at 170 mA for 2 hours using the transfer buffer. After transfer, the membrane was blocked in TBS-Tween-20 (TBST) solution (10 mM Tris-HCl, pH 7.5, 150 mM NaCl, 0.05% Tween-20) containing 3% BSA (#A6003, Sigma-Aldrich)

for 1 h at room temperature with agitation. Membranes were incubated with specific antibodies using the concentrations and conditions recommended by the supplier, in TBST containing 3% BSA, overnight at 4°C with agitation. After washing thrice with TBST for 10 minutes each, the blot was incubated with IRDye secondary antibody at 1:5000 dilution in 3% BSA-TBST for 1 hour at room temperature with agitation. Following a further three washes with TBST for 10 minutes each, the blot was visualised using Odyssey CLx (LI-COR) Imaging system. The intensity of the signal was quantified using Image Studio™ Lite software (LI-COR).

2.2.19 Exosome extraction by PEG precipitation

2.2.19.1 Material preparation

Twenty five grams of Polyethylglycol (PEG, 8 kDa, Sigma) in 50 ml deionised water was ultrasonicated for 1 hour to obtain a homogeneous 50% aqueous solution. The PEG solution was centrifuged at 5,000 × g for 20 minutes at 4°C and the supernatant was filtered through a 0.22 μm syringe filter. Two times PEG solution (20%) was made as 20 ml sonicated, filtered 50% PEG solution mixed with 30 ml MQ water.

2.2.19.2 Protocols

The medium was collected and centrifuged at 2,000 × g for 10 minutes at 4°C to remove detached cells, followed by filtration through a 0.45 μm filter to remove larger particles. Alternatively, centrifugation was performed at 3,000 × g for 15 minutes to remove cells and cell debris. Once centrifuged, the media was added to an equal volume of a 2 × PEG solution, mixed thoroughly by inversion, and incubated at 4°C overnight (for a minimum of 12 hours).The next day, samples were centrifuged in a tabletop centrifuge at 1,500 × g for 30 minutes at 4°C. Conical tubes were then decanted, and allowed to drain for five minutes, tapping occasionally to remove excess PEG. The resulting pellet was suspended in 25-250 μl of MQ water. Samples were then stored at – 80°C.

2.2.20 Luciferase assay

Approximately 48 hours post-transfection, cells were lysed by the addition of 100 µl Passive Lysis Buffer (PLB; Promega) to each well, and plates were rocked gently and continuously for 15-30 minutes to promote complete lysis. Using the Dual-Luciferase Reporter Assay system (Promega), a 30 µl sample of lysate was analysed on a TopCount NXT Luminescence and Scintillation counter (Packard, Australia) for firefly (*Photinus pyralis*) and *renilla* luciferase activity. To minimise the effect of carryover luminescence from neighbouring wells, cell lysates were added to alternate wells of 96-well plates. Lysates were mixed with 40 µl of firefly luciferase reagent (Luciferase Assay Reagent II (LARII), Promega) to measure the activity of firefly luciferase expressed from transiently transfected pGL3-derived vectors. The luminescence of each well was determined 2 minutes after addition of LARII. Addition of 40 µl of Stop and Glo Reagent (Promega) was then added to wells as soon as possible to quench the firefly luciferase activity and provide the substrate for *renilla* luciferase. As previously, the luminescence resulting from the *renilla* luciferase protein was also determined 2 minutes following addition of the substrate.

Relative luciferase activities (ratios of firefly to *renilla* luciferase activity) were calculated for each sample and then averaged to provide a single value for each condition. Cell lysates were stored at -20°C if they were to be assayed again at a later date.

2.2.21 Immunofluorescence Microscopy

For immunofluorescence imaging of primary myoblasts, cells were seeded in 24-well plates at a density of 1.5×10^4 cells/well in 1 ml complete DMEM, 24 hours before treatment. Due to difficulties in the attachment of primary myoblasts to glass coverslips, these cells were seeded directly into collagen-coated wells. Media was removed, and cells were washed twice with PBS before fixing with 500 µl of 3.7%

formaldehyde (37% formaldehyde stock diluted 1:10 in PBS) for 10 minutes at room temperature. Cells were rewashed with PBS and stored in fresh PBS at 4°C if required. Cell membranes were permeabilised by the addition of 0.5% Triton-X in PBS for 5 minutes followed by three rinses with PBS, and then blocked in 1% BSA in PBS (blocking buffer) for 30 minutes. Cells were rinsed once more with PBS before antibody labelling.

2.2.21.1 Antibody labelling

Primary antibodies were used at a concentration of 4 µg/ml. Antibodies were diluted in blocking buffer, added to wells, and left overnight at room temperature. The following day, primary antibodies were removed and cells were washed 3 times with PBS for 5 minutes each time. Secondary antibodies were diluted in PBS to a concentration of 10 µg/ml and placed in each well for about 2 hours at room temperature followed by DAPI (1 µg/ml) counterstaining for nuclei, with an incubation of approximately 8 minutes. Finally, cells were washed three times with PBS for 5 minutes per wash.

2.2.21.2 Imaging

In-well cells were imaged using an Olympus IX71 fluorescence microscope.

2.2.22 Chromatin Immunoprecipitation (ChIP)

ChIP experiments in primary myoblasts were performed using a modified MicroChIP protocol (Dahl and Collas, 2008). Cells were either treated with L-cell or Wnt3a CM or transfected using Lipofectamine LTX (Life Technologies) at a density of 1.8×10^6 cells per T75 flask. Each flask was transfected with a total of 20 µg of DNA and 50 µl Lipofectamine in 3.5 ml serum free (SF)-DMEM. Two flasks were used per condition. Six hours post-transfection, the media was removed and replaced with fresh media to prevent transfection toxicity to the cells. Twenty four hours post-

transfection, cells were trypsinised and resuspended in 2 × T175 flasks per transfection condition. After a further 24 hours, cells were cross-linked by adding 1% final formaldehyde to the growth media. Cells were cross-linked for 30 minutes at 37˚C. Glycine was then added to the growth media at a final concentration of 125 mM, for 10 minutes at room temperature to quench the formaldehyde and stop the fixation reaction. Following fixation, cells were washed twice with ice-cold PBS and then scraped from the flask in 5 ml ice-cold PBS + proteinase inhibitor cocktail (PIC) per flask. Cell suspensions from duplicate flasks were combined in a 10 ml tube and centrifuged at 3,000 × g, 10 minutes at 4°C. The supernatant was aspirated, and the cells were rewashed in 5 ml PBS per tube and centrifuged as per previous step. After removal of the supernatant, the cell pellet was either frozen and stored at -80°C until required, or was lysed immediately. Cells were lysed by the addition of 6 ml ChIP lysis buffer 1 + PIC followed by a 10 minutes incubation on ice. Nuclei were then pelleted by centrifugation at 4,000 × g, 10 minutes, 4°C and supernatant was removed. Nuclear lysis was performed by the addition of 500 µl of ChIP lysis buffer 2 + PIC and incubation on ice for 10 minutes. Sonication of the chromatin was performed as follows on a Sonics Vibracell VCX130 (John Morris Scientific) using a 3 mm stepped microtip probe: 25% amplitude, 20-second pulse followed by a 30 second rest for a total of 15-20 bursts. Chromatin was kept on ice for the whole procedure. To check the efficiency of sonication, 20 µl of chromatin from each sample was reverse crosslinked by adding 80 µl water, 4 µl 5 M NaCl and 1 µl 10 mg/ml RNase A (Cell Signaling Technology) and incubating overnight at 65°C. The remaining sheared chromatin was stored at -80°C until required. The following day, tubes were cooled, 0.5 µl Proteinase K (PNK; 20 mg/ml) was added, and samples were incubated at 42°C for 1 hour. DNA was purified by use of a PCR purification spin kit (Qiagen) as per the manufacturer's instructions, and visualised on a 1.5%

agarose gel. The aim was to generate chromatin fragments that ranged between 300 and 3,000 bp in length. Once chromatin of the appropriate size range was obtained, the samples were centrifuged at 13,000 × g, 10 minutes, 4°C to pellet any insoluble material. The chromatin was then diluted 6-fold in dilution buffer (to a total volume of 3 ml) and pre-cleared for 40 minutes at 4°C by adding 20 µl Protein G ChIP-Grade Magnetic Beads (Cell Signaling Technology). The magnetic beads were captured and removed from the chromatin samples by use of a magnetic rack (Cell Signaling Technology). The chromatin was split as follows: 20 µl was saved for total chromatin (input), 500 µl each for normal rabbit IgG control and each antibody required. Two micrograms of IgG or antibody was used, and samples were slowly rotated overnight at 4°C. Thirty microlitres of Protein G Magnetic Beads were added to all IgG and antibody samples (not input) the following day to capture the immunocomplexes and tubes were left to rotate for a further 2-3 hours. Using the magnetic rack, the magnetic beads were washed twice with dilution buffer + PIC, once with high salt wash buffer, once with LiCl wash buffer and once with TE buffer. Each wash involved slow rotation of the beads in the appropriate buffer for 10 minutes at 4°C. Finally, the beads were captured and resuspended in 200 µl elution buffer and incubated at 65°C overnight. The following day 0.5 µl PNK was added, and samples were incubated for 1 hour at 55°C. DNA purification was performed with the Qiagen PCR purification kit according to the manufacturer's instructions.

2.2.23 Preparation of primary myoblasts

2.2.23.1 Antibody labelling of myoblasts for fluorescence-activated cell sorting (FACS)

Twenty microlitres of isolated cells in PBS + 2% FBS (as above) was placed in a fresh tube and set aside as an unlabelled control sample. The remaining 130 µl was labelled with: 0.3 µl Sca1 (BD Pharmingen, FITC rat anti-mouse, Cy-6A/E (D7) 0.5 mg/ml), 1.2 µl CD45 (BD Pharmingen, APC rat anti-mouse, 30-F11 0.2 mg/ml) and

2 µl CD34 (BD Pharmingen, PE rat anti-mouse, clone RAM34 0.2 mg/ml) and left to incubate in the dark at room temperature for 45 minutes. The cells were washed twice with 1 ml PBS + 2% FBS (2,000 × g, 5 minutes) in a tabletop microcentrifuge before being resuspended in a final volume of 1 ml growth media plus 2 µg/ml doxycycline, and passed through a 50 µm nylon mesh membrane.

2.2.23.2 FACS

Labelled cells from murine muscle were sorted based on Sca1, CD45 and CD34 expression on a BD FACS Aria (BD Biosciences, San Jose, CA). Cells were collected as two populations; the first, CD34+, CD45- and Sca1-, which were considered our primary myoblast population. The second, CD34+, CD45- and Sca1+, were deemed to consist of primary fibroblasts. Sorted cells were collected in 1 ml myoblast growth media plus 2 µg/ml doxycycline to reduce the risk of contamination from the sorter, and grown on collagen-coated flasks.

2.2.24 Maintenance of cell lines

2.2.24.1 Maintenance of mouse primary myoblast cultures

Primary myoblast cultures isolated from mouse were grown at 37°C in a humidified incubator with 5% CO_2 and cultured in either Myoblast Selection Media (Ham's F10 media, 20% FBS, Non-Essential Amino Acids, penicillin-streptomycin (pen-strep) and 5 ng/ml murine basic fibroblast growth factor (bFGF)) or Myoblast Growth Media (1:1 Ham's F10 media:complete DMEM, 20% FBS, Non-Essential Amino Acids, pen-strep and 5 ng/ml murine bFGF). For the primary myoblasts to adhere, all plates and flasks to be used were first coated with a collagen solution (filtered 20 mM acetic acid + 50 µg/ml rat tail collagen). Enough collagen was added to the plate or flask to completely cover the surface and was left on either overnight at room temperature, or for 1 hour at 37°C. After removal of the collagen, the vessel was rinsed twice with sterile PBS. If the vessel was not to be used immediately, it was

stored at 4°C with the PBS. The collagen solution was re-used and was always stored at 4°C.

2.2.24.2 Maintenance of the C3H 10T1/2 cell line

The C3H 10T1/2 cell line was initially generated from primary cultures of 14-17 day whole mouse embryos (inbred C3H Heston strain), disaggregated with 0.25% trypsin (Reznikoff et al., 1973). The resulting cell line was subcloned and selected for immortalisation and contact inhibited growth.

The C3H 10T1/2 cell line was cultured in DMEM with 10% FBS and Non-Essential Amino Acids, grown at 37°C in a humidified incubator with 5% CO_2. When cells reached 50-60% confluence, they were split 1:10 (at most).

2.2.24.3 Maintenance of the HEK293T Cell Culture

HEK293T cells were cultured in DMEM with 10% FBS and Non-Essential Amino Acids at 37ºC in 5% CO_2. The cells were split 1:20, by pipetting, every 3-4 days. Cell stocks were produced by resuspending cell pellet in 0.5 ml FBS + 10% DMSO, and stored at -80ºC.

2.2.24.4 Frozen cell stocks

To generate stocks of cells for later use, cells were centrifuged at 1,500 rpm for 5 minutes and preserved in FBS containing 10% DMSO. They were stored in Nunc cryotube vials, which were initially stored at -80°C overnight, and later moved to liquid nitrogen for long-term storage. On removal from liquid nitrogen, cell stocks were thawed in a 37°C water bath and placed in a T25 or T75 flask. Warm DMEM (or other appropriate media) was added slowly. Media was replaced the following day to remove any remaining traces of DMSO.

2.2.25 Transfection

2.2.25.1 Standard transfection

Transfections were performed using Lipofectamine® LTX with Plus™ Reagent (ThermoFisher), according to the manufacturer's instructions in a 24-well format. Briefly, cells were seeded 1 day before transfection at a density of 1 × 104 cells/cm^2, for cells to reach 70-80% confluence on the day of transfection. Five hundred nanogram DNA, 0.5 µl PLUS reagent and 1.5 µl LTX reagent were combined and diluted with 100 µl of antibiotic- and serum-free DMEM medium and incubated for 30 minutes. The mixture was added dropwise to the cells. The medium was changed to DMEM medium containing antibiotic and serum 4 hours after the transfection and cultured at 37°C.

2.2.25.2 Reverse transfection

For each well of the 24-well plate, 100 µl serum-free DMEM media was added to 333-400 ng plasmid or combination of plasmids, then mixed gently. PLUS reagent was added at a 1:1 ratio (1 µl per µg plasmid), incubated for 5-15 minutes, then a double volume of LTX and PLUS reagent was added to the mixture and incubated for 30 minutes. Approximately 7.5 × 10^4 cells were mixed with the above mixture in a 1.5 ml tube for each corresponding well. Cell and reagent mixture was well mixed and plated in each well. The cells were allowed to sit for approximately 20 minutes on the bench to enable proper distribution. Cells were incubated at 37ºC in 5% CO_2 for 24-48 hours.

Specifically for luciferase assays, pRL-Null was added at a ratio of 1 in 50 of the total plasmid amount. Reporter and effector vectors were added at a 1:2 ratio.

2.2.26 Lentivirus production

To produce retroviral supernatants, HEK293T cells were plated at a density of 4 × 10^5 cells/well in a 6-well plate 24 hours before transfection. The control, or the

specific lentivector (1.5 µg viral DNA plasmid, 1.5 µg pCMV-dvrp8.2, 1 µg VSV-G plasmid), was added to 200 µl of serum-free media. Eight microliters of Lipofectamine® 2000 was added to 200 µl serum-free media (1:2 DNA to Lipofectamine® 2000). Both mixtures were incubated for 5 minutes at room temperature. They were then combined and incubated at room temperature for a further 20 minutes. The complexes were then added to the cells. Cells were grown at 37ºC and 5% CO_2. Virus-containing supernatants were harvested at 48-72 hours post-transfection. Supernatants were either filtered through a 0.45 µm Minisart syringe filter or centrifuged at 1,500 × g for 5 minutes, to remove any packaging cells, and then stored at -80°C.

2.2.27 Lentiviral transduction

Primary myoblasts were plated 24 hours before transduction at a density of 1×10^4 cells/well in a 24-well plate. 4µg/ml of polybrene was added to 0.5 ml viral supernatant for each well. Spinfection was carried out by spinning plates for 2-3hrs at 2,500 rpm, at 32ºC. The viral supernatant was immediately removed and replaced by 0.5 ml of fresh myoblast growth media. The transduced cells were incubated at 37ºC and 5% CO_2 for approximately 48 hours.

Cells were imaged and photographed under a fluorescent microscope (Olympus IX71 inverted microscope) to assess expression of GFP.

2.2.28 Puromycin kill curve

Cells were seeded at a density of 2×10^4 cells/cm^2 for overnight culture. The target cells should be approximately 80-90% confluent. Puromycin was added at various concentrations of 0, 0.25, 0.5, 0.75, 1.0, 1.5, and 2 µg/ml, and changed every other day. The minimum concentration of puromycin that results in complete cell death after 3-5 days is the optimal dose that should be used for selection.

2.2.29 Stable cell line selection

Twenty four hours after transfection, cells were seeded into a 6-well plate at a ratio of 1 in 10. The optimised concentration of antibiotic was added into the medium the next day after subculture. Medium containing antibiotic was changed every other day. The cells were expanded if they reached confluence, and used for an experiment or stored at -80°C.

2.2.30 CRISPR

2.2.30.1 Construction of sgRNA expression vector

Design of targeting components –sgRNA

Target genomic DNA sequences were entered into the online CRISPR design tool *(http://tools.genome-engineering.org*). This tool identified and ranked suitable target sites and matching guide sequences which were 20-bp sequences directly upstream of 5'-NGG, within the input genomic DNA sequence.

Preparation of sgRNA expression constructs

Annealing of oligonucleotides

The top and bottom oligonucleotide strands for each sgRNA design were resuspended to a final concentration of 100 µM. The following reactions were prepared for annealing each pair of oligonucleotides: 1 µl each of 100 µM sgRNA top and bottom strands, 1 µl 10 × T4 ligation buffer, and ddH_20 to bring to a total volume of 10 µl.

Oligonucleotides were annealed in a thermocycler using the following parameters: 37˚C for 30 minutes, 95˚C for 5 minutes and then ramped down to 25˚C at 5˚C/minute.

Lenti-CRISPR V2 digestion

5 µg Lenti-CRISPR V2 was digested by 2 µl BsmbI with NEB 3.1 buffer in 50 µl total volume, at 55˚C for 2 hours.

Ligation and transformation

The ligation reaction was set up containing 50 ng BsmbI digested plasmid, 1:200 diluted annealed oligos, 5 µl 2 × quick ligase buffer and 1 µl Quick Ligase (NEB). The reaction was incubated at room temperature for 10 minutes.

The transformation was performed as described above in section 2.2.10. For each transformed ligation mixture, ten colonies were picked up for PCR screening, and 2 of the screened colonies were inoculated and verified by sequencing with U6 forward primer.

2.2.30.2 Viral transduction and puromycin selection

Correct sgRNA expression lentivectors were transfected into HEK293T cells for lentivirus packing, as per the protocol described in section 2.2.26.. Primary myoblasts were transduced by the produced lentivirus (as described in section 2.2.27). The optimised concentration of puromycin was added to the transduced myoblasts at least 3 days post-transduction. Medium containing puromycin was changed every other day. The cells were split into 10 cm culture dishes if they reached confluence.

2.2.30.3 Cell colony picking and expansion

After at least 2 weeks of puromycin selection, cell colonies were picked up by sterile pipettes and transferred into 96-well plates. Briefly, cell clusters in different areas were selected, the cell cluster was scraped gently with sterile 200 µl pipettes, with the floating cells sucked up immediately, and pipetted into collagen-coated and warm medium filled 96-well plates one by one. Puromycin was added on the second day to

kill the un-transduced wild-type colonies. When the cells reached confluence (approximately one or two weeks), they were split into another two 96-well plates. One plate was prepared for cell freezing; the other was prepared for immunostaining screening of the knock out candidates. The number of picked cell clusters was well labelled for both plates.

2.2.30.4 Enrichment by immunostaining

Immunostaining of target protein was performed in the 96-well plates when the cells reached confluence. Multi-channel pipettes were used for the screening in the 96-well format. The protocol was the same as the method described in section 2.2.21. Well labelled cells were imaged using an Olympus IX70 fluorescence microscope. Candidates with low level or no expression of the target protein were identified.

2.2.30.5 Single cell isolation and expansion

Due to the scattered distribution of primary myoblasts, well-rounded colonies do not form. Therefore the picked cell clusters were cell combinations. To isolate knock out cells with a single genotype, the candidates of the cell mixture enriched by immunostaining were further isolated at the single cell level. Limit dilution or single cell sorting were used to isolate the single cells.

Isolated cell colonies were cultured in 96 well plates and inspected daily to track their appearance. Wells which were empty or that may have been seeded with more than a single cell were marked off. Cells were returned to the incubator and allowed to expand for 3–4 weeks.

When the cells reached 80% confluence, replica plates were prepared for passaging (one well for each clone) by adding 100 µl of myoblast complete medium to each well in the replica plates. The medium was replaced every 2–3 days thereafter, and cells were passaged accordingly. Three plates were prepared: one for making cell

stock, one for immunostaining, and one for DNA isolation and genotyping. The cells in the 96 well plates for making cell stock were further expanded in 48 well plates, 24 well plates, 12 well plates, 6 well plate and T25 flasks, then cell stocks were made from the T25 flasks. Cell status was monitored and recorded every day. Once the cell culture reaches 80% confluence, primary myoblasts must be trypsinized and transferred into bigger containers as these cells would be lost if they differentiate.

2.2.30.6 T7 PCR screening and sequencing

Genomic DNA from above plates was extracted as described in section 2.2.3. PCR was performed with 100 ng of genomic DNA as the template, and specific CRISPR screening primers were used.

Genome Targeting Efficiency was determined by using T7 Endonuclease I (NEB). T7 Endonuclease I (T7 EI) recognises and cleaves non-perfectly matched DNA. The T7 screening was performed according to the manufacturer's instructions. PCR products were purified, annealed and digested with T7 EI. Fragments were analysed to determine the efficiency of genome targeting. Wild type primary myoblasts were used as a negative control. PCR products from T7 screened candidates were purified and sent for sequencing.

2.2.31 Proliferation assay

A dye-retention assay was used to assess proliferation. Briefly, $1x10^6$ wild-type or β-catenin null myoblasts were washed and incubated with 1µL of Vibrant DiI cell-labelling solution (Thermofisher) in 1mL serum-free RPMI at 37^0C for 10 minutes. Labelling efficiency was assessed by flow cytometry using the Accuri C6 (BD Biosciences) and was always > 95%. The cells were plated in a 24-well plate at $5x10^4$ cells/well. After various times in culture the cells were harvested using trypsin and the mean DiI fluorescence level of the population was measured by flow

cytometry. The change (decrement) in mean DiI fluorescence at each time point was calculated as a fold over the initial (time 0) fluorescence level. The experiment was repeated twice in duplicate with similar results and a representative experiment is shown.

2.2.32 RNA-seq

Wild-type and β-catenin null CRISPR myoblasts were plated at 3.3 x 10^5 cells per well in collagen-coated 6-well plates before treatments with Wnt3a or control conditioned L-cell medium. Primary myoblasts were harvested at 24hrs post treatments, and RNA was prepared as previously described. RNA quality was confirmed using the Agilent 2100 Bioanalyzer and RNA-Seq libraries prepared using the TruSeq RNA Sample Preparation Kit v2 according to Illumina protocol. Multiplexed libraries were validated using the Agilent BioAnalyzer, normalized and pooled for sequencing. High-throughput sequencing was performed on the HiSeq 2500 system (Illumina) with a 100-bp read length. Image analysis and base calling were done with Illumina HiSeq Analysis Software. Short read sequences were mapped to a UCSC mm10 reference sequence using the RNA-Seq aligner STAR (Dobin et al., 2013). Known splice junctions from mm10 were supplied to the aligner and de novo junction discovery was also permitted. Differential gene expression analysis, statistical testing and annotation were performed using Cuffdiff 2 (Trapnell et al., 2013). Transcript expression was calculated as gene-level relative abundance in fragments per kilobase of exon model per million mapped fragments and employed correction for transcript abundance bias (Roberts et al., 2011). Results for genes of interest were also explored visually using the UCSC Genome Browser.

2.2.33 ChIP-seq

For ChIP-seq libraries, individual ChIP samples from each condition were pooled,

adaptor ligated, PCR amplified and size selected. Libraries were validated using the 2100 BioAnalyzer (Agilent), normalized, and sequenced on the Illumina HiSeq 2500 using bar-coded multiplexing and either 50 or 100bp read length. Read alignment and peak finding used Bowtie and findPeaks (Homer) respectively. After initial analysis including preparation of bedgraphs for visualization on the UCSC genome browser, bedgraphs were converted to bed format using Bedtools. Custom scripts were developed in perl to identify subpeaks located 3kb from TSS. Two-fold ratio enriched peaks (Wnt3a/L-cell treatment conditions) were selected for motif and gene ontology analysis using Homer tools.

2.2.34 Statistics

Statistical analysis of all results presented in this thesis was performed using GraphPad Prism software (Hearne Scientific). The statistical significance was determined by use of a one-way ANOVA, a two-way ANOVA or the Student's T-test with two-sample unequal variance, as appropriate. A change was deemed statistically significant if $P < 0.05$.

CHAPTER 3: β-catenin interaction with MyoD but not TCF/LEF is essential for Wnt-mediated induction of the myogenic differentiation program

The text and figures presented in this chapter have been submitted as a manuscript to a peer reviewed journal for publication. The style of this Chapter differs slightly from other Chapters because it conforms to the journal publication guidelines. At the time of final thesis amendment, the manuscript, in revised form, was published online (DOI: 10.1242/dev.167080).

3.1 Introduction

Skeletal muscle owes its considerable regenerative capacity to a population of resident muscle stem cells called satellite cells (Lepper et al.; McCarthy et al.; Murphy et al.; Sambasivan et al., 2011). These cells, situated between the basal lamina and myofibre, are largely quiescent in uninjured adult muscle (Buckingham et al.; Mauro; Rudnicki et al.). Soluble factors produced after muscle injury trigger satellite cells to re-enter the cell cycle giving rise to a transit-amplifying population called myoblasts. Myoblasts express a hierarchy of myogenic regulatory factors (MRFs) such as MyoD that is involved in both proliferation and differentiation, and myogenin that drives and modulates the differentiation program (Schultz and Jaryszak; Wozniak et al.). Differentiation involves multiple highly coordinated processes including exit from the cell cycle, migration, adhesion, fusion, and formation of the contractile apparatus that defines functional myofibres.

Several studies have defined critical functions for the canonical Wnt/β-catenin signalling pathway in muscle development and also in adult muscle regeneration (Otto et al.). Wnt ligands bind to membrane receptor co-complexes involving the Frizzled and low-density lipoprotein receptor protein (LRP) families that associate with the so-called destruction complex (Stamos and Weis). Wnt binding elicits a change in the destruction complex that suppresses ubiquitination and degradation of β-catenin (Li et al., 2012). As the core transcriptional effector of the Wnt pathway, β-catenin does not bind DNA directly but instead interacts with partner proteins to regulate target genes. The classical transcriptional partners for β-catenin are the TCF/LEF family factors. In the absence of Wnt signals, TCF/LEF proteins bind and repress Wnt target genes via interaction with Groucho/TLE co-repressors (Arce et al.; Daniels and Weis, 2005a) and HDAC1 (Arce et al.; Billin et al.). Upon binding of Wnt ligand, stabilized β-catenin binds to TCF/LEF proteins and recruits histone

acetyltransferases (HATs) (Hecht et al.; Ogryzko et al.; Parker et al.; Takemaru and Moon) to activate these targets (Hecht et al.; Posokhova et al.; Wodarz and Nusse).

A number of studies including our own have shown that canonical Wnt ligands promote myoblast differentiation (Bernardi et al.; Brack et al.; Pansters et al.; Tanaka et al.; Zhuang et al.), and may increase expression or activity of MyoD and/or myogenin (Jones et al., 2015a; Petropoulos and Skerjanc, 2002; Ridgeway et al., 2000). As an example, very recent work showed that Wnt3a increased expression of myogenin protein and also its binding to the myogenic target Follistatin (Jones et al., 2015a). Yet, the precise mechanism by which Wnt signalling promotes myogenesis has been controversial, particularly the role β-catenin. Murphy *et al* (Murphy et al., 2014a) studied mice with inducible Cre-mediated ablation of β-catenin in satellite cells and observed no defect in adult muscle regeneration (Murphy et al., 2014a). Rudolf *et al* (Rudolf et al., 2016a) performed very similar conditional deletion experiments but with a different Cre-driver line, and found β-catenin to be essential for adult muscle repair in vivo. They also explanted myoblasts lacking β-catenin and showed that they had delayed differentiation in vitro. The reason for the discrepancy between the two studies remains unresolved.

β-catenin interacts with a number of transcription factors in addition to TCF/LEF proteins. For example, we found that β-catenin binds to the Barx2 homeobox protein (Hulin et al., 2016a); while others have shown binding to PITX2 (Vadlamudi et al., 2005) and ARX (Cho et al., 2017). These interactions appear to occur within the context of β-catenin-TCF/LEF complexes, suggesting that they allow the homeobox factors to be recruited to target genes that contain TCF/LEF binding sites. β-catenin also interacts physically with MyoD, and this was shown to promote increased binding of MyoD to its cognate E-box binding motifs (Kim et al., 2008b). We

recently reported that Wnt treatment of myoblasts leads to acquisition of active chromatin marks at the promoters of myogenic genes; notably, these loci were enriched for E-boxes but not for TCF/LEF elements (Hulin et al., 2016a). We proposed that β-catenin may be recruited to E-boxes via its interaction with MyoD and that it may drive differentiation by activating myogenic genes in a TCF/LEF-independent manner; however we did not test the latter explicitly.

In this study we have focused on the mechanisms of Wnt/β-catenin signalling during myogenesis. To clarify the cell-autonomous requirement for β-catenin in differentiation, we developed independent β-catenin null models in adult primary mouse myoblasts using CRISPR. Analysis of null myoblasts confirmed that β-catenin is essential for morphological differentiation and for timely deployment of the myogenic gene expression program. Rescue studies with mutant forms of β-catenin showed that interaction of β-catenin with TCF/LEF factors is not required for differentiation. Instead β-catenin is required for Wnt-mediated enhancement of MyoD binding and for epigenetic activation of myogenic target genes. We also found that interactions of β-catenin with α-catenin at membrane junction complexes play an important role in efficient differentiation.

3.2 Methods

3.3 Results

3.3.1 Characterization of β-catenin null primary myoblasts

To assess the cell-autonomous requirement for β-catenin in myoblasts, we established a primary myoblast model with loss of β-catenin expression and characterized it phenotypically and molecularly. A lentiCRISPRv2 construct targeting exon 5 of β-catenin (Figure 1A) was introduced into low passage primary mouse myoblasts by lentiviral transduction and several clones were expanded. β-

catenin expression in these clones was assessed by RT-PCR (Figure 1B). Loss of β-catenin expression appeared to be mediated by NMD (nonsense mediated mRNA decay) as mRNA levels were less than 5% of parental levels (Figure 1B). All null clones had a similar phenotype (Supplemental Figure 2), which included a rounded morphology and impaired differentiation as discussed further below. Loss of β-catenin protein was confirmed at the protein level by immunostaining and immunoblotting for selected lines (e.g. Figures 1C, 1E). Consistent with the loss of β-catenin, Axin2 failed to be induced in null cells after Wnt3a treatment (Figure 1D). Sequencing analysis of selected clones revealed frameshift deletions generating premature stop codons in both alleles; the resulting predicted proteins would be truncated to <40 aa (see Supplemental Figure 2A, B), although these are unlikely to be made due to NMD-mediated loss of the transcript.

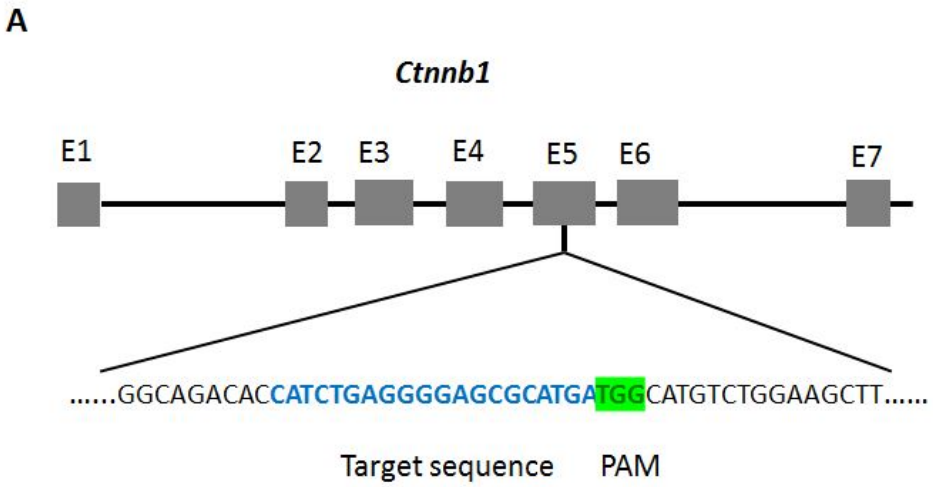

B

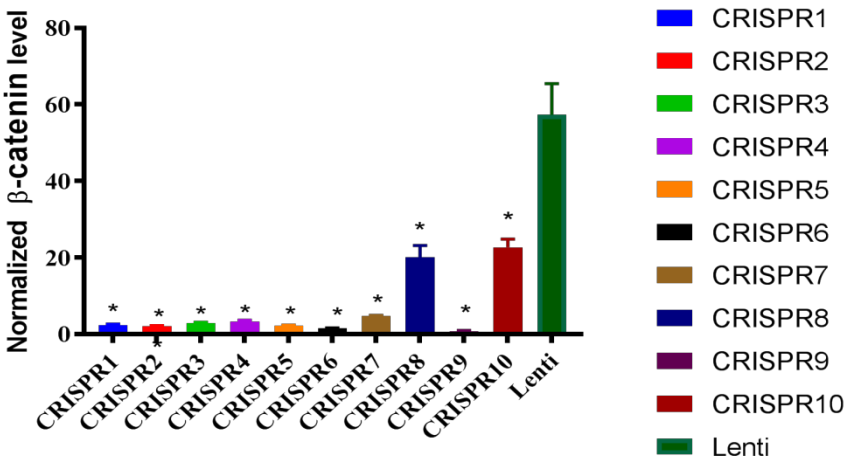
Normalized β-catenin level
80
60
40
20
0
CRISPR1
CRISPR2
CRISPR3
CRISPR4
CRISPR5
CRISPR6
CRISPR7
CRISPR8
CRISPR9
CRISPR10
Lenti
CRISPR1
CRISPR2
CRISPR3
CRISPR4
CRISPR5
CRISPR6
CRISPR7
CRISPR8
CRISPR9
CRISPR10
Lenti

C

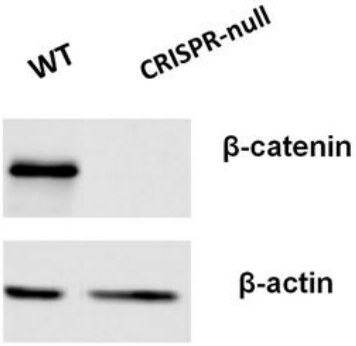
WT
CRISPR-null
β-catenin
β-actin

D

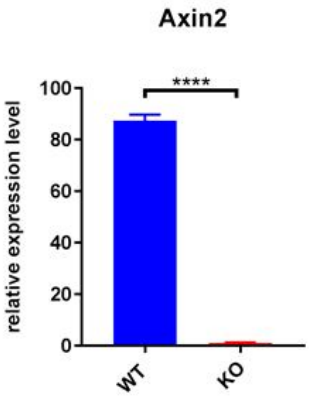
Axin2
****
relative expression level
100
80
60
40
20
0
WT
KO

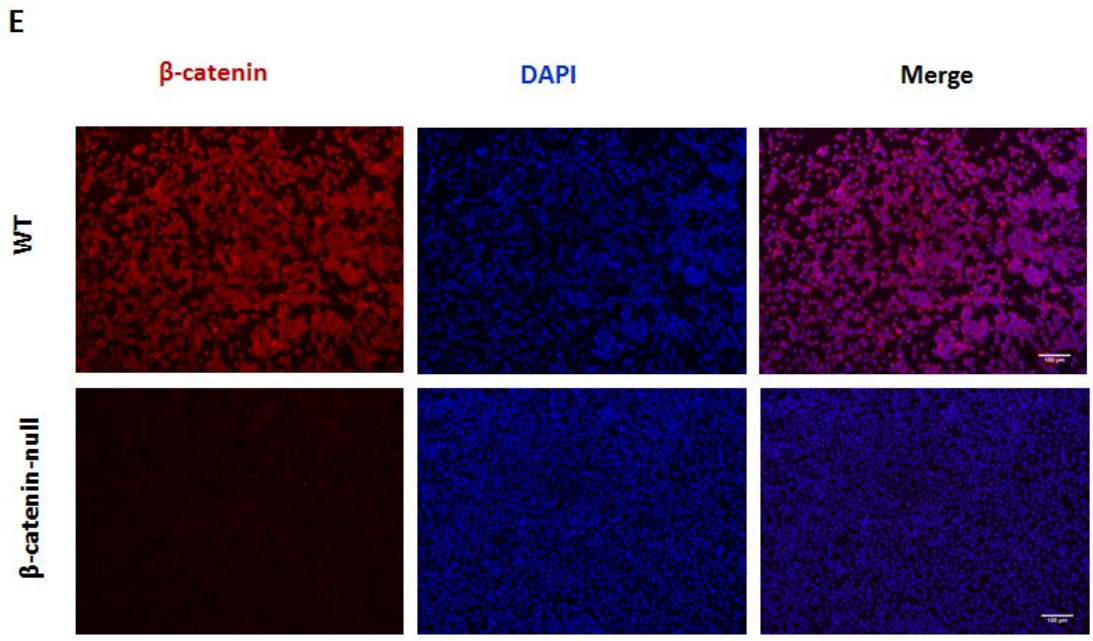

Figure 3.1: Characterization of β-catenin null primary myoblasts

(A) Strategy for Cas9/gRNA-mediated mutation of β-catenin. **(B)** β-catenin mRNA expression was measured by RT-PCR in multiple independent CRISPR-generated myoblast lines and compared to that in wild-type myoblasts transfected with the empty vector (LentiCRISPRv2). Data are normalized to the housekeeping gene RPS26 and show the average of two experiments performed in duplicate. Statistical analysis used one-way ANOVA with $p<0.05$ considered significant. **(C)** Western blot analysis using β-catenin antibody show β-catenin null primary myoblasts are completely absent of β-catenin protein expression. β-actin is used as a loading control. **(D)** β-catenin-null myoblasts show no induction of Axin2 mRNA after treatment with Wnt3a for 24hrs. Statistical analysis used t-test with $p<0.05$ considered significant. **(E)** Immunofluorescence labelling of β-catenin (red) in wild-type and β-catenin null primary myoblasts cultured; nuclei are stained with DAPI (blue). Scale bar represents 25 µm. n = 3.

3.3.2 Differentiation capacity of wild-type and β-catenin-null primary myoblasts and immunostaining analysis of myogenic markers

As mentioned, all null clones had a similar phenotype; a representative line is shown in Figure 2 in comparison to wild-type control cells that were transduced with empty lentiCRISPRv2 vector and passaged a similar number of times. When cultured in growth media, the β-catenin null cells appeared rounded relative to wild-type cells, and failed to undergo spontaneous differentiation upon reaching confluence (Figure

2A). Treatment with Wnt3a induced differentiation of wild-type cells leading to formation of aligned fibres that began to beat after 5 days in culture (Figure 2B and Supplemental Figures 3 and 4). In contrast, β-catenin null cells continued to proliferate after Wnt3a treatment (Supplemental Figure 2B) and fused slowly and infrequently giving rise to only very short fibres that were poorly aligned and did not beat even after 5 days in culture (Figure 2B and Supplemental Figures 3 and 4 videos). Upon long term culture, some β-catenin null cells fused into syncytia that became detached from the substrate and formed spherical balls (Figure 2B), indicating that loss of β-catenin impaired substrate attachment. We immunostained cultures with myogenin and MyHC antibodies at different time points after treating cells with Wnt3a to monitor differentiation, and found a substantial delay in the expression of both myogenin (Figure 3A) and MyHC (Figure 3B). In wild-type myoblasts myogenin and MyHC were first detected on day 1, whereas in β-catenin null myoblasts myogenin was detected on day 2-3 after induction of differentiation. While most β-catenin null cells eventually acquired myogenin and MyHC, they formed few multinucleated elongated myofibers. Interestingly, MyHC was expressed robustly in unfused cells and in syncytia that did not elongate. These data suggest that β-catenin is important for coupling of fusion and cytoskeletal remodelling with acquisition of molecular markers of differentiation.

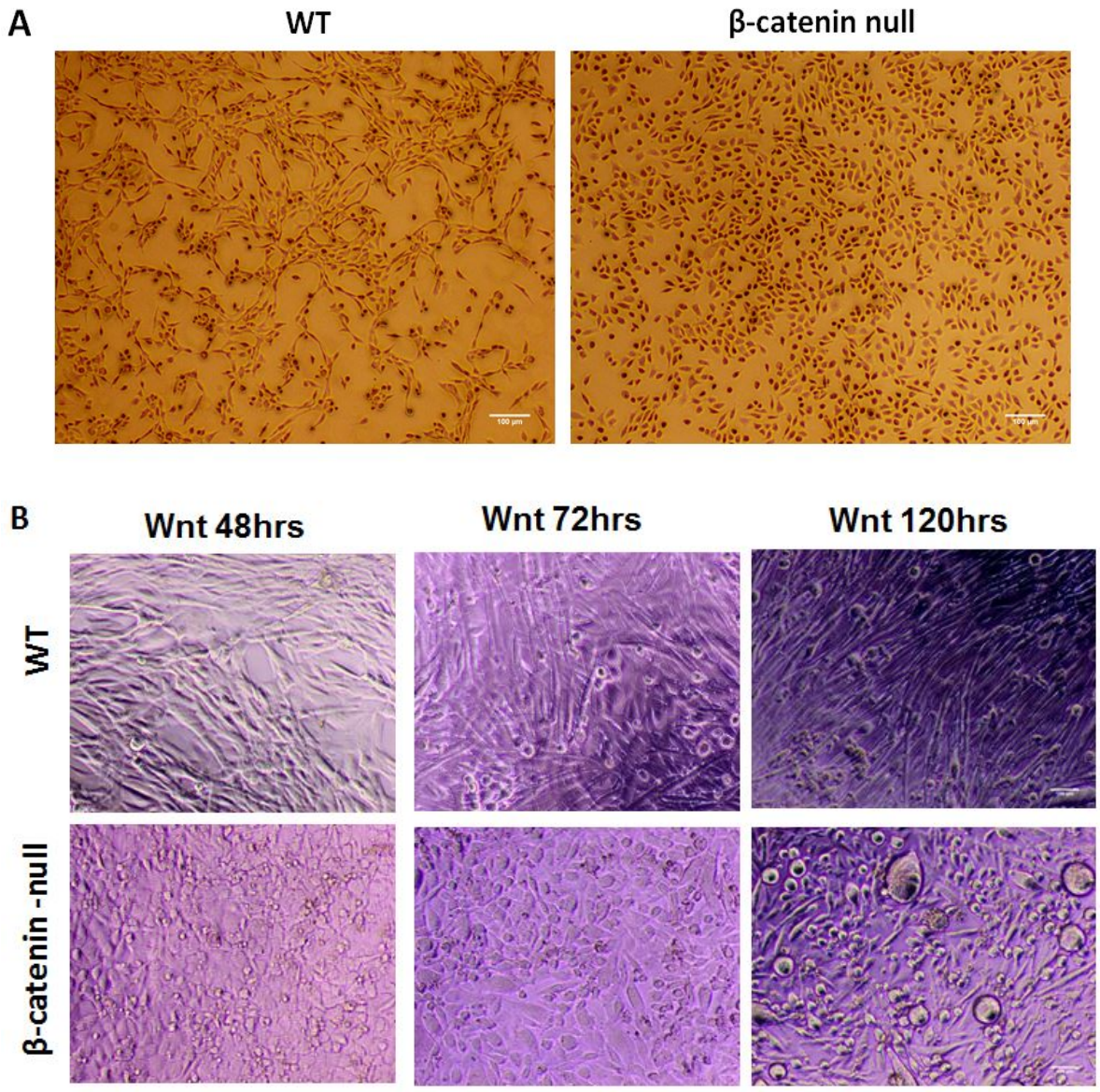

Figure 3.2: Differentiation capacity of wild-type and β-catenin-null primary myoblasts
(A) Phenotype of wild-type and β-catenin-null primary myoblasts cultured in growth media (GM) showing lack of spontaneous differentiation. **(B)** Phenotype of wild-type and β-catenin-null primary myoblasts after 5 days of culture in Wnt3a-containing media showing greatly impaired differentiation. n = 3.

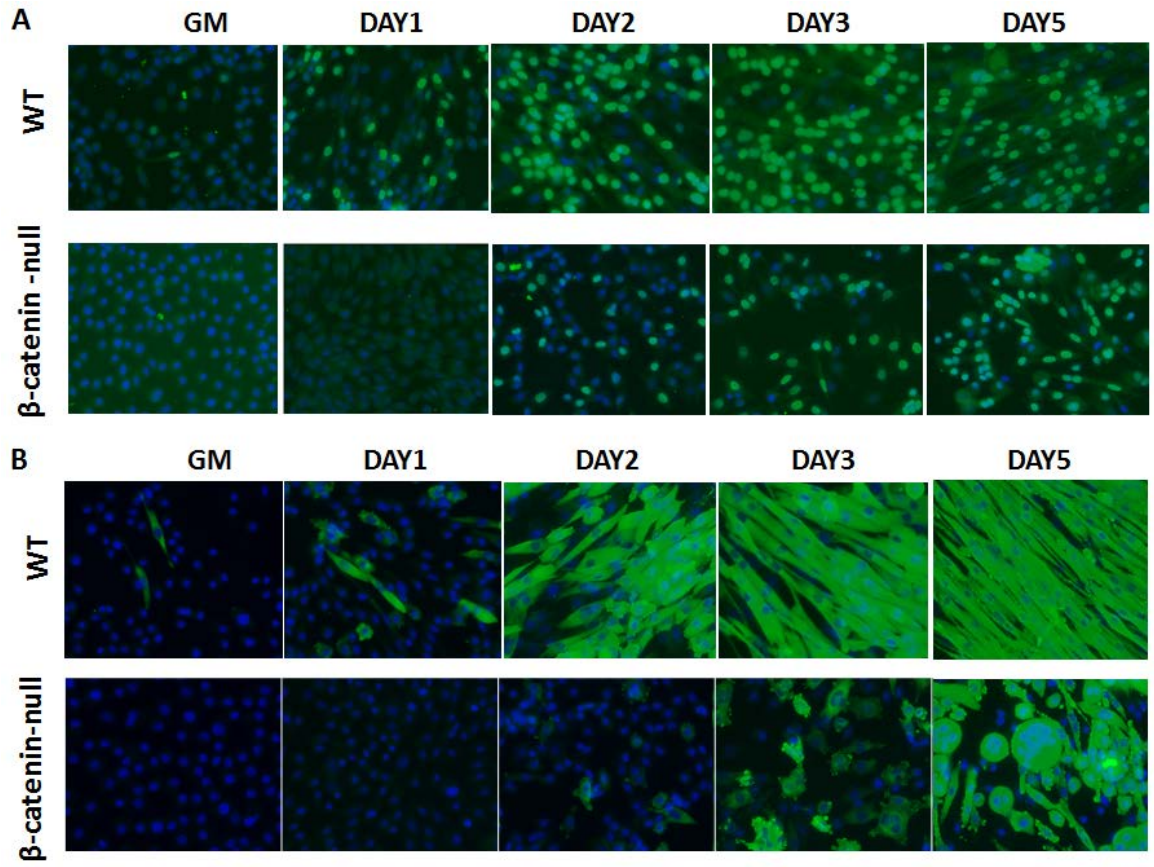

Figure 3.3: Immunostaining analysis of myogenic markers in wild-type and β-catenin-null primary myoblasts after Wnt3a-treatment

Immunofluorescence staining for Myogenin **(A)** or MyHC **(B)**, both green. Nuclei were stained with DAPI (blue). Images were captured at 0, 24, 48, 72, and 120hrs post treatment. n=3.

3.3.3 Transcriptomic analysis of wild-type and β-catenin-null cells after Wnt3a treatment identifies the Wnt-induced gene set

To understand the molecular changes underlying the phenotypic effects of loss of β-catenin, we performed transcriptomic analysis of wild-type myoblasts and two of the β-catenin null lines, after 24 hours of Wnt3a treatment. Comparative enrichment clustering of RNAseq data using Toppcluster (Kaimal et al., 2010) showed a large number of enriched Gene Ontology (GO) terms associated with muscle in wild-type cells but not in null cells (Figure 4A, B). The observation that Wnt3a treatment robustly induces the myogenic transcriptional program in wild-type cells has not been previously reported; however it is consistent with our recent epigenomic

analyses showing acquisition of activating histone modifications at myogenic genes (Hulin et al., 2016a). When comparing the most significantly enriched GO terms, muscle contraction and striated muscle formation were the top two hits in wild-type cells; no muscle-associated terms appeared in the top 10 hits in β-catenin null cells and the most significantly enriched GO categories were related to cholesterol and lipid metabolism (Figure 4C, D). The failure of null cells to activate myogenic gene expression programs within 24 hours of induction of differentiation is consistent with the delay in myogenin acquisition seen in Figure 3.

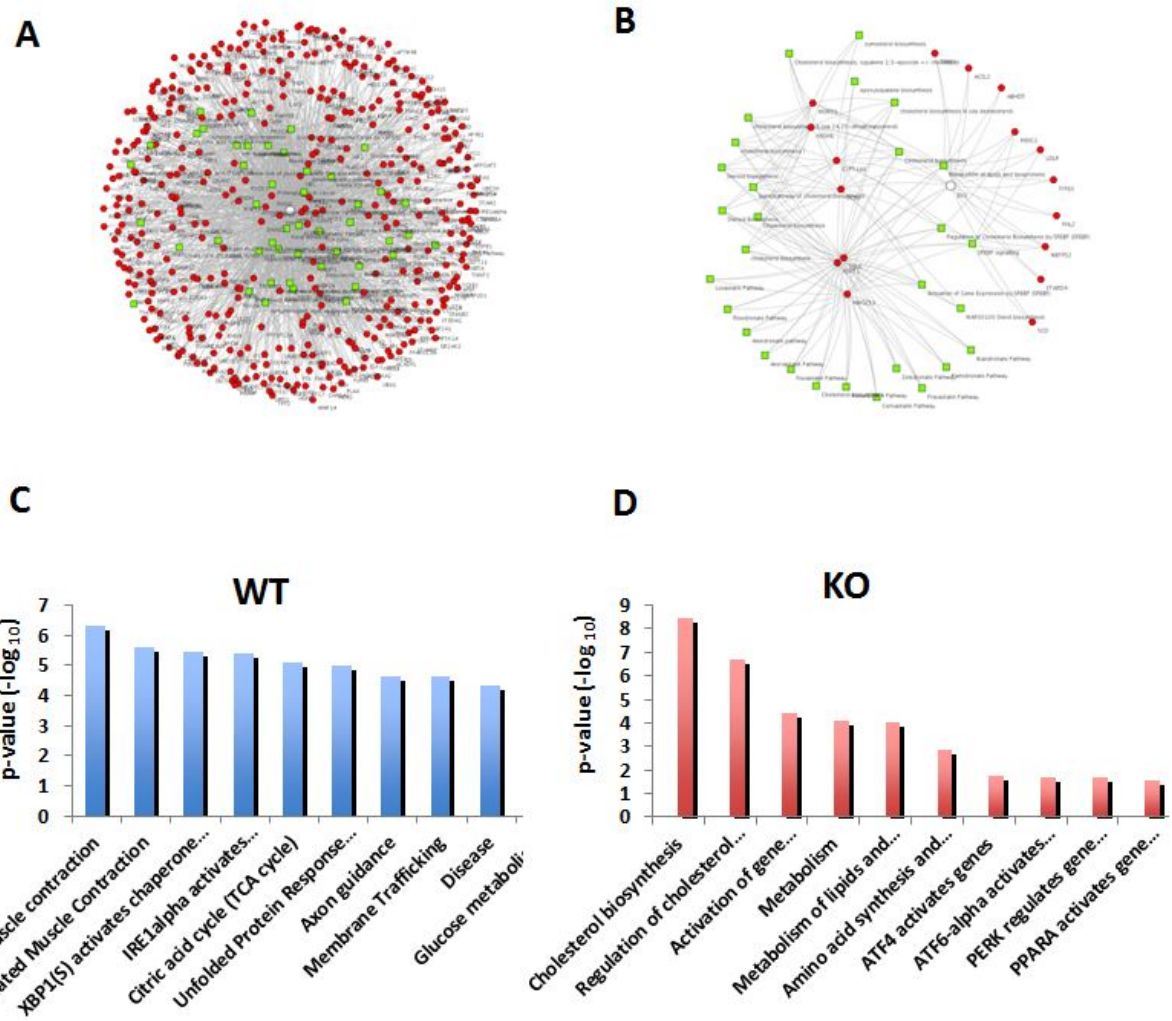

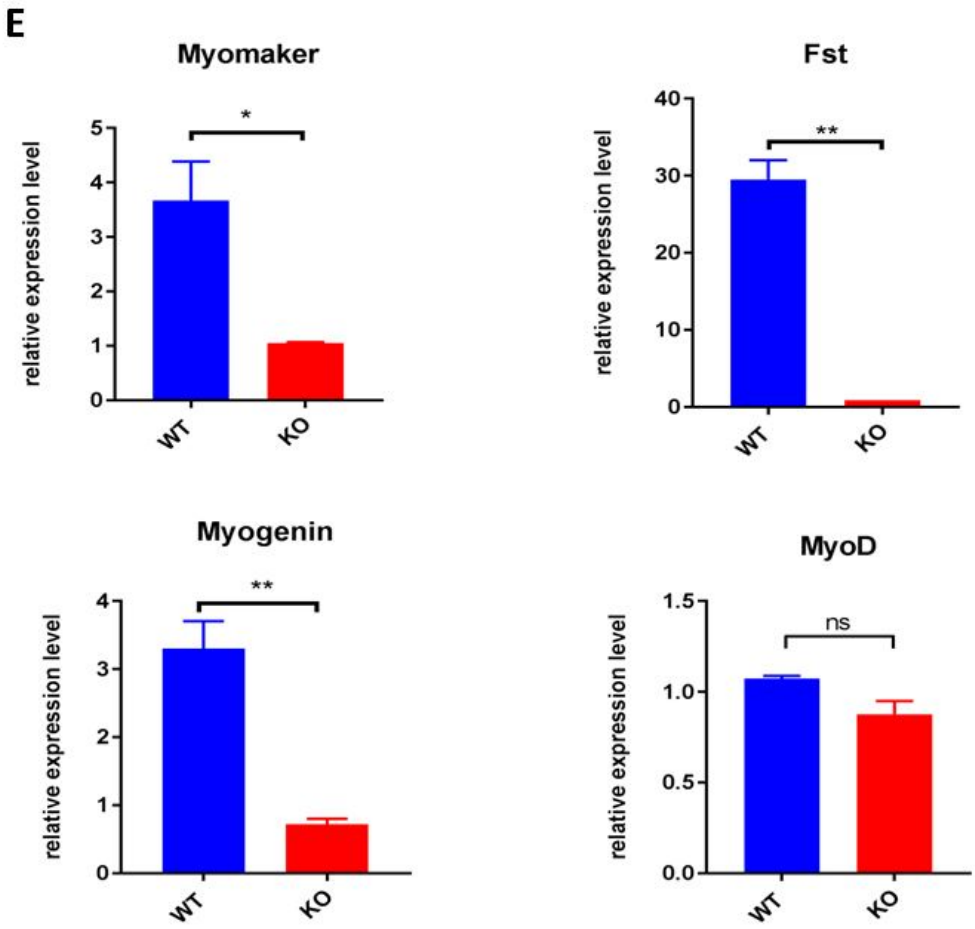

Figure 3.4: Transcriptomic analysis of wild-type and β-catenin-null cells after Wnt3a treatment identifies the Wnt-induced gene set

(A) and **(B)**: RNA-Seq was performed on wild-type (A) and β-catenin-null (B) myoblasts treated with Wnt3a or control (L-cell) medium for 24hrs. Genes upregulated by Wnt3a treatment (Wnt3a/L cell ≥ two fold - red nodes) were analyzed using Toppcluster to define associated pathways (green nodes). Network analysis of global gene expression changes in wild-type shows many genes upregulated by Wnt3a in wild-type but not in β-catenin-null myoblasts. **(C)** and **(D)**: Gene Ontology (GO) terms significantly enriched in the differentially expressed gene set (Wnt3a/L cell ≥ two fold) identified in wild-type (C) and β-catenin-null (D) myoblasts. **(E)** Wnt3a induces expression of myogenic genes Myomaker (Tmem8c), Fst, and Myogenin in myoblasts in a β-catenin-dependent manner. Quantitative RT-PCR was performed on wild-type and β-catenin-null myoblasts treated with Wnt3a or control (L-cell) medium for 24hrs. Data are normalized to the housekeeping gene RPS26 and are the average of three experiments performed in duplicate. Statistical analysis used t-test with $p<0.05$ considered significant. n = 3.

To validate the genome-wide analysis, we performed qRT-PCR for selected Wnt targets and myogenic markers after Wnt3a treatment (Figure 4E). There was significantly less induction of the key myogenic regulator and MyoD target myogenin (Figure 4E). Follistatin (Fst) was previously shown to be a Wnt-target (Jones et al., 2015b) and its induction was almost completely abolished. Myomaker (Tmem8c) is a gene that we have identified as being a target of β-catenin using ChIP (not shown), and is also essential for myoblast fusion (Millay et al., 2014a); Myomaker induction by Wnt was also abolished in null cells (Figure 4E).

3.3.4 Transfecting constitutively-active β-catenin is sufficient to rescue morphological differentiation and expression of myogenic genes in β-catenin-null myoblasts

Although all of our independent β-catenin null lines showed a similar phenotype of impaired differentiation; it was important to confirm the phenotype using a rescue experiment. We transfected β-catenin-null myoblasts with either a constitutively-active/stable β-catenin expression plasmid or an empty vector control, together with a GFP-expression plasmid to assess transfection efficiency. Of note, null myoblasts transfected substantially more efficiently than wild-type myoblasts (~80% of null cells were GFP-positive relative to 50-60% of wild-type myoblasts), possibly due to their rounded/poorly-attached phenotype, or possibly due to other unknown membrane changes. When transfected with stable β-catenin, the null cells began to elongate and fuse (Figure 5A); control transfected cells remained rounded and unfused. β-catenin transfection also induced expression of Fst, Myomaker (Tmem8c) and myogenin in null cells and wild-type cells (Figure 5B, C). The induction of Myomaker in null cells was higher than the other targets examined, possibly showing a high sensitivity of this target to β-catenin levels (Figure 5B, C). Overall the results support the conclusion that absence of β-catenin is responsible for the loss of differentiation capacity and myogenic gene expression in the null cells.

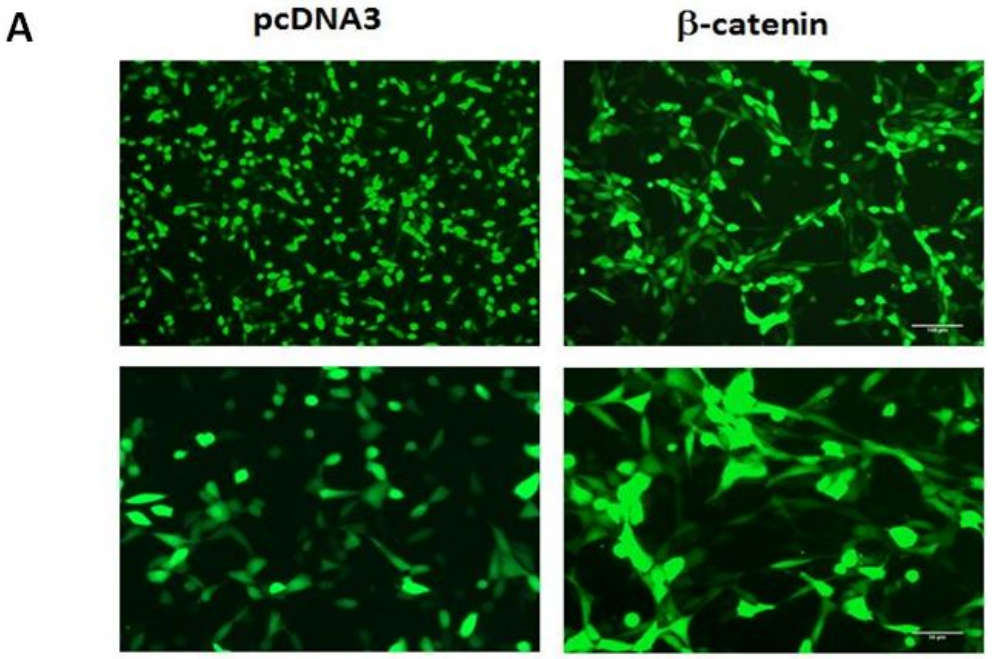
A
pcDNA3
β-catenin

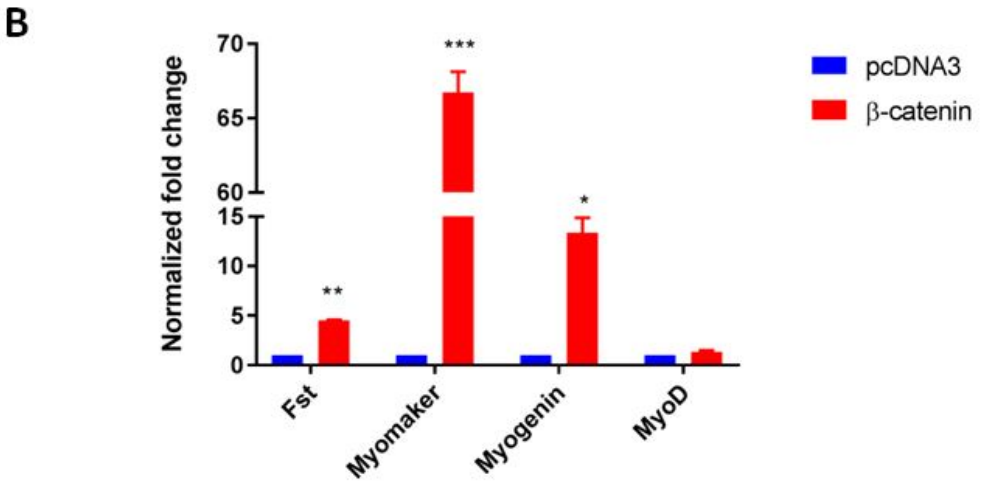
B
Normalized fold change
70
65
60
15
10
5
0
***
**
*
pcDNA3
β-catenin
Fst
Myomaker
Myogenin
MyoD

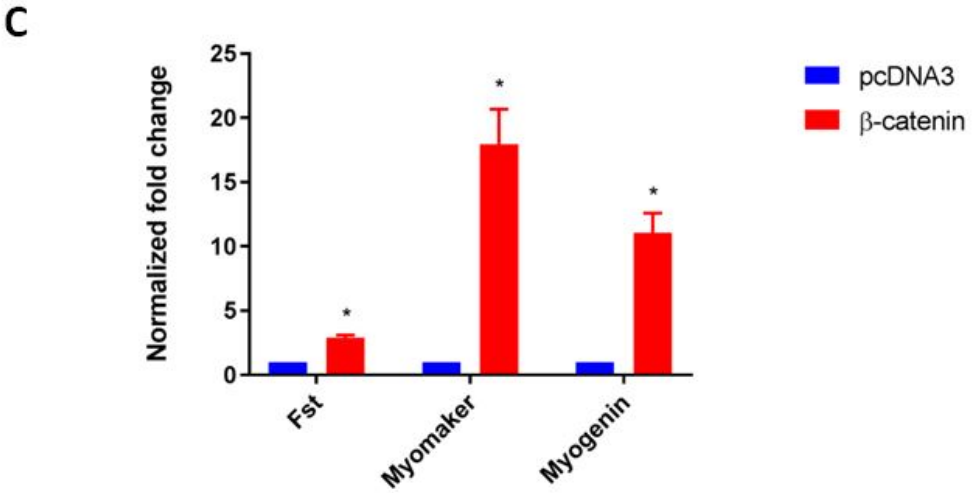
C
Normalized fold change
25
20
15
10
5
0
*
*
*
pcDNA3
β-catenin
Fst
Myomaker
Myogenin

Figure 3.5: Transfecting constitutively-active β-catenin is sufficient to rescue morphological differentiation and expression of myogenic genes in β-catenin-null myoblasts

(A) The constitutively active β-catenin expression plasmid was co-transfected with a GFP-expression plasmid to identify transfected cells. β-catenin-transfected cells show fusion into myotubes whereas those transfected with empty vector do not. Upper panel, scale bar represents 25 μm; Bottom panel, scale bar represents 50 μm. **(B, C)** Myogenic gene induction after transfection of β-catenin in β-catenin null myoblasts **(B)** or wild-type myoblasts **(C)**. Quantitative RT-PCR analysis was performed 48hrs post transfection. Data are normalized to the housekeeping gene RPS26 and then to pcDNA3 empty vector transfection (set to a value of 1). The results shown are the average of at least three independent experiments performed in duplicate. Statistical analysis in panels B and C used multiple t-test with $p<0.05$ considered significant.

3.3.5 genome-wide analysis of activating-histone modifications in wild-type and β-catenin null cells

To further examine the mechanism of action of β-catenin, we performed genome-wide analysis of activating-histone modifications in wild-type and β-catenin null cells. As we found previously (Hulin et al., 2016a), in wild-type cells, activating modifications (H3KAc, H3K4me3) were enriched at myogenic gene promoters 24 hrs after Wnt3a treatment. In contrast, in β-catenin null cells there was no enrichment of activating histone modifications at myogenic genes. Motif analysis showed that, consistent with our earlier study (Hulin et al., 2016a), in wild-type cells, promoters enriched in activating modifications after Wnt3a treatment were enriched for MRF and MEF binding motifs but not TCF/LEF binding motifs (Figure 6A). In null cells, there were no significantly enriched motifs (with P values $>10^4$). These data suggest that β-catenin may promote MRF (e.g. MyoD) recruitment to myogenic gene targets: to test this model we performed MyoD-ChIP-seq in wild-type and β-catenin null cells after treatment with Wnt3a. We identified genomic regions showing increased binding of endogenous MyoD 24 hrs after Wnt3a treatment, and then performed GO and motif analysis. In wild-type cells, GO analysis showed significant enrichment of MyoD binding to genes associated with myogenic differentiation (Figure 6B, left),

specifically at loci that were enriched in MRF and MEF binding motifs (Figure 6C). In null cells, there was a slight increase in MyoD binding after Wnt3a treatment, but the loci showing enhanced binding were not associated with myogenic genes (Figure 6B, right), and contained no statistically-enriched motifs (not shown), suggesting that this was non-specific. These data suggest that in wild-type myoblasts, Wnt3a promotes increased binding of MyoD to myogenic target loci in a β-catenin-dependent manner. This may be mediated by the direct interaction of MyoD with β-catenin (Kim et al., 2008b). We also considered that increased binding of MyoD to Myomaker after Wnt3a treatment could be due to an increase in MyoD levels. However immunoblotting analysis of myoblasts treated with or without Wnt3a showed no difference in MyoD protein levels (Supplemental Figure 5 A, B). Levels of the inhibitory partner of MyoD, ID1, were also comparable in wild-type and myoblasts cells after Wnt3a treatment (Supplemental Figure 5 C, D).

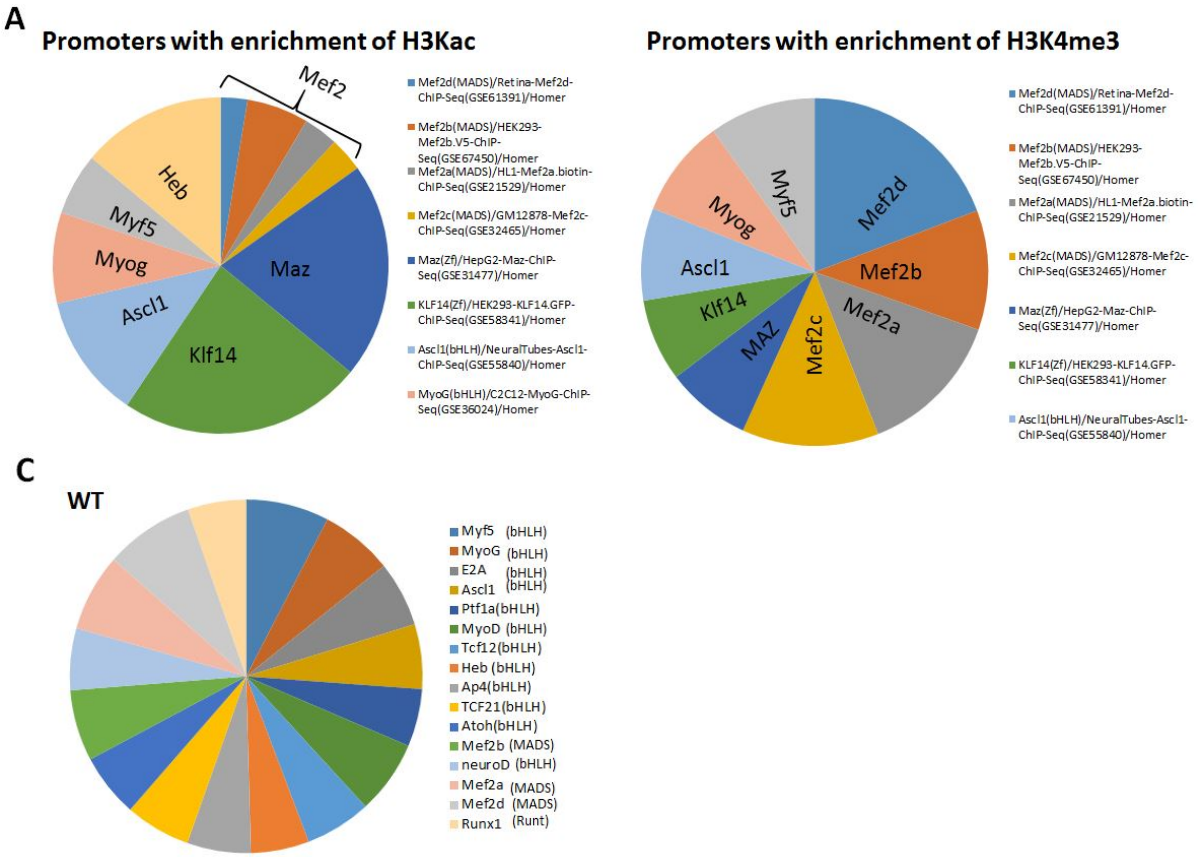

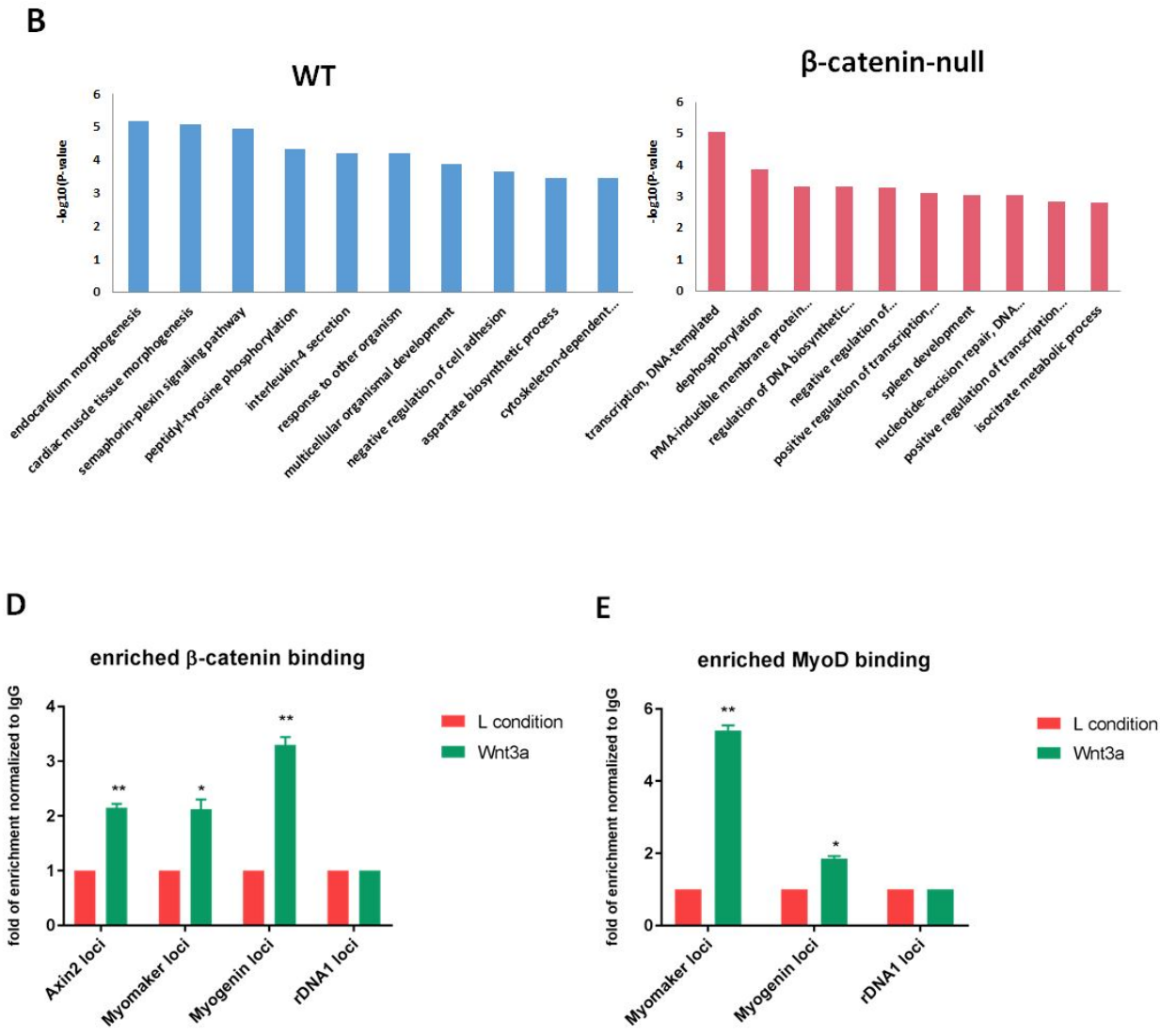

Figure 3.6: Epigenomic analyses suggest that β-catenin may promote MyoD association with chromatin

(A) H3Kac and H3K4me3 ChIP-seq was performed using chromatin from wild-type myoblasts treated with control- or Wnt3a-media for 24hrs. Homer analysis was used to identify the top 10 motifs that are enriched in promoter regions that show increased levels of H3Kac and H3K4me3 (>3fold) after Wnt3a induction (represented as target sequences with motif/total sequences with motif). **(B)** MyoD ChIP-seq analyses of wild-type and β-catenin null primary myoblasts treated with Wnt3a medium for 24hrs. Gene Ontology (GO) analysis was performed on the set of genes showing increased MyoD binding after Wnt3a-treatment (Wnt/L cell ≥ two fold) in wild-type (left) and β-catenin CRIPSR-null (right) myoblasts. Wild-type myoblasts show significant enrichment of muscle-associated GO categories; β-catenin-null myoblasts do not show enrichment in any muscle specific categories. **(C)** The top 15 motifs (Homer analysis) seen in promoter regions showing increased MyoD binding (>2fold) after Wnt3a-treatment of wild-type myoblasts (target sequences with motif/total

sequences with motifs). Statistical analysis in panels B and C used multiple t-test with $p<0.05$ considered significant. **(D-E)** Wnt3a increases binding of β-catenin and MyoD to the proximal promoters of the Myomaker and myogenin genes as shown by ChIP-qPCR analysis. Chromatin from wild-type primary myoblasts treated with control or Wnt3a medium for 48 hrs was used for ChIP with β-catenin **(D)** or MyoD **(E)** antibodies. qPCR was used to assess enrichment of the Myomaker and myogenin promoters in both β-catenin- and MyoD-ChIP samples; the Axin2 enhancer was used as a control for β-catenin-ChIP. Data were first normalised to a control non-target locus (rDNA1) and then to the mock ChIP with preimmune IgG, set to a value of 1. N = 3. Error bars represent SEM. * $p < 0.05$ and ** $p < 0.001$.

To further explore the potential for co-recruitment of β-catenin and MyoD to myogenic targets, we focussed on the target genes Myomaker and myogenin. The mouse myogenin gene is a well-defined MyoD target (Yee and Rigby, 1993). The chicken Myomaker gene was reported to be a MyoD target (Luo et al., 2015b); however regulation of mouse Myomaker has not been investigated. We identified putative E-box motifs (Supplemental Figure 6) within the region of the mouse Myomaker proximal promoter that showed enrichment of H3KAc after Wnt3a treatment of myoblasts; moreover we showed that this region recruits heterologously expressed MyoD (Supplemental Figure 6). ChIP-qPCR analysis showed that β-catenin was recruited to the E-box-containing regions of both the Myomaker and myogenin promoters after Wnt3a treatment of myoblasts, with enrichment values similar to that at the Axin2 enhancer (Figure 6D; and also see (Hulin et al., 2016a)). Endogenous MyoD was recruited to the same promoter regions after Wnt3a treatment as shown by ChIP (Figure 6E); supporting the idea that both factors bind these targets.

3.3.6 Comparison of the ability of wild-type and mutant forms of β-catenin to rescue differentiation of β-catenin null myoblasts

To directly test the model that β-catenin may be recruited via its interactions with MRFs such as MyoD (Kim et al., 2008b), rather than interactions with TCF/LEF

family members, we attempted to rescue the phenotype of the β-catenin-null cells using a variant of β-catenin that does not interact with TCF/LEF. Previous structure-function studies revealed residues in β-catenin essential for interaction with TCF/LEF proteins, specifically two positively charged residues that are referred to as 'charged buttons' (Graham et al., 2000). We generated a mutant form of the constitutively active/stable β-catenin protein in which these residues were mutated to negative charges and tested its ability to induce Axin2 (Supplemental Fig 7). The mutant form of stable β-catenin (referred to here as the TCF-binding site mutant) was unable to induce Axin2, confirming functional ablation of TCF/LEF interaction. When this TCF-binding site mutant was transfected into β-catenin null myoblasts, morphological differentiation was indistinguishable from that of cells transfected with wild-type β-catenin (Figure 7A). That the TCF-binding site mutant fully rescued differentiation was confirmed by quantifying the number of nuclei in MyHC positive fibers (Figure 7B, C). Overall, these data support the model that β-catenin may induce differentiation via its direct interactions with MyoD, rather than via TCF/LEF. Unfortunately the residues involved in interaction of β-catenin with MyoD have not been defined, so this interaction could not be specifically ablated to confirm this model. To better understand the relative roles of β-catenin and MyoD in myogenesis, we also compared the effects of expressing MyoD or constitutively active/stable β-catenin in the mesenchymal progenitor cell line C3H10T1/2 that does not endogenously express MyoD. Ectopic expression of MyoD in C3H10T1/2 cells induced myogenic conversion (Supplemental Figure 8) as previously reported (Aurade et al., 1994), as shown by elongation and interaction of the myoblasts (Figure 3.7A) resulting in increased fusion (Figure 3.7C). In contrast, expression of stable β-catenin in C3H10T1/2 cells did not produce a myogenic phenotype, suggesting that it is not sufficient to induce MyoD expression. These data provide

further support for the model that β-catenin cooperates with MyoD, rather than acting genetically upstream of this factor.

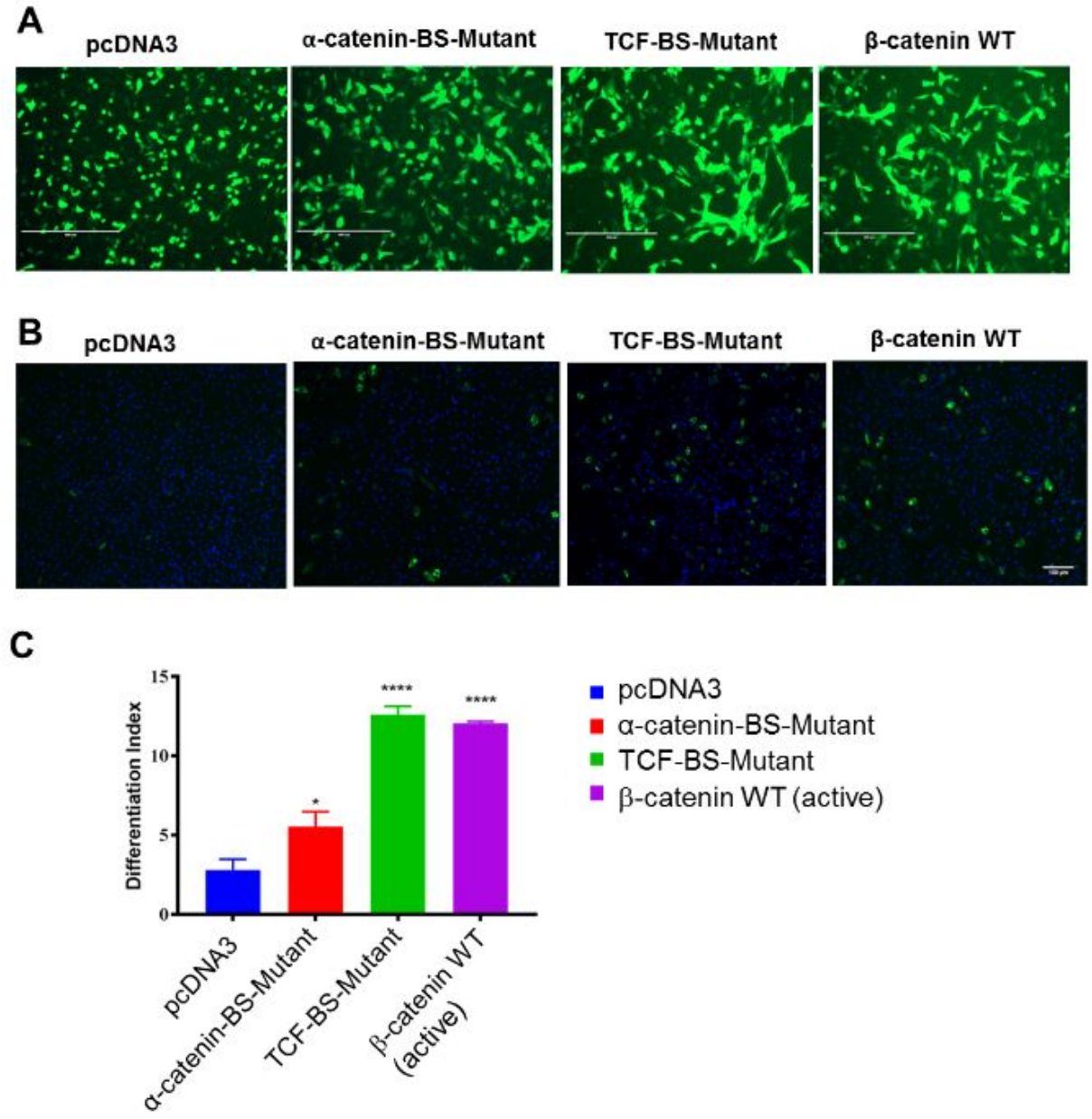

Figure 3.7: Comparison of the ability of wild-type and mutant forms of β-catenin to rescue differentiation of β-catenin null myoblasts

(A) β-catenin null myoblasts were cotransfected with GFP and one of the following expression plasmids: empty pcDNA3, α-catenin-binding site (BS) mutant form of β-catenin (cannot interact with α-catenin), TCF-binding site (BS) mutant form of β-catenin (cannot interact with TCF/LEF), wild-type β-catenin (constitutively active/stable). Scale bar represents 100 μm. **(B, C)** Quantitation of differentiation was achieved by immunostaining with MyHC **(B)** and counting the percentage of nuclei in MyHC positive myofibers **(C)**.

Statistical analysis used one-way ANOVA with $p<0.05$ considered significant. n = 3.

Although the studies reported here focus on the nuclear β-catenin pool, the majority of β-catenin molecules in the cell are associated with cadherins at membrane in junction complexes. This core complex includes α-catenin as a key linker between cadherin/β-catenin complexes and the actin microfilament system (Huveneers and de Rooij, 2013); interaction of β-catenin with α-catenin is proposed to uncouple interaction of the latter with actin thus controlling local filament assembly (Xu and Kimelman, 2007; Yamada et al., 2005). We examined whether expression of a mutant form of β-catenin that cannot interact with α-catenin could promote differentiation of β-catenin null myoblasts. The residues that control interaction of β-catenin with α-catenin have been previously defined (Aberle et al., 1996; Nieset et al., 1997); we mutated these residues (Threonine 120 and Valine 122) in constitutively active/stable β-catenin to alanine generating a variant that does not bind to α-catenin. This mutant (referred to here as the α-catenin binding site mutant) was able to induce Axin2 expression as effectively as wild-type β-catenin (supplemental Figure 7). The α-catenin-binding site mutant only partially rescued differentiation (Figure 7), suggesting that both the nuclear functions of β-catenin, and interactions between β-catenin and α-catenin at membrane junction complexes, are required for efficient differentiation.

3.4 Conclusions and Discussion

The goal of this study was to confirm and define mechanistically the cell-autonomous requirement for β-catenin in myoblast differentiation. A previous study by Murphy et al (Murphy et al., 2014a) had reported that β-catenin expression in satellite cells and their myoblast progeny was not required for adult (regenerative) myogenesis. That study tested the effects of β-catenin ablation *in vivo*, but did not

examine the ability of the null myoblasts to differentiate in culture (Murphy et al., 2014a). The result was sufficiently unexpected that an independent replication was performed (Rudolf et al., 2016a). The results of the latter study were in sharp disagreement with those of the former (Murphy et al., 2014a), showing that myogenesis was impaired both *in vivo*, and *in vitro* in the absence of β-catenin. The reason for the discrepancy between these studies is not clear, although the possibility that the earlier study was compromised by the presence of unrecognized 'recombination escapers' has been put forth (Rudolf et al., 2016a). Given that both of these studies ablated β-catenin via recombination *in vivo*, we felt that it was important to generate an independent *in vitro* model in which the cell autonomous requirement for β-catenin could be examined. Our model is clonal, hence our results are not confounded by residual (e.g. unrecombined) wild-type cells that might be selectively enriched during manipulations; moreover the behaviour of the cells has not been pre-programmed by myofibre/niche interactions prior to loss of β-catenin.

Our findings are consistent with those of Rudolf et al (Rudolf et al., 2016a), in that β-catenin was critical for effective differentiation of myoblasts. When fusion occurred it appeared largely uncoupled from the assembly of the myofibrils that maintain myofibre architecture; hence the formation of ball-shaped syncytia that were poorly attached to the substrate in long term cultures. Moreover, we observed cells that expressed myogenin and MyHC without fusing or elongating; further supporting the idea that β-catenin is important for coupling of molecular differentiation, fusion, and myofibril assembly. These morphological data are consistent with, but extend beyond, that shown by Rudolf *et al* (Rudolf et al., 2016a). Our gene expression data are also consistent with, but extended beyond those of Rudolf *et al* who focussed on the role of β-catenin in promoting TGF β signalling (Rudolf et al., 2016a). We found that β-catenin null cells were highly deficient in activation of the myogenic gene

expression program after Wnt3a treatment. The functions of targets that failed to be induced within 24 hours of Wnt treatment span transcriptional regulation (myogenin), signalling (Fst), and mechanochemistry (Myomaker). While loss any of these targets individually might have led to failure of differentiation, our RNAseq and histone ChIP-seq data suggests that global deregulation of the myogenic program is the fundamental basis for the phenotype of the null cells.

We previously proposed that β-catenin might cooperate with MyoD to promote myogenic differentiation. This model was based on our previously published genome-wide epigenomic analyses of myoblasts (Hulin et al., 2016a), which showed that Wnt3a increased chromatin accessibility at loci that were highly enriched in binding sites for MRFs, but not enriched in binding sites for TCF/LEF. In this study we found that loss of β-catenin prevents Wnt-induced enhancement of MyoD binding at myogenic target loci. Moreover, analytical ChIP studies suggested that β-catenin and MyoD bind to common myogenic loci. Genome-wide analysis of β-catenin and MyoD binding after Wnt3a treatment would ideally generalize the co-binding model; however we were unable to obtain consistent β-catenin ChIP-seq results in myoblasts; possibly because β-catenin associates in large complexes that are inconsistently represented after the shearing/size selection steps of library construction. Critically however, we were able to exploit our null cells to dissect the functions of β-catenin using rescue studies. A key finding was that the variant of β-catenin that could not interact with TCF/LEF proteins was able to rescue differentiation. This provides strong support for our contention that β-catenin may promote myogenesis via its interactions with MRFs such as MyoD (Kim et al., 2008b), rather than interactions with TCF/LEF family members. Furthermore, β-catenin-dependent increase in binding of MyoD to target loci after Wnt treatment was not due to any increase in MyoD levels or reduction in levels of the MyoD

inhibitor ID1. It is possible however that Wnt/β-catenin signalling promotes acetylation of MyoD or other post-transcriptional changes that promote its association with E-boxes. This remains to be tested. Given that MyoD binds to β-catenin directly (Kim et al., 2008b) it is possible that β-catenin helps promotes local histone remodelling through its co-activators to increase accessibility of MyoD to E-boxes. Of note, β-catenin and MyoD share the coactivator p300. p300 is known to be required for myogenic differentiation (Polesskaya et al., 2001). Moreover, we have found that chemical inhibition of the interaction between β-catenin and p300 blocks differentiation (data not shown), supporting the idea that β-catenin may ensure a critical mass of HAT activity at MyoD-target loci and this leads to increased MyoD binding, as well as recruitment of other MRFs and MEFs that acts as transcriptional activators.

The apparent redundancy of β-catenin-TCF/LEF interactions for myogenic differentiation in our study is in conflict with a very recent publication that suggested that TCF4 is required for differentiation (Agley et al., 2017). In this study by Agley *et al*, overexpression of active β-catenin or dominant-negative (DN)-TCF4 in human myoblasts impaired differentiation resulting in thin fibres. Overexpression of Wnts or active β-catenin has been previously reported to produce thinner myofibers due to precocious differentiation of myoblasts at the expense of proliferation (Brack et al., 2008b; Murphy et al., 2014a; Rudolf et al., 2016a). We did not see unusually thin myofibers when we expressed active β-catenin in our null cells; however rescue and over-expression are different, and our response may represent the normal behaviour of cells with physiological levels of active β-catenin, rather than the disruptive effects of excess β-catenin. The inhibitory effect of DN-TCF4 on differentiation seen by Agley *et al* was taken to indicate that β-catenin-TCF complexes are required for myogenesis (Agley et al., 2017). However, DN-TCF4 expression dramatically

reduced levels of active β-catenin relative to control cells (Agley et al., 2017); a state that would be expected to impair differentiation based on our findings and those of Rudolf et al (Rudolf et al., 2016a), regardless of the mechanism of β-catenin action. Previous knockout studies also suggest that expression of TCF4 in myoblasts is not essential for myogenesis, but that it helps specify muscle fiber type (Mathew et al., 2011). Formation of appropriately sized myofibers clearly requires a balance of myoblast proliferation and differentiation. Our overall model that β-catenin-TCF interactions are not required to activate the myogenic program, but are required for appropriate feedback to the Wnt pathway (via targets such as Axin2) to prevent precocious/excessive fusion, is not inconsistent with any of the previous published findings, including those of Agley *et al* (Agley et al., 2017).

Our data also showed for the first time that interaction of β-catenin with α-catenin was important although not essential for myoblast differentiation. This result is consistent with reports that cadherins are essential in this process (Ozawa, 2015; Wrobel et al., 2007) and in line with the prevailing notion that differentiation involves cooperation and feedback between membrane signalling events and the nuclear program. Future work could further explore the requirements for different functions of β-catenin by transfecting additional mutant forms.

In summary, we have provided strong support for a new model in which myoblast differentiation requires the cooperation of β-catenin with MyoD and not TCF/LEF, and that this myogenic complex targets a suite of genes that coordinate the differentiation program. Further work to dissect the coactivator requirements of this complex may ultimately allow differential targeting of desirable pro-myogenic vs deleterious (e.g. pro-fibrotic) functions of β-catenin in muscle. In addition, our *in vitro* studies suggest that the transient inhibition of β-catenin in transplanted

myoblasts might be a useful approach to suppress spontaneous differentiation and promote sustained proliferation *in vivo* thus increasing engraftment rates, prior to reactivation of β-catenin to allow fusion into myofibers.

3.5 Supplemental Figures

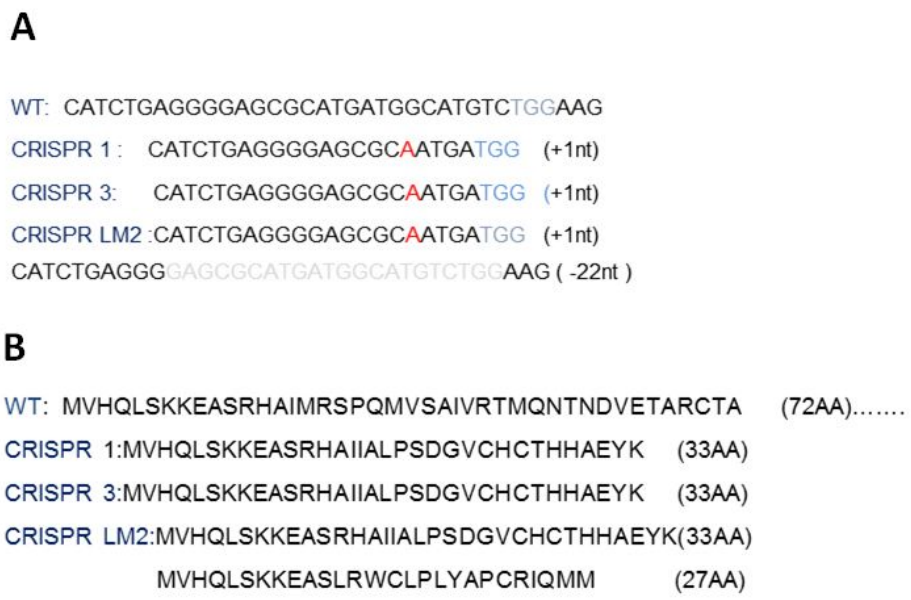

Supplemental Figure 3.1: Sequences of mutations in three selected β-catenin-null lines
(A) Mutant No.1 and No.3 show one nt ("A") insertion before the PAM (TGG), in each case the second allele did not amplify suggesting a large deletion. Mutant LM2 shows one nt ("A") insertion before PAM in one allele, and 22nt missing from the second another allele. **(B)** Predicted translation of β-catenin-null alleles showing protein truncation. Wild-type β-catenin exon5 is predicted to be translated into 72 corresponding amino acids; Mutant No.1 and No.3 are predicted to stop translation at 33 amino acids; Mutant LM2 is predicted to stop translation at the 33 amino acids for one allele and 27 amino acids for the second allele.

A

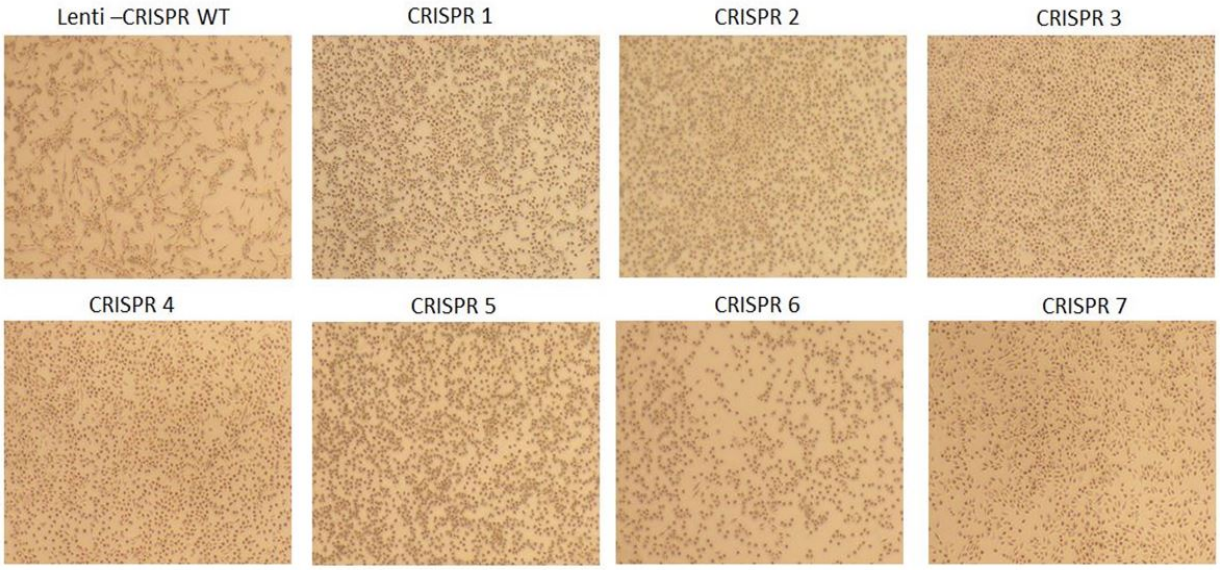

B

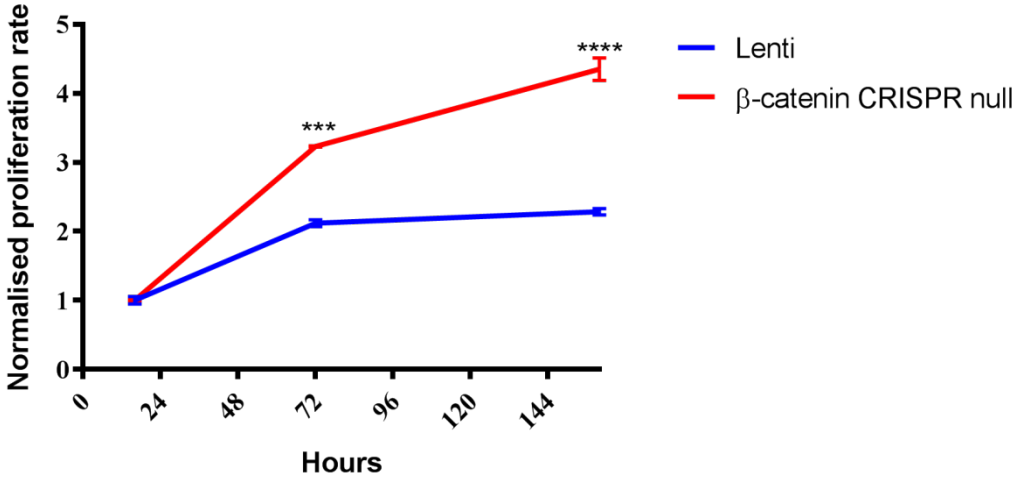

Supplemental Figure 3.2:

(A) Images of multiple independent β-catenin CRISPR null myoblast lines and wild-type myoblasts maintained in GM. The consistent phenotype of β-catenin null cells was rounded morphology and lack of spontaneous differentiation. **(B)** β-catenin CRISPR null myoblasts show continued proliferation in high-density culture while proliferation of wild-type myoblasts (Lenti) plateaus. Statistical analysis used two-way ANOVA. n = 3.

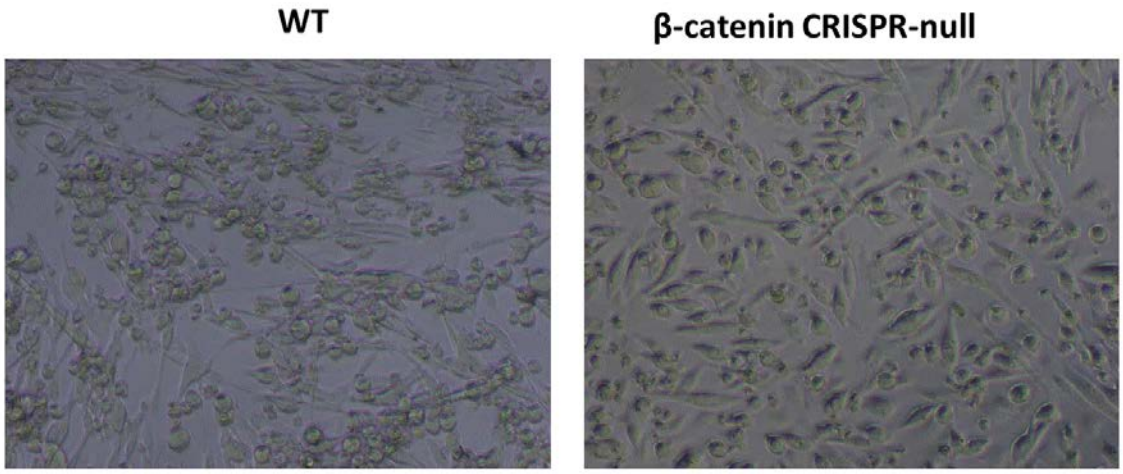

Supplemental Figure 3.3: Videos showing that long-term cultures of wild-type, but not β-catenin-null myoblasts can form contracting myofibers (see attached files for videos)

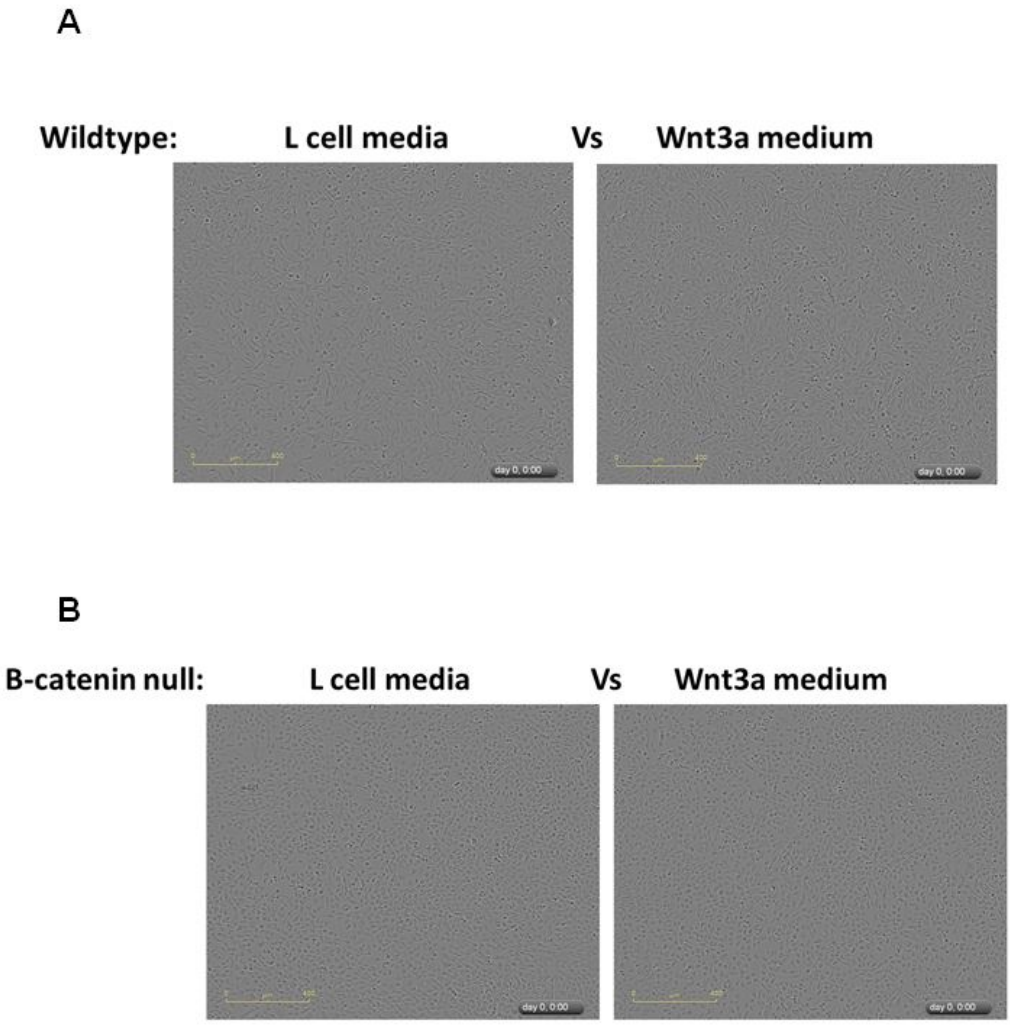

Supplemental Figure 3.8: (see attached files for videos)

(A) Incucyte recordings of wild-type myoblasts cultured with Wnt3a-conditioned or L cell control medium. Wnt3a induces the formation of highly aligned myofibers; spontaneous differentiation in the absence of Wnt3a generates unaligned fibers with poor substrate attachment. **(B)** Incucyte recordings of β-catenin null myoblasts cultured with Wnt3a-conditioned or L cell control medium. Wnt3a has no effect on null myoblasts, both cultures show delayed formation of fibers that remain short, unaligned and with poor substrate attachment.

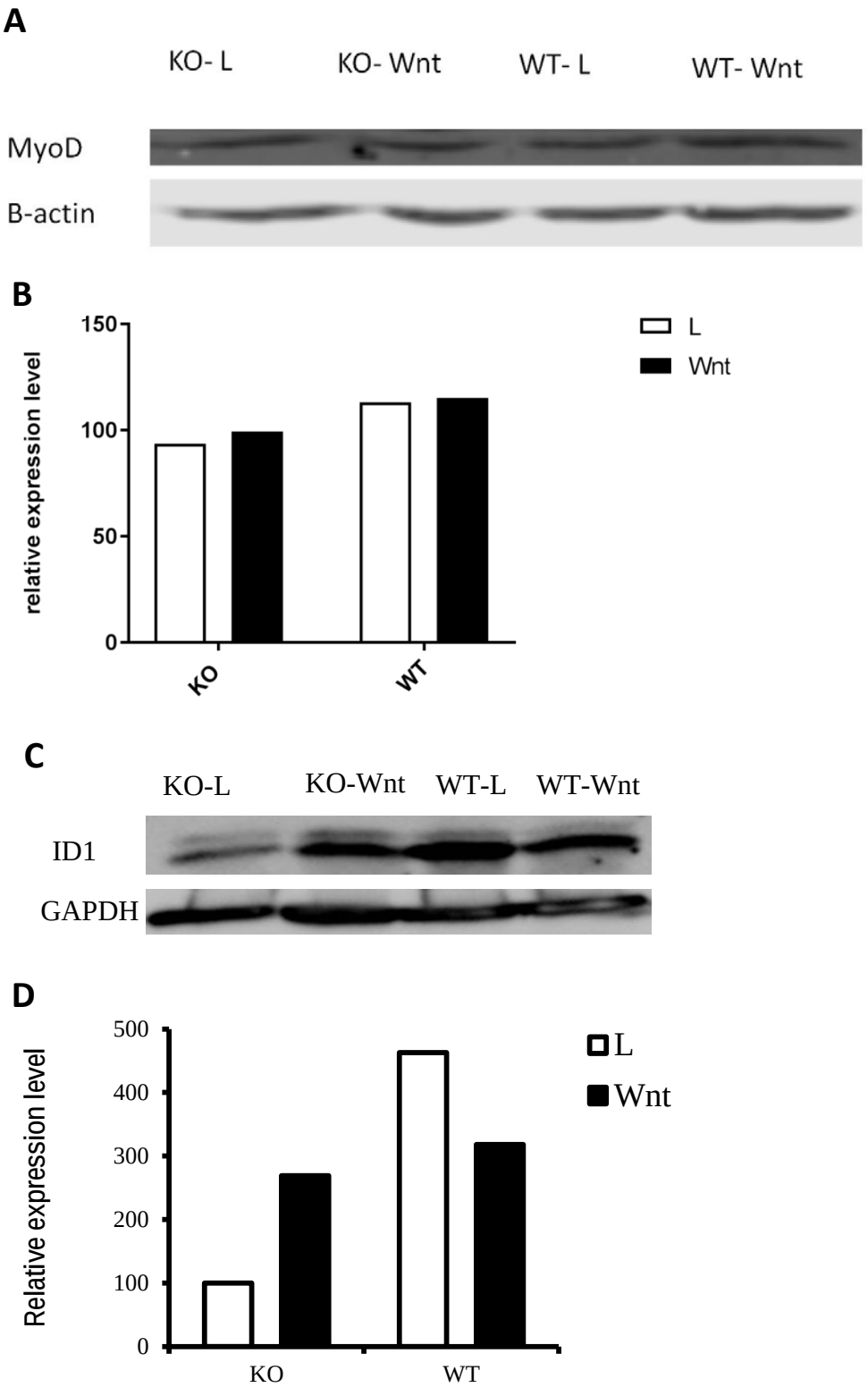

Supplemental Figure 3.9:

(A, C) Immunoblotting analysis of MyoD **(A)** and ID1 **(C)** expression after Wnt3a treatment of wild-type or β-catenin null myoblasts. **(B, D)** Quantification by densitometry and normalization of MyoD **(B)** or ID1 **(D)** levels to houskeeping protein (β-actin or GAPDH) levels.

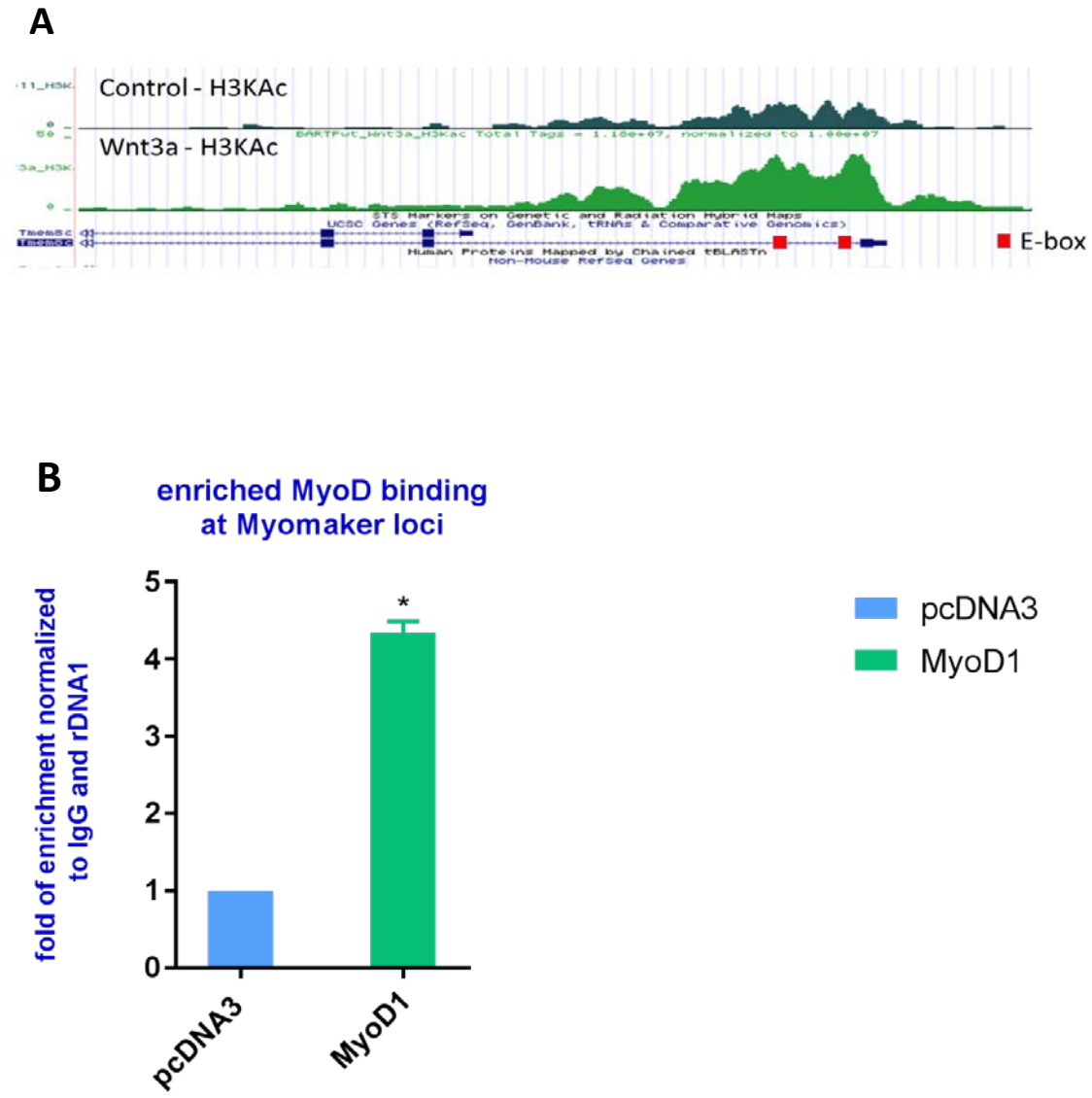

Supplemental Figure 3.6: ChIP-qPCR analysis validates the Myomaker promoter as a MyoD target

(A) Proximal promoter of the mouse Myomaker (Tmem8c) gene showing predicted E-box motifs within the region that showed enrichment of H3KAc after Wnt3a treatment of myoblasts (image from UCSC Genome Browser mm9) **(B)** Chromatin from wild-type primary myoblasts transfected with MyoD expression plasmid was subjected to ChIP with MyoD antibodies. Data are normalised to amplification values for a control non-target locus

(rDNA1), and to pcDNA3 empty vector transfection. Enrichment values were subsequently normalised to the mock ChIP with preimmune IgG, set to a value of 1. Error bars represent SEM. Statistical analysis used t-test. * $p < 0.05$ and ** $p < 0.001$. n = 3.

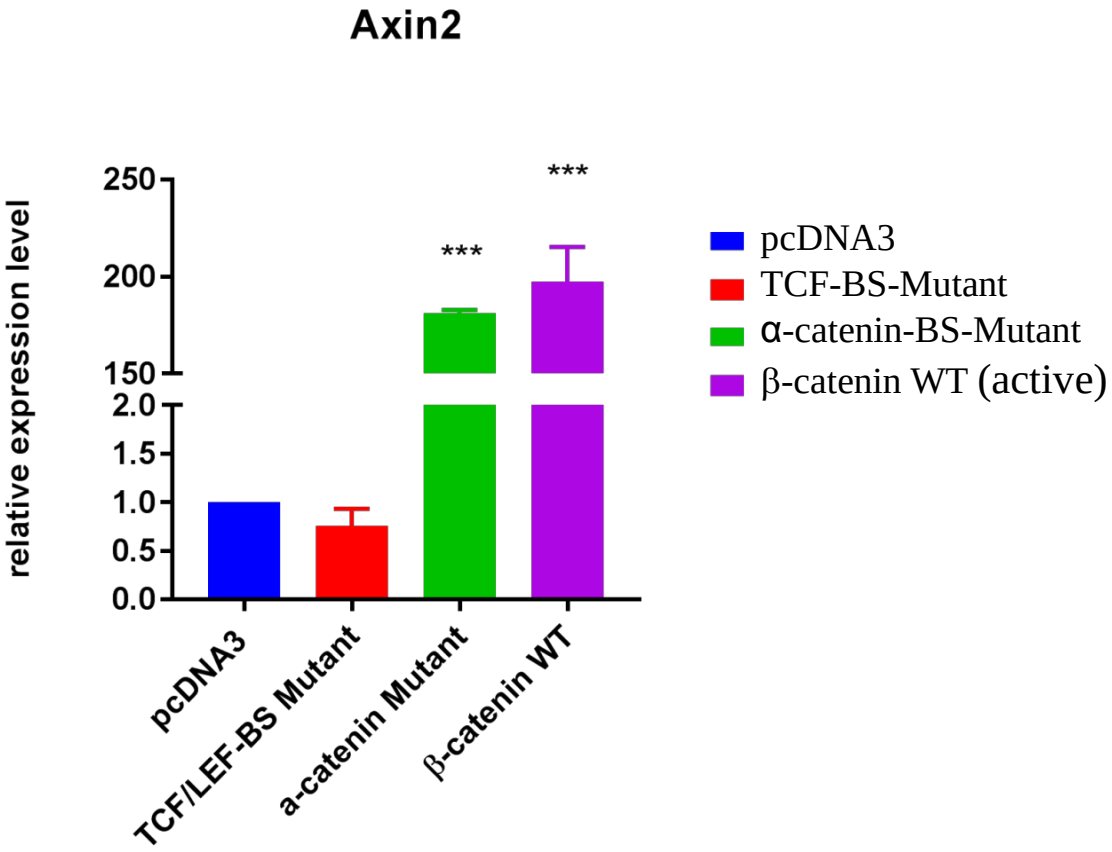

Supplemental Figure 3.10: RT-PCR analysis of Axin2 expression in β-catenin null myoblasts that have been transfected with various mutant forms of stable β-catenin

Cells were cotransfected with GFP and one of the following expression plasmids: empty pcDNA3, TCF-binding site (BS) mutant form of β-catenin (cannot interact with TCF/LEF), α-catenin-binding site (BS) mutant form of β-catenin (cannot interact with α-catenin), wild-type β-catenin (constitutively active/stable). Statistical analysis used one-way ANOVA. n = 3.

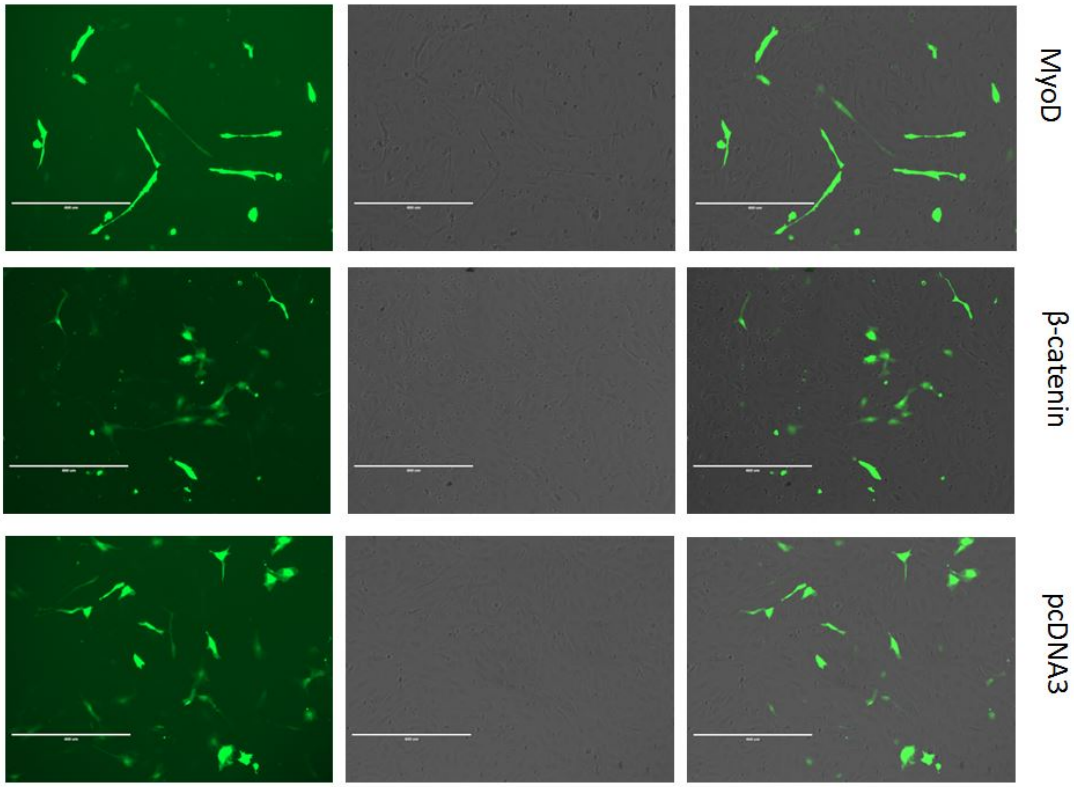

Supplemental Figure 3.8: C3H10T1/2 mesenchymal progenitor cells co-transfected with GFP expression plasmid and either β-catenin, MyoD, or empty pcDNA3 expression plasmids

MyoD expression converted the cells to the myogenic lineage as evidenced by formation of thin myotubes; β-catenin overexpression could not induce myogenic conversion of C3H10T1/2 cells. n = 3.

CHAPTER 4: Wnt regulated microRNAs modulate Pax7 expression

The figures presented in this chapter have been submitted as a manuscript to a peer reviewed journal for publication. At the time of final thesis amendment, the manuscript, in revised form, was published online (DOI: 10.1002/jcb.28542).

4.1 Introduction and aims

MicroRNAs (miRNAs) are small non-coding RNA molecules that regulate gene expression post-transcriptionally (Bartel, 2004). miRNAs bind to the 3'UTR of their target genes, which leads to mRNA degradation and/or protein translation inhibition (Krol et al., 2010). Gene regulation by miRNAs has been widely reported, and involves nearly all cellular processes. Computational studies indicate that about one-third of human genes are possibly regulated by miRNAs, and each miRNA potentially targets more than 200 genes (Krek et al., 2005; Lewis et al., 2005).

In myogenesis, miRNAs have been identified as important players in myogenic gene regulation. The essential role of miRNAs in skeletal muscle development was demonstrated by knock-out of the key factor in miRNA biogenesis dicer, which led to embryonic lethality (O'Rourke et al., 2007). Specifically, depletion of dicer resulted in a decrease in skeletal muscle mass, reduction of myofibre number, increase in myogenic cell apoptosis and acceleration of myoblast death.

The expression of miRNAs is not ubiquitous; many miRNAs are expressed in a tissue-specific manner (Lagos-Quintana et al., 2002; Lee and Ambros, 2001). The miRNAs exclusively or preferentially expressed in striated muscle are called myomiRs (McCarthy, 2008). Currently there are eight miRNAs recognised as myomiRs: miR-1, miR-133a, miR-206, miR-133b, miR-208a, miR-208b, miR-486 and miR-499 (Sempere et al., 2004; Small et al., 2010; van Rooij et al., 2009; van Rooij et al., 2007). Of these myomiRs, miR-133a, miR-206, miR-133b and miR-1 are the most abundant in muscle and the most extensively studied.

It is reported that myomiR-208a, myomiR-208b, myomiR-499, and myomiR-486 are encoded within the introns of the muscle expressed genes *MYH6, MYH7*, *MYH7B* and *ANK1* respectively (van Rooij et al., 2009; van Rooij et al., 2007). At the

genomic level, miR-1 is encoded by two paralogous genes (miR-1-1 and miR-1-2), and miR-133a is encoded by two paralogous genes (miR-133a-1 and miR-133a-2). In contrast miR-206 and miR-133b have no paralogues. The genes encoding miR-1 and miR-133a are organised as two bicistronic clusters (miR-1/miR-133a-2 and miR-1-2/miR-133a-1). Each of these loci is thought to be transcribed as a single bicistronic primary RNA from which the individual miRNAs are later processed. Similarly, miR-206/miR-133b are organised in a cluster. It is reported that miR-206 and miR-133b may produce a bicistronic; however they may also be indepdently transcribed from separate promoters generating different primary RNAs under certain conditions (Cesana et al., 2011). The miR-206/miR-133b gene cluster is located on human chromosome 6 (mouse chromosome 1) within an intergenic region adjacent a long non-coding RNA gene called LINCMD1, which is also involved in myogenesis. The miR-1-1/miR-133a-2 cluster is located on human Chromosome 20 (mouse chromosome 2) in an intergenic region. The paralogous miR-1-2/miR-133a-1 cluster is located on human Chromosome 18 (mouse chromosome 18) and are intragenic being located within an intron of the mindbomb (MIB1) gene; which encodes a protein involved in Notch signalling.

The primary miRNA transcripts are processed to highly similar mature miRNAs. The sequence of mature miR-1-1 is identical to that of miR-1-2, as is mature miR-133a-1 and miR-133a-2; miR-133b differs from miR-133a only by one nucleotide at the 3' end; miR-206 differs from miR-1 by four nucleotides, also at the 3' end.

The expression of each of these four myomiRs is reported to be induced during muscle differentiation (Chen et al., 2006a; Kim et al., 2006). However, they may play distinct roles at different stages of myogenesis, and the literature regarding their functions includes a number of contradictory findings. For example, miR-1 was

reported to promote differentiation through the inhibition of myogenic gene repressor histone deacetylase 4 (HDAC4) (Chen et al., 2006b), and similarly, miR-206 has been found to inhibit HDAC4 which also promotes differentiation (Williams et al., 2009; Winbanks et al., 2011). In contrast, miR-133a was found to enhance myoblast proliferation via suppression of serum response factor (SRF) (Chen et al., 2006b). However, another study reported that miR-133 suppressed myoblast proliferation by targeting SP1 (Zhang et al., 2012). That some studies have not distinguished miR-133a from miR-133b may explain some of the apparently contradictory functions reported for miR-133.

Pax7 is one of the key players in regulating satellite function during regenerative myogenesis. miR-206 is induced during myoblast differentiation and directly targets the 3'UTR of Pax7, which restricts myoblast proliferative potential and accelerates differentiation (Chen et al., 2010a; Dey et al., 2011a). miR-1 also targets Pax7 via its 3'UTR, inhibiting satellite cell proliferation and facilitating expression of the gene program associated with differentiation (Chen et al., 2010a). Although binding sites for miR-133b were predicted in the Pax7 3'UTR by bioinformatics software, no study has yet examined whether miR-133b (or miR-133a) can inhibit Pax7 expression. Moreover, as discussed above, the role of miR-133a/b in myogenic differentiation remains unclear. In addition, it is unknown whether other Pax7 regulating miRNAs are expressed in myoblasts.

A previous unpublished study from our laboratory found that Wnt3a specifically increased the level of miR-133b and miR-206 primary transcripts, but not miR-133a or miR-1 primary transcripts, in the C2C12 cell line. This suggested that these two miRNAs are a part of the program by which Wnts induce differentiation. Although C2C12 cells are a commonly used myoblast model, primary myoblasts are generally

preferred as more physiologically relevant for studying myogenesis *in vitro*. Hence in studies reported in this Chapter we used primary myoblasts, including our β-catenin CRISPR null model, to examine how miR-206/miR-133b are regulated by canonical Wnt signalling, and to examine their roles in Wnt-induced differentiation.

Because β-catenin cannot bind to DNA directly, other transcriptional factors must be involved in its function. As described in Chapter 3, it appears that MRFs such as MyoD, rather than TCF/LEF factors, may be the primary partners for β-catenin in the activation of differentiation-associated genes. MRFs have been previously implicated in the regulation of myomiRs. ChIP experiments identified binding sites for MyoD and myogenin upstream of the miR-1, miR-133 and miR-206 genes in C2C12 cells (Rao et al., 2006). miR-206 was upregulated by MyoD during the embryonic fibro-myogenic transition (Rosenberg et al., 2006). miR-1 and miR-206 were induced by MRFs during chicken embryonic development, and their expression was lost when Myf5 was deficient (Sweetman et al., 2008). These data suggest that β-catenin might cooperate with MRFs in the regulation of miR-206/miR-133b downstream of Wnt signals.

miRNAs can be secreted from cells and have been identified in serum, plasma, milk, urine, spinal fluid and other extracellular body fluids (Alexandrov et al., 2012; Allegra et al., 2012; He et al., 2014). These circulating miRNAs exist in micro-vesicles called exosomes. Exosomes are small membrane vesicles (typically 30-200 nm) of endocytic origin which are secreted by most cells in culture. Recently, exosomes have attracted considerable attention as important new players in cell-cell communication. Very recent evidence has shown that exosomes carrying specific myomiRs, such as miR-1, miR-206 and miR-133, can target myocytes and modulate the behaviour of these cells via gene expression regulation (He et al., 2014;

Matsuzaka and Hashido, 2015). However, it is unknown whether canonical Wnt signalling may influence the abundance or nature of exosomal myomiRs.

The specific aims of this chapter are:

1. To confirm whether miR-206/miR-133b are specific targets of Wnt/β-catenin signalling in adult primary myoblasts.
2. To assess the requirement for β-catenin in regulation of miR-206/miR-133b.
3. To identify the role of MRFs in regulation of miR-206/miR-133b.
4. To investigate the role of miR-206/miR-133b in the modulation of Pax7.
5. To identify other miRNAs that may be involved in the regulation of Pax7 downstream of Wnt signals.
6. To investigate the expression of miR-206/miR-133b in exosomes secreted by primary myoblasts in the context of Wnt signalling.

4.2 Results

4.2.1 Wnt3a induces the expression of miR-206 and miR-133b primary transcripts in wild-type myoblasts but not in β-catenin CRISPR null myoblasts

To test if canonical Wnt signalling can induce miR-206 and miR-133b expression, wild-type and β-catenin CRISPR null myoblasts were treated with Wnt3a and then harvested and the level of primary miRNA transcripts was measured by real-time PCR.

Primary miR-206 and miR-133b transcripts were induced by 2.5 and 3 fold respectively in Wnt3a-treated myoblasts compared to L-cell medium control treatment (Figure 4.1). No induction of primary miR-1 and miR-133a transcripts was observed. This result was consistent with previous observations in C2C12 cells (not shown). There was no induction of primary miR-206, miR-133b, miR-1, or miR-133a in the β-catenin CRISPR null myoblasts. These results indicated that Wnt3a induces primary miR-206 and primary miR-133b in a β-catenin dependent manner.

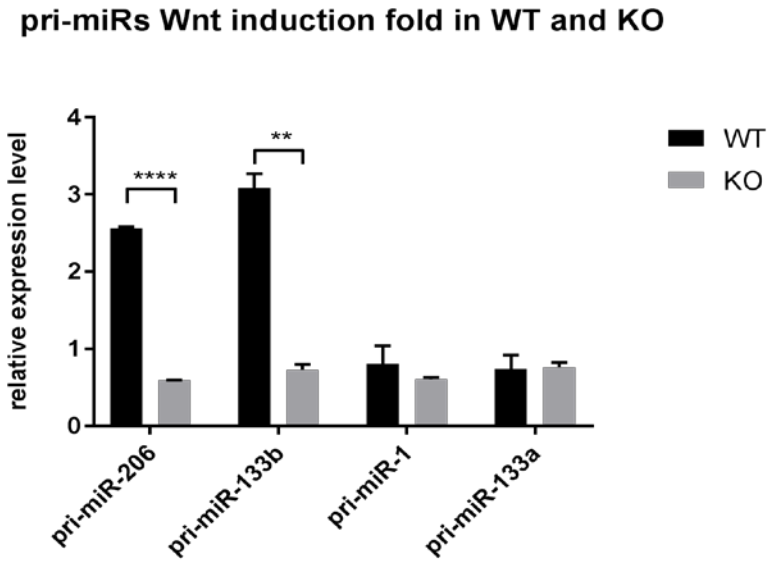

Figure 4.1: Wnt3a induces expression of primary miR-206 and miR-133b in wild-type myoblasts but not in β-catenin CRISPR null myoblasts

Cells were plated at 20% confluence, treated with Wnt3a medium or L cell control medium, and harvested 24 hours post-treatment for isolation of RNA. Levels of primary miRNA

expression were normalised against the housekeeping gene RPS26, then normalised over the results from cells treated with L-cell control medium (set to a value of 1). Three independent experiments were performed. Error bars represent SEM. ** $p < 0.01$ and **** $p < 0.0001$.

4.2.2 Wnt3a induces the expression of mature miR-206 and mature miR-133 in the wild-type myoblasts but not in the β-catenin CRISPR null myoblasts

Primary miRNAs are long non-coding transcripts that are processed into short-hairpin precursors of about 70-100 nucleotides called pre-miRNAs by the RNAase 3 endonuclease Drosha. Pre-miRNAs are further processed by another RNAase, Dicer, to form the mature miRNA of about 22 nucleotides. Therefore, the modulation of miRNAs may occur at multiple levels, and the abundance of primary transcripts may not mirror the abundance of mature miRNAs (Winter et al., 2009).

To test if mature miR-206, miR-133b, miR-1, or miR-133a were induced by Wnt signalling, Wnt3a treated wild-type and β-catenin CRISPR null myoblasts were harvested and the level of mature miRNAs was measured by real-time PCR (Figure 4.2). In the wild-type myoblasts, mature miR-206 and miR-133b were induced by five to seven-fold in Wnt3a-treated condition compared to L-cell medium control. Mature miR-133a also appeared to be induced; however the qRT-PCR primers used for the analysis were found to be unable to distinguish between mature miR-133a and miR-133b. Given that the miR-133a primary transcript was not induced (Figure 4.1), it is likely that the qRT-PCR analysis of mature miR-133a is artefactual due to the lack of primer specificity. Mature miR-1 was not induced by Wnt3a, which was consistent with the lack of induction of its primary transcript (Figure 4.1). In the β-catenin CRISPR null myoblasts, none of the four mature miRNAs were induced. Taken together, these data suggest that Wnt signals induce miR-206 and 133b in a β-catenin-dependent manner at the level of the primary transcripts, and that this translates into elevated levels of their mature forms.

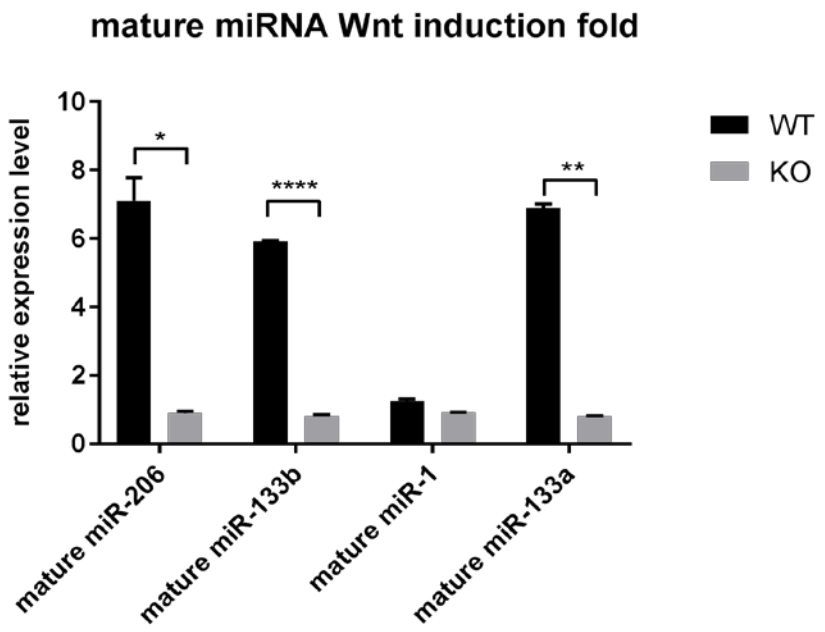

Figure 4.2: Wnt3a induces the expression of mature miR-206 and miR-133 in wild-type myoblasts but not in the β-catenin CRISPR null myoblasts

Cells were plated at 20% confluence, treated with Wnt3a medium or L cell control medium, and harvested 24 hours post-treatment for isolation of RNA. RNA was poly-A tailed and reverse transcribed using a poly-T adaptor method (see Methods). Mature miRNA expression was assessed by quantitative real-time PCR, normalised to the housekeeping gene snoRNA234, and is presented as fold induction over cells treated with L-cell control medium (set to a value of 1). Three independent experiments were performed. Error bars represent SEM. * $p < 0.05$, ** $p < 0.001$ and **** $p < 0.0001$.

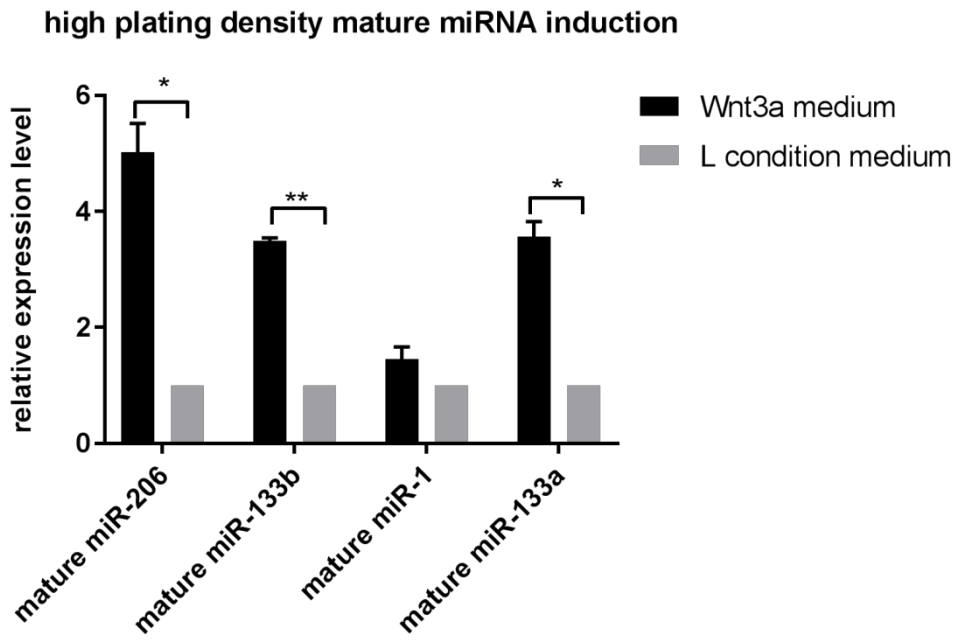

Figure 4.3: Wnt3a induces the expression of mature miR-206 and miR-133 in wild-type myoblasts at high density

Cells were plated at 35% confluence, treated with Wnt3a medium or L cell control medium, and harvested 24 hours post treatment. Total RNA was isolated and reverse transcribed. Mature miRNA expression was assessed by quantitative real-time PCR, normalised to the housekeeping gene snoRNA234, and is presented as fold induction over cells treated with L-cell medium control (set to a value of 1). Three independent experiments were performed. Error bars represent SEM. * $p < 0.05$ and ** $p < 0.001$.

Interestingly, the level of induction of miR-206 and miR-133 by Wnt3a was influenced considerably by myoblast confluence. Experiments shown in Figures 4.1 and 4.2 used a low plating density such that myoblasts did not reach confluence before harvesting. When myoblasts were plated at higher density such that they were confluent by harvest, miR-206 and miR-133 were induced to a lower level (about 3-4 fold) by Wnt3a (Figure 4.3). This may have been partly due to an increase in the baseline expression of these miRNAs at higher confluence (not shown).

4.2.3 Expression of active β-catenin induces expression of miR-206 and miR-133b

To further investigate the role of β-catenin in the specific induction of miR-206 and

miR-133b, we used a viral vector to introduce constitutively active (stable) β-catenin into wild-type myoblasts, and measured the expression level of primary miRNAs (Figure 4.4).

Constitutive overexpression of active β–catenin led to approximately 8-9 fold induction of the primary transcripts encoding miR-206 and miR-133b, but no induction of miR-1 and miR-133a. These results are consistent with results showing that miR-206 and miR-133b are specifically induced by Wnt3a (Figure 4.1) and suggest that β–catenin is not only necessary, but sufficient to induce these miRNA in myoblasts.

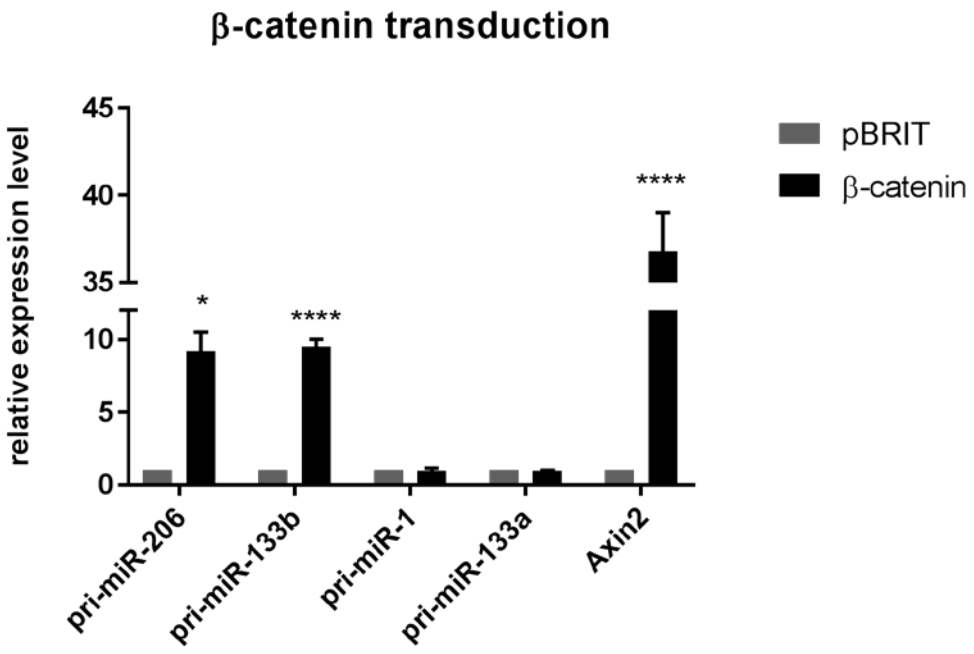

Figure 4.4: Primary miR-206 and miR-133b are induced by transduction of active β-catenin in wild-type myoblasts

Primary myoblasts were harvested 48 hours post retrovirus transduction. Levels of primary miRNA and mAxin2 expression were normalised against the housekeeping gene RPS26, then normalised over the results from cells transduced with empty pBRIT control (set to a value of 1). Three independent experiments were performed. Error bars represent SEM.* $p < 0.05$ and **** $p < 0.0001$.

4.2.4 β-catenin transfection in wild-type myoblasts increases the expression of miR-206 and miR-133b

During the course of this project, I optimized a plasmid transfection protocol for primary myoblasts in order to obviate the need for viral transduction. To determine whether transfection was as effective as viral transduction, I transfected a non-viral active β-catenin expression plasmid and measured the change in miR-206 and miR-133b. β-catenin transfection increased the expression of primary miR-206 and miR-133b by 7 and 5 fold respectively relative to transfection of empty vector (Figure 4.5); the primary transcripts of miR-1 and miR-133a were not increased. This suggests that plasmid transfection has only slightly lower efficacy than viral transduction in these cells (compare miRNA induction in Fig 4.4 and 4.5). This was further supported by studies that used GFP transfection and expression analysis to assess transfection efficiency (not shown).

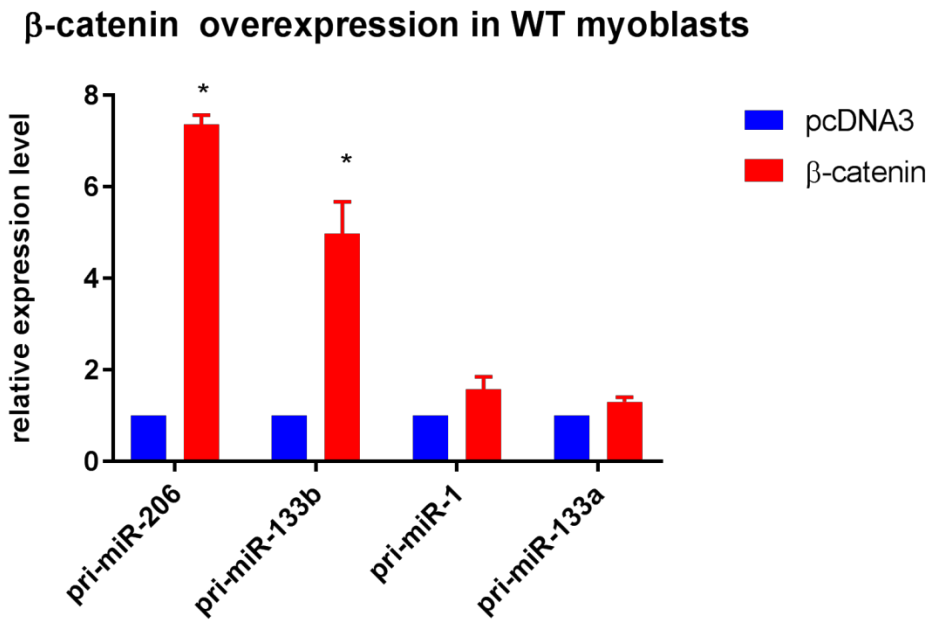

Figure 4.5: Primary miR-206 and miR-133b are induced by β-catenin transfection in wild-type myoblasts

Wild-type myoblasts were harvested 48 hours post transfection of a β-catenin expression

vector. Levels of primary miRNA expression were normalised against the housekeeping gene RPS26, then normalised over the results from cells transfected with pcDNA3 control (set to a value of 1). Three independent experiments were performed. Error bars represent SEM. * $p < 0.05$.

4.2.5 β-catenin transfection in β-catenin CRISPR null myoblasts rescues the expression of miR-206 and miR-133b

As shown in Chapter 3, β-catenin transfection in the β-catenin CRISPR null myoblasts increased ('rescued') the expression of myogenic factors and myogenic target genes. To determine if myogenic miRNAs were also rescued by β-catenin, β-catenin CRISPR null myoblasts were transfected with β-catenin and harvested 48 hours post transfection (Figure 4.6). As expected, the expression of primary miR-206 and miR-133b were 'rescued' in the β-catenin CRISPR null myoblasts, with their expression increased by approximately 4.5 and 3 fold respectively. In terms of absolute level, rescued primary miR-206 and miR-133b was 5.5 and 2.7 fold higher than the level in WT myoblasts.

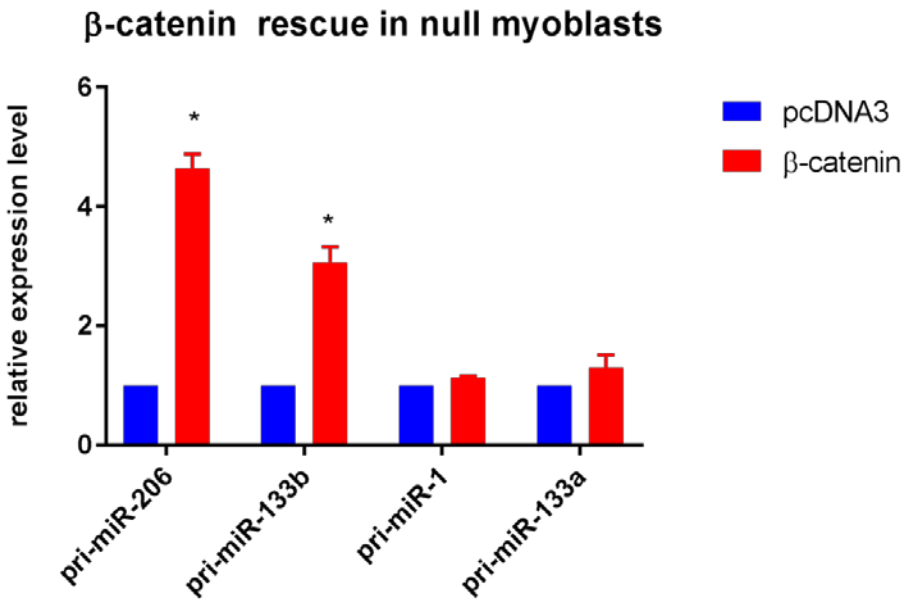

Figure 4.6: Primary miR-206 and miR-133b expression is rescued by β-catenin transfection in β-catenin CRISPR null myoblasts

β-catenin CRISPR null myoblasts were harvested 48 hours post β-catenin transfection.

Levels of primary miRNA expression were normalised against the housekeeping gene RPS26, then normalised over the results from cells transfected with pcDNA3 control (set to a value of 1). Three independent experiments were performed. Error bars represent SEM. * $p < 0.05$.

4.2.6 miR-206 and miR-133b mimics inhibit Pax7 expression

Pax7 downregulation is required for myoblast differentiation (Seale et al., 2000). miRNA modulation of Pax7 expression has been reported, including by miR-1, miR-206, miR-486 and miR-431 (Chen et al., 2010a; Dey et al., 2011a; Wu et al., 2015). Moreover, we found that canonical Wnt signals reduce Pax7 levels (Hulin et al., 2016b).Thus the observation that Wnt3a specifically induces the expression of miR-206 provides a mechanism by which it can reduce Pax7 expression facilitating differentiation (Chen et al., 2010a; Dey et al., 2011a). However, the function of miR-133b in adult myogenesis remains less clear, and miR-133b has not yet been reported to regulate Pax7.

Bioinformatics analysis predicted that miR-133b could bind to the 3'UTR of Pax7, prompting the following experiments to investigate if miR-133b modulates Pax7.

4.2.6.1 miR-206 and miR-133b mimics reduce luciferase activity of Pax7 3'UTR

The Pax7-3'UTR was cloned into a pGL3-basic luciferase reporter vector downstream of the luciferase gene. This allows the expression of luciferase to be controlled post-transcriptionally by factors (e.g. miRNAs) that can interact with the 3'UTR sequence.

To determine whether the Pax7-3'UTR was responsive to miR-206 or miR-133b, wild-type or β-catenin CRISPR null myoblasts were transfected with the luciferase reporter construct and either miR-206 mimics, miR-133b mimics, an equal mixture of miR-206 and miR-133b mimics, or negative control mimics (Figure 4.7). Twenty

seven hours post-transfection cells were harvested for analysis of luciferase activity. In wild-type myoblasts, miR-206 mimics reduced luciferase activity by 20%, which is highly consistent with a previously published study performed in C2C12 cells (Chen et al., 2010a). Transfection of miR-133b mimics was more effective, reducing Pax7 3'UTR-controlled luciferase activity by about 60%. Interestingly, while miR-133b mimics also reduced luciferase activity in the β-catenin CRISPR null myoblasts (by about 35%), miR-206 did not show any effect in these cells. In both cell lines, the combination of both miRNA mimics did not lead to an increased reduction; thus there is no synergistic effect between miR-133b and miR-206.

When luciferase activity was measured at forty hours post-transfection, the inhibitory effect of miR-133b mimics of luciferase activity was still seen in both wild-type and null cells; however the reduction in activity produced miR-206 mimics disappeared. Taken together, these data suggest that miR-133b may be the dominant post-transcriptional regulator of Pax7 activity.

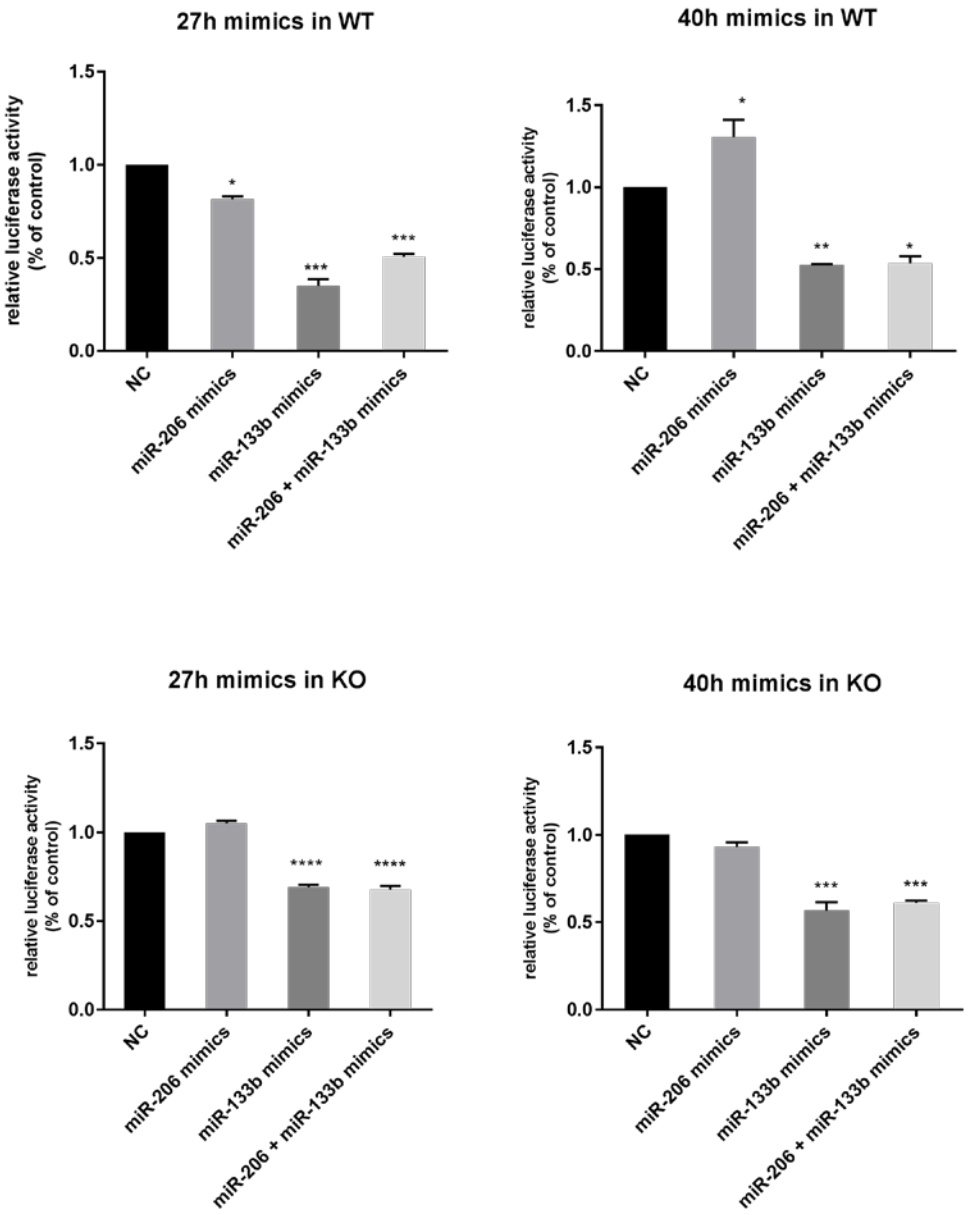

Figure 4.7: Activity of the pGL3-Pax7 3'UTR luciferase reporter construct after co-transfection with miRNA mimics in wild-type and β-catenin CRISPR null myoblasts

Wild-type myoblasts and β-catenin CRISPR null myoblasts were co-transfected with pGL3-Pax7 3'UTR and with 30 nM miR-206 mimics, miR-133b mimics, a mixture of miR-206 and miR-133b mimics (each making up 50%) or negative control mimics. Cells were harvested 27 and 40 hours post-transfection. All data are normalised to a Renilla luciferase internal control, expressed as the mean firefly/Renilla luciferase ratio. Data were then normalised to the negative control (set to a value of 1). Three independent experiments were performed. Error bars represent SEM. * $p < 0.05$, ** $p < 0.01$, *** $p < 0.001$ and **** $p < 0.0001$ relative to negative control unless otherwise marked.

4.2.6.2 miR-206 and miR-133b mimics inhibit Pax7 expression at the transcriptional level

To test whether modulation of Pax7 expression by miR-206 and miR-133b occurs at mRNA and protein levels, myoblasts were transfected with miR-206 or miR-133b mimics, and the level of mRNA and protein of Pax7 was measured and analysed.

As shown in Figure 4.8, miR-133b mimics dramatically reduced the Pax7 mRNA level by 70%, whereas miR-206 mimics reduced Pax7 mRNA by only 15%, compared to negative control mimics. This result is in line with the luciferase activity data (Figure 4.7), and again shows that miR-133b is more potent than miR-206 in targeting Pax7 mRNA, and hence might lead to greater Pax7 protein reduction.

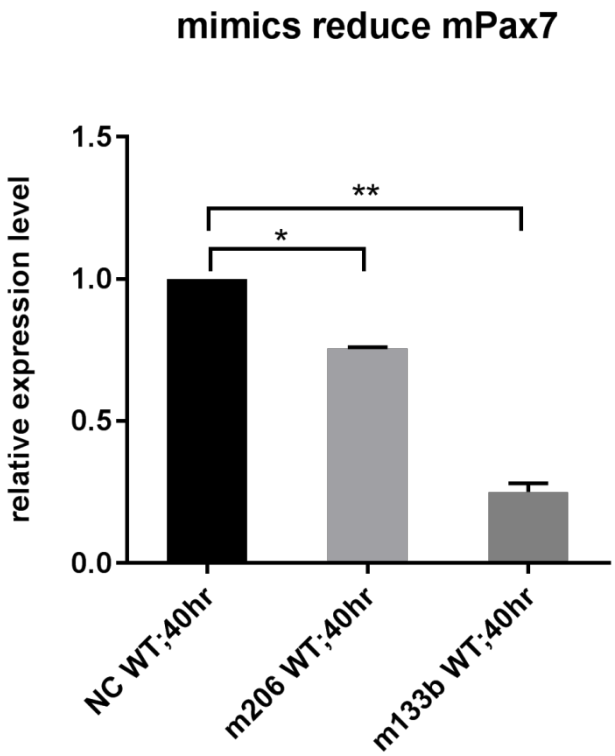

Figure 4.8: Pax7 mRNA level in wild-type myoblasts transfected with miR-206 and miR-133b mimics

Cells were harvested 40 hours post transfection. The level of mRNA expression is shown relative to the expression of the housekeeping gene RPS26, then normalised over the results from the cells transfected with negative control mimics. Three independent experiments were performed. Error bars represent SEM. * $p < 0.05$ and ** $p < 0.001$.

4.2.6.3 miR-206 and miR-133b mimics inhibit Pax7 expression at the protein level

To determine the effects of these two miRNAs on Pax7 protein levels, we performed immunostaining and western blot for Pax7 protein in wild-type myoblasts that had been transfected with miRNA mimics.

Immunostaining of Pax7 following transfection with miR-206 and miR-133b mimics

Wild-type myoblasts were transfected with miR-206, miR-133b, negative control mimics at 30 nM concentration; forty hours post transfection, myoblasts were fixed for immunostaining with fluorescently labeled Pax7 antibodies and nuclei were counterstained with DAPI. The total cell numbers (DAPI stained) and Pax7 positive cells were counted and the proportion of Pax7 positive cells was calculated.

Pax7 was expressed at a high ratio in the cells transfected with negative control mimics, about 95% were Pax7-positive (Figure 4.9B). Transfection with miR-206 mimics resulted in a 20% decrease in Pax7 Pax7-positive cells; miR-133b transfection led to approximately 30% reduction in Pax7 Pax7-positive cells.

Analysis of the immunostaining images showed that myoblasts transfected with miR-206 or miR-133b were sparser than cells transfected with negative control mimics (Figure 4.9A). Counting the total number of DAPI positive cells in each condition showed that miR-206 and miR-133b mimic transfection led to significant reduction of cell numbers by approximately 20% and 25% respectively (Figure 4.9C). These data suggest that both mimics reduced cell proliferation.

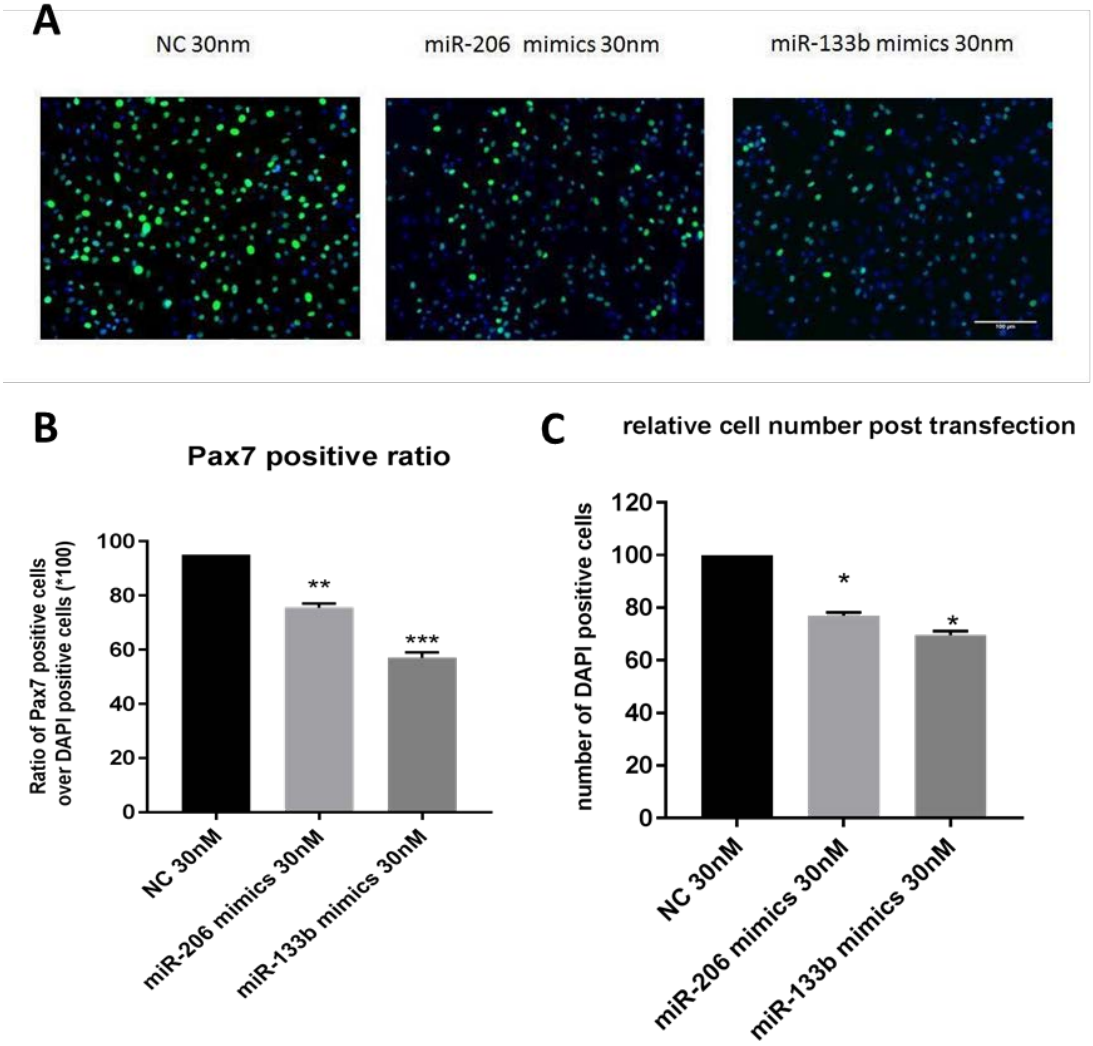

Figure 4.9: Immunostaining for Pax7 following transfection with miR-206 and miR-133b mimics

Wild-type myoblasts were harvested 40 hours post-transfection. **(A)** Overlaid images of Pax7 (green) and nuclear staining (blue). Scale bar indicates 100 µm. **(B)** Pax7 positive ratio in the cells transfected with scrambled control mimics, miR-206 and miR-133b mimics. **(C)** Relative cell number post transfection. The number of cells in the cultures transfected with scrambled mimics (control) was set to 100. Three independent experiments were performed. Error bars represent SEM. * $p < 0.05$, ** $p < 0.01$, and *** $p < 0.001$.

Western blot analysis of Pax7 following transfection of mi-R133b and miR-206 mimics

Immunostaining showed that the mimics changed in the frequency of Pax7 expression in cells; to confirm changes in the total Pax7 protein level we performed a western blot assay (Figure 4.10).

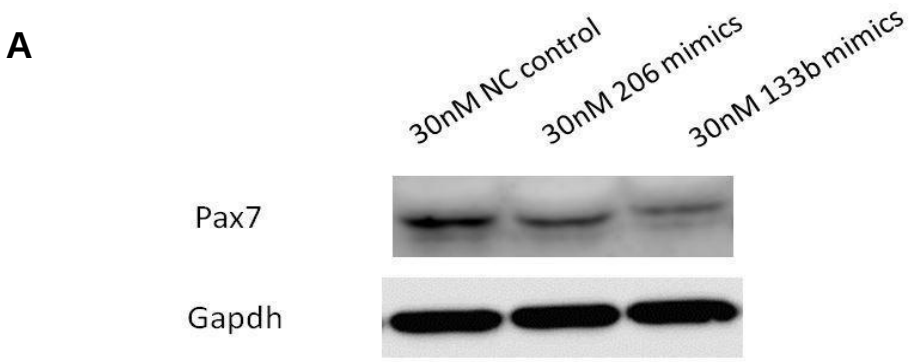

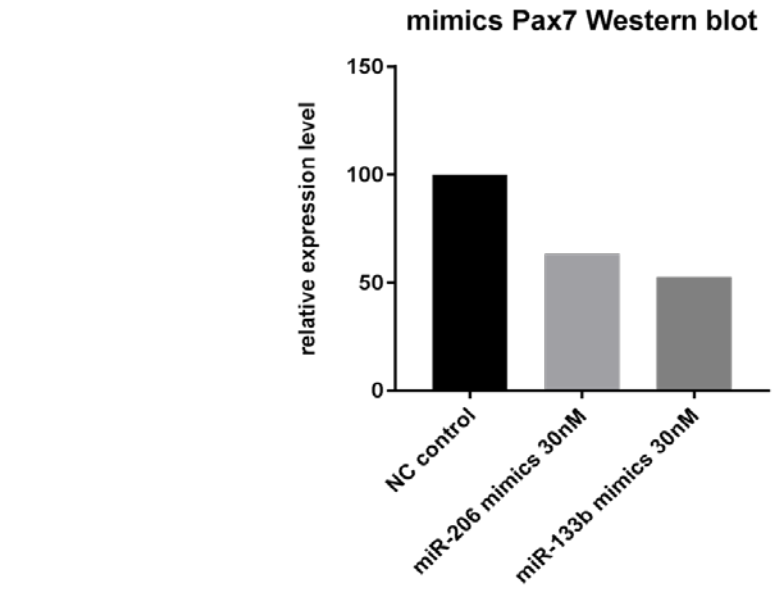

Figure 4.10: Pax7 protein level in wild-type myoblasts transfected with miR-206 and miR-133b mimics

Cells were harvested 40 hours post transfection. **(A)** Pax7 protein level was detected using a Pax7 specific antibody. Detection of GAPDH protein served as loading control. A representative blot of two independent experiments is shown. **(B)** Quantification of western blot. Pax7 expression with NC control set as 100.

The western blot assay indicated that the level of Pax7 protein was reduced approximately 50% by transfection of miR-133b mimics relative to negative control mimics. miR-133b mimics appeared to produce a greater reduction in Pax7 than miR-206 mimics, which further supports the idea that miR-133b may be more critical

than miR-206 for Pax7 regulation.

4.2.7 Wnt3a inhibits Pax7 expression in a β-catenin dependent manner

β-catenin is the central player in the canonical Wnt signalling pathway and is required for upregulation of primary miR-206 and miR-133b transcription (Figure 4.1). Overexpression of miR-206 or miR-133b led to the decreased expression of Pax7 (Figures 4.8-4.10). We previously showed that Wnt3a is able to downregulate Pax7 expression (Hulin et al., 2016b); however, it was still unknown whether β-catenin was specifically required for this regulation. To answer this question, we used western blot analysis to assess Pax7 protein expression post Wnt3a treatment in wild-type and the β-catenin CRISPR null myoblasts (Figure 4.11).

Twenty four hours post Wnt3a treatment, wild-type and β-catenin CRISPR null myoblasts were harvested for western blot assays. Pax7 protein bands were apparent in wild-type and null myoblasts treated with L-cell control medium. In wild-type myoblasts, Wnt3a treatment led to dramatic reduction in the intensity of the Pax7 protein band. However, in β–catenin null myoblasts, Wnt3a treatment had little or no effect on Pax7 protein band intensity relative to control treatment. This result indicates that Wnt3a inhibition of Pax7 expression occurs in a β–catenin dependent manner.

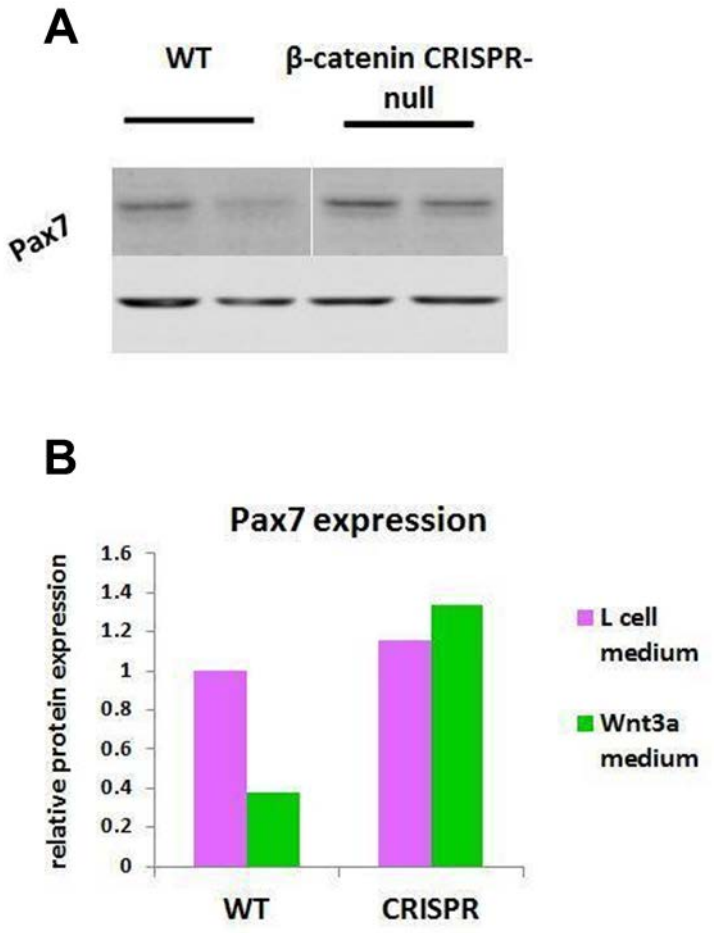

Figure 4.11: Wnt3a reduces Pax7 protein expression in wild-type myoblasts but not in β-catenin CRISPR null myoblasts

Wild-type and β-catenin CRISPR-null myoblasts were harvested 24 hours post Wnt3a or L – cell medium treatment. Pax7 protein level was detected by a Pax7 specific antibody, and β-actin served as loading control. A representative blot of three independent experiments is shown.

4.2.8 Site-directed mutagenesis of miRNA binding sites in the Pax7 3'UTR

The next question that I wanted to address was whether the inhibition of Pax7 by Wnt3a was mediated by the induction of miR-133b and miR-206. A miR-206 binding site had been previously identified in the Pax7-3'UTR (Chen et al., 2010b; Dey et al., 2011b). Our bioinformatics analysis predicted that miR-133b might bind to an adjacent sequence, "GGACCAAUC", within the 3'UTR. To test if this predicted binding site indeed responds to miR-133b, we performed site directed

mutagenesis of this binding site. The mutant and wild-type versions of the pGL3-Pax7 3'UTR luciferase vector were then co-transfected with miR-133b mimics in wild-type myoblasts; luciferase activity was measured 24 hours post-transfection (Figure 4.12).

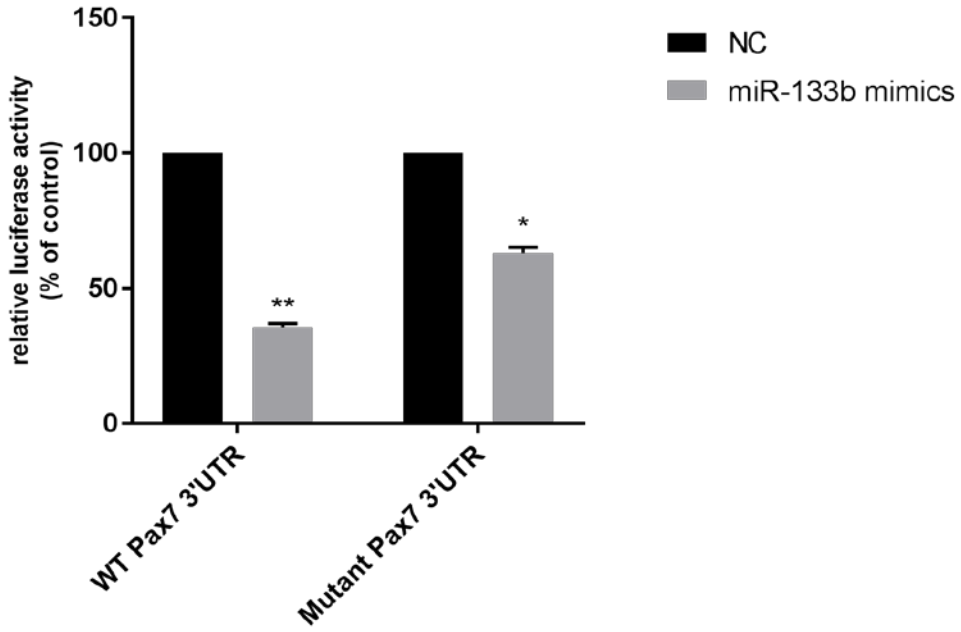

Figure 4.12: Mutation of predicted miR-133b binding site in the Pax7 3'UTR reduces the repressive effect of miR-133b mimics

Wild-type primary myoblasts were transfected with WT Pax7 3'UTR or miR-133b binding site mutated Pax7 3'UTR (Mutant Pax7 3'UTR); 20 nM miR-133b mimics or negative control mimics were co-transfected in each case. Cells were harvested 24 hours post-transfection. All values were normalised to Renilla activity, then normalised to the cells transfected with negative control. Three independent experiments were performed. Error bars represent SEM. * $p < 0.05$ and ** $p < 0.001$. Pax7 3'UTR was cloned by Siti and mutation of miR-133b binding site was performed by Liang Li.

miR-133b reduced the activity of the wild-type Pax7 3'UTR luciferase reporter by approximately 70%,; however it reduced the activity of the mutated Pax7 3'UTR by only 40%. This result suggests that the predicted miR-133b binding site is involved in the recruitment of miR-133b to the Pax7 3'UTR; however that fact that the

mutation did not abolish the effect of miR-133b suggests the possibility that additional binding sites for miR-133b might exist in the 3'UTR.

4.2.9 MRFs activate the promoter of miR-206/miR-133b

The studies described so far have shown that Wnt induces miRNAs that can target the Pax7-3'UTR; however they have not determined the specific mechanism by which these miRNAs are regulated. The primary sequences of miR-206 and miR-133b are located in a gene cluster, possibly sharing the same promoter. Previously our laboratory developed a luciferase reporter construct containing the putative promoter region of miR-206/miR-133b; using this construct, MyoD was found to induce the promoter approximately 5 fold in C2C12 cells.

To further investigate the regulation of miR-206 and miR-133b in primary myoblasts, wild-type myoblasts were co-transfected with the miR-206/miR-133b promoter luciferase construct and with MyoD, myogenin, or β–catenin. Luciferase assays were performed 24 or 44 hours post transfection.

These data showed that the miR-206/133b promoter was activated by the MRFs, MyoD and myogenin (Figure 4.13). MyoD and myogenin induced promoter activity by 2-3 fold at 24 hours post-transfection, and by 12 and 8 fold at 44 hours post-transfection. Compared to the results from the studies performed previously in our laboratory in C2C12 cells (not shown), the level of miR-206/miR-133b promoter activity induced by MyoD in the primary myoblasts was much higher.

Interestingly, β–catenin did not induce promoter activity; in fact it slightly reduced activity at 24 hours post-transfection; moreover there was no synergy between the MRFs and β–catenin at any time point (Figure 4.13). It therefore appears that β–catenin does not directly regulate this miR-206/miR-133b promoter region.

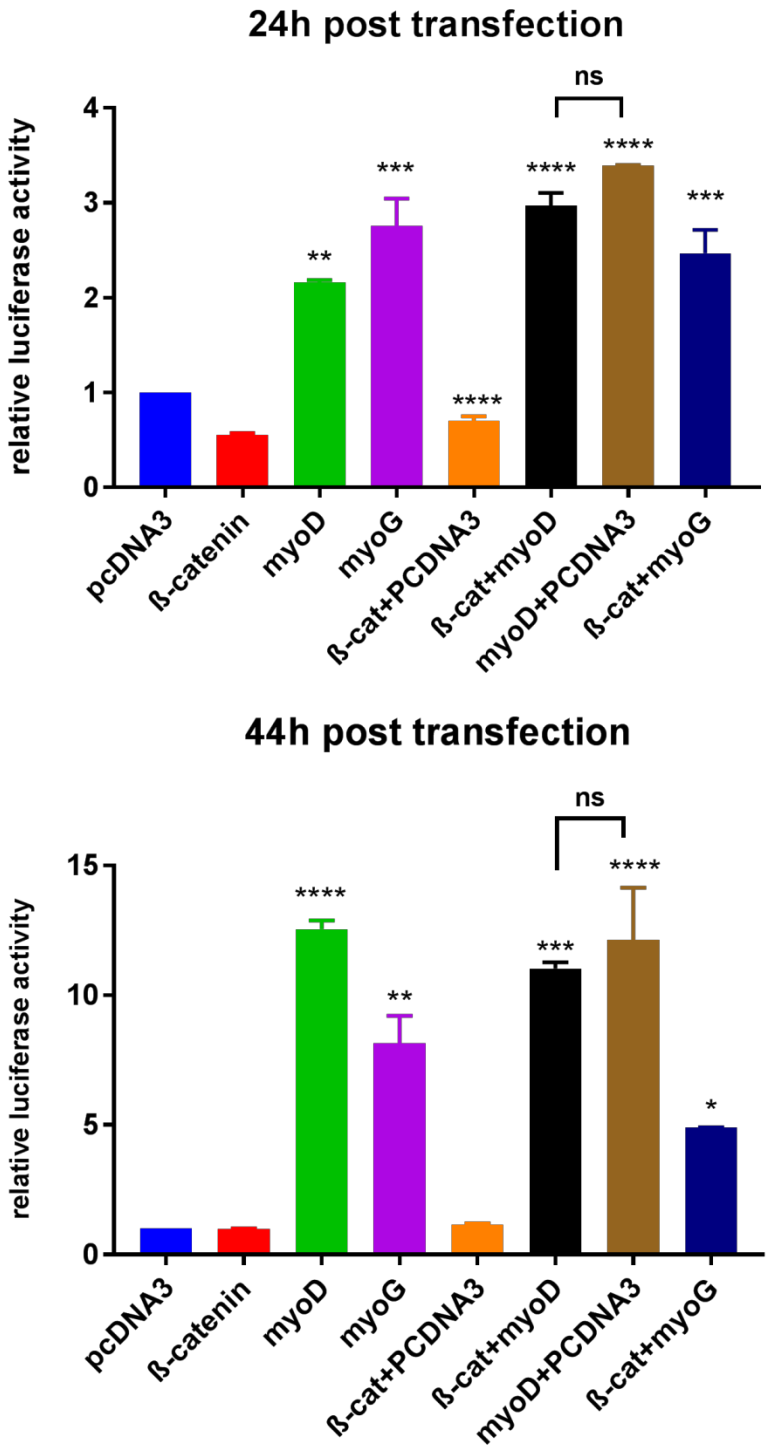

Figure 4.13: Activation of miR-206/miR-133b promoter region by various effector genes involved in myoblast differentiation

Wild-type primary myoblasts were co-transfected in duplicate with the miR-206/miR-133b promoter-luciferase construct, and an equal amount of each effector construct. Cells were harvested at 24 and 44 hours post-transfection and assayed for firefly and Renilla luciferase activity. All data are normalised to a Renilla luciferase internal control, expressed as the

mean firefly/Renilla luciferase ratio. Data were then normalised to the empty vector pcDNA3 transfection (set to a value of 1). Three independent experiments were performed. Data represent mean induction ± SEM and were analyzed by one-way ANOVA or t-test to to determine significance (*P < 0.05; **P < 0.01, *** p < 0.001 and **** p < 0.0001 relative to pcDNA3).

4.2.10 Screening for Wnt3a responsive miRNAs that regulate Pax7

To explore whether there are other Wnt3a-responsive miRNAs that might play a role in regulating Pax7, we screened a number of miRNA candidates to determine if they are regulated by Wnt3a in myoblasts. Twelve miRNA candidates were selected based on 1) prediction of miRNAs that are likely to bind to the Pax7-3'UTR and 2) the prediction of miRNAs with involvement in Wnt pathways by the website miRNA.org- Targets and Expression (http://34.236.212.39/microrna/home.do).

Wild-type and β–catenin null myoblasts were treated with Wnt3a for 24 hours and harvested for the measurement of twelve mature miRNAs by real-time RT-PCR (Figure 4.14). Four miRNAs were significantly induced more than 1.5 fold, including miR-143 (2.27 fold), miR-150-5P (1.61 fold), miR-1192 (1.53 fold) and miR-23b-3p (1.56 fold). Two miRNAs showed a non-significant trend towards induction: miR-431 (1.41 fold) and miR-22-3P (1.33 fold). Six other miRNAs were not induced by Wnt3a treatment: miR-15-a, miR-16, miR-183, miR-23a-3p, miR-410 and miR-495.

Among the induced mature miRNAs, miR-143 was the most abundantly expressed (based on raw RTPCR data not shown). Furthermore, miR-143 was induced at the highest level by Wnt3a, which suggested that miR-143 might be a promising candidate for mediating responses to Wnt in primary myoblasts, although it is less abundant than miR-206 or miR-133b, and its level of induction is somewhat lower.

.

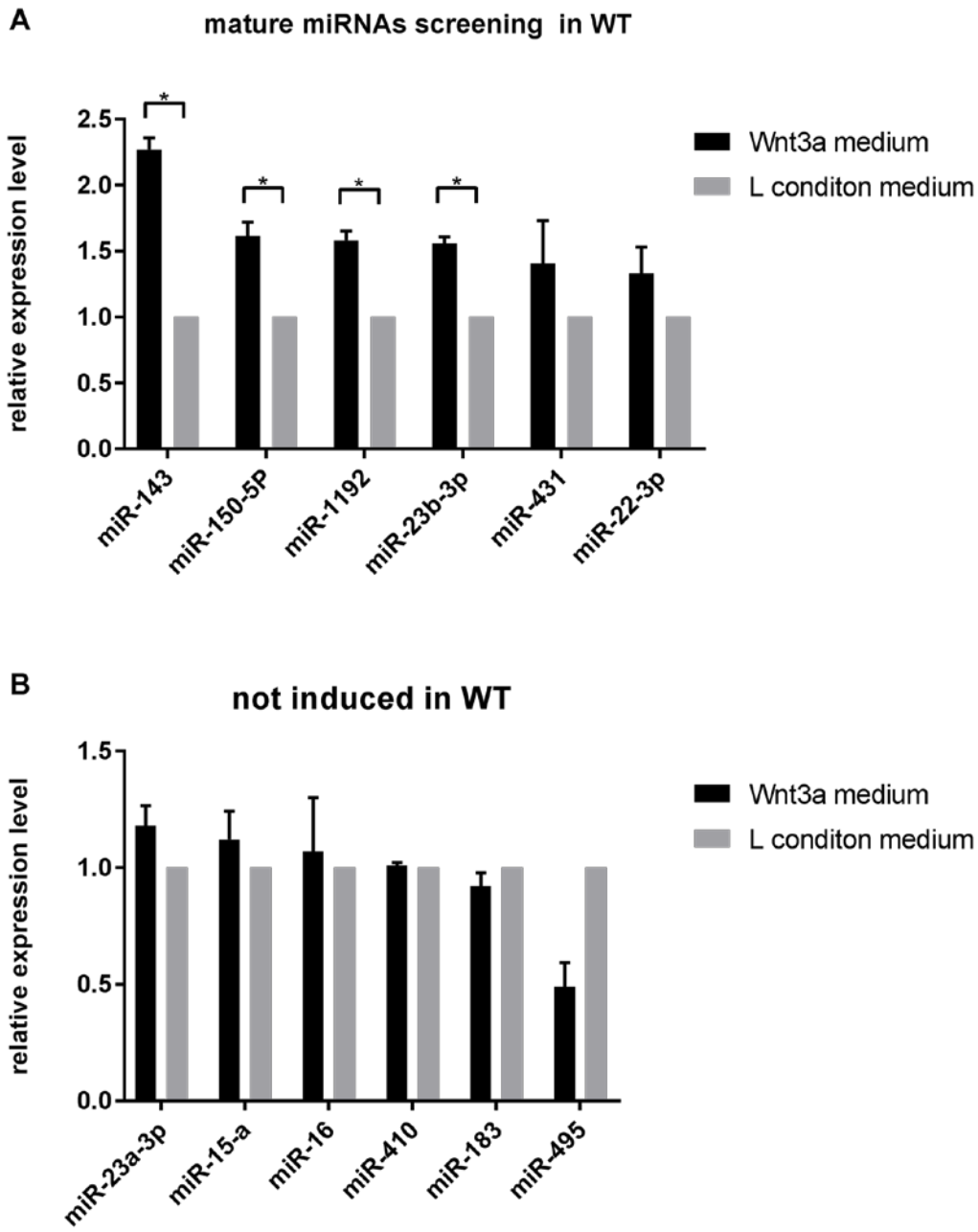

Figure 4.14: Screening for Wnt-induced miRNAs in primary myoblasts. (A) Mature miRNAs induced by Wnt3a and (B) mature miRNAs not induced by Wnt3a

Wild-type primary myoblasts were treated with Wnt3a for 24 hours and harvested for mature miRNA assay. Total RNA was isolated and reverse transcribed. Mature miRNA expression was assessed by quantitative real-time PCR, normalised to the housekeeping gene snoRNA234 and is presented as fold induction over cells treated with L-cell medium control (set to a value of 1). Three independent experiments were performed. Error bars represent SEM. * $p < 0.05$.

We next examined whether induction of these newly identified Wnt responsive

miRNAs was β–catenin dependent. β–catenin CRISPR null myoblasts were treated with Wnt3a medium for 24 hours and their levels measured by qRT-PCR. The mature miRNAs (miR-143, miR-150-5P, miR-1192, miR-23b-3p and miR-431) that were induced in the wild-type myoblasts were not induced in the β–catenin CRISPR null myoblasts (Figure 4.15), showing that their regulation was β–catenin dependent.

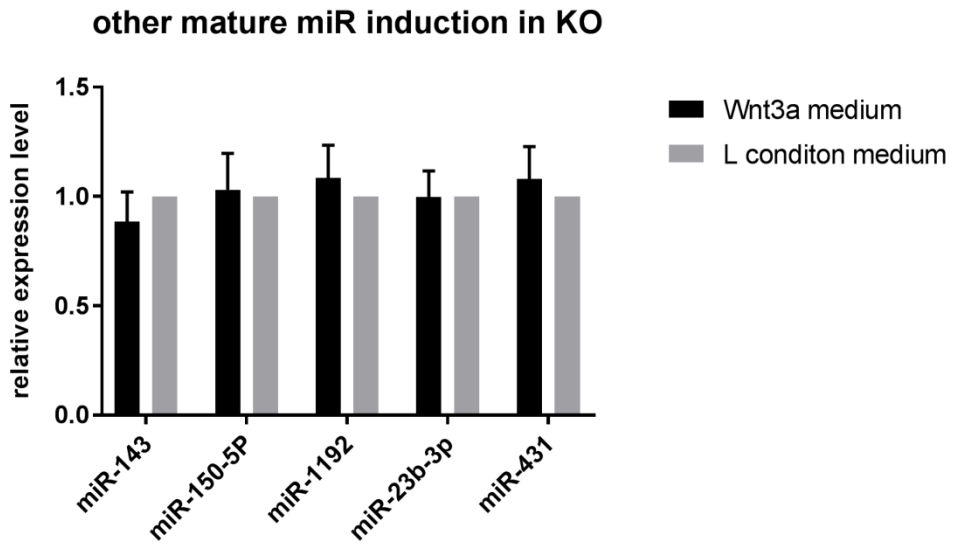

Figure 4.15: miRNA expression profile in β-catenin CRISPR null myoblasts post Wnt treatment

β–catenin CRISPR null myoblasts were treated with Wnt3a for 24 hours and harvested for mature miRNA assay. Total RNA was isolated and reverse transcribed. Mature miRNA expression was assessed by quantitative real-time PCR, normalised to the housekeeping gene snoRNA234 and is presented as fold induction over cells treated with L-cell medium control (set to a value of 1). Three independent experiments were performed. Error bars represent SEM.

4.2.11 Expression of mature miR-206/miR-133b and miR-1/miR-133a in exosomes

Exosomes are nano-sized small membrane vesicles that are secreted by many cell types into the extracellular space (Théry et al., 2002). Many miRNAs have been identified in the exosomal lumen, which may suggest a role in intercellular communication. We wished to determine whether Wnt-mediated induction of

miRNAs in primary myoblasts also led to their secretion into exosomes. We decided to focus on the highly Wnt-induced myomiRs miR-206 and miR-133b for this analysis; miR-1 was used as a non-Wnt regulated control.

I developed a protocol for enrichment of micro/nanovesicles (a mixture of membrane-bounded particles that include exosomes) from the myoblast media using polyethylene glycol (PEG) precipitation, and applied this method to wild-type and β-catenin CRISPR null myoblasts that were treated with Wnt3a on L cell control media. RNA was prepared from the microvesicular pellet and the expression levels of mature miR-206, miR-133, and miR-1 were measured. In both wild-type and β-catenin CRISPR null myoblasts, mature miR-206, miR-133b, miR-1, and 133a were detected in the secreted exosomes (Figure 4.16). After normalization of the expression level to miRNA-let7, mature miR-206 was the most abundant among the four miRNAs tested. The level of miR-206 in exosomes was induced by about two-fold by Wnt3a in wild-type myoblasts, but this induction was not seen in the β–catenin CRISPR null cells. Mature miR-133b and miR-133a (as noted previously, the analysis could not distinguish mature miR-133b from miR-133a) were found in exosomes at a relatively low level compared to miR-206. Mature miR-133b was increased by two fold in exosomes from Wnt3a treated wild-type myoblasts, but not null β–catenin myoblasts. As discussed previously, the apparent increase in mature miR-133a in exosomes is likely an artefact because the miR-133a primers also amplify miR-133b. No increase in expression of miR-1 by Wnt3a was found in either myoblast type.

These data suggested that in the extracellular exosomes, the expression profile of the four mature myomiRs in response to Wnt3a mirrors their profile in cells.

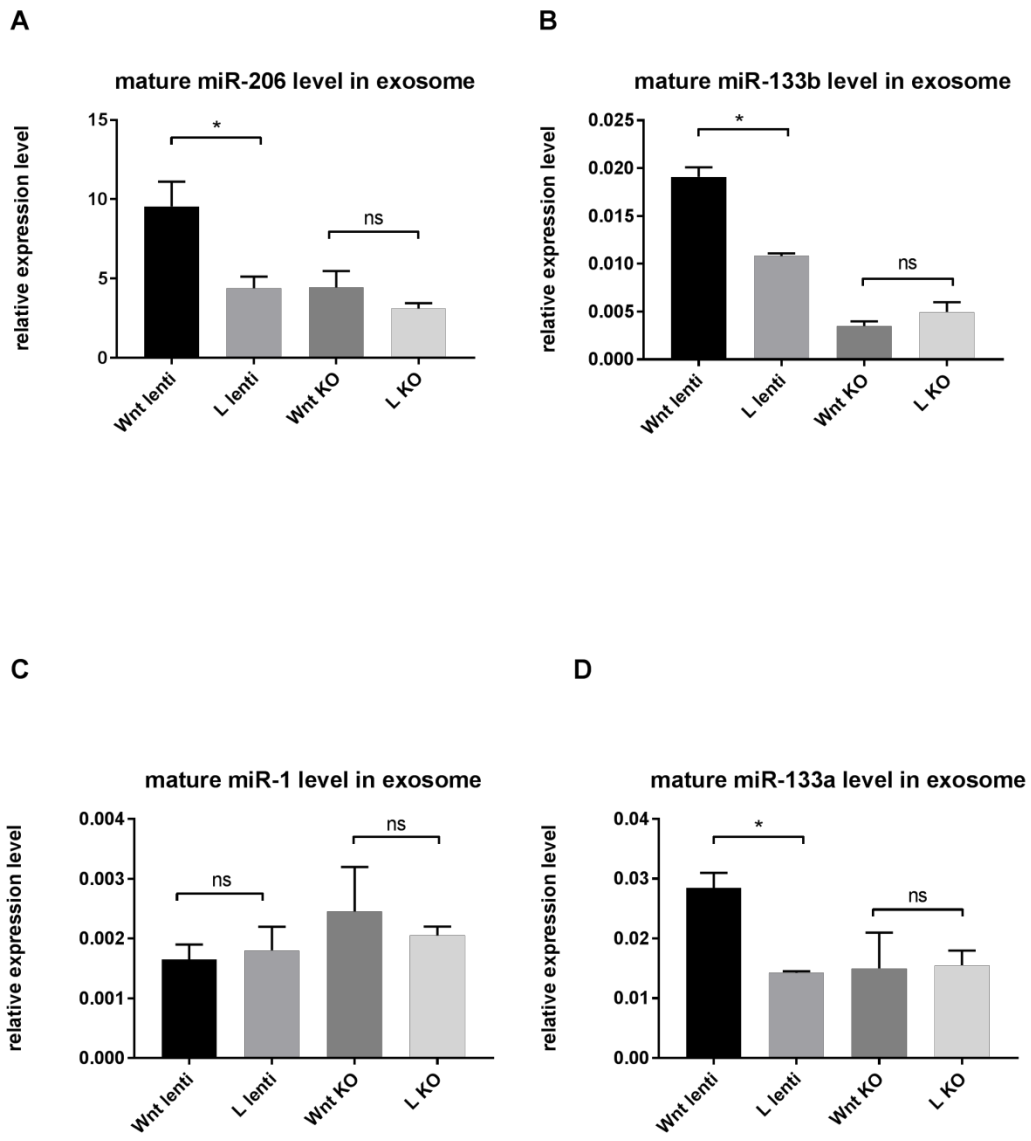

Figure 4.16: Relative expression levels of mature miRNAs in myoblast-derived exosomes

Wild-type and β–catenin CRISPR null myoblasts were treated with Wnt3a medium for 24 hours, then harvested for exosome extraction. Levels of mature miRNA were normalised to miRNA-let7. Relative expression levels of **(A)** mature miR-206, **(B)** mature miR-133b, **(C)** mature miR-1, **(D)** mature miR-133a in Wnt3a and L-cell medium condition cultured wild-type and β–catenin CRISPR null myoblasts. Three independent experiments were performed. Error bars represent SEM. * $p < 0.05$.

4.3 Conclusions and discussion

Here we showed for the first time that Wnt3a induces the expression of miR-206 and miR-133b at the primary transcript level (2-3 fold increase) and the mature miRNA level (6-7 fold increase) in wild-type primary myoblasts. This elevation of miRNA level did not occur in the β–catenin CRISPR null myoblasts, showing that induction of miR-206/miR-133b by Wnt is β–catenin dependent. The observation that overexpression of β–catenin by transfection or infection in wild-type myoblasts induces miR-133b and miR-206 expression, and that expression of β–catenin rescues miR-206/miR-133b expression in null myoblasts, strongly supports the idea that these miRNAs are direct β–catenin targets.

The biological functions of miR-206/miR-133b in muscle have been somewhat ambiguous. Only miR-206 was previously reported to promote muscle differentiation via direct repression of Pax7; there are insufficient studies to precisely delineate the function of miR-133b (relative to miR-133a) in myogenesis. Moreover, no reports have previously linked these miRNAs to Wnt/β–catenin signalling. As bioinformatics prediction showed that miR-133b also potentially binds to Pax7-3'UTR, we focused on the roles of miR-206/miR-133b on Pax7 regulation downstream of Wnt/β–catenin signalling in primary myoblasts.

Several pieces of data presented in this Chapter allow us to construct a pathway from Wnt signals to Pax7 inhibition via miR-206 and miR-133b. Luciferase reporter assays showed that transfection of miR-206 and miR-133b mimics into primary myoblasts reduced the activity of constructs containing the Pax7-3'UTR by 20% and 50% respectively. The 20% reduction by miR-206 is entirely consistent with the published data of Chen *et al.* (Chen et al., 2010a), where they also showed a 20% reduction in the activity of a reporter containing the Pax7-3'UTR after miR-206

overexpression. However Chen et al, did not test whether miR-133b could inhibit the Pax7 3'UTR.

Importantly, we found that miR-133b mimics had a stronger inhibitory effect than miR-206, at both time points and in both cell lines (wild-type or β–catenin null myoblasts) tested. At 27 hours post transfection, the extent of the decrease in Pax7-3'UTR reporter activity by miR-206 or miR-133b mimics was greater in the wild-type than in the β–catenin null myoblasts; in fact miR-206 mimics were completely ineffective in null cells (Figure 4.7). This finding might suggest that other factors that promote the function of these miRNAs (particularly miR-206) are lacking in the null cells. In wild-type cells, although miR-206 mimics reduced reporter activity at the 27 hour time point, they were no longer effective at 40 hours post transfection. This finding may be due to instability of miRNA mimics, although given that miR-133b mimics were similarly effective at both time points, it is also possible that miR-206 mimics are subject to some feedback regulatory effects that specifically diminish their activity. In contrast to the inconsistent effect of miR-206 mimics, the effect of miR-133b mimics was robust at around 50-60% reduction in reporter activity at both early and late time points in wild-type myoblasts and 30-40% reduction in β–catenin null myoblasts.

While a functional binding site for miR-206 in the 3'UTR of Pax7 had previously been reported (Chen et al., 2010a), our luciferase reporter studies showed for the first time that miR-133b could also target the Pax7-3'UTR. Moreover, using site-directed mutagenesis, we were able to show that the sole predicted miR-133b binding site containing the core sequence "GGACCAAUC" is likely to be involved in miR-133b function. However, the inability of mutation in this site to completely abolish the response of the reporter to miR-133b suggests that additional binding sites may exist.

Deletion analysis of the 3'UTR may be required to delineate the locations of such sites. Alternatively, it is possible that miR-133b expression enhances the expression of other miRNAs that can target the Pax7 3'UTR, thus acting indirectly. Future work could examine the relationship between miR-133b and other miRNAs, including the novel Wnt-responsive miRNAs identified in our studies.

The studies in this Chapter showed that both miR-206 and miR-133b could inhibit transcription of endogenous Pax7. In particular, miR-133b mimics reduced Pax7 mRNA levels by almost 75% in wild-type myoblasts. This was a much more dramatic effect than that produced by miR-206 mimics, which only reduced the level of Pax7 by about 20%. The effects of these miRNAs on Pax7 protein was assessed by immunostaining and western blot analysis. Immunostaining for Pax7 showed that both miRNAs reduced the number of Pax7-positive cells, with miR-133b mimics exerting a stronger effect (>40% reduction) than the miR-206 mimics (~25% reduction) at the same dose. Western blot analysis indicated that the total level of Pax7 protein was reduced by miR-133b and miR-206 mimics by approximately 50% and 40% respectively. The discrepancy between these two measures of Pax7 protein might be explained by the fact that the immunostaining analysis scored cells as Pax7 positive over a range of expression levels (indicated by fluorescence intensity).

The effects of miR-133b and miR-206 expression on myoblast behavior and morphology were consistent with the reduction in Pax7 and suggested enhanced differentiation. Transfection miR-133b and miR-206 mimics in wild-type myoblasts led to 35% and 20% reduction in proliferation respectively, relative to transfection of negative control mimics. Moreover, we observed that myoblasts transfected with miR-133b mimics became more elongated and began to fuse; these changes were not seen in cells transfected with negative control mimics (data not shown). Taken

together these results suggested that miR-206/miR-133b reduce proliferation, and promote the process of differentiation; moreover, miR-133b is likely to be a more potent inducer of myoblast differentiation.

Overall, these results provide a more detailed understanding of the mechanism of miRNA modulation of Pax7, and provide a mechanism for the β–catenin dependent repression of Pax7 by Wnt3a in adult myoblasts. Interestingly, the western blot of Pax7 suggests that the basal level of Pax7 in the β–catenin CRISPR null myoblasts is higher than in wild-type myoblasts. This may be in part explained by the relatively lower level of miR-206/miR-133b in the β–catenin null myoblasts. Moreover, this may be part of the reason that null myoblasts are refractory to differentiation (a process that requires Pax7 inhibition).

The next major goal of studies in this chapter was to define the specific transcription factors involved in the control of miR-206/miR-133b expression in adult myoblasts. Previous published studies on the promoter region of miR-206/miR-133b indicated that there was a functional E-box motif present (Rao et al., 2006). Previous work by our laboratory using miR-206/miR-133b and miR-1/miR-133a promoter-reporter constructs found that MyoD increased the activity of the miR-206/miR-133b promoter in C2C12 cells. However, neither Wnt3a nor β–catenin influenced the activity of the miR-206/miR-133b promoter in these cells. At that time, the C2C12 cell line was used as a myoblast model because efficient transfection protocols for the primary myoblasts had not yet been developed. After we optimised the transfection method in primary myoblasts, around 50% efficiency was achieved (based on the percentage of cells expressing GFP plasmid). Hence, we were able to test the effect of MyoD, myogenin, and β–catenin on miR-206/miR-133b promoter activity using the luciferase reporter assay in primary myoblasts, which represent a

more native myoblast model than C2C12 cells. MyoD and myogenin induced the miR-206/miR-133b promoter, with substantially (up to 6-fold) greater effect at 44 hours than 24 hours post-transfection (Figure 4.13). The delayed response might be explained by the requirement to first overcome the effects of an inhibitor of promoter activation (for example, Pax7), although the nature of such an inhibitor will require further study. Interestingly, tranfecting half of the amount of MyoD or myogenin plasmids led to a similar level of induction (not shown), which indicated that MyoD and myogenin might have saturated their binding sites on the promoter.

The miR-206/miR-133b promoter did not respond to transfection of β–catenin plasmid (Figure 4.13) or treatment with Wnt3a medium (data not shown). This was unexpected, as β–catenin and Wnt3a both increased the native miRNA expression. It is possible that the elements required for the Wnt/β–catenin response are not present within the cloned promoter region. Moreover, a transiently transfected (episomal) promoter-reporter construct will not recapitulate the native chromatin structure around the promoter. If the action of Wnt/β–catenin involves chromatin remodeling events, these effects might not be observable in the synthetic promoter-reporter system. Altogether, these results indicate that miR-206/miR-133b is directly regulated by MyoD and myogenin via elements within the proximal promoter region. β–catenin might regulate miR-206/miR-133b gene through distal elements, such elements could possibly have long-range interactions with MRFs bound proximally. Alternatively, its effects could be mediated by changes in native chromatin structure.

Just as one miRNA can regulate multiple genes, a single gene is able to be modulated by various miRNAs. Bioinformatics indicated that there were binding sites for multiple miRNAs within the 3'UTR of Pax7, twelve of which were selected for study here based on prediction of possible involvement in Wnt pathways. The level

of mature miR-143, miR-150-5P, miR-1192 and miR-23b-3p were all increased by Wnt3a in wild-type myoblasts, but did not change in β–catenin null myoblasts. Whether these Wnt/β–catenin-regulated miRNAs are also involved in Pax7 modulation will require further analysis, including expression of miRNA mimics in primary myoblasts and analysis of Pax7 levels, as well as site-directed mutagenesis of their predicted binding sites in the Pax7 3'UTR. Any functional relationships (such as synergy or cross-regulation) between these miRNAs and miR-206/miR-133b are also important to investigate.

In the final part of these studies, the expression of mature miR-206/miR-133b and miR-1/miR-133a were detected in exosomes secreted from primary myoblasts (Figure 4.16). Wnt3a increased the levels of exosomal miR-206/miR-133 in a β–catenin-dependent manner, which mirrors their regulation in the cells. The possibility that miR-206/miR-133 could be secreted extracellularly and taken up by surrounding cells suggests a possible mechanism to control the differentiation of a local population of primary myoblasts through cell to cell communication. Because this effect occurs downstream of Wnt signalling, it could allow the sustained response of a population of cells to the initial Wnt signal, even after feedback inhibition has reduced levels of β–catenin itself. In addition, exosomal miR-206 produced by myoblasts was recently shown to influence the behavior of neighbouring fibroblasts, specifically inhibiting collagen production (Fry et al., 2017). Currently the functions of exosomal miR-133b have not been defined. Future studies could examine whether any of the miRNAs whose expression is enhanced by Wnt signals in myoblasts can alter the behavior of neighbouring cells (both myoblasts and fibroblasts), thus providing another way for Wnt signals to propagate.

CHAPTER 5: Coactivators of β-catenin in Wnt regulation of muscle stem cells and fibroblasts

5.1 Introduction

5.1.1 CBP and p300

CREB binding protein (CBP) and p300 are two coactivators of β-catenin. They were initially identified as factors binding to the transcription factor cAMP response element-binding protein (CREB) and the adenoviral-transforming protein E1A, respectively (Chrivia et al., 1993; Eckner et al., 1994). These two proteins are evolutionarily related, and it has been suggested that they are involved in multiple cellular activities, such as cell proliferation, differentiation and apoptosis (Goodman and Smolik, 2000; Shiama, 1997).

CBP and p300 are quite similar in amino acid sequence (63% identity), they have similar structures, and both contain five common protein interaction domains, suggesting that they possess overlapping functions. However, gene perturbation experiments in mouse demonstrated that both genes are necessary and not interchangeable during embryonic development, as homozygous CBP-/- and p300-/- mice were inviable, and distinct developmental defects were observed in each model (Tanaka et al., 2000; Yao et al., 1998).

CBP and p300 can interact with a wide range of transcription factors and co-factors. These interactions are mainly regulated by upstream signals, such as phosphorylation (Ait-Si-Ali et al., 1999) and hormone stimulation. CBP and p300 are reported to act as a stabilising “bridge” between transcription factors and the core transcriptional machinery, or to function as a scaffold to help assemble the transcriptional complexes. CBP and p300 exert acetyl-transferase function and can acetylate both histone and non-histone proteins. In most cases, acetylation of transcription factors has been shown to increase their DNA-binding capacity. Furthermore, CBP and p300 can interact with other acetyltransferases or bind to other chromatin modifiers and

remodeling factors to alter chromatin structure and function (Ogryzko et al., 1998; Vandel and Trouche, 2001).

5.1.2 CBP and p300 play distinct roles in β–catenin signalling

A major paradox in understanding CBP/p300 function is that despite their similarities in structure and binding partners, they appear to be capable of contributing to functionally opposed cellular processes as described below.

CBP and p300 have been shown to play distinct roles, particularly in Wnt/β-catenin signalling and stem cell regulation. When Wnt signalling is activated and β-catenin is stabilized, accumulated cytoplasmic β-catenin translocates to the nucleus, recruiting either CBP or p300 to generate a transcriptionally active complex, thereby activating downstream pathways to regulate stem cell maintenance or differentiation. In haematopoietic stem cells (HSC), CBP was demonstrated to be crucial for HSC proliferation, while p300 was shown to be essential for HSC differentiation (Rebel et al., 2002). In neuronal cells, TCF/β-catenin/CBP mediated transcription was essential for neuronal stem cell/progenitor self-renewal, while TCF/β-catenin/p300 mediated transcription is critical to promote neuronal progenitor differentiation and inhibit proliferation (Teo et al., 2005).

In muscle stem cells, studies have implicated both CBP and p300 in MRF regulated transcription and myogenesis. *In vitro* studies showed that MyoD and Myf5 can cooperate with CBP, p300 and Mef2 to activate myogenin and Mrf4 during myogenesis (Eckner et al., 1996; Sartorelli et al., 1997). CBP was shown to acetylate MyoD to facilitate its heterodimer formation with E-box protein (Polesskaya et al., 2000; Sartorelli et al., 1999). However, chemical inhibition of CBP acetyltransferase (AT) activity could not block the activation of myogenin by MyoD in C2C12 cells, suggesting that CBP activity can be compensated for, possibly by p300 (Polesskaya

et al., 2001). In contrast, *in vivo* studies have suggested that p300 plays a critical role in myogenesis that may not be compensated by CBP. A single allele mutation which causes inactivation of p300 AT activity in mouse embryos led to deceased expression of MRFs and impaired myogenesis (Roth et al., 2003). In contrast, AT activity mutation in *cbp* in mouse embryos did not lead to any apparent muscle deficiency (Roth et al., 2003).

Furthermore, ES cells deficient in p300 or p300 AT activity showed significantly impaired capability to activate *MyoD* and *Myf5* during skeletal muscle formation, but ES cells lacking CBP or CBP AT activity retained the ability to form muscles (Roth et al., 2003).

Overall, these results indicate that CBP and p300 play distinct roles in embryo myogenesis, and p300 might be essential for embryonic muscle differentiation. However, the exact roles which CBP and p300 play in Wnt regulated adult myogenesis are less well studied, and the mechanisms involved remain unclear.

5.1.3 Inhibiting β–catenin/CBP for treating fibrosis

Adult myogenesis is under the control of Wnt signalling, which is one of the most important cascades regulating development and stemness. However, aberrant Wnt signalling has been shown to lead to a wide range of diseases including human fibrosis.

Fibrosis occurs in different tissues, and treatment strategies involving β–catenin/CBP inhibition are being developed. ICG-001 has been identified as a novel pharmacological inhibitor that specifically blocks β–catenin/CBP interaction via competition for the β–catenin binding site (Ma et al., 2005). Recent studies have shown that elevated Wnt signalling is associated with parasite infection and

contributes to liver fibrosis (Wang et al., 2017). Selective inhibitors PRI-724 and ICG-001 targeting Wnt/β-catenin/CBP ameliorated liver fibrosis in mice (Akcora et al., 2017; Tokunaga et al., 2017). Similar to liver fibrosis, aberrant activation of the Wnt/β-catenin signalling pathway occurs in patients with idiopathic pulmonary fibrosis (IPF). Administration of ICG-001 blocked Wnt/β-catenin signalling, attenuated and even reversed bleomycin-induced lung fibrosis and significantly improved survival in mice (Henderson et al., 2010). ICG-001 treatment also remarkably improved cardiac contractile function in a rat myocardial infarction model (Sasaki et al., 2013).

Altogether, these studies suggest that modulation of Wnt signalling via Wnt/β-catenin/CBP inhibition offers a promising therapeutic approach towards the restoration of fibrotic organs and tissues.

In skeletal muscle, fibrosis is usually associated with the muscular dystrophies (e.g. DMD), which compromises patient mobility and leads to people becoming confined to a wheelchair. However, currently there is no practical therapy available for DMD patients and the only relatively effective therapy requires corticosteroid administration, which leads to undesirable secondary effects (Angelini, 2007). Moreover, the relevant mechanism of skeletal muscle fibrosis regulation and muscle regeneration remains unclear. Recently, elevated Wnt signalling has been reported to accelerate skeletal muscle atrophy/fibrosis (Brack et al., 2007; Trensz et al., 2010). However, the effect of Wnt/β-catenin/CBP inhibition on fibrotic skeletal muscle has not yet been investigated.

5.2 Aims

For these reasons, we decided to investigate whether treatment by the Wnt/β-catenin/CBP inhibitor ICG-001 is effective in fibrotic skeletal muscle. Moreover, we

also aimed to study the underlying mechanisms of β-catenin coactivator usage in primary myoblast differentiation, which is crucial for muscle regeneration. IQ-1 is a small molecular inhibitor that specifically disrupts the interaction between β-catenin and p300, thus we can use IQ-1 and ICG-001 to study the roles of p300 and CBP in Wnt/β-catenin signalling. By dissecting the roles of CBP and p300 in adult myogenesis, we expect to gain a more in-depth understanding of the pro-differentiation and pro-fibrotic effects of Wnt, which are closely related to the mechanisms of muscle regeneration and pathogenesis of muscle fibrosis. We can then modulate Wnt signalling more safely and efficiently to help develop therapies for patients with fibrosis in muscle.

The specific aims of this chapter were to:

1. Examine the roles of p300 and CBP during primary myoblast differentiation using chemical inhibition.
2. Examine the role of CBP during fibroblast activation using chemical inhibition.
3. Identify the effect of ICG-001 for treating skeletal muscle fibrosis in mice.

5.3 Results

5.3.1 IQ-1 inhibits myoblast differentiation *in vitro*

Primary myoblasts were plated in 24-well plates 24 hours prior to treatment with Wnt3a medium or L-cell medium control with IQ-1 at 5 μM and 10 μM, and ICG-001 at 10 μM. DMSO was added as a control. Primary myoblasts were harvested for RNA extraction 48 hours post-treatment. Results are displayed in Figure 5.1.

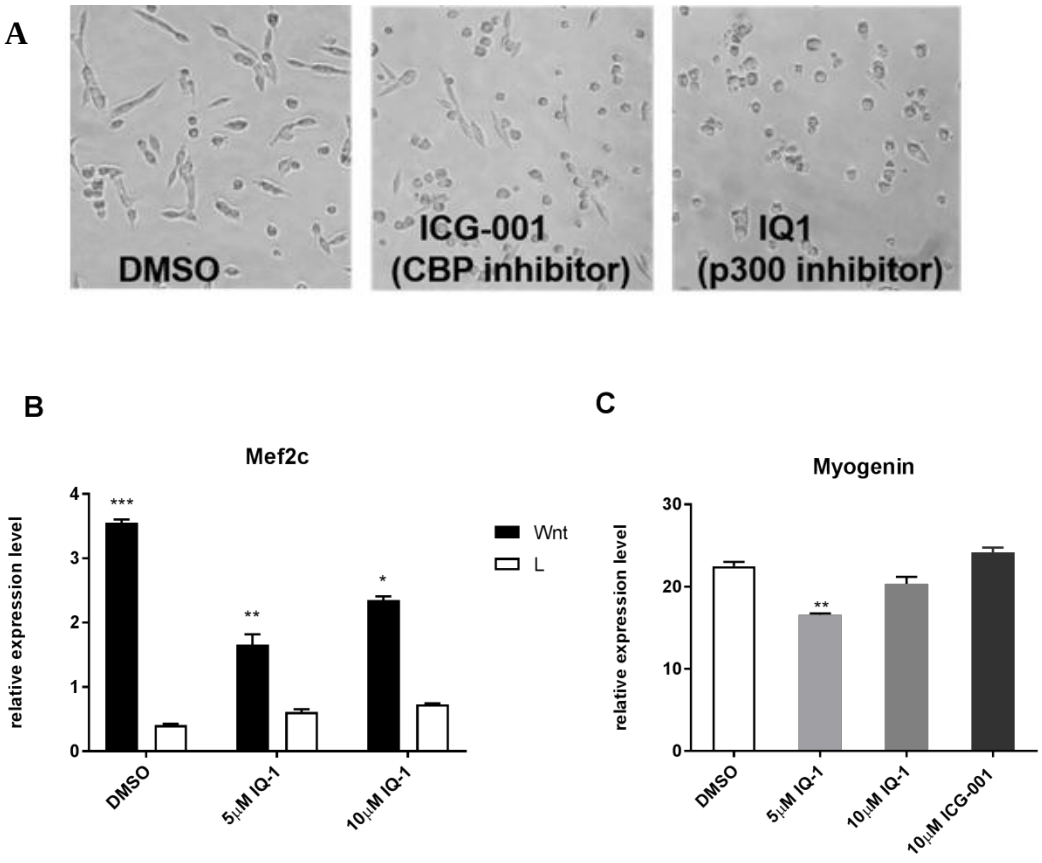

Figure 5.1: Images Morphological and gene expression changes in cells treated with Wnt3a with and without ICG-001 or IQ-1.and expression of MRFs in primary myoblasts post treatment

(A) Images of wild-type primary myoblasts post treatment with 5μM ICG-001 or 10μM IQ-1. **(B)** Expression of Mef2c in primary myoblasts treated with Wnt3a or control media, with or without IQ-1. **(C)** Expression of myogenin in IQ-1 or ICG-001 treated primary myoblasts. DMSO is used as the vehicle control. Primary myoblasts were harvested for RNA extraction 48 hours post-treatment. Total RNA was isolated and reverse transcribed. mRNA expression was assessed by quantitative real-time PCR, normalised to the housekeeping gene RPS26, then normalised over the results from cells treated with L-cell medium control for figure B.

Three independent experiments were performed. Error bars represent SEM. * $p < 0.05$, ** $p < 0.01$ and *** $p < 0.0001$ relative to the control unless otherwise marked.

Primary myoblasts treated with only DMSO elongated consistent with the early stages of differentiation. Myoblasts treated with IQ-1 remained very rounded, which indicated that their differentiation was impaired compared to the control condition. In contrast, ICG-001 did not appear to impair the morphological differentiation of the myoblasts.

The expression of the myogenic marker Mef2c was induced about nine fold by Wnt3a treatment in combination with DMSO vehicle, consistent with a strong pro-differentiative effect of the Wnt ligand. Compared to the DMSO control, IQ-1 treatment reduced the ability of Wnt3a to induce Mef2c to only three fold. This result showed that targeting p300 with IQ-1 impaired myoblast differentiation at the molecular level and supports the idea that p300 is a pro-differentiation factor of β-catenin.

The expression of myogenin was also reduced by treatment with 5 μM IQ-1, although the effect was more modest than the effect on Mef2c expression. The effect of IQ1 was not dose-dependent and actually the higher dose was less effective, possibly related to cell toxicity. In contrast, ICG-001 treatment did not reduce the level of myogenin. These results indicate that ICG-001 has no negative impact on myoblast differentiation; which suggests that CBP may not be involved in the pro-differentiation effect of Wnt/β-catenin signalling in muscle. Interestingly, ICG-001 appeared to slightly increase myogenin expression compared to the control condition; this may be due to inhibition of formation of β-catenin/CBP complexes, freeing β-catenin to recruit p300.

5.3.2 ICG-001 inhibits fibrosis *in vitro*

C3H10T1/2 cells were plated in 24-well plates 24 hours before being treated with Wnt3a medium or L-cell medium control in combination with ICG-001 or DMSO vehicle. C3H10T1/2 cells were harvested for RNA extraction 48 hours post treatment.

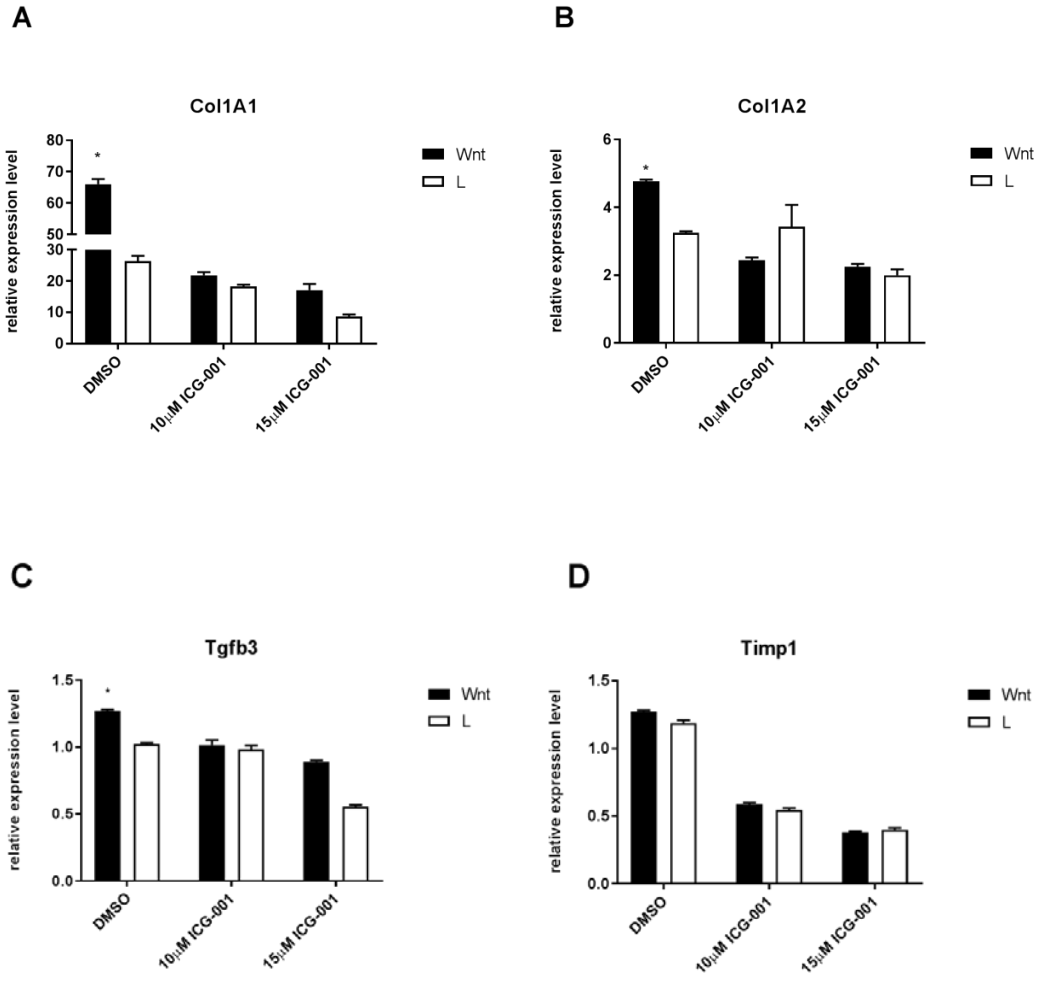

Figure 5.2: Relative expression of Col1A1 (A), Col1A2 (B), Tgfb3 (C) and Timp1 (D) in ICG-001 treated C3H10T1/2 cells

C3H10T1/2 cells were treated with Wnt3a or control media, with or without ICG-001 (10μM or 15μM), or DMSO control, and harvested for RNA extraction 48 hours post-treatment. Total RNA was isolated and reverse transcribed. mRNA expression was assessed by quantitative real-time PCR, normalised to the housekeeping gene RPS26, then normalised

over the results from cells treated with L-cell medium control. Three independent experiments were performed. Error bars represent SEM. * $p < 0.05$ relative to the control unless otherwise marked.

As shown in in Figure 5.2, the expression of fibrotic markers Col1A1 and Col1A2 were significantly induced by Wnt treatment, with ColA1 induced approximately 2.5 fold and Col1A2 induced around 40%. ICG-001 treatment at two different doses inhibited this induction of Col1A1 and Col1A2 by Wnt3a.

The fibrotic markers Tgfb3 and Timp1 were only slightly induced by Wnt (Tgfb3 induction was statistically significant while Timp1 was not); the induction of Tgfb3 was prevented by ICG-001 and the basal expression was also reduced at the higher dose. The levels of Timp1 were reduced by about one third with 10 µM ICG-001 and one half with 15 µM ICG-001, regardless of the medium (Wnt3a or L- cell medium control).

The fact that the expression of all four fibrotic markers was decreased by ICG-001 suggests that their regulation by Wnt involves CBP and supports the idea that ICG-001 may be used to inhibit pro-fibrotic Wnt signalling.

5.3.3 ICG-001 inhibits fibrosis *in vivo*

To determine whether ICG-001 could be effective in inhibiting fibrosis *in vivo*, we used a muscle injury model with cardiotoxin (CTX). Four mice (2 pairs per condition) were injected with CTX into the tibialis anterior (TA) in both hind limbs; three days later, the left hind limb was injected again with CTX while the right hind limb was injected with saline as a control. The left hind limb that received the double-injury thus represents an ‘asynchronous regeneration’ model in which the first regeneration process is disrupted by the initiation of the second injury leading to activation of fibrotic pathways (Dadgar et al., 2014). The right limb (single injury) is

expected to repair efficiently with no activation of fibrotic markers. ICG-001(12mg/kg) was injected IP to one of each pair of mice on day 5 days post second injury and subsequently every second day for 4 days (3 doses in total). At 9 days post injury, the mice were euthanized and the injured muscles were dissected for RNA extraction. The expression of Connective tissue growth factor (Ctgf), a Wnt target and early fibrosis marker, was assessed by qRT-PCR as previously described. Rps26 was used a housekeeping reference gene. Ctgf expression level in the double injured limb was normalized to that in the single injured limb for each mouse. Ctgf was induced an average of 4 fold in the double injured limb compared to the single injected limb. This induction was completely blocked by ICG-001 in both pairs of mice (Figure 5.3, data was generated in our laboratory with technical assistance). This very small pilot study indicated that 'asynchronous regeneration' model indeed promotes the pro-fibrotic pathway. Moreover, it suggests that ICG-001 inhibits activation of this pathway *in vivo* and may be a promising candidate for treating fibrosis in muscle.

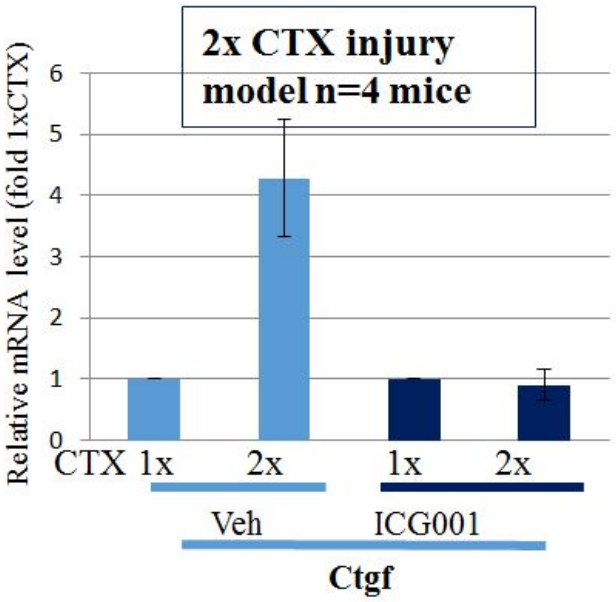

Figure 5.3: CTX injury study

CTX was injected once or twice (3 days apart) and ICG-001 was injected IP over 4 days,

starting 5 days post injury. Ctgf = connective tissue growth factor. n=4.

5.4 Conclusion and discussion

5.4.1 CBP is involved in the pro-fibrotic effect of Wnt/β-catenin signalling and p300 is associated with the pro-differentiation effect of Wnt/β-catenin signalling

Our results indicate that CBP and p300 have distinct roles in Wnt/β-catenin regulated muscle stem cell differentiation.

The CBP/β-catenin complex inhibitor ICG-001 did not inhibit differentiation of myoblasts (Figure 5.1C). However, ICG-001 did inhibit fibrotic pathways in the C3H10T1/2 cells, as indicated by decreased expression of four fibrotic markers (Figure 5.2).

In contrast, p300/β-catenin blocker IQ-1 inhibited myoblast differentiation phenotypically (Figure 5.1 A), and also reduced the expression of myogenic markers Mef2c and Myogenin (Figure 5.1 B and C). Our ChIP-PCR data also showed that p300 was recruited to Tmem8c promoter in Wnt treated wild-type myoblasts, which indicated that p300 may facilitate the expression of Tmem8c (Myomaker). Together these data suggest that p300 is associated with the pro-differentiation effect of Wnt/β-catenin signalling in muscle.

5.4.2 ICG-001 is a promising candidate for treating fibrosis in muscle

Canonical Wnt is a double-edged sword as it is associated with fibrosis, but also is important for muscle regeneration, which makes it difficult to target for therapeutic applications in muscle.

Based on our observations of distinct usage of coactivators CBP and p300 in Wnt/β-catenin signalling, we propose that we might be able to specifically inhibit the pro-fibrotic effect of Wnt/β-catenin (involving CBP) without blocking differentiation

(involving p300) using chemical inhibitors such as ICG-001. The in vitro results shown here including the inhibition the expression of four genes that are important in different aspects of muscle fibrosis, including collagens, the matrix remodeling factor Timp1, and the Tgfb3, suggest that the fibrosis pathway may be broadly inhibited; however genome wide studies would be required to confirm this.

In line with this result, we also observed ICG-001 treatment reduced the expression of fibrotic marker Ctgf in CTX-injured mice during muscle repair. These findings further support the idea that CBP is involved in the pro-fibrotic effect of Wnt/β-catenin signalling in muscle. They also suggest that ICG-001 may be a promising candidate for treating fibrosis in muscle *in vivo*. However, it will be critical to repeat these *in vivo* studies with larger number of mice and more a thorough analysis of fibrosis including histological characterization of matrix deposition and myofiber regeneration, as well as expression profile of more fibrotic makers. Of note, we did not see increased expression of collagen genes in our asynchronous regeneration model (not shown), suggesting that other models (i.e. older mice, or other types of injury) may be more useful to study the later stages of fibrosis.

An another important consideration is whether inhibition of β-catenin-CBP complexes with drugs such as ICG-001 will influence the Wnt feedback pathways, in particular, the inhibition of β-catenin activity by Axin. Previous studies have suggested that failure to switch off β-catenin activity compromises muscle regeneration because it disrupts the balance of myoblast proliferation and differentiation (Murphy et al., 2014b). Future studies could examine the possibility of transient or fibroblast-specific β-catenin-CBP inhibition as an approach for inhibiting fibrosis without disrupting Wnt-feedback in muscle progenitors. Ultimately, we hope that such research can help to expedite the development of

therapies for treating fibrosis in muscle by identifying the Wnt/β-catenin-CBP pathway as a tractable target.

CHAPTER 6: General Discussion and Conclusions

Canonical Wnt signalling has been proposed to promote muscle stem cell differentiation during muscle development and regeneration. However, the underlying mechanisms are unclear, particularly regarding the role of the core mediator β-catenin. The existing reports in literature describing the effects of β-catenin perturbation in muscle stem cells are inconsistent, and hence its function remains controversial. To address this controversy we created a β-catenin null model of adult mouse primary myoblasts using CRISPR. This model was expected to improve our understanding of the cell-autonomous functions of β-catenin during myoblast differentiation.

Through a series of studies described in this thesis we addressed not only the requirement for β-catenin in myogenesis, but also the mechanisms of β-catenin action in terms of molecular partners and target genes. We also began to explore possible avenues for therapeutic perturbation of Wnt/β-catenin signalling in muscle.

The main findings of this thesis can be summarised as below, and each of these findings are expanded upon in the subsequent sections.

1) There is a cell-autonomous requirement for β-catenin in differentiation of adult myoblasts;
2) β-catenin interacts with MyoD but not TCF/LEF to induce myogenic differentiation;
3) Wnt/β-catenin signalling promotes myogenic differentiation by inducing the expression of myogenic genes including miRNAs that inhibit Pax7;
4) miR-133b is induced by Wnt/β-catenin and is more potent than miR-206 in repressing Pax7;
5) The fusogenic protein Myomaker is a novel direct target of Wnt/β-catenin signalling;

6) CBP is involved in the pro-fibrotic effect of Wnt/β-catenin signalling and p300 is associated with the pro-differentiation effect of Wnt/β-catenin signalling;
7) The β-catenin-TCF-CBP complex inhibitor ICG-001 is a promising candidate for treating fibrosis in muscle.

Characterization of β-catenin null adult myoblasts shows a requirement for β-catenin in differentiation.

As described in Chapter 3, the β-catenin CRISPR null model was successfully generated in primary myoblasts and characterised using a series of molecular and cellular approaches. An immediate observation was that the differentiation of β-catenin null myoblasts was greatly delayed relative to wild-type myoblasts; this phenotype was demonstrated by imaging, time-lapse recording of differentiation, qPCR analysis of myogenic gene expression, and immunostaining of myogenic markers. After this extensive phenotypic analysis, we verified this knockout model by rescue with exogenously expressed β-catenin, and performed RNA-seq to better understand how the mutant and wild-type primary myoblasts respond to canonical Wnt ligand. Essentially all of the muscle specific genes that were induced by Wnt3a in wild-type myoblasts, failed to be induced in the β-catenin null myoblasts. Our interpretation of this data was that in the absence of β-catenin, myoblasts cannot respond to Wnt3a by inducing the myogenic program.

Consistent with our findings, Suzuki *et al.* (Suzuki et al., 2015) reported that Wnt/β-catenin signalling regulates multiple steps of myogenesis. Using the Wnt inhibitor IWR1-endo, they showed that fusion of myoblasts was largely blocked, and that this regulation involved Fermt2. Myofibres that did form under Wnt inhibitor treatment were short with fewer nuclei, and the expression of MyHC in myoblasts and

myofibres was significantly reduced compared to the control condition. This abnormal myofiber phenotype due to the chemical disruption of β-catenin activity is very similar to our β-catenin null model, where fusion of null myoblasts is delayed and fibres that form are short and show reduced MyHC expression. More recently, Rudolf *et al.* (Rudolf et al., 2016b) reported that Wnt/β-catenin signalling controls muscle regeneration *in vivo*. By using a satellite-cell/myoblast specific conditional recombination approach, they created knockout and constitutively active β-catenin mouse models. They observed that myoblasts with β-catenin deficiency had delayed differentiation, and myoblasts with constitutively active β-catenin precociously differentiated *in vivo* and *in vitro*. After TA muscle injury, both mutants showed impaired regeneration with aberrant extracellular matrix remodelling. Their study agrees with ours and supports our conclusion that β-catenin function is required for differentiation during muscle regeneration. However, a previous study by Murphy *et al.* (Murphy et al., 2014b) contradicts both our findings and the above research. They concluded that β-catenin activity is not required but needs to be silenced during muscle regeneration. The genetic approach (satellite cell/myoblast specific conditional recombination) used by Murphy *et al.* is similar to that of Rudolf *et al.*, but the observations are opposite. One possible explanation may be that 'recombination escaper' cells mediated muscle repair in the Murphy *et al.* model. The recombination efficiency was only evaluated by FACS at one time point after induction of recombination (5 days after the final tamoxifen injection), revealing only a small number of escaper cells (estimated at ~1%) that were considered functionally insignificant. However, these escaper cells may have expanded later during the regenerative process and ultimately have reached numbers sufficient for normal repair capability, thus masking the functional deficiency of the β-catenin knockout cells. If this indeed occurred then it would suggest that cells that are able to

regenerate the muscle have a strong selective advantage over defective (e.g. β-catenin null) cells.

Mechanisms of β-catenin action in myoblasts during differentiation.

To date there is limited research uncovering the detailed mechanisms of β-catenin action during myoblast differentiation. We previously performed histone ChIP-seq analysis in wild-type myoblasts had identified regions of chromatin that were activated by Wnt3a treatment; moreover motif analysis had shown that these regions were enriched in MEF and MRF binding sites, but not the classical Wnt responsive DNA element, the TCF/LEF site. This had suggested a model in which Wnt signals were transduced to myogenic target genes by MRFs and MEFs rather than by TCF/LEF.

To test this model explicitly, we generated a β-catenin variant that could not bind to TCF/LEF factors and found that it could still rescue the differentiation of the β-catenin null myoblasts. Taken together with research by Kim *et al.* (Kim et al., 2008b) that showed that MyoD and β-catenin physically interact, this prompted a model in which β-catenin and MyoD might be co-recruited to myogenic genes. To test this model, we performed MyoD and β-catenin ChIP-PCR analysis, as well as MyoD ChIP-seq analysis in wild-type and β-catenin null myoblasts. ChIP-PCR analysis of a set of activated myogenic promoters showed that Wnt3a simultaneously increased the binding of MyoD and β-catenin to these promoters. Next, we performed MyoD ChIP-seq to explore the relationship of MyoD and β-catenin at the global genomic level. While wild-type cells showed increased binding of MyoD to promoter regions containing E-box and MADS motifs after Wnt3a treatment, β-catenin null cells showed no such increase in MyoD binding. Overall, we concluded from these studies that TCF/LEF is not involved in the differentiation program of

muscle stem cells, and that MyoD is the partner required by β-catenin during myoblast differentiation. This notion is further supported by two previous studies (Kim et al., 2008a; Tanaka et al., 2011). Kim *et al.* (Kim et al., 2008a) showed that interaction of β-catenin with MyoD increases the binding of MyoD to the E-box element in DNA. The same group also showed that TCF/LEF was not expressed in myotubes (Kim et al., 2008a). In another study, β-catenin/TCF complex inhibitor FH535 impaired the proliferation of myoblasts (Tanaka et al., 2011), which suggested that TCF/LEF is involved in myoblast proliferation rather than differentiation.

The notion that MyoD is the main mediator of Wnt-β-catenin signalling during myogenic differentiation is consistent with its role as the master regulator that controls gene expression during this process. In particular, MyoD binds to promoters and intergenic regions in myoblasts and myotubes (Blais et al., 2005; Cao et al., 2010), and the binding at these regulatory regions increases during myoblast differentiation (Cao et al., 2010). Additionally, MyoD recruits factors needed for enhancer assembly and histone-modifying enzymes (such as p300) that control the acquisition of activating histone modifications such as H3K4mel and H3K27ac (Blum et al., 2012).

The observation that there is less binding of MyoD to chromatin after Wnt3a treatment of β-catenin null myoblasts, relative to wild-type myoblasts, could suggest that the level of MyoD is reduced, or that the occupancy of MyoD at relevant genomic loci is altered in the absence of β-catenin. We found that the amount of MyoD protein was not reduced in the null cells compared to wild-type myoblasts; moreover the level of MyoD protein was not increased by Wnt3a or β-catenin overexpression in the wild-type myoblasts. This data indicates that it is MyoD

occupancy, and not the level of MyoD, that is altered by Wnt3a in a β-catenin-dependent manner. We will require further study to determine exactly how β-catenin alters MyoD recruitment to its target elements in DNA. Two possibilities are 1) that it enhances the stability of the MyoD-DNA binding complex, and 2) that it promotes a modification of MyoD that enhances its binding, such as acetylation. These possibilities can be tested in the future using chromatin-based assays in our null myoblasts. Ideally, it would also be desirable to perform both MyoD and β-catenin ChIP-seq analysis in the same cells and determine the extent to which their target loci overlap. Moreover, Re-ChIP analysis, in which DNA-transcription factor complexes captured with one antibody (i.e. MyoD) are eluted are re-captured with another antibody (i.e. β-catenin) might be an effective way to test for simultaneous adjacent binding of these factors. No data for β-catenin ChIP-seq was presented in this thesis as various attempts to perform this analysis were unsuccessful, with even known canonical targets (such as Axin2) not showing enrichment in the ChIP-seq data. In contrast, analytical ChIP (analysed by qPCR) performed with the same β-catenin antibodies has reproducibly shown enrichment of numerous Wnt targets including Axin2. We suspect that this discrepancy between the efficacy of β-catenin ChIP and ChIP-seq relates to the size of the crosslinked protein-DNA complexes formed in myoblasts and the specific protocols employed in ChIP-seq library construction. If the complexes formed by β-catenin and its cofactors with target DNA are very large, then they may be lost during the size-selection step of library construction. It the future, it would be useful to optimize the library construction process for β-catenin, perhaps by adding a DNA shearing step after the crosslinks between the captured DNA and proteins have been reversed. This could reduce the size of large fragments making them amenable to cloning and increasing their representation in the resultant library.

With respect to the targets of putative β-catenin-MyoD complexes that are involved in differentiation, we propose that the broad network of known pro-differentiation genes may be subject to this regulatory pathway downstream of Wnt. This network includes other transcriptional regulators, miRNAs (as discussed further below), and direct mechano-chemical effectors of cell adhesion, cell fusion, and cytoskeletal remodelling. In support of this idea, we saw genes corresponding to each of these functional categories (especially those related to contractile apparatus assembly) in the GO analysis of our RNA-seq study comparing the transcriptomes of wild-type and null cells after Wnt3a treatment.

We also identified novel direct targets of Wnt-β-catenin signalling that are worthy of discussion including Myomaker. Myomaker (Tmem8c) was named in 2013 based on its crucial role during myoblast fusion and muscle formation (Millay et al., 2013). Myomaker is an eight transmembrane protein which is expressed on the surface of myoblasts during fusion and downregulated thereafter. It is not only required for fusion during embryonic myogenesis, but is also critical for adult muscle regeneration (Millay et al., 2014b). How myomaker is regulated has been unclear. One study in chicken myoblasts reported that myomaker is regulated by MyoD, myogenin and miR-140-3P (Luo et al., 2015a). However the activity of the chicken myomaker gene promoter was only induced very modestly (less than 1.5 fold) by MyoD or myogenin in their study. We found that the mouse myomaker promoter is induced around 10-15 fold by MyoD and myogenin in reporter assays (data not shown). Based on data from both ChIP-PCR and promoter-reporter assays we could conclude that myomaker is regulated directly by Wnt signalling via β-catenin binding to the proximal promoter region. Moreover, we found that Wnt increased binding of MyoD to the promoter. Thus it is likely that Wnt/β-catenin regulates myoblast fusion in part through upregulation of myomaker in a precise spatiotemporal manner.

It is important to note that the adhesion function of β-catenin itself was also implicated in our studies in promoting myoblast fusion/differentiation. β-catenin is known to function at the plasma membrane in a complex with α-catenin, with α-actinin and cadherins at intercellular adherens junction complexes that transduce cell contact into various cellular responses including actin reorganization (Aberle et al., 1994; Hinck et al., 1994; Knudsen et al., 1995; Pokutta and Weis, 2000). By generating a mutant form of β-catenin that could not interact with α-catenin, we found that loss of this interaction reduced its ability to rescue myoblast differentiation. This finding is in general agreement with those of Suzuki *et al.* (Suzuki et al., 2015) who reported that inhibition of β-catenin with IWR1-endo disrupted actin accumulation and alignment and prevented colocalization of cadherin and β-catenin in myofibers. Exactly how the functions of β-catenin at membrane adherens junction complexes and in the nucleus are coordinated remains to be determined and will be an important area for future studies.

MicroRNAs as targets of Wnt/β-catenin signalling: a mechanism for de-repression of myogenesis.

Canonical Wnt not only promotes the transcription of protein-coding myogenic genes, but also increased the expression of specific miRNAs. Previous studies in our laboratory indicated that two of the four MyomiRs, miR-206 and miR-133b, were specifically induced by Wnt3a in the C2C12 cell line. miR-206 is reported to be involved in Pax7 regulation (Chen et al., 2010a; Dey et al., 2011a), and our bioinformatics study predicted that miR-133b would also bind to Pax7 3'UTR. In studies described in Chapter 4, we explored the role of miR-206 and miR-133b in Pax7 regulation downstream of Wnt/β-catenin signalling. We found that Pax7 is repressed by Wnt3a in wild-type myoblasts, but remains expressed in the absence of

β-catenin, indicating that inhibition of Pax7 protein is β-catenin dependent. In parallel with the loss of Pax7, we found that Wnt3a induced the primary transcripts and the mature processed forms of miR-206 and miR-133b in wild-type, but not β-catenin null, myoblasts. This suggested that miR-133b and miR-206 might be key mediators of Wnt/β-catenin-induced downregulation of Pax7. miRNA mimic experiments proved that miR-133b was more potent than miR-206 in Pax7 downregulation at both the mRNA and protein levels. Studies using a luciferase reporter construct containing the Pax7 3'UTR indicated that this was mediated through the 3'UTR; moreover mutagenesis of the predicted miR-133b binding site indicated that miR-133b functions in part through this site, but that there are possibly other binding sites as well. Future studies should identify these sites, which could involve deletion and mutagenesis of the Pax7 3'UTR. There may also be other Wnt-responsive miRNAs produced by myoblasts that target Pax7. In particular, future studies should examine whether any of the novel Wnt-regulated miRNAs that we identified in Chapter 4 might also target Pax7.

Overall, the work reported in Chapter 4 showed for the first time that miR-133b was a direct regulator of Pax7, and also mapped a pathway from Wnt3a to the posttranscriptional regulation of Pax7. Pax7 is known to be an inhibitor of differentiation and its downregulation is essential for myogenic differentiation to proceed (Olguin and Olwin, 2004; Zammit et al., 2004), in part by allowing allow myogenin to accumulate and drive the myogenic program. We propose that the Wnt/β-catenin pathway has two essential roles in myogenesis: de-repression of the differentiation pathway by removing Pax7, and active induction of differentiation-associated genes.

We also showed that exosomes secreted into myoblast media contained all of the

mature MyomiRs: miR-133a/b, miR-206, and miR-1; moreover, the induction of exosomal miRNA levels by Wnt treatment mirrored that of cellular miRNAs. By packaging miRNAs such as miR-133b and miR-206 into exosomes that can be exported into the microenvironment, the pro-differentiation effect of these miRNAs might be spread to neighbouring myoblasts and enhance their differentiation. However, the capacity of these exosomes to transmit such a signal remains to be shown empirically. In the future this could be achieved by isolating exosomes from Wnt3a- and control- treated cells, and applying them to naïve myoblasts, and assessing whether they are sufficient to induce differentiation.

An interesting observation about miR-133b is that both the primary and mature miRNA levels are much lower in the β-catenin CRISPR null cells compared to the wild-type myoblasts. This is consistent with the higher level of Pax7 found in the null cells. Our RNA-seq data also suggests that lipid metabolism pathways are elevated in the β-catenin null cells. miR-133 has been reported to control brown adipose determination in adult skeletal muscle stem cells (Yin et al., 2013). In particular, miR-133 inhibits brown adipose commitment in satellite cells, and antagonism of miR-133 was shown to induce satellite cells to convert to brown adipocytes during muscle regeneration. Hence, reduced miR-133 in β-catenin null cells might promote plasticity and acquisition of an adipogenic phenotype. However, additional experiments will need to be performed to test this idea, such as lipid staining and lipid content measurement, and assessment of brown and white adipocyte markers in the wild-type and null myoblast lines.

The main findings from Chapters 3 and 4 have been distilled into the model shown in Figure 6.1 which depicts the proposed different roles for β-catenin in MyoD-containing complexes that activate and de-repress differentiation, and in TCF/LEF-

complexes that are involved in Wnt feedback as well as having other functions (such as fibrosis as discussed further below).

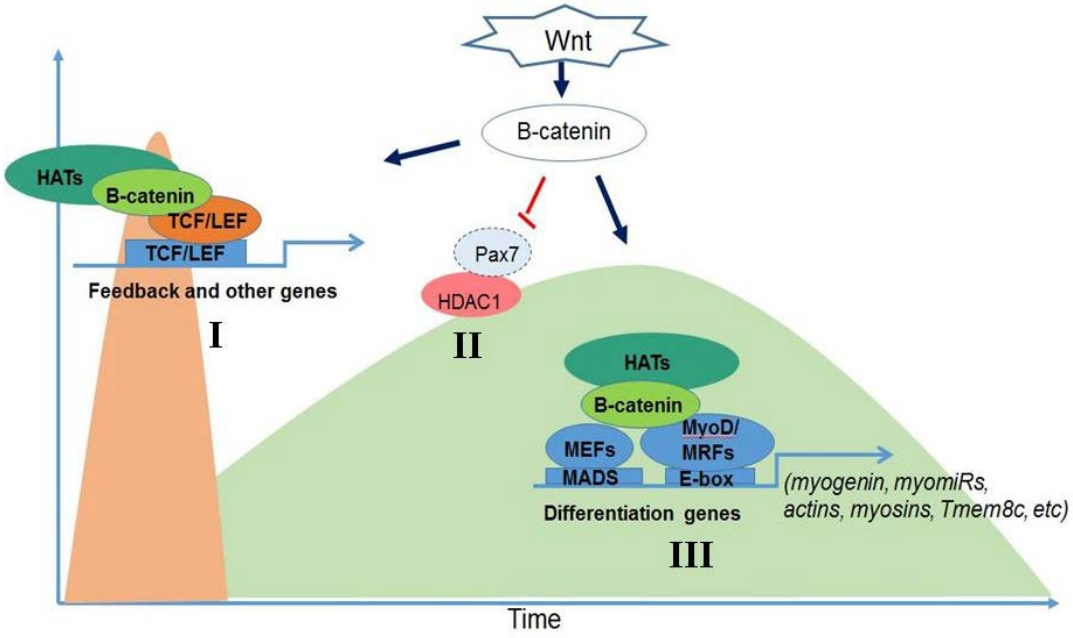

Figure 6.1: Working model for the role of Wnt/β-catenin signalling in myoblasts

Wnt signalling in myoblasts operates through three molecular pathways (I, II, III). The first **(I)** is initiated when stabilised β-catenin interacts with TCF/LEF to drive transcription of Axin2 and other Wnt feedback genes. In the second pathway **(II)**, Wnt signalling leads to the reduction of Pax7 protein and therefore the Pax7-HDAC1 inhibitory complex, thereby de-repressing the myogenic program. Reduction of Pax7 is most likely by Wnt mediated activation of pro-myogenic miRNAs. In the third pathway **(III)**, stabilised β-catenin cooperates with MyoD and possibly also MEFs, which bind to E-box and MADS sites in pro-myogenic differentiation genes. This enhances MyoD binding and likely the recruitment of HATs, leading to increased transcription thus directly promoting differentiation.

Wnt – signalling and fibrosis: a possible therapeutic target?

Canonical Wnt is a double-edged sword as it can promote myogenic differentiation but it can also contribute to fibrosis. We cannot block Wnt/β-catenin signalling completely in muscle to ameliorate fibrosis, as this would almost certainly inhibit muscle regeneration. In many cell types, complexes of β-catenin-TCF/LEF are reported to be involved in Wnt-promoted fibrosis (Hao et al., 2011; Henderson et al.,

2010; Sasaki et al., 2013); moreover, these profibrotic complexes also involve the coactivator CBP (Hao et al., 2011; Henderson et al., 2010; Sasaki et al., 2013). In Chapter 3, it was concluded that TCF/LEF is not directly involved in activating pro-differentiation genes; this suggested that transcriptional complexes required for myoblast differentiation may be different from those involved in fibrotic signalling. To further explore this idea, we investigated the role of CBP in different aspects of Wnt signalling in Chapter 5. The CBP/β-catenin inhibitor ICG-001 can specifically block the interaction between CBP and β-catenin. Our results showed that ICG-001 reduced the expression of fibrotic markers in the C3H10T1/2 mesenchymal progenitor cell line and also reduced the expression of fibrotic gene Ctgf by about four fold in a fibrosis mouse model. In contrast, differentiation of myoblasts in response to Wnt signals was not impaired by ICG-001, which was shown by induction of myogenic markers. However myoblast differentiation was affected by the administration of the p300/β-catenin complex inhibitor IQ-1. Taking the effect of IQ-1 on myoblasts together with prior literature (Higuchi et al., 2016; Rieger et al., 2016),we postulate that the pro-myogenic effect of Wnt involves the cooperation of β-catenin, MRFs, MEFs and the coactivator p300. In contrast CBP is likely to be important for Wnt/β-catenin mediated pro-fibrotic signalling. Based on these observations, we proposed that it might be possible to exploit the differential usage of β-catenin coactivators to chemically block the fibrotic effect of Wnt/β-catenin signalling (involving CBP) without blocking differentiation (involving p300).

Currently, our data on the inhibitory effect of ICG-001 on fibrosis is quite preliminary. In particular, we only studied one fibrogenic cell type *in vitro* (C3H10T1/2), which are an immortal cell line variously described in literature as resembling fibroblasts and multipotent mesenchymal progenitor cells. In injured and dystrophic muscle, muscle associated fibroblasts and fibroadipogenic progenitors

(FAPs) are likely to be the main origin of fibrotic inclusions (Dong et al., 2017; Lemos et al., 2015; Li et al., 2008). It will be important to examine whether ICG-001 can inhibit pro-fibrotic genes in these primary cell types isolated directly from muscle. Moreover, the pilot *in vivo* studies will need to be repeated with larger numbers of mice, and a more detailed analysis of muscle fibrosis occurring *in vivo* carried out. It has also been reported that excessive Wnt signalling can induce transdifferentiation of myoblasts to fibroblasts (Brack et al., 2007), although the extent to which this is a major contributor to fibrosis is unclear. Nevertheless, it would be useful to assess whether ICG-001 can also prevent this fibrogenic conversion of myoblasts. The model shown in Figure 6.2 summarizes the proposed different roles of Wnt/β-catenin in myogenesis and fibrosis.

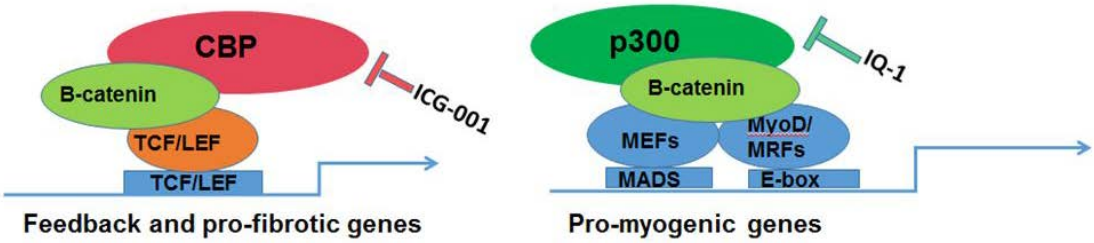

Figure 6.2: Working model for the differential role of different coactivator complexes in pro-myogenic and pro-fibrotic signalling

Wnt signalling in muscle stem cells has two major effects, promoting fibrosis and myogenic differentiation, and this is dependent on the specific β-catenin coactivator recruited to the transcriptional complex. CBP (which can be inhibited by ICG-001), associates with the β-catenin-TCF/LEF complexes to activate Wnt responsive pro-fibrotic genes at TCF/LEF binding motifs. Conversely, p300 (which can be inhibited by IQ-1) associates with the β-catenin/MRF/MEF complex to bind to E-box and MADS binding motifs, thereby activating the transcription of Wnt responsive pro-myogenic genes.

One last issue when considering the potential of therapeutic inhibition of β-catenin-TCF/LEF-CBP complexes to ameliorate fibrosis is the extent to which these

complexes may also be required for particular steps of muscle regeneration. As has been discussed in Chapter 1, after muscle injury, satellite cells are activated, proliferate and differentiate to form new myofibers. The balance between proliferation and differentiation is clearly essential for effective regeneration. This is evident from observations that driving excessive differentiation at the expense of sufficient proliferation leads to smaller thinner fibres (Brack et al., 2008b). As also discussed in Chapter 1, negative feedback to the Wnt signalling pathways constrains Wnt signalling into cyclical on-off loops, this feedback involves direct activation of the Axin2 gene by β-catenin/TCF complexes. It is quite possible that disrupting β-catenin/TCF/CBP complexes with ICG-001 would disrupt this feedback. Thus, although activation of pro-differentiation genes may not be impaired, the disruption of the normal cyclical pattern of Wnt signalling could interfere with the balance of proliferation and differentiation causing inadequate repair. Future studies will need to more carefully examine the role of different β-catenin cofactors in the different aspects of Wnt signalling in myogenesis and fibrosis. We already have evidence that there is crosstalk between the pro-differentiation and feedback associated transcriptional complexes/pathways. In particular, we showed previously that the homeobox factor Barx2 interacts with β-catenin and is part of both pro-myogenic MyoD-containing complexes, and also β-catenin/TCF complexes that activate Axin2 (Hulin et al., 2016b). Similarly, Pax7 represses activation of pro-myogenic E-box-containing genes, but also represses Axin2 expression via interaction with β-catenin/TCF complexes (Hulin et al., 2016b).

It is clear that there is much still to be understood about the molecular mechanisms by Wnt/β-catenin signalling controls different cellular processes in muscle, including differentiation, Wnt feedback, and fibrosis. Ultimately however, we hope our research may provide an avenue to develop new therapies for muscle fibrosis

associated with muscle degenerative diseases.

References

Aberle, H., Butz, S., Stappert, J., Weissig, H., Kemler, R., and Hoschuetzky, H. (1994). Assembly of the cadherin-catenin complex in vitro with recombinant proteins. Journal of cell science *107*, 3655-3663.

Aberle, H., Schwartz, H., Hoschuetzky, H., and Kemler, R. (1996). Single Amino Acid Substitutions in Proteins of the armadillo Gene Family Abolish Their Binding to -Catenin. Journal of Biological Chemistry *271*, 1520-1526.

Agley, C., Lewis, F., Jaka, O., Lazarus, N., Velloso, C., Francis-West, P., M. Ellison-Hughes, G., and D. R. Harridge, S. (2017). Active GSK3β and an intact β-catenin TCF complex are essential for the differentiation of human myogenic progenitor cells, Vol 7.

Ait-Si-Ali, S., Carlisi, D., Ramirez, S., Upegui-Gonzalez, L.-C., Duquet, A., Robin, P., Rudkin, B., Harel-Bellan, A., and Trouche, D. (1999). Phosphorylation by p44 MAP Kinase/ERK1 stimulates CBP histone acetyl transferase activity in vitro. Biochemical and biophysical research communications *262*, 157-162.

Akcora, B.O., Storm, G., and Bansal, R. (2017). Inhibition of canonical WNT signaling pathway by beta-catenin/CBP inhibitor ICG-001 ameliorates liver fibrosis in vivo through suppression of stromal CXCL12. Biochim Biophys Acta *1864*, 804-818.

Akhmetshina, A., Palumbo, K., Dees, C., Bergmann, C., Venalis, P., Zerr, P., Horn, A., Kireva, T., Beyer, C., and Zwerina, J. (2012). Activation of canonical Wnt signalling is required for TGF-β-mediated fibrosis. Nature communications *3*, 735.

Alexandrov, P.N., Dua, P., Hill, J.M., Bhattacharjee, S., Zhao, Y., and Lukiw, W.J. (2012). microRNA (miRNA) speciation in Alzheimer's disease (AD) cerebrospinal fluid (CSF) and extracellular fluid (ECF). International journal of biochemistry and molecular biology *3*, 365.

Allegra, A., Alonci, A., Campo, S., Penna, G., Petrungaro, A., Gerace, D., and Musolino, C. (2012). Circulating microRNAs: new biomarkers in diagnosis, prognosis and treatment of cancer. International journal of oncology *41*, 1897-1912.

Angelini, C. (2007). The role of corticosteroids in muscular dystrophy: a critical appraisal. Muscle & nerve *36*, 424-435.

Arce, L., Pate, K.T., and Waterman, M.L. (2009). Groucho binds two conserved regions of LEF-1 for HDAC-dependent repression. BMC cancer *9*, 159.

Arnold, L., Henry, A., Poron, F., Baba-Amer, Y., Van Rooijen, N., Plonquet, A., Gherardi, R.K., and Chazaud, B. (2007). Inflammatory monocytes recruited after skeletal muscle injury switch into antiinflammatory macrophages to support myogenesis. Journal of Experimental Medicine *204*, 1057-1069.

Aurade, F., Pinset, C., Chafey, P., Gros, F., and Montarras, D. (1994). Myf5, MyoD, myogenin and MRF4 myogenic derivatives of the embryonic mesenchymal cell line C3H10T1/2 exhibit the same adult muscle phenotype. Differentiation; research in biological diversity *55*, 185-192.

Bartel, D.P. (2004). MicroRNAs: genomics, biogenesis, mechanism, and function. cell *116*, 281-297.

Beauchamp, J.R., Heslop, L., David, S., Tajbakhsh, S., Kelly, R.G., Wernig, A., Buckingham, M.E., Partridge, T.A., and Zammit, P.S. (2000). Expression of CD34 and Myf5 defines the majority of quiescent adult skeletal muscle satellite cells. The Journal of cell biology *151*, 1221-1234.

Beccafico, S., Riuzzi, F., Puglielli, C., Mancinelli, R., Fulle, S., Sorci, G., and Donato, R. (2011). Human muscle satellite cells show age-related differential expression of S100B protein and RAGE. Age *33*, 523-541.

Bengtsson, N.E., Hall, J.K., Odom, G.L., Phelps, M.P., Andrus, C.R., Hawkins, R.D., Hauschka, S.D., Chamberlain, J.R., and Chamberlain, J.S. (2017). Muscle-specific CRISPR/Cas9 dystrophin gene editing ameliorates pathophysiology in a mouse model for Duchenne muscular dystrophy. Nature communications *8*, 14454.
Bentzinger, C., von Maltzahn, J., and Rudnicki, M.A. (2010). Extrinsic regulation of satellite cell specification. Stem cell research & therapy *1*, 27.
Bernardi, H., Gay, S., Fedon, Y., Vernus, B., Bonnieu, A., and Bacou, F. (2011). Wnt4 activates the canonical β-catenin pathway and regulates negatively myostatin: functional implication in myogenesis. American Journal of Physiology - Cell Physiology *300*, C1122-C1138.
Bienz, M., and Clevers, H. (2000). Linking colorectal cancer to Wnt signaling. Cell *103*, 311-320.
Billin, A.N., Thirlwell, H., and Ayer, D.E. (2000). Beta-catenin-histone deacetylase interactions regulate the transition of LEF1 from a transcriptional repressor to an activator. Mol Cell Biol *20*, 6882-6890.
Bischoff, R. (1975). Regeneration of single skeletal muscle fibers in vitro. The Anatomical Record *182*, 215-235.
Blais, A., Tsikitis, M., Acosta-Alvear, D., Sharan, R., Kluger, Y., and Dynlacht, B.D. (2005). An initial blueprint for myogenic differentiation. Genes & development *19*, 553-569.
Blum, R., Vethantham, V., Bowman, C., Rudnicki, M., and Dynlacht, B.D. (2012). Genome-wide identification of enhancers in skeletal muscle: the role of MyoD1. Genes & development *26*, 2763-2779.
Borello, U., Coletta, M., Tajbakhsh, S., Leyns, L., De Robertis, E.M., Buckingham, M., and Cossu, G. (1999). Transplacental delivery of the Wnt antagonist Frzb1 inhibits development of caudal paraxial mesoderm and skeletal myogenesis in mouse embryos. Development *126*, 4247-4255.
Bour, B.A., O'Brien, M.A., Lockwood, W.L., Goldstein, E.S., Bodmer, R., Taghert, P.H., Abmayr, S.M., and Nguyen, H.T. (1995). Drosophila MEF2, a transcription factor that is essential for myogenesis. Genes & development *9*, 730-741.
Brack, A.S., Conboy, I.M., Conboy, M.J., Shen, J., and Rando, T.A. (2008a). A temporal switch from notch to Wnt signaling in muscle stem cells is necessary for normal adult myogenesis. Cell stem cell *2*, 50-59.
Brack, A.S., Conboy, I.M., Conboy, M.J., Shen, J., and Rando, T.A. (2008b). A temporal switch from notch to Wnt signaling in muscle stem cells is necessary for normal adult myogenesis. Cell Stem Cell *2*, 50-59.
Brack, A.S., Conboy, M.J., Roy, S., Lee, M., Kuo, C.J., Keller, C., and Rando, T.A. (2007). Increased Wnt signaling during aging alters muscle stem cell fate and increases fibrosis. Science *317*, 807-810.
Braun, T., and Arnold, H.H. (1995). Inactivation of Myf-6 and Myf-5 genes in mice leads to alterations in skeletal muscle development. The EMBO journal *14*, 1176-1186.
Braun, T., Bober, E., Rudnicki, M.A., Jaenisch, R., and Arnold, H.-H. (1994). MyoD expression marks the onset of skeletal myogenesis in Myf-5 mutant mice. Development *120*, 3083-3092.
Braun, T., Buschhausen-Denker, G., Bober, E., Tannich, E., and Arnold, H. (1989). A novel human muscle factor related to but distinct from MyoD1 induces myogenic conversion in 10T1/2 fibroblasts. The EMBO journal *8*, 701-709.
Braun, T., Rudnicki, M.A., Arnold, H.-H., and Jaenisch, R. (1992). Targeted inactivation of the muscle regulatory gene Myf-5 results in abnormal rib development and perinatal death. Cell *71*, 369-382.
Breitbart, R.E., Liang, C.S., Smoot, L.B., Laheru, D.A., Mahdavi, V., and Nadal-

Ginard, B. (1993). A fourth human MEF2 transcription factor, hMEF2D, is an early marker of the myogenic lineage. Development *118*, 1095-1106.
Buckingham, M., Bajard, L., Chang, T., Daubas, P., Hadchouel, J., Meilhac, S., Montarras, D., Rocancourt, D., and Relaix, F. (2003). The formation of skeletal muscle: from somite to limb. Journal of Anatomy *202*, 59-68.
Buckingham, M., and Relaix, F. (2007). The role of Pax genes in the development of tissues and organs: Pax3 and Pax7 regulate muscle progenitor cell functions. Annu Rev Cell Dev Biol *23*, 645-673.
Cao, Y., Yao, Z., Sarkar, D., Lawrence, M., Sanchez, G.J., Parker, M.H., MacQuarrie, K.L., Davison, J., Morgan, M.T., and Ruzzo, W.L. (2010). Genome-wide MyoD binding in skeletal muscle cells: a potential for broad cellular reprogramming. Developmental cell *18*, 662-674.
Carlson, M.E., and Conboy, I.M. (2007). Loss of stem cell regenerative capacity within aged niches. Aging cell *6*, 371-382.
Carthy, J.M., Garmaroudi, F.S., Luo, Z., and McManus, B.M. (2011). Wnt3a induces myofibroblast differentiation by upregulating TGF-β signaling through SMAD2 in a β-catenin-dependent manner. PloS one *6*, e19809.
Cesana, M., Cacchiarelli, D., Legnini, I., Santini, T., Sthandier, O., Chinappi, M., Tramontano, A., and Bozzoni, I. (2011). A long noncoding RNA controls muscle differentiation by functioning as a competing endogenous RNA. Cell *147*, 358-369.
Chang, N.C., Chevalier, F.P., and Rudnicki, M.A. (2016). Satellite cells in muscular dystrophy–Lost in polarity. Trends in molecular medicine *22*, 479-496.
Chen, J.-F., Mandel, E.M., Thomson, J.M., Wu, Q., Callis, T.E., Hammond, S.M., Conlon, F.L., and Wang, D.-Z. (2006a). The role of microRNA-1 and microRNA-133 in skeletal muscle proliferation and differentiation. Nature genetics *38*, 228-233.
Chen, J.-F., Mandel, E.M., Thomson, J.M., Wu, Q., Callis, T.E., Hammond, S.M., Conlon, F.L., and Wang, D.-Z. (2006b). The role of microRNA-1 and microRNA-133 in skeletal muscle proliferation and differentiation. Nature genetics *38*, 228.
Chen, J.-F., Tao, Y., Li, J., Deng, Z., Yan, Z., Xiao, X., and Wang, D.-Z. (2010a). microRNA-1 and microRNA-206 regulate skeletal muscle satellite cell proliferation and differentiation by repressing Pax7. The Journal of cell biology *190*, 867-879.
Chen, J.F., Tao, Y., Li, J., Deng, Z., Yan, Z., Xiao, X., and Wang, D.Z. (2010b). microRNA-1 and microRNA-206 regulate skeletal muscle satellite cell proliferation and differentiation by repressing Pax7. J Cell Biol *190*, 867-879.
Cho, I.T., Lim, Y., Golden, J.A., and Cho, G. (2017). Aristaless Related Homeobox (ARX) Interacts with beta-Catenin, BCL9, and P300 to Regulate Canonical Wnt Signaling. PLoS One *12*, e0170282.
Christ, B., and Ordahl, C.P. (1995). Early stages of chick somite development. Anatomy and embryology *191*, 381-396.
Christov, C., Chrétien, F., Abou-Khalil, R., Bassez, G., Vallet, G., Authier, F.-J., Bassaglia, Y., Shinin, V., Tajbakhsh, S., and Chazaud, B. (2007). Muscle satellite cells and endothelial cells: close neighbors and privileged partners. Molecular biology of the cell *18*, 1397-1409.
Chrivia, J.C., Kwok, R.P., Lamb, N., Hagiwara, M., Montminy, M.R., and Goodman, R.H. (1993). Phosphorylated CREB binds specifically to the nuclear protein CBP. Nature *365*, 855-859.
Clevers, H. (2006). Wnt/β-catenin signaling in development and disease. Cell *127*, 469-480.
Collins, C.A., Olsen, I., Zammit, P.S., Heslop, L., Petrie, A., Partridge, T.A., and Morgan, J.E. (2005). Stem cell function, self-renewal, and behavioral heterogeneity of cells from the adult muscle satellite cell niche. Cell *122*, 289-301.
Conerly, M.L., Yao, Z., Zhong, J.W., Groudine, M., and Tapscott, S.J. (2016).

Distinct activities of Myf5 and MyoD indicate separate roles in skeletal muscle lineage specification and differentiation. Developmental cell *36*, 375-385.
Cong, L., Ran, F.A., Cox, D., Lin, S., Barretto, R., Habib, N., Hsu, P.D., Wu, X., Jiang, W., and Marraffini, L. (2013). Multiplex genome engineering using CRISPR/Cas systems. Science, 1231143.
Cornelison, D., and Wold, B.J. (1997). Single-cell analysis of regulatory gene expression in quiescent and activated mouse skeletal muscle satellite cells. Developmental biology *191*, 270-283.
Cossu, G., and Borello, U. (1999). Wnt signaling and the activation of myogenesis in mammals. The EMBO journal *18*, 6867-6872.
CRISPR, R. (2011). maturation by trans-encoded small RNA and host factor RNase III Deltcheva. Nature *471*, 602-607.
Crist, C.G., Montarras, D., and Buckingham, M. (2012). Muscle satellite cells are primed for myogenesis but maintain quiescence with sequestration of Myf5 mRNA targeted by microRNA-31 in mRNP granules. Cell stem cell *11*, 118-126.
Dadgar, S., Wang, Z., Johnston, H., Kesari, A., Nagaraju, K., Chen, Y.-W., Hill, D.A., Partridge, T.A., Giri, M., and Freishtat, R.J. (2014). Asynchronous remodeling is a driver of failed regeneration in Duchenne muscular dystrophy. J Cell Biol *207*, 139-158.
Dahl, J.A., and Collas, P. (2008). A rapid micro chromatin immunoprecipitation assay (ChIP). Nature protocols *3*, 1032.
Daniels, D.L., and Weis, W.I. (2005a). Beta-catenin directly displaces Groucho/TLE repressors from Tcf/Lef in Wnt-mediated transcription activation. Nat Struct Mol Biol *12*, 364-371.
Daniels, D.L., and Weis, W.I. (2005b). β-catenin directly displaces Groucho/TLE repressors from Tcf/Lef in Wnt-mediated transcription activation. Nature Structural and Molecular Biology *12*, 364.
Davis, R.L., Weintraub, H., and Lassar, A.B. (1987). Expression of a single transfected cDNA converts fibroblasts to myoblasts. Cell *51*, 987-1000.
Day, K., Shefer, G., Richardson, J.B., Enikolopov, G., and Yablonka-Reuveni, Z. (2007). Nestin-GFP reporter expression defines the quiescent state of skeletal muscle satellite cells. Developmental biology *304*, 246-259.
Dey, B.K., Gagan, J., and Dutta, A. (2011a). miR-206 and-486 induce myoblast differentiation by downregulating Pax7. Molecular and cellular biology *31*, 203-214.
Dey, B.K., Gagan, J., and Dutta, A. (2011b). miR-206 and -486 induce myoblast differentiation by downregulating Pax7. Mol Cell Biol *31*, 203-214.
Dobin, A., Davis, C.A., Schlesinger, F., Drenkow, J., Zaleski, C., Jha, S., Batut, P., Chaisson, M., and Gingeras, T.R. (2013). STAR: ultrafast universal RNA-seq aligner. Bioinformatics *29*, 15-21.
Dong, J., Dong, Y., Chen, Z., Mitch, W.E., and Zhang, L. (2017). The pathway to muscle fibrosis depends on myostatin stimulating the differentiation of fibro/adipogenic progenitor cells in chronic kidney disease. Kidney international *91*, 119-128.
Doudna, J.A., and Charpentier, E. (2014). The new frontier of genome engineering with CRISPR-Cas9. Science *346*, 1258096.
Drees, F., Pokutta, S., Yamada, S., Nelson, W.J., and Weis, W.I. (2005). α-catenin is a molecular switch that binds E-cadherin-β-catenin and regulates actin-filament assembly. Cell *123*, 903-915.
Du, M., Perry, R.L., Nowacki, N.B., Gordon, J.W., Salma, J., Zhao, J., Aziz, A., Chan, J., Siu, K.M., and McDermott, J.C. (2008). Protein kinase A represses skeletal myogenesis by targeting myocyte enhancer factor 2D. Molecular and cellular biology *28*, 2952-2970.

Eckner, R., Ewen, M.E., Newsome, D., Gerdes, M., DeCaprio, J.A., Lawrence, J.B., and Livingston, D.M. (1994). Molecular cloning and functional analysis of the adenovirus E1A-associated 300-kD protein (p300) reveals a protein with properties of a transcriptional adaptor. Genes & development *8*, 869-884.
Eckner, R., Yao, T.-P., Oldread, E., and Livingston, D.M. (1996). Interaction and functional collaboration of p300/CBP and bHLH proteins in muscle and B-cell differentiation. Genes & development *10*, 2478-2490.
Edmondson, D.G., Cheng, T., Cserjesi, P., Chakraborty, T., and Olson, E.N. (1992). Analysis of the myogenin promoter reveals an indirect pathway for positive autoregulation mediated by the muscle-specific enhancer factor MEF-2. Molecular and cellular biology *12*, 3665-3677.
Enesco, M., and Puddy, D. (1964). Increase in the number of nuclei and weight in skeletal muscle of rats of various ages. Developmental Dynamics *114*, 235-244.
Fairman, R., Beran-Steed, R.K., Anthony-Cahill, S.J., Lear, J.D., Stafford, W.F., DeGrado, W.F., Benfield, P.A., and Brenner, S.L. (1993). Multiple oligomeric states regulate the DNA binding of helix-loop-helix peptides. Proceedings of the National Academy of Sciences *90*, 10429-10433.
Fry, C.S., Kirby, T.J., Kosmac, K., McCarthy, J.J., and Peterson, C.A. (2017). Myogenic progenitor cells control extracellular matrix production by fibroblasts during skeletal muscle hypertrophy. Cell stem cell *20*, 56-69.
Gasiunas, G., Barrangou, R., Horvath, P., and Siksnys, V. (2012). Cas9–crRNA ribonucleoprotein complex mediates specific DNA cleavage for adaptive immunity in bacteria. Proceedings of the National Academy of Sciences *109*, E2579-E2586.
Gavard, J., Marthiens, V., Monnet, C., Lambert, M., and Mège, R.M. (2004). N-cadherin Activation Substitutes for the Cell Contact Control in Cell Cycle Arrest and Myogenic Differentiation INVOLVEMENT OF p120 AND β-CATENIN. Journal of Biological Chemistry *279*, 36795-36802.
Gilbert, L.A., Larson, M.H., Morsut, L., Liu, Z., Brar, G.A., Torres, S.E., Stern-Ginossar, N., Brandman, O., Whitehead, E.H., and Doudna, J.A. (2013). CRISPR-mediated modular RNA-guided regulation of transcription in eukaryotes. Cell *154*, 442-451.
Goodman, R.H., and Smolik, S. (2000). CBP/p300 in cell growth, transformation, and development. Genes & development *14*, 1553-1577.
Gordon, M.D., and Nusse, R. (2006). Wnt signaling: multiple pathways, multiple receptors, and multiple transcription factors. Journal of Biological Chemistry *281*, 22429-22433.
Gossett, L.A., Kelvin, D.J., Sternberg, E., and Olson, E. (1989). A new myocyte-specific enhancer-binding factor that recognizes a conserved element associated with multiple muscle-specific genes. Molecular and cellular biology *9*, 5022-5033.
Graham, T.A., Weaver, C., Mao, F., Kimelman, D., and Xu, W. (2000). Crystal Structure of a β-Catenin/Tcf Complex. Cell *103*, 885-896.
Grégoire, S., Tremblay, A.M., Xiao, L., Yang, Q., Ma, K., Nie, J., Mao, Z., Wu, Z., Giguère, V., and Yang, X.-J. (2006). Control of MEF2 transcriptional activity by coordinated phosphorylation and sumoylation. Journal of Biological Chemistry *281*, 4423-4433.
Grégoire, S., Xiao, L., Nie, J., Zhang, X., Xu, M., Li, J., Wong, J., Seto, E., and Yang, X.-J. (2007). Histone deacetylase 3 interacts with and deacetylates myocyte enhancer factor 2. Molecular and cellular biology *27*, 1280-1295.
Grifone, R., Demignon, J., Houbron, C., Souil, E., Niro, C., Seller, M.J., Hamard, G., and Maire, P. (2005). Six1 and Six4 homeoproteins are required for Pax3 and Mrf expression during myogenesis in the mouse embryo. Development *132*, 2235-2249.
Gros, J., Manceau, M., Thomé, V., and Marcelle, C. (2005). A common somitic

origin for embryonic muscle progenitors and satellite cells. Nature *435*, 954.
Gumbiner, B.M. (2000). Regulation of cadherin adhesive activity. The Journal of cell biology *148*, 399-404.
Günther, S., Kim, J., Kostin, S., Lepper, C., Fan, C.-M., and Braun, T. (2013). Myf5-positive satellite cells contribute to Pax7-dependent long-term maintenance of adult muscle stem cells. Cell stem cell *13*, 590-601.
Guy, C.P., Majerník, A.I., Chong, J.P., and Bolt, E.L. (2004). A novel nuclease-ATPase (Nar71) from archaea is part of a proposed thermophilic DNA repair system. Nucleic acids research *32*, 6176-6186.
Haberland, M., Arnold, M.A., McAnally, J., Phan, D., Kim, Y., and Olson, E.N. (2007). Regulation of HDAC9 gene expression by MEF2 establishes a negative-feedback loop in the transcriptional circuitry of muscle differentiation. Molecular and cellular biology *27*, 518-525.
Han, J., Jiang, Y., Li, Z., Kravchenko, V., and Ulevitch, R. (1997). Activation of the transcription factor MEF2C by the MAP kinase p38 in inflammation. Nature *386*, 296.
Han, X.H., Jin, Y.-R., Seto, M., and Yoon, J.K. (2011). A WNT/β-catenin signaling activator, R-spondin, plays positive regulatory roles during skeletal myogenesis. Journal of Biological Chemistry *286*, 10649-10659.
Hao, S., He, W., Li, Y., Ding, H., Hou, Y., Nie, J., Hou, F.F., Kahn, M., and Liu, Y. (2011). Targeted Inhibition of β-Catenin/CBP Signaling Ameliorates Renal Interstitial Fibrosis. Journal of the American Society of Nephrology : JASN *22*, 1642-1653.
Hasty, P., Bradley, A., Morris, J.H., Edmondson, D.G., Venuti, J.M., Olson, E.N., and Klein, W.H. (1993). Muscle deficiency and neonatal death in mice with a targeted mutation in the myogenin gene. Nature *364*, 501.
He, W.A., Calore, F., Londhe, P., Canella, A., Guttridge, D.C., and Croce, C.M. (2014). Microvesicles containing miRNAs promote muscle cell death in cancer cachexia via TLR7. Proceedings of the National Academy of Sciences *111*, 4525-4529.
He, X., Semenov, M., Tamai, K., and Zeng, X. (2004). LDL receptor-related proteins 5 and 6 in Wnt/β-catenin signaling: arrows point the way. Development *131*, 1663-1677.
Hecht, A., Vleminckx, K., Stemmler, M.P., van Roy, F., and Kemler, R. (2000a). The p300/CBP acetyltransferases function as transcriptional coactivators of [beta]-catenin in vertebrates. EMBO J *19*, 1839-1850.
Hecht, A., Vleminckx, K., Stemmler, M.P., Van Roy, F., and Kemler, R. (2000b). The p300/CBP acetyltransferases function as transcriptional coactivators of β-catenin in vertebrates. The EMBO journal *19*, 1839-1850.
Henderson, W.R., Chi, E.Y., Ye, X., Nguyen, C., Tien, Y.-t., Zhou, B., Borok, Z., Knight, D.A., and Kahn, M. (2010). Inhibition of Wnt/β-catenin/CREB binding protein (CBP) signaling reverses pulmonary fibrosis. Proceedings of the National Academy of Sciences *107*, 14309-14314.
Higuchi, Y., Nguyen, C., Yasuda, S.-Y., McMillan, M., Hasegawa, K., and Kahn, M. (2016). Specific direct small molecule p300/β-catenin antagonists maintain stem cell potency. Current molecular pharmacology *9*, 272-279.
Hinck, L., Näthke, I.S., Papkoff, J., and Nelson, W.J. (1994). Dynamics of cadherin/catenin complex formation: novel protein interactions and pathways of complex assembly. The Journal of cell biology *125*, 1327-1340.
Hinterberger, T.J., Sassoon, D.A., Rhodes, S.J., and Konieczny, S.F. (1991). Expression of the muscle regulatory factor MRF4 during somite and skeletal myofiber development. Developmental biology *147*, 144-156.

Hu, P., Geles, K.G., Paik, J.-H., DePinho, R.A., and Tjian, R. (2008). Codependent activators direct myoblast-specific MyoD transcription. Developmental cell *15*, 534-546.
Hulin, J.A., Nguyen, T.D., Cui, S., Marri, S., Yu, R.T., Downes, M., Evans, R.M., Makarenkova, H., and Meech, R. (2016a). Barx2 and Pax7 Regulate Axin2 Expression in Myoblasts by Interaction with beta-Catenin and Chromatin Remodelling. Stem Cells *34*, 2169-2182.
Hulin, J.A., Nguyen, T.D.T., Cui, S., Marri, S., Yu, R.T., Downes, M., Evans, R.M., Makarenkova, H., and Meech, R. (2016b). Barx2 and Pax7 Regulate Axin2 Expression in Myoblasts by Interaction with β-Catenin and Chromatin Remodelling. Stem Cells *34*, 2169-2182.
Huveneers, S., and de Rooij, J. (2013). Mechanosensitive systems at the cadherin–F-actin interface. Journal of Cell Science *126*, 403-413.
Inoue, H., Nojima, H., and Okayama, H. (1990). High efficiency transformation of Escherichia coli with plasmids. Gene *96*, 23-28.
Ishino, Y., Shinagawa, H., Makino, K., Amemura, M., and Nakata, A. (1987). Nucleotide sequence of the iap gene, responsible for alkaline phosphatase isozyme conversion in Escherichia coli, and identification of the gene product. Journal of bacteriology *169*, 5429-5433.
Ivana, L., Ohkawa, Y., Berkes, C.A., Bergstrom, D.A., Dacwag, C.S., Tapscott, S.J., and Imbalzano, A.N. (2005). MyoD targets chromatin remodeling complexes to the myogenin locus prior to forming a stable DNA-bound complex. Molecular and cellular biology *25*, 3997-4009.
Joe, A.W., Yi, L., Natarajan, A., Le Grand, F., So, L., Wang, J., Rudnicki, M.A., and Rossi, F.M. (2010). Muscle injury activates resident fibro/adipogenic progenitors that facilitate myogenesis. Nature cell biology *12*, 153.
Jones, A.E., Price, F.D., Le Grand, F., Soleimani, V.D., Dick, S.A., Megeney, L.A., and Rudnicki, M.A. (2015a). Wnt/beta-catenin controls follistatin signalling to regulate satellite cell myogenic potential. Skelet Muscle *5*, 14.
Jones, A.E., Price, F.D., Le Grand, F., Soleimani, V.D., Dick, S.A., Megeney, L.A., and Rudnicki, M.A. (2015b). Wnt/β-catenin controls follistatin signalling to regulate satellite cell myogenic potential. Skeletal Muscle *5*, 14.
Kaimal, V., Bardes, E.E., Tabar, S.C., Jegga, A.G., and Aronow, B.J. (2010). ToppCluster: a multiple gene list feature analyzer for comparative enrichment clustering and network-based dissection of biological systems. Nucleic Acids Research *38*, W96-W102.
Kassar-Duchossoy, L., Gayraud-Morel, B., Gomès, D., Rocancourt, D., Buckingham, M., Shinin, V., and Tajbakhsh, S. (2004). Mrf4 determines skeletal muscle identity in Myf5: Myod double-mutant mice. Nature *431*, 466.
Kassar-Duchossoy, L., Giacone, E., Gayraud-Morel, B., Jory, A., Gomès, D., and Tajbakhsh, S. (2005). Pax3/Pax7 mark a novel population of primitive myogenic cells during development. Genes & development *19*, 1426-1431.
Kato, Y., Zhao, M., Morikawa, A., Sugiyama, T., Chakravortty, D., Koide, N., Yoshida, T., Tapping, R.I., Yang, Y., and Yokochi, T. (2000). Big mitogen-activated kinase regulates multiple members of the MEF2 protein family. Journal of Biological Chemistry *275*, 18534-18540.
Kawabe, Y.-i., Wang, Y.X., McKinnell, I.W., Bedford, M.T., and Rudnicki, M.A. (2012). Carm1 regulates Pax7 transcriptional activity through MLL1/2 recruitment during asymmetric satellite stem cell divisions. Cell stem cell *11*, 333-345.
Kim, C.-H., Neiswender, H., Baik, E.J., Xiong, W.C., and Mei, L. (2008a). β-Catenin interacts with MyoD and regulates its transcription activity. Molecular and cellular biology *28*, 2941-2951.

Kim, C.H., Neiswender, H., Baik, E.J., Xiong, W.C., and Mei, L. (2008b). Beta-catenin interacts with MyoD and regulates its transcription activity. Mol Cell Biol *28*, 2941-2951.
Kim, H.K., Lee, Y.S., Sivaprasad, U., Malhotra, A., and Dutta, A. (2006). Muscle-specific microRNA miR-206 promotes muscle differentiation. The Journal of cell biology *174*, 677-687.
Knudsen, K.A., Soler, A.P., Johnson, K.R., and Wheelock, M.J. (1995). Interaction of alpha-actinin with the cadherin/catenin cell-cell adhesion complex via alpha-catenin. The Journal of cell biology *130*, 67-77.
Konigsberg, U.R., Lipton, B.H., and Konigsberg, I.R. (1975). The regenerative response of single mature muscle fibers isolated in vitro. Developmental biology *45*, 260-275.
Krek, A., Grün, D., Poy, M.N., Wolf, R., Rosenberg, L., Epstein, E.J., MacMenamin, P., Da Piedade, I., Gunsalus, K.C., and Stoffel, M. (2005). Combinatorial microRNA target predictions. Nature genetics *37*, 495.
Krol, J., Loedige, I., and Filipowicz, W. (2010). The widespread regulation of microRNA biogenesis, function and decay. Nature Reviews Genetics *11*, 597-610.
Kuang, S., Chargé, S.B., Seale, P., Huh, M., and Rudnicki, M.A. (2006). Distinct roles for Pax7 and Pax3 in adult regenerative myogenesis. J Cell Biol *172*, 103-113.
Kuang, S., Kuroda, K., Le Grand, F., and Rudnicki, M.A. (2007). Asymmetric self-renewal and commitment of satellite stem cells in muscle. Cell *129*, 999-1010.
Kühl, M., Sheldahl, L.C., Park, M., Miller, J.R., and Moon, R.T. (2000). The Wnt/Ca2+ pathway: a new vertebrate Wnt signaling pathway takes shape. Trends in genetics *16*, 279-283.
Lagos-Quintana, M., Rauhut, R., Yalcin, A., Meyer, J., Lendeckel, W., and Tuschl, T. (2002). Identification of tissue-specific microRNAs from mouse. Current biology *12*, 735-739.
Le Grand, F., Jones, A.E., Seale, V., Scimè, A., and Rudnicki, M.A. (2009). Wnt7a activates the planar cell polarity pathway to drive the symmetric expansion of satellite stem cells. Cell stem cell *4*, 535-547.
Le Grand, F., and Rudnicki, M.A. (2007). Skeletal muscle satellite cells and adult myogenesis. Current opinion in cell biology *19*, 628-633.
Lee, R.C., and Ambros, V. (2001). An extensive class of small RNAs in Caenorhabditis elegans. Science *294*, 862-864.
Lemos, D.R., Babaeijandaghi, F., Low, M., Chang, C.-K., Lee, S.T., Fiore, D., Zhang, R.-H., Natarajan, A., Nedospasov, S.A., and Rossi, F.M. (2015). Nilotinib reduces muscle fibrosis in chronic muscle injury by promoting TNF-mediated apoptosis of fibro/adipogenic progenitors. Nature medicine *21*, 786.
Lepper, C., Conway, S.J., and Fan, C.-M. (2009). Adult satellite cells and embryonic muscle progenitors have distinct genetic requirements. Nature *460*, 627.
Lepper, C., Partridge, T.A., and Fan, C.-M. (2011). An absolute requirement for Pax7-positive satellite cells in acute injury-induced skeletal muscle regeneration. Development *138*, 3639-3646.
Lewis, B.P., Burge, C.B., and Bartel, D.P. (2005). Conserved seed pairing, often flanked by adenosines, indicates that thousands of human genes are microRNA targets. cell *120*, 15-20.
Li, Vivian S.W., Ng, Ser S., Boersema, Paul J., Low, Teck Y., Karthaus, Wouter R., Gerlach, Jan P., Mohammed, S., Heck, Albert J.R., Maurice, Madelon M., Mahmoudi, T., *et al.* (2012). Wnt Signaling through Inhibition of β-Catenin Degradation in an Intact Axin1 Complex. Cell *149*, 1245-1256.
Li, Z.B., Kollias, H.D., and Wagner, K.R. (2008). Myostatin directly regulates skeletal muscle fibrosis. Journal of Biological Chemistry.

Lilly, B., Zhao, B., Ranganayakulu, G., Paterson, B.M., Schulz, R.A., and Olson, E.N. (1995). Requirement of MADS domain transcription factor D-MEF2 for muscle formation in Drosophila. Science *267*, 688-693.
Lin, Q., Schwarz, J., Bucana, C., and Olson, E.N. (1997). Control of mouse cardiac morphogenesis and myogenesis by transcription factor MEF2C. Science *276*, 1404-1407.
Liu, F., Liang, Z., Xu, J., Li, W., Zhao, D., Zhao, Y., and Yan, C. (2016). Activation of the wnt/β-Catenin Signaling Pathway in Polymyositis, Dermatomyositis and Duchenne Muscular Dystrophy. Journal of Clinical Neurology *12*, 351-360.
Liu, N., Nelson, B.R., Bezprozvannaya, S., Shelton, J.M., Richardson, J.A., Bassel-Duby, R., and Olson, E.N. (2014). Requirement of MEF2A, C, and D for skeletal muscle regeneration. Proceedings of the National Academy of Sciences, 201401732.
Liu, Q.-C., Zha, X.-H., Faralli, H., Yin, H., Louis-Jeune, C., Perdiguero, E., Pranckeviciene, E., Muñoz-Cànoves, P., Rudnicki, M.A., and Brand, M. (2012). Comparative expression profiling identifies differential roles for Myogenin and p38α MAPK signaling in myogenesis. Journal of molecular cell biology *4*, 386-397.
Logan, C.Y., and Nusse, R. (2004). The Wnt signaling pathway in development and disease. Annu Rev Cell Dev Biol *20*, 781-810.
Luo, W., Li, E., Nie, Q., and Zhang, X. (2015a). Myomaker, regulated by MYOD, MYOG and miR-140-3p, promotes chicken myoblast fusion. International journal of molecular sciences *16*, 26186-26201.
Luo, W., Li, E., Nie, Q., and Zhang, X. (2015b). Myomaker, Regulated by MYOD, MYOG and miR-140-3p, Promotes Chicken Myoblast Fusion. Int J Mol Sci *16*, 26186-26201.
Luz, M., Marques, M., and Santo Neto, H. (2002). Impaired regeneration of dystrophin-deficient muscle fibers is caused by exhaustion of myogenic cells. Brazilian journal of medical and biological research *35*, 691-695.
Ma, H., Naseri, A., Reyes-Gutierrez, P., Wolfe, S.A., Zhang, S., and Pederson, T. (2015). Multicolor CRISPR labeling of chromosomal loci in human cells. Proceedings of the National Academy of Sciences *112*, 3002-3007.
Ma, H., Nguyen, C., Lee, K.-S., and Kahn, M. (2005). Differential roles for the coactivators CBP and p300 on TCF/β-catenin-mediated survivin gene expression. Oncogene *24*, 3619.
Massari, M.E., and Murre, C. (2000). Helix-loop-helix proteins: regulators of transcription in eucaryotic organisms. Molecular and cellular biology *20*, 429-440.
Mathew, S.J., Hansen, J.M., Merrell, A.J., Murphy, M.M., Lawson, J.A., Hutcheson, D.A., Hansen, M.S., Angus-Hill, M., and Kardon, G. (2011). Connective tissue fibroblasts and Tcf4 regulate myogenesis. Development *138*, 371-384.
Matsuzaka, Y., and Hashido, K. (2015). Roles of miR-1, miR-133a, and miR-206 in calcium, oxidative stress, and NO signaling involved in muscle diseases. RNA & DISEASE *2*.
Mauro, A. (1961). Satellite cell of skeletal muscle fibers. The Journal of biophysical and biochemical cytology *9*, 493.
McCarthy, J.J. (2008). MicroRNA-206: the skeletal muscle-specific myomiR. Biochimica et Biophysica Acta (BBA)-Gene Regulatory Mechanisms *1779*, 682-691.
McCarthy, J.J., Mula, J., Miyazaki, M., Erfani, R., Garrison, K., Farooqui, A.B., Srikuea, R., Lawson, B.A., Grimes, B., Keller, C., *et al.* (2011). Effective fiber hypertrophy in satellite cell-depleted skeletal muscle. Development *138*, 3657-3666.
McDermott, J.C., Cardoso, M.C., Yu, Y.T., Andres, V., Leifer, D., Krainc, D., Lipton, S.A., and Nadal-Ginard, B. (1993). hMEF2C gene encodes skeletal muscle- and brain-specific transcription factors. Molecular and cellular biology *13*, 2564-2577.

McKinnell, I.W., Ishibashi, J., Le Grand, F., Punch, V.G., Addicks, G.C., Greenblatt, J.F., Dilworth, F.J., and Rudnicki, M.A. (2008). Pax7 activates myogenic genes by recruitment of a histone methyltransferase complex. Nature cell biology *10*, 77.
Metcalfe, C., Mendoza-Topaz, C., Mieszczanek, J., and Bienz, M. (2010). Stability elements in the LRP6 cytoplasmic tail confer efficient signalling upon DIX-dependent polymerization. J Cell Sci *123*, 1588-1599.
Millay, D.P., O'Rourke, J.R., Sutherland, L.B., Bezprozvannaya, S., Shelton, J.M., Bassel-Duby, R., and Olson, E.N. (2013). Myomaker is a membrane activator of myoblast fusion and muscle formation. Nature *499*, 301.
Millay, D.P., Sutherland, L.B., Bassel-Duby, R., and Olson, E.N. (2014a). Myomaker is essential for muscle regeneration. Genes Dev *28*, 1641-1646.
Millay, D.P., Sutherland, L.B., Bassel-Duby, R., and Olson, E.N. (2014b). Myomaker is essential for muscle regeneration. Genes & development *28*, 1641-1646.
Mintz, B., and Baker, W.W. (1967). Normal mammalian muscle differentiation and gene control of isocitrate dehydrogenase synthesis. Proceedings of the National Academy of Sciences *58*, 592-598.
Mojica, F.J., Díez-Villaseñor, C., Soria, E., and Juez, G. (2000). Biological significance of a family of regularly spaced repeats in the genomes of Archaea, Bacteria and mitochondria. Molecular microbiology *36*, 244-246.
Molkentin, J.D., and Olson, E.N. (1996). Combinatorial control of muscle development by basic helix-loop-helix and MADS-box transcription factors. Proceedings of the National Academy of Sciences *93*, 9366-9373.
Moon, R.T., Bowerman, B., Boutros, M., and Perrimon, N. (2002). The promise and perils of Wnt signaling through β-catenin. Science *296*, 1644-1646.
Moss, F., and Leblond, C. (1971). Satellite cells as the source of nuclei in muscles of growing rats. The Anatomical Record *170*, 421-435.
Muir, A., Kanji, A., and Allbrook, D. (1965). The structure of the satellite cells in skeletal muscle. Journal of anatomy *99*, 435.
Murphy, M.M., Keefe, A.C., Lawson, J.A., Flygare, S.D., Yandell, M., and Kardon, G. (2014a). Transiently active Wnt/beta-catenin signaling is not required but must be silenced for stem cell function during muscle regeneration. Stem Cell Reports *3*, 475-488.
Murphy, M.M., Keefe, A.C., Lawson, J.A., Flygare, S.D., Yandell, M., and Kardon, G. (2014b). Transiently active Wnt/β-catenin signaling is not required but must be silenced for stem cell function during muscle regeneration. Stem Cell Reports *3*, 475-488.
Murphy, M.M., Lawson, J.A., Mathew, S.J., Hutcheson, D.A., and Kardon, G. (2011). Satellite cells, connective tissue fibroblasts and their interactions are crucial for muscle regeneration. Development *138*, 3625-3637.
Nabeshima, Y., Hanaoka, K., Hayasaka, M., Esuml, E., Li, S., Nonaka, I., and Nabeshima, Y.-i. (1993). Myogenin gene disruption results in perinatal lethality because of severe muscle defect. Nature *364*, 532.
Nagata, Y., Kobayashi, H., Umeda, M., Ohta, N., Kawashima, S., Zammit, P.S., and Matsuda, R. (2006). Sphingomyelin levels in the plasma membrane correlate with the activation state of muscle satellite cells. Journal of Histochemistry & Cytochemistry *54*, 375-384.
Nieset, J.E., Redfield, A.R., Jin, F., Knudsen, K.A., Johnson, K.R., and Wheelock, M.J. (1997). Characterization of the interactions of alpha-catenin with alpha-actinin and beta-catenin/plakoglobin. J Cell Sci *110 (Pt 8)*, 1013-1022.
Niessen, C.M., and Gumbiner, B.M. (1998). The juxtamembrane region of the cadherin cytoplasmic tail supports lateral clustering, adhesive strengthening, and

interaction with p120ctn. The Journal of cell biology *141*, 779-789.
Nishimasu, H., Ran, F.A., Hsu, P.D., Konermann, S., Shehata, S.I., Dohmae, N., Ishitani, R., Zhang, F., and Nureki, O. (2014). Crystal structure of Cas9 in complex with guide RNA and target DNA. Cell *156*, 935-949.
Nusse, R., Fuerer, C., Ching, W., Harnish, K., Logan, C., Zeng, A., Ten Berge, D., and Kalani, Y. (2008). Wnt signaling and stem cell control. Paper presented at: Cold Spring Harbor symposia on quantitative biology (Cold Spring Harbor Laboratory Press).
O'Rourke, J.R., Georges, S.A., Seay, H.R., Tapscott, S.J., McManus, M.T., Goldhamer, D.J., Swanson, M.S., and Harfe, B.D. (2007). Essential role for Dicer during skeletal muscle development. Developmental biology *311*, 359-368.
Ogryzko, V.V., Kotani, T., Zhang, X., Schiltz, R.L., Howard, T., Yang, X.-J., Howard, B.H., Qin, J., and Nakatani, Y. (1998). Histone-like TAFs within the PCAF histone acetylase complex. Cell *94*, 35-44.
Ogryzko, V.V., Schiltz, R.L., Russanova, V., Howard, B.H., and Nakatani, Y. (1996). The transcriptional coactivators p300 and CBP are histone acetyltransferases. Cell *87*, 953-959.
Olguin, H.C., and Olwin, B.B. (2004). Pax-7 up-regulation inhibits myogenesis and cell cycle progression in satellite cells: a potential mechanism for self-renewal. Developmental biology *275*, 375-388.
Olguin, H.C., Yang, Z., Tapscott, S.J., and Olwin, B.B. (2007). Reciprocal inhibition between Pax7 and muscle regulatory factors modulates myogenic cell fate determination. J Cell Biol *177*, 769-779.
Ono, Y., Boldrin, L., Knopp, P., Morgan, J.E., and Zammit, P.S. (2010). Muscle satellite cells are a functionally heterogeneous population in both somite-derived and branchiomeric muscles. Developmental biology *337*, 29-41.
Otto, A., Collins-Hooper, H., and Patel, K. (2009). The origin, molecular regulation and therapeutic potential of myogenic stem cell populations. Journal of Anatomy *9999*.
Otto, A., Schmidt, C., Luke, G., Allen, S., Valasek, P., Muntoni, F., Lawrence-Watt, D., and Patel, K. (2008). Canonical Wnt signalling induces satellite-cell proliferation during adult skeletal muscle regeneration. Journal of cell science *121*, 2939-2950.
Oustanina, S., Hause, G., and Braun, T. (2004). Pax7 directs postnatal renewal and propagation of myogenic satellite cells but not their specification. The EMBO journal *23*, 3430-3439.
Ozawa, M. (2015). E-cadherin cytoplasmic domain inhibits cell surface localization of endogenous cadherins and fusion of C2C12 myoblasts. Biology Open *4*, 1427-1435.
Pansters, N., van der Velden, J., Kelders, M., Laeremans, H., Schols, A., and Langen, R. (2011). Segregation of myoblast fusion and muscle-specific gene expression by distinct ligand-dependent inactivation of GSK-3β. Cellular and Molecular Life Sciences *68*, 523-535.
Parker, D.S., Ni, Y.Y., Chang, J.L., Li, J., and Cadigan, K.M. (2008). Wingless signaling induces widespread chromatin remodeling of target loci. Mol Cell Biol *28*, 1815-1828.
Patapoutian, A., Yoon, J.K., Miner, J.H., Wang, S., Stark, K., and Wold, B. (1995). Disruption of the mouse MRF4 gene identifies multiple waves of myogenesis in the myotome. Development *121*, 3347-3358.
Peifer, M., and Polakis, P. (2000). Wnt signaling in oncogenesis and embryogenesis--a look outside the nucleus. Science *287*, 1606-1609.
Petropoulos, H., and Skerjanc, I.S. (2002). Beta-catenin is essential and sufficient for skeletal myogenesis in P19 cells. J Biol Chem *277*, 15393-15399.

Pokutta, S., and Weis, W.I. (2000). Structure of the dimerization and β-catenin-binding region of α-catenin. Molecular cell *5*, 533-543.
Polesskaya, A., Duquet, A., Naguibneva, I., Weise, C., Vervisch, A., Bengal, E., Hucho, F., Robin, P., and Harel-Bellan, A. (2000). CREB-binding protein/p300 activates MyoD by acetylation. Journal of Biological Chemistry *275*, 34359-34364.
Polesskaya, A., Naguibneva, I., Fritsch, L., Duquet, A., Ait-Si-Ali, S., Robin, P., Vervisch, A., Pritchard, L., Cole, P., and Harel-Bellan, A. (2001). CBP/p300 and muscle differentiation: no HAT, no muscle. The EMBO journal *20*, 6816-6825.
Polesskaya, A., Seale, P., and Rudnicki, M.A. (2003). Wnt signaling induces the myogenic specification of resident CD45+ adult stem cells during muscle regeneration. Cell *113*, 841-852.
Posokhova, E., Shukla, A., Seaman, S., Volate, S., Hilton, M.B., Wu, B., Morris, H., Swing, D.A., Zhou, M., Zudaire, E., *et al.* (2015). GPR124 functions as a WNT7-specific coactivator of canonical beta-catenin signaling. Cell Rep *10*, 123-130.
Potthoff, M.J., Arnold, M.A., McAnally, J., Richardson, J.A., Bassel-Duby, R., and Olson, E.N. (2007). Regulation of skeletal muscle sarcomere integrity and postnatal muscle function by Mef2c. Molecular and cellular biology *27*, 8143-8151.
Potthoff, M.J., and Olson, E.N. (2007). MEF2: a central regulator of diverse developmental programs. Development *134*, 4131-4140.
Pourcel, C., Salvignol, G., and Vergnaud, G. (2005). CRISPR elements in Yersinia pestis acquire new repeats by preferential uptake of bacteriophage DNA, and provide additional tools for evolutionary studies. Microbiology *151*, 653-663.
Qi, L.S., Larson, M.H., Gilbert, L.A., Doudna, J.A., Weissman, J.S., Arkin, A.P., and Lim, W.A. (2013). Repurposing CRISPR as an RNA-guided platform for sequence-specific control of gene expression. Cell *152*, 1173-1183.
Ran, F.A., Hsu, P.D., Lin, C.-Y., Gootenberg, J.S., Konermann, S., Trevino, A.E., Scott, D.A., Inoue, A., Matoba, S., and Zhang, Y. (2013). Double nicking by RNA-guided CRISPR Cas9 for enhanced genome editing specificity. Cell *154*, 1380-1389.
Rao, P.K., Kumar, R.M., Farkhondeh, M., Baskerville, S., and Lodish, H.F. (2006). Myogenic factors that regulate expression of muscle-specific microRNAs. Proceedings of the National Academy of Sciences *103*, 8721-8726.
Rebel, V.I., Kung, A.L., Tanner, E.A., Yang, H., Bronson, R.T., and Livingston, D.M. (2002). Distinct roles for CREB-binding protein and p300 in hematopoietic stem cell self-renewal. Proceedings of the National Academy of Sciences *99*, 14789-14794.
Relaix, F., Montarras, D., Zaffran, S., Gayraud-Morel, B., Rocancourt, D., Tajbakhsh, S., Mansouri, A., Cumano, A., and Buckingham, M. (2006). Pax3 and Pax7 have distinct and overlapping functions in adult muscle progenitor cells. J Cell Biol *172*, 91-102.
Relaix, F., Rocancourt, D., Mansouri, A., and Buckingham, M. (2005). A Pax3/Pax7-dependent population of skeletal muscle progenitor cells. Nature *435*, 948.
Renault, V., Thorne, L.E., Eriksson, P.O., Butler-Browne, G., and Mouly, V. (2002). Regenerative potential of human skeletal muscle during aging. Aging cell *1*, 132-139.
Reynolds, A.B., Daniel, J., McCrea, P.D., Wheelock, M.J., Wu, J., and Zhang, Z. (1994). Identification of a new catenin: the tyrosine kinase substrate p120cas associates with E-cadherin complexes. Molecular and cellular biology *14*, 8333-8342.
Reznikoff, C.A., Bertram, J.S., Brankow, D.W., and Heidelberger, C. (1973). Quantitative and qualitative studies of chemical transformation of cloned C3H mouse embryo cells sensitive to postconfluence inhibition of cell division. Cancer research *33*, 3239-3249.

Rhodes, S.J., and Konieczny, S.F. (1989). Identification of MRF4: a new member of the muscle regulatory factor gene family. Genes & development *3*, 2050-2061.
Ridgeway, A.G., Petropoulos, H., Wilton, S., and Skerjanc, I.S. (2000). Wnt signaling regulates the function of MyoD and myogenin. J Biol Chem *275*, 32398-32405.
Rieger, M.E., Zhou, B., Solomon, N., Sunohara, M., Li, C., Nguyen, C., Liu, Y., Pan, J.-h., Minoo, P., and Crandall, E.D. (2016). p300/β-catenin interactions regulate adult progenitor cell differentiation downstream of WNT5a/protein kinase C (PKC). Journal of Biological Chemistry *291*, 6569-6582.
Roberts, A., Pimentel, H., Trapnell, C., and Pachter, L. (2011). Identification of novel transcripts in annotated genomes using RNA-Seq. Bioinformatics *27*, 2325-2329.
Rochat, A., Fernandez, A., Vandromme, M., Moles, J.-P., Bouschet, T., Carnac, G., and Lamb, N.J. (2004). Insulin and wnt1 pathways cooperate to induce reserve cell activation in differentiation and myotube hypertrophy. Molecular biology of the cell *15*, 4544-4555.
Rocheteau, P., Gayraud-Morel, B., Siegl-Cachedenier, I., Blasco, M.A., and Tajbakhsh, S. (2012). A subpopulation of adult skeletal muscle stem cells retains all template DNA strands after cell division. Cell *148*, 112-125.
Rosenberg, M.I., Georges, S.A., Asawachaicharn, A., Analau, E., and Tapscott, S.J. (2006). MyoD inhibits Fstl1 and Utrn expression by inducing transcription of miR-206. The Journal of cell biology *175*, 77-85.
Rosenblatt, J.D. (1992). A time course study of the isometric contractile properties of rat extensor digitorum longus muscle injected with bupivacaine. Comparative biochemistry and physiology Comparative physiology *101*, 361-367.
Roth, J.F., Shikama, N., Henzen, C., Desbaillets, I., Lutz, W., Marino, S., Wittwer, J., Schorle, H., Gassmann, M., and Eckner, R. (2003). Differential role of p300 and CBP acetyltransferase during myogenesis: p300 acts upstream of MyoD and Myf5. The EMBO journal *22*, 5186-5196.
Rudnicki, M., Le Grand, F., McKinnell, I., and Kuang, S. (2008a). The molecular regulation of muscle stem cell function. Paper presented at: Cold Spring Harbor symposia on quantitative biology (Cold Spring Harbor Laboratory Press).
Rudnicki, M.A., Braun, T., Hinuma, S., and Jaenisch, R. (1992). Inactivation of MyoD in mice leads to up-regulation of the myogenic HLH gene Myf-5 and results in apparently normal muscle development. Cell *71*, 383-390.
Rudnicki, M.A., Le Grand, F., McKinnell, I., and Kuang, S. (2008b). The molecular regulation of muscle stem cell function. Cold Spring Harbor symposia on quantitative biology *73*, 323-331.
Rudnicki, M.A., Schnegelsberg, P.N., Stead, R.H., Braun, T., Arnold, H.-H., and Jaenisch, R. (1993). MyoD or Myf-5 is required for the formation of skeletal muscle. Cell *75*, 1351-1359.
Rudolf, A., Schirwis, E., Giordani, L., Parisi, A., Lepper, C., Taketo, M.M., and Le Grand, F. (2016a). beta-Catenin Activation in Muscle Progenitor Cells Regulates Tissue Repair. Cell Rep *15*, 1277-1290.
Rudolf, A., Schirwis, E., Giordani, L., Parisi, A., Lepper, C., Taketo, M.M., and Le Grand, F. (2016b). β-catenin activation in muscle progenitor cells regulates tissue repair. Cell reports *15*, 1277-1290.
Rupp, L.J., Schumann, K., Roybal, K.T., Gate, R.E., Chun, J.Y., Lim, W.A., and Marson, A. (2017). CRISPR/Cas9-mediated PD-1 disruption enhances anti-tumor efficacy of human chimeric antigen receptor T cells. Scientific reports *7*, 737.
Sacco, A., Mourkioti, F., Tran, R., Choi, J., Llewellyn, M., Kraft, P., Shkreli, M., Delp, S., Pomerantz, J.H., and Artandi, S.E. (2010). Short telomeres and stem cell

exhaustion model Duchenne muscular dystrophy in mdx/mTR mice. Cell *143*, 1059-1071.
Sambasivan, R., and Tajbakhsh, S. (2007). Skeletal muscle stem cell birth and properties. Paper presented at: Seminars in cell & developmental biology (Elsevier).
Sambasivan, R., Yao, R., Kissenpfennig, A., Van Wittenberghe, L., Paldi, A., Gayraud-Morel, B., Guenou, H., Malissen, B., Tajbakhsh, S., and Galy, A. (2011). Pax7-expressing satellite cells are indispensable for adult skeletal muscle regeneration. Development *138*, 3647-3656.
Sartorelli, V., Huang, J., Hamamori, Y., and Kedes, L. (1997). Molecular mechanisms of myogenic coactivation by p300: direct interaction with the activation domain of MyoD and with the MADS box of MEF2C. Molecular and cellular biology *17*, 1010-1026.
Sartorelli, V., Puri, P.L., Hamamori, Y., Ogryzko, V., Chung, G., Nakatani, Y., Wang, J.Y., and Kedes, L. (1999). Acetylation of MyoD directed by PCAF is necessary for the execution of the muscle program. Molecular cell *4*, 725-734.
Sasaki, T., Hwang, H., Nguyen, C., Kloner, R.A., and Kahn, M. (2013). The small molecule Wnt signaling modulator ICG-001 improves contractile function in chronically infarcted rat myocardium. PloS one *8*, e75010.
Schienda, J., Engleka, K.A., Jun, S., Hansen, M.S., Epstein, J.A., Tabin, C.J., Kunkel, L.M., and Kardon, G. (2006). Somitic origin of limb muscle satellite and side population cells. Proceedings of the National Academy of Sciences of the United States of America *103*, 945-950.
Schmalbruch, H., and Lewis, D. (2000). Dynamics of nuclei of muscle fibers and connective tissue cells in normal and denervated rat muscles. Muscle & nerve *23*, 617-626.
Schultz, E., and Jaryszak, D.L. (1985). Effects of skeletal muscle regeneration on the proliferation potential of satellite cells. Mechanisms of ageing and development *30*, 63-72.
Seale, P., Sabourin, L.A., Girgis-Gabardo, A., Mansouri, A., Gruss, P., and Rudnicki, M.A. (2000). Pax7 is required for the specification of myogenic satellite cells. Cell *102*, 777-786.
Sempere, L.F., Freemantle, S., Pitha-Rowe, I., Moss, E., Dmitrovsky, E., and Ambros, V. (2004). Expression profiling of mammalian microRNAs uncovers a subset of brain-expressed microRNAs with possible roles in murine and human neuronal differentiation. Genome biology *5*, R13.
Shiama, N. (1997). The p300/CBP family: integrating signals with transcription factors and chromatin. Trends in cell biology *7*, 230-236.
Small, E.M., O'Rourke, J.R., Moresi, V., Sutherland, L.B., McAnally, J., Gerard, R.D., Richardson, J.A., and Olson, E.N. (2010). Regulation of PI3-kinase/Akt signaling by muscle-enriched microRNA-486. Proceedings of the National Academy of Sciences *107*, 4218-4223.
Snow, M.H. (1977). Myogenic cell formation in regenerating rat skeletal muscle injured by mincing II. An autoradiographic study. The Anatomical Record *188*, 201-217.
Soleimani, V.D., Punch, V.G., Kawabe, Y.-i., Jones, A.E., Palidwor, G.A., Porter, C.J., Cross, J.W., Carvajal, J.J., Kockx, C.E., and van IJcken, W.F. (2012). Transcriptional dominance of Pax7 in adult myogenesis is due to high-affinity recognition of homeodomain motifs. Developmental cell *22*, 1208-1220.
Stamos, J.L., and Weis, W.I. (2013). The beta-catenin destruction complex. Cold Spring Harbor perspectives in biology *5*, a007898.
Studitsky, A. (1965). Free auto-and homografts of muscle tissue in experiments on animals. Annals of the New York Academy of Sciences *120*, 789-801.

Su, S., Zou, Z., Chen, F., Ding, N., Du, J., Shao, J., Li, L., Fu, Y., Hu, B., and Yang, Y. (2017). CRISPR-Cas9-mediated disruption of PD-1 on human T cells for adoptive cellular therapies of EBV positive gastric cancer. Oncoimmunology *6*, e1249558.
Suzuki, A., Pelikan, R.C., and Iwata, J. (2015). WNT/β-catenin signaling regulates multiple steps of myogenesis by regulating step-specific targets. Molecular and cellular biology *35*, 1763-1776.
Sweetman, D., Goljanek, K., Rathjen, T., Oustanina, S., Braun, T., Dalmay, T., and Münsterberg, A. (2008). Specific requirements of MRFs for the expression of muscle specific microRNAs, miR-1, miR-206 and miR-133. Developmental biology *321*, 491-499.
Takemaru, K.-I., and Moon, R.T. (2000a). The transcriptional coactivator CBP interacts with β-catenin to activate gene expression. The Journal of cell biology *149*, 249-254.
Takemaru, K.I., and Moon, R.T. (2000b). The transcriptional coactivator CBP interacts with beta-catenin to activate gene expression. J Cell Biol *149*, 249-254.
Tanaka, S., Terada, K., and Nohno, T. (2011). Canonical Wnt signaling is involved in switching from cell proliferation to myogenic differentiation of mouse myoblast cells. Journal of molecular signaling *6*, 12.
Tanaka, Y., Naruse, I., Hongo, T., Xu, M.-J., Nakahata, T., Maekawa, T., and Ishii, S. (2000). Extensive brain hemorrhage and embryonic lethality in a mouse null mutant of CREB-binding protein. Mechanisms of development *95*, 133-145.
Teo, J.-L., Ma, H., Nguyen, C., Lam, C., and Kahn, M. (2005). Specific inhibition of CBP/β-catenin interaction rescues defects in neuronal differentiation caused by a presenilin-1 mutation. Proceedings of the National Academy of Sciences of the United States of America *102*, 12171-12176.
Théry, C., Zitvogel, L., and Amigorena, S. (2002). Exosomes: composition, biogenesis and function. Nature Reviews Immunology *2*, 569.
Tokunaga, Y., Osawa, Y., Ohtsuki, T., Hayashi, Y., Yamaji, K., Yamane, D., Hara, M., Munekata, K., Tsukiyama-Kohara, K., and Hishima, T. (2017). Selective inhibitor of Wnt/β-catenin/CBP signaling ameliorates hepatitis C virus-induced liver fibrosis in mouse model. Scientific Reports *7*.
Trapnell, C., Hendrickson, D.G., Sauvageau, M., Goff, L., Rinn, J.L., and Pachter, L. (2013). Differential analysis of gene regulation at transcript resolution with RNA-seq. Nature biotechnology *31*, 10.1038/nbt.2450.
Trensz, F., Haroun, S., Cloutier, A., Richter, M.V., and Grenier, G. (2010). A muscle resident cell population promotes fibrosis in hindlimb skeletal muscles of mdx mice through the Wnt canonical pathway. American Journal of Physiology-Cell Physiology *299*, C939-C947.
Vadlamudi, U., Espinoza, H.M., Ganga, M., Martin, D.M., Liu, X., Engelhardt, J.F., and Amendt, B.A. (2005). PITX2, β-catenin and LEF-1 interact to synergistically regulate the LEF-1 promoter. Journal of Cell Science *118*, 1129-1137.
van der Velden, J.L., Langen, R.C., Kelders, M.C., Wouters, E.F., Janssen-Heininger, Y.M., and Schols, A.M. (2006). Inhibition of glycogen synthase kinase-3β activity is sufficient to stimulate myogenic differentiation. American Journal of Physiology-Cell Physiology *290*, C453-C462.
van Rooij, E., Quiat, D., Johnson, B.A., Sutherland, L.B., Qi, X., Richardson, J.A., Kelm, R.J., and Olson, E.N. (2009). A family of microRNAs encoded by myosin genes governs myosin expression and muscle performance. Developmental cell *17*, 662-673.
van Rooij, E., Sutherland, L.B., Qi, X., Richardson, J.A., Hill, J., and Olson, E.N. (2007). Control of stress-dependent cardiac growth and gene expression by a microRNA. Science *316*, 575-579.

Vandel, L., and Trouche, D. (2001). Physical association between the histone acetyl transferase CBP and a histone methyl transferase. EMBO reports *2*, 21-26.
von Maltzahn, J., Chang, N.C., Bentzinger, C.F., and Rudnicki, M.A. (2012). Wnt signaling in myogenesis. Trends in cell biology *22*, 602-609.
von Maltzahn, J., Jones, A.E., Parks, R.J., and Rudnicki, M.A. (2013). Pax7 is critical for the normal function of satellite cells in adult skeletal muscle. Proceedings of the National Academy of Sciences *110*, 16474-16479.
Wang, Q., Chou, X., Guan, F., Fang, Z., Lu, S., Lei, J., Li, Y., and Liu, W. (2017). Enhanced Wnt Signalling in Hepatocytes is Associated with Schistosoma japonicum Infection and Contributes to Liver Fibrosis. Scientific Reports *7*.
Williams, A.H., Valdez, G., Moresi, V., Qi, X., McAnally, J., Elliott, J.L., Bassel-Duby, R., Sanes, J.R., and Olson, E.N. (2009). MicroRNA-206 delays ALS progression and promotes regeneration of neuromuscular synapses in mice. Science *326*, 1549-1554.
Winbanks, C.E., Wang, B., Beyer, C., Koh, P., White, L., Kantharidis, P., and Gregorevic, P. (2011). TGF-β regulates miR-206 and miR-29 to control myogenic differentiation through regulation of histone deacetylase 4 (HDAC4). Journal of Biological Chemistry, jbc. M110. 192625.
Winter, J., Jung, S., Keller, S., Gregory, R.I., and Diederichs, S. (2009). Many roads to maturity: microRNA biogenesis pathways and their regulation. Nature cell biology *11*, 228.
Wodarz, A., and Nusse, R. (1998). Mechanisms of Wnt signaling in development. Annu Rev Cell Dev Biol *14*, 59-88.
Wozniak, A.C., Kong, J., Bock, E., Pilipowicz, O., and Anderson, J.E. (2005). Signaling satellite-cell activation in skeletal muscle: Markers, models, stretch, and potential alternate pathways. Muscle & Nerve *31*, 283-300.
Wright, W.E., Sassoon, D.A., and Lin, V.K. (1989). Myogenin, a factor regulating myogenesis, has a domain homologous to MyoD. Cell *56*, 607-617.
Wrobel, E., Brzoska, E., and Moraczewski, J. (2007). M-cadherin and beta-catenin participate in differentiation of rat satellite cells. European journal of cell biology *86*, 99-109.
Wu, H., Naya, F.J., McKinsey, T.A., Mercer, B., Shelton, J.M., Chin, E.R., Simard, A.R., Michel, R.N., Bassel-Duby, R., and Olson, E.N. (2000). MEF2 responds to multiple calcium-regulated signals in the control of skeletal muscle fiber type. The EMBO journal *19*, 1963-1973.
Wu, R., Li, H., Zhai, L., Zou, X., Meng, J., Zhong, R., Li, C., Wang, H., Zhang, Y., and Zhu, D. (2015). MicroRNA-431 accelerates muscle regeneration and ameliorates muscular dystrophy by targeting Pax7 in mice. Nature communications *6*, 7713.
Xu, W., and Kimelman, D. (2007). Mechanistic insights from structural studies of β-catenin and its binding partners. Journal of cell science *120*, 3337-3344.
Yablonka-Reuveni, Z., and Rivera, A.J. (1994). Temporal expression of regulatory and structural muscle proteins during myogenesis of satellite cells on isolated adult rat fibers. Developmental biology *164*, 588-603.
Yamada, S., Pokutta, S., Drees, F., Weis, W.I., and Nelson, W.J. (2005). Deconstructing the cadherin-catenin-actin complex. Cell *123*, 889-901.
Yao, T.-P., Oh, S.P., Fuchs, M., Zhou, N.-D., Ch'ng, L.-E., Newsome, D., Bronson, R.T., Li, E., Livingston, D.M., and Eckner, R. (1998). Gene dosage–dependent embryonic development and proliferation defects in mice lacking the transcriptional integrator p300. Cell *93*, 361-372.
Yee, S.P., and Rigby, P.W. (1993). The regulation of myogenin gene expression during the embryonic development of the mouse. Genes & Development *7*, 1277-1289.

Yin, H., Pasut, A., Soleimani, V.D., Bentzinger, C.F., Antoun, G., Thorn, S., Seale, P., Fernando, P., van IJcken, W., and Grosveld, F. (2013). MicroRNA-133 controls brown adipose determination in skeletal muscle satellite cells by targeting Prdm16. Cell metabolism *17*, 210-224.
Yu, Y.-T., Breitbart, R.E., Smoot, L.B., Lee, Y., Mahdavi, V., and Nadal-Ginard, B. (1992). Human myocyte-specific enhancer factor 2 comprises a group of tissue-restricted MADS box transcription factors. Genes & development *6*, 1783-1798.
Zammit, P.S., Golding, J.P., Nagata, Y., Hudon, V., Partridge, T.A., and Beauchamp, J.R. (2004). Muscle satellite cells adopt divergent fates: a mechanism for self-renewal? J Cell Biol *166*, 347-357.
Zammit, P.S., Heslop, L., Hudon, V., Rosenblatt, J.D., Tajbakhsh, S., Buckingham, M.E., Beauchamp, J.R., and Partridge, T.A. (2002). Kinetics of myoblast proliferation show that resident satellite cells are competent to fully regenerate skeletal muscle fibers. Experimental cell research *281*, 39-49.
Zetsche, B., Gootenberg, J.S., Abudayyeh, O.O., Slaymaker, I.M., Makarova, K.S., Essletzbichler, P., Volz, S.E., Joung, J., Van Der Oost, J., and Regev, A. (2015). Cpf1 is a single RNA-guided endonuclease of a class 2 CRISPR-Cas system. Cell *163*, 759-771.
Zhang, D., Li, X., Chen, C., Li, Y., Zhao, L., Jing, Y., Liu, W., Wang, X., Zhang, Y., and Xia, H. (2012). Attenuation of p38-mediated miR-1/133 expression facilitates myoblast proliferation during the early stage of muscle regeneration. PloS one *7*, e41478.
Zhang, W., Behringer, R.R., and Olson, E.N. (1995). Inactivation of the myogenic bHLH gene MRF4 results in up-regulation of myogenin and rib anomalies. Genes & development *9*, 1388-1399.
Zhuang, L., Hulin, J.A., Gromova, A., Tran Nguyen, T.D., Yu, R.T., Liddle, C., Downes, M., Evans, R.M., Makarenkova, H.P., and Meech, R. (2014). Barx2 and Pax7 have antagonistic functions in regulation of wnt signaling and satellite cell differentiation. Stem Cells *32*, 1661-1673.